

**ELECTRICAL ENGINEERING SERIES**



# **Lithium Batteries and Other Electrochemical Storage Systems**

**Christian Glaize and Sylvie Geniès**

**ISTE**

**WILEY**



## Lithium Batteries and Other Electrochemical Storage Systems





# **Lithium Batteries and Other Electrochemical Storage Systems**

Christian Glaize  
Sylvie Geniès

*Series Editor*  
*Bernard Multon*

**ISTE**

**WILEY**

First published 2013 in Great Britain and the United States by ISTE Ltd and John Wiley & Sons, Inc.

Apart from any fair dealing for the purposes of research or private study, or criticism or review, as permitted under the Copyright, Designs and Patents Act 1988, this publication may only be reproduced, stored or transmitted, in any form or by any means, with the prior permission in writing of the publishers, or in the case of reprographic reproduction in accordance with the terms and licenses issued by the CLA. Enquiries concerning reproduction outside these terms should be sent to the publishers at the undermentioned address:

ISTE Ltd  
27-37 St George's Road  
London SW19 4EU  
UK

[www.iste.co.uk](http://www.iste.co.uk)

John Wiley & Sons, Inc.  
111 River Street  
Hoboken, NJ 07030  
USA

[www.wiley.com](http://www.wiley.com)

© ISTE Ltd 2013

The rights of Christian Glaize and Sylvie Geniès to be identified as the authors of this work have been asserted by them in accordance with the Copyright, Designs and Patents Act 1988.

Library of Congress Control Number: 2013941764

---

British Library Cataloguing-in-Publication Data

A CIP record for this book is available from the British Library

ISBN: 978-1-84821-496-5

---



Printed and bound in Great Britain by CPI Group (UK) Ltd., Croydon, Surrey CR0 4YY

## Table of Contents

|  |      |
|--|------|
| <b>Preface</b> . . . . .   | xiii |
| <b>Acknowledgements</b> . . . . .  | xv   |
| <b>Introduction</b> . . . . .  | xvii |
| <b>PART 1. STORAGE REQUIREMENTS CHARACTERISTICS OF<br/>SECONDARY BATTERIES EXAMPLES OF USE</b> . . . . . | 1    |
| <b>Chapter 1. Breakdown of Storage Requirements</b> . . . . .  | 3    |
| 1.1. Introduction . . . . .  | 3    |
| 1.2. Domains of application for energy storage . . . . .   | 3    |
| 1.2.1. Starter batteries . . . . .   | 4    |
| 1.2.2. Traction batteries . . . . .  | 6    |
| 1.2.3. Stationary batteries . . . . .  | 10   |
| 1.2.4. Batteries for mobile or nomadic devices . . . . .   | 17   |
| 1.3. Review of storage requirements and appropriate<br>technologies . . . . .                            | 18   |
| 1.4. Conclusion . . . . .  | 19   |
| <b>Chapter 2. Definitions and Measuring Methods</b> . . . . .  | 21   |
| 2.1. Introduction . . . . .  | 21   |
| 2.2. Terminology . . . . .   | 21   |
| 2.2.1. Accumulator . . . . .   | 22   |
| 2.2.2. Element, elementary cell, electrolyte . . . . .   | 22   |
| 2.2.3. Electrode, half-element, half-cell . . . . .  | 23   |

|   |    |
|---|----|
| 2.2.4. Oxidation, reduction, anode, cathode . . . . .   | 24 |
| 2.2.5. Active material . . . . .  | 25 |
| 2.2.6. Voltage . . . . .  | 25 |
| 2.2.7. Battery of accumulators, modules, packs, BMS . . . . .   | 26 |
| 2.3. Definitions of the characteristics . . . . .   | 27 |
| 2.3.1. Nominal voltage . . . . .  | 27 |
| 2.3.2. Voltage under current . . . . .  | 27 |
| 2.3.3. Capacities . . . . .   | 30 |
| 2.4. States of the battery . . . . .  | 40 |
| 2.4.1. Depth of discharge . . . . .   | 40 |
| 2.4.2. State of charge . . . . .  | 41 |
| 2.4.3. State of energy . . . . .  | 41 |
| 2.4.4. State of health . . . . .  | 41 |
| 2.4.5. State of function . . . . .  | 45 |
| 2.4.6. Theoretical gravimetric capacity . . . . .   | 45 |
| 2.4.7. Practical gravimetric capacity . . . . .   | 46 |
| 2.4.8. Volumetric capacity . . . . .  | 46 |
| 2.4.9. Specific capacity . . . . .  | 46 |
| 2.4.10. Direct-current internal resistance and short-circuit<br>current . . . . .   | 47 |
| 2.4.11. AC internal resistance . . . . .  | 48 |
| 2.4.12. Impedance, impedancemetry, impedance<br>spectroscopy . . . . .  | 49 |
| 2.4.13. Stored energy and deliverable energy . . . . .  | 62 |
| 2.4.14. Gravimetric energy density . . . . .  | 63 |
| 2.4.15. Volumetric energy density . . . . .   | 64 |
| 2.4.16. Specific energy . . . . .   | 64 |
| 2.4.17. Gravimetric power and volumetric power . . . . .  | 65 |
| 2.5. Faradaic efficiency . . . . .  | 66 |
| 2.6. Self-discharge . . . . .   | 67 |
| 2.7. Acceptance current . . . . .   | 68 |
| 2.8. Conclusion . . . . .   | 69 |
| 2.9. Appendix 1: Nernst's law . . . . .   | 69 |
| 2.9.1. Redox potential of an electrode . . . . .  | 69 |
| 2.9.2. Electromotive force of an electrochemical cell . . . . .   | 70 |
| 2.9.3. Nernst's law . . . . .   | 71 |
| 2.9.4. Activity of the species . . . . .  | 73 |
| 2.9.5. Example of the application of Nernst's law to a lithium<br>secondary battery using the insertion mechanism . . . . . | 74 |
| 2.10. Appendix 2: Double layer . . . . .  | 78 |
| 2.11. Appendix 3: Warburg impedance . . . . .   | 79 |
| 2.12. Solutions to the exercises in Chapter 2 . . . . .   | 82 |

|  |                |
|--|----------------|
| <b>Chapter 3. Practical Examples Using Electrochemical Storage . . .</b>   | <b>89</b>      |
| 3.1. Introduction . . . . .  | 89             |
| 3.1.1. Starter currents for internal combustion engines<br>in cars . . . . .   | 89             |
| 3.1.2. Power required by a telecommunications transceiver<br>in an isolated site . . . . .                               | 94             |
| 3.1.3. House in an isolated site . . . . .   | 98             |
| 3.1.4. Currents in an operational electric car battery . . . . .   | 101            |
| 3.1.5. Currents during the phase of recharging of batteries<br>in electric cars . . . . .                                | 104            |
| 3.1.6. Autonomous urban lighting . . . . .   | 107            |
| 3.2. Conclusion . . . . .  | 109            |
| 3.3. Solution to the exercises in Chapter 3 . . . . .  | 110            |
| <br><b>PART 2. LITHIUM BATTERIES. . . . .</b>  | <br><b>115</b> |
| <b>Chapter 4. Introduction to Lithium Batteries. . . . .</b>   | <b>117</b>     |
| 4.1. History of lithium batteries . . . . .  | 117            |
| 4.2. Categories of lithium batteries . . . . .   | 121            |
| 4.3. The different operational mechanisms for lithium<br>batteries . . . . .   | 122            |
| 4.3.1. Intercalation (or insertion) materials . . . . .  | 122            |
| 4.3.2. Alloys . . . . .  | 123            |
| 4.3.3. Direction conversion materials . . . . .  | 128            |
| 4.3.4. Differences of voltage profiles between intercalation<br>materials, alloys and conversion materials . . . . .     | 129            |
| 4.3.5. Properties of the electrode materials . . . . .   | 130            |
| 4.4. Appendices . . . . .  | 131            |
| 4.4.1. Appendix 1: Examples of redox couples . . . . .   | 131            |
| 4.4.2. Appendix 2: Dendrites . . . . .   | 131            |
| 4.4.3. Appendix 3: Transition metals . . . . .   | 132            |
| <br><b>Chapter 5. The Basic Elements in Lithium-ion Batteries:<br/>Electrodes, Electrolytes and Collectors . . . . .</b> | <br><b>135</b> |
| 5.1. Introduction . . . . .  | 135            |
| 5.2. Operation of lithium-ion technology . . . . .   | 136            |
| 5.3. Positive electrodes. . . . .  | 138            |
| 5.3.1. Lithiated transition metal oxides . . . . .   | 138            |
| 5.3.2. Manganese oxide . . . . .   | 142            |
| 5.3.3. Lithiated iron oxyphosphate . . . . .   | 143            |

|   |            |
|---|------------|
| 5.3.4. Crystalline structures . . . . .   | 145        |
| 5.3.5. Mass capacities . . . . .  | 146        |
| 5.4. Negative electrodes . . . . .  | 146        |
| 5.4.1. Carbonaceous materials . . . . .   | 146        |
| 5.4.2. Other carbonaceous materials . . . . .   | 150        |
| 5.4.3. Lithium titanate oxide . . . . .   | 152        |
| 5.4.4. Electrochemical potentials . . . . .   | 156        |
| 5.4.5. Mass capacities . . . . .  | 156        |
| 5.5. Electrolyte . . . . .  | 158        |
| 5.5.1. Liquid electrolyte . . . . .   | 158        |
| 5.5.2. Polymer electrolyte . . . . .  | 160        |
| 5.6. Current collectors . . . . .   | 161        |
| 5.7. Conclusion . . . . .   | 162        |
| 5.8. Solution to exercises in Chapter 5 . . . . .   | 162        |
| <b>Chapter 6. Usual Lithium-ion Batteries.</b> . . . .  | <b>167</b> |
| 6.1. Principle of operation of conventional assemblies<br>of electrodes . . . . .   | 167        |
| 6.1.1. Principle of operation of a C-LiMO <sub>2</sub> element . . . . .  | 168        |
| 6.1.2. Principle of operation of a C-LiCoO <sub>2</sub> element . . . . .   | 168        |
| 6.1.3. Principle of operation of a C-LiFePO <sub>4</sub> element . . . . .  | 171        |
| 6.1.4. Principle of operation of a Li <sub>4</sub> Ti <sub>5</sub> O <sub>12</sub> -LiMn <sub>2</sub> O <sub>4</sub><br>element . . . . . | 173        |
| 6.1.5. Principle of operation of a Li <sub>4</sub> Ti <sub>5</sub> O <sub>12</sub> -LiFePO <sub>4</sub><br>element . . . . .              | 176        |
| 6.2. Major characteristics . . . . .  | 177        |
| 6.2.1. Voltage of an element . . . . .  | 178        |
| 6.2.2. Usage for “energy” or “power” . . . . .  | 179        |
| 6.2.3. Window of voltage explored . . . . .   | 181        |
| 6.2.4. Charge . . . . .   | 183        |
| 6.2.5. Safety management in cells . . . . .   | 187        |
| 6.2.6. Internal failures . . . . .  | 188        |
| 6.2.7. Operating temperatures . . . . .   | 189        |
| 6.2.8. Self-discharge . . . . .   | 189        |
| 6.2.9. Memory effect . . . . .  | 190        |
| 6.2.10. Commercially available capacities . . . . .   | 190        |
| 6.2.11. Dependency of the capacity on the discharge<br>current and the temperature. Peukert’s law . . . . .                               | 190        |
| 6.2.12. Gauges . . . . .  | 192        |
| 6.2.13. Practical gravimetric energy density . . . . .  | 198        |
| 6.2.14. Practical volumetric energy density . . . . .   | 202        |

|   |            |
|---|------------|
| 6.2.15. Plot of the gravimetric energy densities as a function of the volumetric energy densities . . . . . | 203        |
| 6.2.16. Gravimetric and volumetric power densities . . . . .  | 204        |
| 6.2.17. Faradaic efficiency of a charge/discharge cycle . . . . .   | 206        |
| 6.2.18. Energy efficiency of a charge/discharge cycle . . . . .   | 207        |
| 6.2.19. Average cycling lifetime . . . . .  | 210        |
| 6.2.20. Calendar lifetime . . . . .   | 210        |
| 6.2.21. Degradation phenomena. . . . .  | 214        |
| 6.2.22. Operational safety. . . . .   | 217        |
| 6.2.23. Transport and storage of lithium batteries. . . . .   | 219        |
| 6.2.24. Packaging. . . . .  | 221        |
| 6.2.25. Manufacturing procedures . . . . .  | 222        |
| 6.2.26. Energy cost throughout lifecycle . . . . .  | 226        |
| 6.2.27. Purchasing cost . . . . .   | 228        |
| 6.2.28. Manufacturers and suppliers/integrators. . . . .  | 228        |
| 6.2.29. Main outlets . . . . .  | 229        |
| 6.2.30. Recycling options. . . . .  | 230        |
| 6.3. Solution to exercises from Chapter 6 . . . . .   | 230        |
| <b>Chapter 7. Present and Future Developments Regarding Lithium-ion Batteries . . . . .</b>                 | <b>235</b> |
| 7.1. Improvement of the operation and safety of current technologies . . . . .                              | 236        |
| 7.1.1. Developments of advanced BMSs (Battery Management Systems). . . . .                                  | 236        |
| 7.1.2. Development of high-performance management systems . . . . .   | 238        |
| 7.1.3. Synthesis of new solvents . . . . .  | 239        |
| 7.1.4. Introduction of redox shuttle molecules to prevent over-charging . . . . .                           | 240        |
| 7.2. Improvement of the intrinsic performances (energy, power) . . . . .                                    | 244        |
| 7.2.1. Synthesis of new materials . . . . .   | 244        |
| 7.3. New formats of batteries. . . . .  | 252        |
| 7.3.1. Development of specific architectures: bipolar . . . . .   | 252        |
| 7.3.2. Development of thin and soft batteries . . . . .   | 253        |
| 7.3.3. Development of micro-batteries. . . . .  | 254        |
| 7.4. Conclusion . . . . .   | 255        |
| <b>Chapter 8. Lithium-Metal Polymer Batteries . . . . .</b>   | <b>257</b> |
| 8.1. Principle of operation. . . . .  | 258        |
| 8.1.1. Positive electrode. . . . .  | 259        |

|  |            |
|--|------------|
| 8.1.2. Negative electrode . . . . .  | 260        |
| 8.1.3. Electrolyte . . . . .   | 260        |
| 8.2. Manufacturing process . . . . .   | 260        |
| 8.3. Main characteristics . . . . .  | 261        |
| 8.3.1. Operating voltage . . . . .   | 261        |
| 8.3.2. Capacity . . . . .  | 261        |
| 8.3.3. Practical gravimetric energy density . . . . .                                | 261        |
| 8.3.4. Practical volumetric energy density . . . . .                                 | 262        |
| 8.3.5. Power . . . . .   | 262        |
| 8.3.6. Operating temperature . . . . .   | 262        |
| 8.3.7. Self-discharge . . . . .  | 262        |
| 8.3.8. Average cycling lifetime . . . . .  | 262        |
| 8.3.9. Recyclability . . . . .   | 262        |
| <b>Chapter 9. Lithium-Sulfur Batteries . . . . .</b>                                 | <b>263</b> |
| 9.1. Introduction . . . . .  | 263        |
| 9.2. The element Sulfur . . . . .  | 264        |
| 9.3. Principle of operation . . . . .  | 264        |
| 9.4. Discharge curve . . . . .   | 269        |
| 9.5. Advantages to Li-S . . . . .  | 270        |
| 9.6. Limitations and disadvantages of a Li-S battery . . . . .                       | 271        |
| 9.6.1. Positive electrode . . . . .  | 271        |
| 9.6.2. Electrolyte . . . . .   | 278        |
| 9.6.3. Negative electrode . . . . .  | 283        |
| 9.7. Conclusion . . . . .  | 285        |
| <b>Chapter 10. Lithium-Air Batteries . . . . .</b>                                   | <b>287</b> |
| 10.1. Introduction . . . . .   | 287        |
| 10.2. Operational principle . . . . .  | 289        |
| 10.2.1. Aqueous Li O <sub>2</sub> . . . . .  | 290        |
| 10.2.2. Organic Li-O <sub>2</sub> . . . . .  | 292        |
| 10.3. Electrolytes . . . . .   | 295        |
| 10.4. Main limitations . . . . .   | 297        |
| 10.4.1. General limitations . . . . .  | 298        |
| 10.5. Main actors . . . . .  | 304        |
| 10.6. Conclusion . . . . .   | 306        |
| 10.7. Appendix: calculation of theoretical gravimetric<br>energy densities . . . . . | 307        |



|   |     |
|---|-----|
| <b>Chapter 11. Lithium Resources</b> . . . . .  | 309 |
| 11.1. State of the art in terms of availability of lithium resources . . . . .          | 310 |
| 11.2. Comparison of resources with the needs of the electrical industry . . . . .       | 312 |
| 11.3. State of the art of extraction techniques and known production reserves . . . . . | 315 |
| 11.4. Nature and geological origin of all potential lithium resources . . . . .         | 318 |
| 11.5. Global geographic distribution of raw lithium resources . . . . .                 | 320 |
| 11.6. Evolution of the cost of lithium . . . . .  | 323 |
| 11.7. Summary . . . . .   | 325 |
| <b>PART 3. OTHER TYPES OF BATTERIES</b> . . . . .                                       | 327 |
| <b>Chapter 12. Other Types of Batteries</b> . . . . .                                   | 329 |
| 12.1. Introduction . . . . .  | 329 |
| 12.2. Sodium–Sulfur technology . . . . .  | 330 |
| 12.2.1. Operational principle . . . . .   | 330 |
| 12.2.2. Main characteristics . . . . .  | 333 |
| 12.3. Nickel chloride batteries . . . . .   | 335 |
| 12.3.1. Operational principle . . . . .   | 336 |
| 12.3.2. Main characteristics . . . . .  | 338 |
| 12.3.3. Availability . . . . .  | 339 |
| 12.4. Conclusions about high-temperature batteries . . . . .                            | 340 |
| 12.5. Redox flow systems . . . . .  | 340 |
| 12.5.1. Vanadium redox battery . . . . .  | 343 |
| 12.5.2. Operational principle . . . . .   | 343 |
| 12.5.3. Main characteristics . . . . .  | 345 |
| 12.5.4. Availability . . . . .  | 347 |
| 12.5.5. Other redox flow battery technologies . . . . .                                 | 349 |
| 12.5.6. Conclusion about redox flow batteries . . . . .                                 | 350 |
| <b>Conclusion</b> . . . . .   | 351 |
| <b>Index</b> . . . . .  | 353 |



## Preface

Whether for mobile, on-board or stationary applications, it is of crucial importance to have high-performing storage systems, whose manufacturing, use and recycling costs are reasonable and which offer good operational safety. In view of the extent of application domains, and of the diversity of usage profiles and technical/economic criteria which need to be satisfied, it is undeniable that no single technology can serve all these needs. The first part of this book (Chapters 1–3) outlines the storage requirements and the most widely-used technologies for each of these, the definitions used to characterize accumulators, and gives examples of the usage of electrochemical storage. The rest of the book describes the most recently introduced electrochemical secondary batteries<sup>1</sup>: lithium technologies and the most recent accumulators (redox-flow batteries, high-temperature batteries, etc.).

This book will show the reader that batteries are complex systems, whose successful commercialization has been the fruit of a great many projects in scientific research, empiricism and industrial know-how. The design of electrochemical accumulators has been the focus of a great deal of work, and sometimes compromise with a view to keeping them competitive and economically viable. Their design is not set in stone. Quite the opposite, in fact – it is constantly changing, thanks to feedback from experience on the ground, but at the cost of lengthy and painstaking validation testing, because the lifetimes are increasingly long and the laws of accelerated aging are not always usable or representative of real-life operation. We also wished to

---

<sup>1</sup> Lead and nickel-based electrochemical secondary batteries are described in detail in: C. Glaize and S. Geniès – Lead and Nickel Electrochemical Batteries, ISTE, London, John Wiley & Sons, New York, 2012.

demonstrate that it is not possible to consider a group of batteries as having fixed characteristics which are applicable regardless of the application and the technology used to manufacture them. For this reason, we made a quite deliberate choice to outline the fundamental electrochemical and chemical phenomena involved, as simply and clearly as possible, sometimes “by hand”. Indeed, we feel it is essential to have knowledge of these mechanisms in order to develop appropriate theoretical models and understand the possible applications for each technology.

The challenge for us was to explain how to choose and properly use an secondary battery for a given usage, without falling into the trap of merely giving a list of “recipes”. For this purpose, the reader needs to be given a detailed understanding of the function of secondary batteries and a description of their different (and often numerous) technological variants. This is not something which can be done in merely a few pages. Also, it is no easy task to give a pedagogical explanation of the electrochemical processes and the industrial constraints to readers with a background in electrical engineering, but who are not specialists in electrochemistry.

We have not neglected always keeping sight of the economic approach which is important when choosing between different storage possibilities. In addition, although we have tried to make this book as complete as possible and present the maximum possible number of examples, we of course make no pretense of exhaustivity, and no claim of having flawless understanding (the secondary reactions that take place in the oldest accumulators are not all completely elucidated and therefore *a fortiori*, neither are those of the most recent technologies, which are still subject to diverse and sometimes contradictory explanations). We have cited a great many academic publications, because development has never ceased, even on the commercialized lithium secondary batteries, and the more recently introduced technologies are far from finished. Finally, the data presented (particularly technical-economic data) are those which were available at the time of writing, commenced in 2010 and completed in early 2013. With the advancement of research and development in the field of storage, compounded by the performance requirements for electric vehicles and the storage of electricity – be it of renewable or non-renewable origin – batteries will certainly continue to evolve rapidly in years to come. Hence, this point must be borne in mind.

Christian GLAIZE and Sylvie GENIÈS  
June 2013

## Acknowledgements

The writing of this book was punctuated by numerous and enriching scientific discussions – between ourselves but also and above all the discussions we have had with fellow researching university professors, researchers, doctoral candidates and industrial partners. In naming all these people (listed below in alphabetical order), we wish to extend to them our heartfelt thanks for their availability and the time which they have given us. Their knowledge, experience and skills have greatly enriched this book and have advanced our own knowledge of accumulators.

Thanks go, therefore, to Jean-Jacques Huselstein, Thierry Martiré, Laure Monconduit, Lorenzo Stievano and Yaël Thiaux, who are researchers and teaching researchers at the Université Montpellier II; to Loïc Goemaere and Adrien Soares, who at the time were doctoral candidates at the Université Montpellier II; to Yann Bultel, Professor at the Institut National Polytechnique de Grenoble; and to Bernard Multon, Professor at the Ecole Normale Supérieure de Cachan and the commissioning editor of this series of books. At CEA-Liten, thanks go to the researchers Mélanie Alias, Philippe Azaïs, Céline Barchasz, Florence Fusalba, Frédéric Le Cras, Sébastien Patoux and Marion Perrin, and to Charles Gayot, Camille Grosjean, Jérémie Jousse, and Mathieu Quenard, who were doctoral candidates and some of whom have now obtained their doctorates. Our thanks to Benoît Connes and Matthieu Prigent from Phaesun France, and to Jean-Pierre Belliard at Novéa Energies.

To those to whom we owe thanks but who are not explicitly thanked above, we beg forgiveness for this unintentional oversight. These people know who they are.

Christian GLAIZE and Sylvie GENIÈS

On a personal note, I would like to express my gratitude to Jean Alzieu, who is a fount of scientific knowledge and innovative ideas, who introduced me to the world of electrochemistry. Further thanks go to Josette Fourcade, Jean-Claude Jumas, Laure Monconduit and Lorenzo Stievano, who then introduced me to the domain of lithium accumulators.

Christian GLAIZE

And now to you, the reader: enjoy this book!

## Introduction

Since the presentation of the lead-acid electrochemical accumulator by Gaston Planté at the French *Académie des Sciences* in 1859, many other material couples for the purpose have emerged. Some have been abandoned or are very underdeveloped, because a number of disadvantages have not been completely resolved, rendering the technology insufficiently viable.<sup>1</sup> Others have endured, such as nickel-cadmium (NiCd), introduced in 1899 by the Swede Waldemar Jungner (1869–1924) and developed primarily by Edison. Yet it was not until 1947 that Neumann succeeded in making the battery completely sealed, giving us the modern nickel-cadmium battery. The new generations of batteries are mostly sealed, either by obligation (lithium, NaS, chlorides, redox flow batteries, etc.) or to limit the need for maintenance.

The description of these different types of batteries is important, because the criteria for choosing a technology appropriate for a given application do not depend solely on the mass energy or the cost per kWh stored, as we might be led to think on the basis of the most commonplace analyses. There are other factors to be considered, such as the lifetime, the type of cycling, safety, etc. Therefore, this book will begin with a chapter which will show the diversity of applications for batteries and the main characteristics

---

<sup>1</sup> For instance, the nickel-iron battery, invented almost at the same time (Edison, 1901) as the nickel-cadmium battery, has a poor charge efficiency, which causes excessive heating and hydrogen release. Another example is nickel-zinc technology, for which further study seems necessary, because it is subject to the formation of dendrites which limit its lifetime.

required of them in terms of storage. This first chapter will also demonstrate the diversity of the levels of current summed and energy stored (from the few mWh of a lithium battery in a wristwatch to the tens of MWh electricity storage for grid support), and also the diversity of the durations of discharge (which can range from a few minutes for emergency supply for computers to hundreds of hours to preserve data in an electronic device). Thus, it is clear that no single type of accumulator can serve for such diverse applications. Already, with lead and then nickel accumulators, there were different technologies to choose from, but the elements introduced recently – particularly lithium-based solutions – offer a far broader range of different technologies.

After a second chapter which presents the definitions and measuring methods used in the world of electrochemical storage, and a third which gives examples of the applications of batteries, in the rest of this book we propose to describe the electrochemical cells developed recently (end of the 20<sup>th</sup> Century) which are now being commercialized, as well as those whose future looks bright. We shall begin with lithium secondary batteries (Chapters 4–10). Then, in Chapter 12, we shall describe high-temperature technologies (sodium/sulfur (NaS), ZEBRA and chlorides) and redox flow systems.

We shall also touch upon the increasing rapid evolution of the technologies, particularly as regards lithium batteries, for which the avenues of research are extremely varied. The substance couples used in tomorrow's world will probably be different to those widely used today. These advances will be discussed in Chapter 7 for lithium-ion elements. Then we shall go on to describe the promising lithium-sulfur batteries (Chapter 9) and lithium-air cells (Chapter 10).



PART 1

Storage Requirements  
Characteristics of Secondary  
Batteries Examples of Use



## Chapter 1

# Breakdown of Storage Requirements

### 1.1. Introduction

Electrochemical electricity storage has been in use for as long as electricity has been industrially used. The earliest secondary battery was introduced by Gaston Planté in 1859, i.e. between the first laboratory primary battery created by Alessandro Volta in 1800 and the industrial dynamo from Zénobe Gramme in 1869.

### 1.2. Domains of application for energy storage

Energy storage systems are used in many fields of application. Each of these domains is characterized by specific operational profiles and, consequently, different types and technologies of secondary batteries. They are described below.

Of the major domains of application, we might cite:

- starter batteries;
- traction batteries and on-board batteries;
- stationary deep cycle batteries (batteries for storage in decentralized microgrids with photovoltaic generation, for grid support, etc.);

– standby power batteries (batteries for uninterruptible power supply, for safeguarding information, etc.);

– and, more recently, batteries for mobile devices: portable computers and mobile telephones – in billions of units produced each year – digital cameras, audio and video players, camcorders, PDAs (Personal Digital Assistants), etc.

### **1.2.1. Starter batteries**

Better known as “SLI” batteries (for “Start, Lighting and Ignition”), these batteries are used to fire up internal combustion engines (in cars and trucks but also tractors, electrogen groups, or even boats or airplanes, etc.) as well as to provide lighting and many other functions. These batteries have an average specific energy<sup>1</sup> and a low cost.

The profile of the current entering<sup>2</sup> into an SLI battery, and the evolution of the state of charge (SOC, defined in section 2.4.2) are shown qualitatively below (Figure 1.1). Typically, car batteries have a nominal voltage of 12 V. Their capacity is usually between 40 and 80 Ah. Start currents can reach up to several hundred amperes.<sup>3</sup> Measured values are given in section 3.1.1.

In a car with a combustion engine, the battery only supplies energy when the engine is not running, or is running at a slowed speed. When the vehicle is moving, it is the alternator which supplies the demands. When the battery is supplying energy, it is usually quickly recharged by the alternator, and is therefore subjected only to a microcycle. Conversely, in certain trucks, the battery may have to supply certain functions such as the raising/lowering of an unloading tailgate, a refrigeration group, a crane, etc. The battery is then subject to deeper discharges (Figure 1.2).

---

1 Volume energy or mass energy: the ratio of the energy stored to the volume or mass (see section 2.4.9).

2 Here we choose to work with receiver convention, meaning that the current entering at the positive terminal of the battery, i.e. the current that recharges the battery, is counted positively.

3 For motorcycles, we find 6 V and 12 V batteries. The capacities range from a few Ah to over 30 Ah.

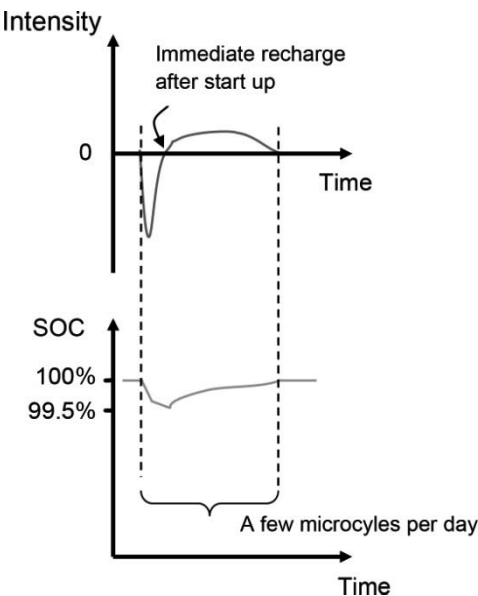


**Figure 1.1.** Car SLI battery: profile of the current flowing into the battery and change in its SOC

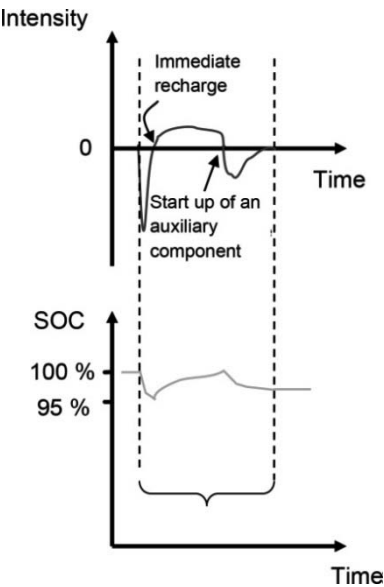


**Figure 1.2.** SLI battery for a truck with auxiliary functions: profile of current entering into the battery and evolution of its SOC

### 1.2.2. Traction batteries

Traction batteries are used in forklift trucks, handling and lifting machines, wheelchairs, electrically assisted pedal cycles (EAPCs), electric vehicles (EVs) or hybrid electric vehicles (HEVs), golf buggies, etc. These applications require power to be supplied to the engine but also need sufficient energy to deliver a range (capacity for autonomous operation) which is compatible with their usage.

#### 1.2.2.1. Vehicle batteries without brake energy recovery

The slow speed of certain electrically-motorized vehicles means that, even if the electric power chain is capable of it, kinetic energy is not recovered during braking. Such is the case with many handling and lifting machines, wheelchairs, EAPCs, etc.<sup>4</sup>

For these vehicles, the profile of current running into the battery and the evolution of the SOC are shown in Figure 1.3. They are used in a simple cycle: a discharge of greater or lesser depth, followed by a complete charge. The periods of discharging and charging are thus clearly distinct.

EAPCs have batteries of 24, 36 or 48 V and a capacity of around ten Ah. The batteries used for wheelchairs are generally 12 or 24 V, with capacities of up to a few tens of Ah (usually 20–40 Ah). For handling vehicles such as forklift trucks, several 6 or 12 V batteries are connected in series, with unitary capacities of several hundred Ah.

For this type of application, the technology needs to be adapted: we favor electrode/electrolyte interfaces which offer the largest possible exchange surfaces so as to be able to supply and receive a significant peak power. However, for each application, there is a compromise to be found between the peak power and the stored energy (an explanation of the difference between “energy” batteries and “power” batteries is given in section 5.2.2).

---

<sup>4</sup> Motorization by a direct-current (DC) engine and a non-reversible chopper used to be the most widely-used solution. In more modern vehicles, an induction motor is installed, supplied by an inverter. Both the induction motor and the power part of the inverter are naturally reversible, but as yet this possibility has not always been built into the inverter control.

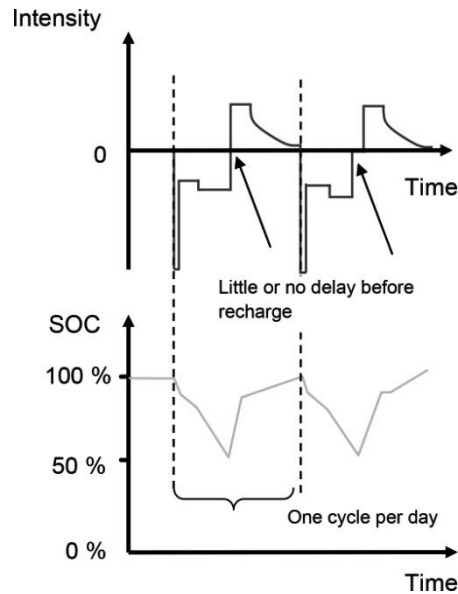


**Figure 1.3.** *Traction battery: profile of current entering into the battery and evolution of its SOC*

#### 1.2.2.2. *Vehicle batteries with brake energy recovery*

Electric or hybrid cars use batteries whose sizing and design are appropriate to supply the power and/or energy needs to respond to the different usage profiles. In contrast to the applications discussed above, energy is recovered by the battery on braking. Current peaks appear during the phases of braking. The same is true of golf buggies, electric karts, etc. To set these apart from the previous uses, we sometimes find the term “on-board batteries”.

Three usage profiles can be defined for operation in a hybrid vehicle, a hybrid plug-in vehicle (i.e. a rechargeable hybrid) or a pure electric vehicle.

##### 1.2.2.2.1. *Hybrid vehicle batteries*

Generally speaking, the batteries fitted to a hybrid vehicle tend to be sized for power, because they need to be capable of providing peaks of power during acceleration and being recharged with high intensities during braking. They play the role of an energy buffer between the primary energy source – the combustion engine – and the vehicle’s running needs. The

excursion of the depth of discharge (DOD, see section 2.4.1) is therefore very limited. In order to prevent too high or too low a state of charge (SOC, see section 2.4.2), which may be damaging for the NiMH batteries used, the charge oscillates by a few % around an average state of charge between 40 and 80% (54-56% for the Toyota Prius 2001 in hybrid operation<sup>5</sup>) (Figure 1.4). In the Toyota Prius and the Honda Insight, even with fully electrical operation, the battery management system (BMS) prevents the battery from discharge below a ~40% SOC or from reaching complete charge.

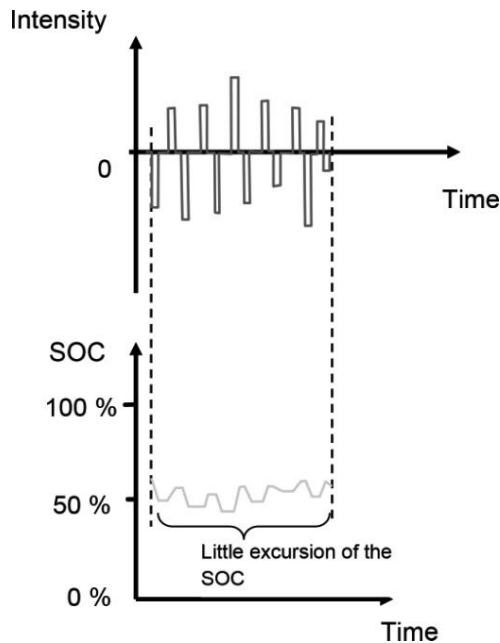


**Figure 1.4.** *Profile of current entering into the battery and evolution of the SOC for a battery in a hybrid vehicle*

#### 1.2.2.2.2. “Plug-in” hybrid vehicle batteries

For batteries in hybrid vehicles which can be connected to the electrical grid to be recharged (plug-in), the battery can be subjected to a deeper

<sup>5</sup> K.J. KELLY, M. MIHALIC, M. ZOLOT (National Renewable Energy Laboratory), “Battery usage and thermal performance of the Toyota Prius and Honda Insight during chassis dynamometer testing”, *The Seventeenth Annual Battery Conference on Applications and Advances*, Long Beach, California, 14–18 January 2002.



discharge, because additional recharging from the grid is possible, provided there is a charge point nearby. The batteries have to be able to withstand charge/discharge cycles over a broader range of SOC's used than in the case of batteries for hybrid vehicles (Figure 1.5).

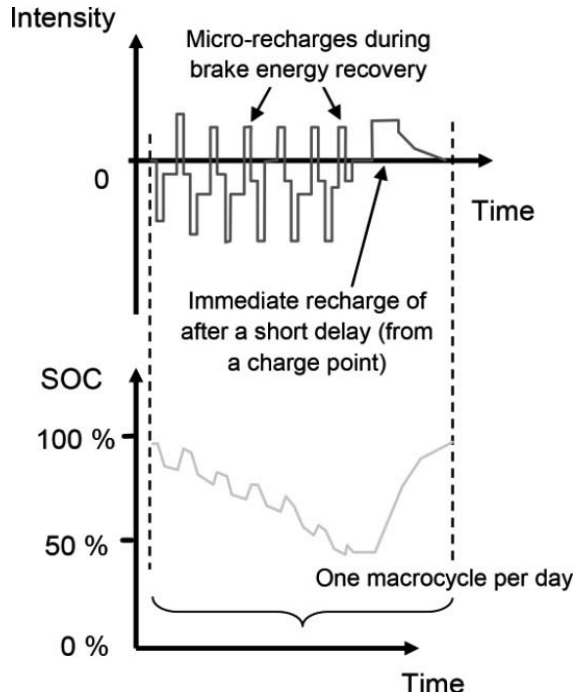


**Figure 1.5.** Profile of current entering into the battery and evolution of its SOC for a battery in a plug-in hybrid vehicle

#### 1.2.2.2.3. Batteries for all-electric vehicles

The batteries used for an all-electric vehicle tend to be sized for energy (significant capacity) in order to ensure a sufficient range. They undergo a cycle of complete charge and deep discharge nearly every day (see Figure 1.6) and must be designed for such a cycle.

Today, whilst some EVs are to be found which are equipped with lead batteries or ZEBRA batteries (described in Chapter 12), most production uses lithium-ion or lithium polymer metal batteries.

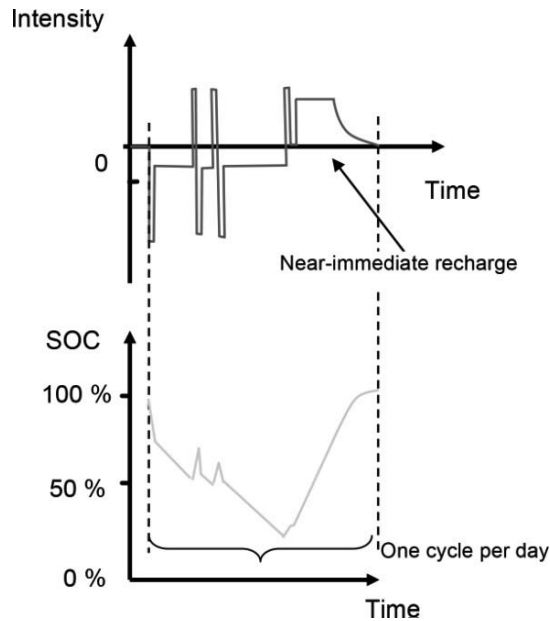


**Figure 1.6.** Profile of current entering into the battery and evolution of its SOC for an onboard battery in a fully-electric vehicle

### 1.2.3. Stationary batteries

Stationary batteries are used in very varied applications: Uninterruptible Power Supply (UPS), memory saving, decentralized power supply, grid support, etc.

#### 1.2.3.1. Batteries for autonomous supply

Autonomous supply batteries are usually used when no other source of electricity is available. They are specifically developed to perfectly supply the required cycling profiles. The most apt example is the application of solar power at stand-alone sites, supplying electricity requirements in places far from electrical networks (chalets, mountain shelters, telecommunications outposts, highway information panels, weather stations, etc.).

For a domestic application, the profiles of current entering into the battery and the evolution of the SOC are illustrated diagrammatically in Figure 1.8 and given quantitatively in section 3.1.3.

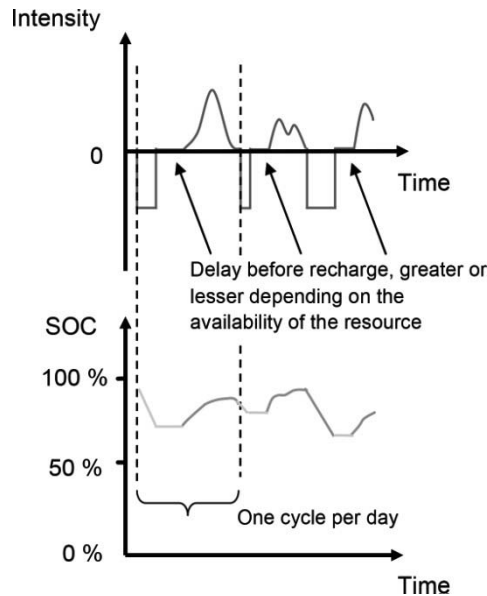


**Figure 1.7.** *Decentralized domestic power supply battery for an isolated site: profile of current entering into the battery and evolution of its SOC (in reality, the discharge currents have more complex profiles)*

Applications such as transmitters for cellphone networks (BTS: Base Transceiver Station) require a far more regular power supply throughout the day and even throughout the year. For the sizing of a transceiver in an isolated site, we assume a constant power requirement of a few kW. The capacity of the battery is calculated on the basis of the level of sunshine the site receives, the desired level of autonomy in case of lack of sun (e.g. five days or only two or three if the power supply is backed up by an electrogen group). Figure 1.8 shows the profile of current entering into the battery for a purely solar power supply, and the evolution of the SOC. Real-life data are given in section 3.1.2.

However, we can also use autonomous supply in urban areas (street furniture) in order to limit installation and operational costs. Such is the case for many parking meters or streetlamps, whose power is supplied by photovoltaic cells and batteries, preventing the need to dig trenches to lay electrical cables and then resurface the sidewalks. This autonomous power supply also enables us to avoid having to hire an energy meter, the cost of which may be greater than the energy consumed.

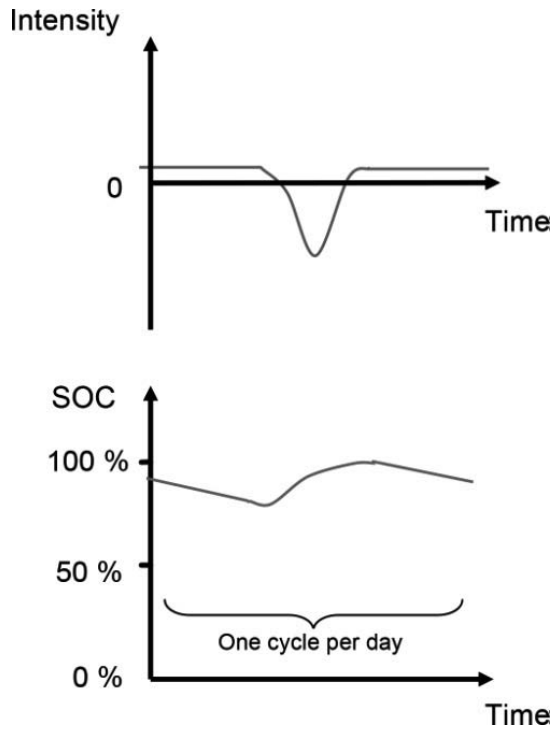
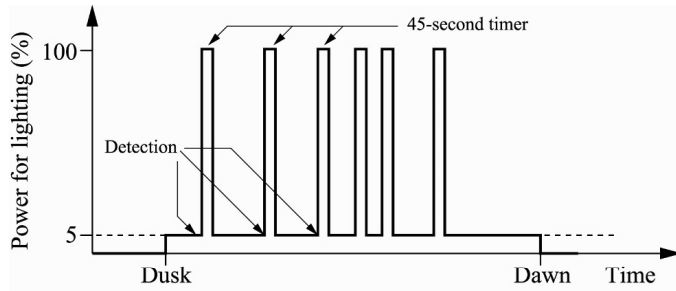


**Figure 1.8.** *Battery supplying a telecommunications transceiver on an isolated site: profile of current entering into the battery and evolution of its SOC*

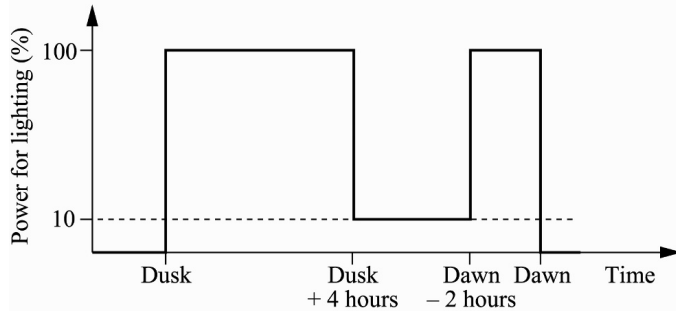
With recent urban lighting installations, there have been attempts to decrease energy bills and light pollution during the night. Decreasing energy consumption is even more crucial in autonomous urban lighting with a view to minimizing the size of the battery and those of the photovoltaic modules. For this purpose, the level of lighting is modulated depending on the time and the presence or absence of pedestrians or vehicles. Examples of the profiles of current required from the battery are shown in Figure 1.9.

A real-world example of the current and voltage for an autonomous urban lighting application is given in section 3.1.6.

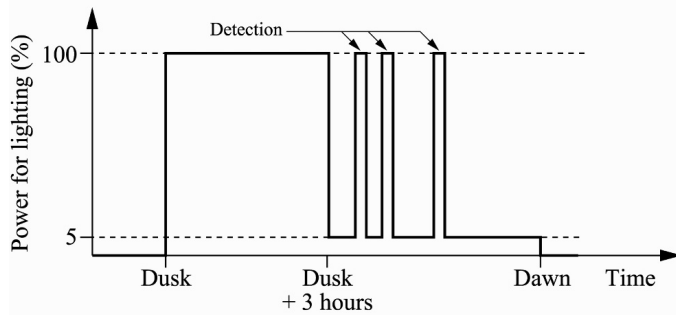
In an entirely different domain, electricity is supplied to pleasure boats by batteries which are recharged by the alternator of the engine and/or solar panels and/or a wind/water turbine. One might also cite gadgets such as garden lights, pocket torches, etc.



a) Presence detection



b) Maximum (&gt; 6 hours per night) + Reduction of light intensity



c) Maximum for 3 hours + detection

**Figure 1.9.** Power required of the battery of a streetlamp  
(source: Novéa Energies – [www.novea-energies.com](http://www.novea-energies.com))

### 1.2.3.2. Batteries for grid support

Nowadays, the increase in the number of renewable energy systems connected to the electrical grid (solar or wind systems, for instance) makes it more difficult to manage the grid because of the intermittence and variability of production, and because of its unpredictability or prediction errors.

Studies are being carried out and prototypes tested to evaluate the advantage of integrating storage systems into these grid-connected systems, which would help improve the planning of production means, optimize the global energy efficiency of the system and shift the bulk of energy provision to times when the need is greatest.

However, the issue of the stability of power supply grids is not a new one. Electrochemical systems for energy accumulation have been installed on the grid for over 20 years, with lead-acid or nickel-cadmium batteries. More recently, we are witnessing a significant development of sodium-sulfur batteries (which are discussed in detail in Chapter 12). Experiments have been performed with redox flow systems (also detailed in Chapter 12). The unitary powers range from several MW to several tens of MW, and the quantities of energy stored from several MWh to tens of MWh.

Various configurations have been studied, with very different usage profiles, owing to their time constants: smoothing or elimination of the peaks, smoothing of daily consumption<sup>6</sup>, injection into the grid on demand from a distributor, etc. Hence, batteries of very different technologies are capable of responding to the functional requirements.

The profiles of the current entering into the battery and the evolution of its SOC are given in Figure 1.10.

#### 1.2.3.3. *Uninterruptible power supply batteries*

Uninterruptible power supply batteries<sup>7</sup> are used for communication networks, computers and IT centers, nuclear power plants, etc. They are able to respond to peak power or energy requirements as a function of the reliability of the grid which they are stabilizing. They take over in case of failure of the electricity supply grid, providing power (DC or AC power depending on the application) over a greater or lesser duration (around fifteen minutes for the safeguarding of data and shutdown of a domestic or

---

<sup>6</sup> Interseasonal storage by electrochemical batteries is difficult to envisage with the current technologies or those which should emerge in the near future.

<sup>7</sup> Often incorrectly called “inverters” in ICT-specific language. Indeed, the core of an uninterruptible power supply is constituted by an energy storage device: an electrochemical battery. This battery is kept in the fully-charged state by a charger. If the electrical grid fails, an inverter takes the energy stored in the battery and supplies it as an alternative form (AC) to the charge.

office computer<sup>8</sup>, or up to several hours for strategic applications).<sup>9</sup> These batteries are usually maintained in a fully charged state by a so-called “floating” current<sup>10</sup>, which compensates for self-discharge. Thus, they are fully charged for whenever they are called upon, given that that moment is not predictable. These batteries are identified by the term “floating batteries”.

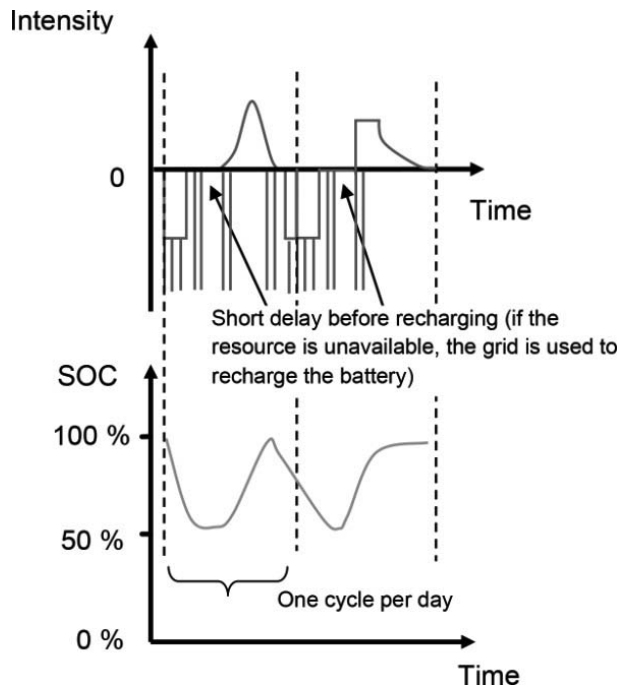


**Figure 1.10.** *Electricity supply battery connected to the grid for the smoothing or elimination of consumption peaks: profile of current entering into the battery and evolution of its SOC*

In the category of emergency supply batteries, we also find illuminating safety signage. If the general lighting grid fails, these devices (called

<sup>8</sup> Such inverters deliver between one and several hundred watts. They use 12, 18 or 24 V batteries of a few Ah.

<sup>9</sup> With a view to limiting the size of the batteries, we can use an electrogen group. The battery serves as a power supply until the electrogen group is able to start up and take over.

<sup>10</sup> This term stems from the fact that it is a voltage to which the battery is subjected, and the current fluctuates depending on the temperature, the age of the battery, etc.

Standalone Emergency Lighting Units – SELUs) are able to offer sufficient lighting with autonomy of at least an hour to prevent panic and indicate the emergency exits. The battery used is also floating.

With chargers controlled by a microcontroller, there are other types of charge which are more elaborate than floating and which help extend the lifetime of the batteries, decrease maintenance operations and ensure that the batteries are indeed capable of providing the necessary energy if and when required.

The profile of current entering into the battery and the evolution of its SOC are shown in Figure 1.11.

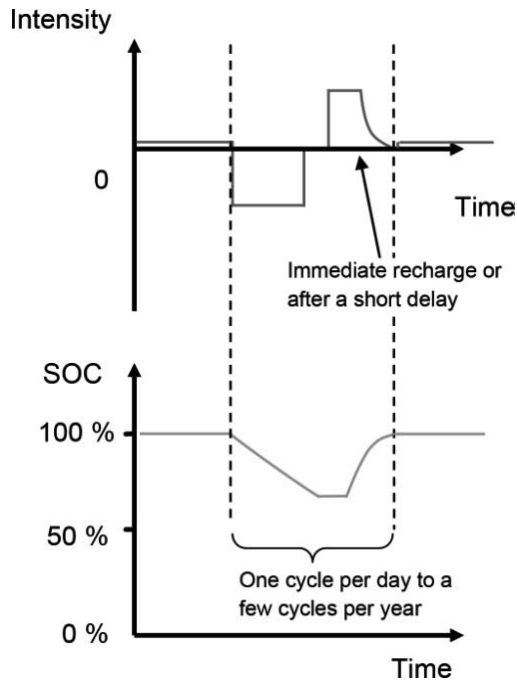


**Figure 1.11.** *Emergency power supply battery: profile of current entering into the battery and evolution of its SOC*

#### 1.2.3.4. Batteries for memory- and data saving

In the same category of ideas but with extremely low powers and energies, we can cite memory-saving or the operation of the internal



timekeeper in computers or, indeed, no-primary-battery watches (such as the Casio range of photovoltaic watches or the Seiko Kinetic®) or other systems requiring some of the electronic components to be powered between the normal operating times. In such cases, an element of a few mAh is used, because the power required is a few  $\mu\text{W}$ .

#### 1.2.4. Batteries for mobile or nomadic devices

The design of high-specific-energy batteries facilitated the rapid advent of mobile or nomadic devices. These batteries are used to supply energy to mobile equipment: cellular and wireless telephones, computers, music players, digital cameras, video players, cameras, games consoles, wireless tools, and so on) requiring excellent performances in terms of power, volume- and mass energy and cyclability.

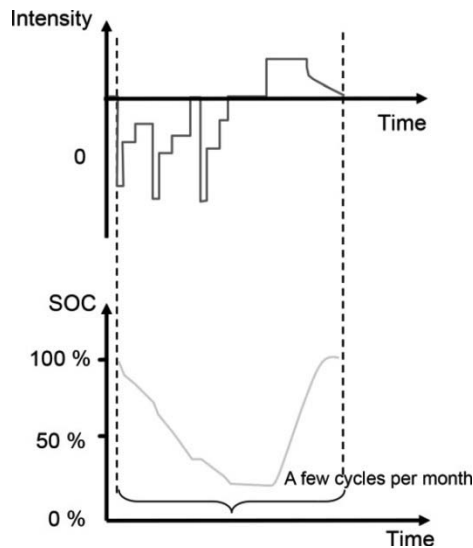


**Figure 1.12.** Battery for a nomadic device: profile of current entering into the battery and evolution of its SOC

The profile of current entering into the battery and the evolution of its SOC are illustrated in Figure 1.12. In many such applications, we see a succession of periods of slow discharge and periods of rapid discharge. Such is the case, for instance, with a cellphone which goes from standby or receiver mode – which are not particularly energy-hungry – to transmission

mode, which requires a significant power level. The batteries of nomadic devices function in cycling mode (conversation for a cellphone, autonomous operation for a computer, etc.) and then are charged from the mains where they may remain plugged in for long periods of time. For these low-power devices, the management of the charge is usually entrusted to specialized integrated circuits.

### 1.3. Review of storage requirements and appropriate technologies

Table 1.1 shows different domains which require electricity storage. We have indicated the different battery technologies used or envisaged for each of these domains, on the basis of technico-economic requirements.

|          | Examples of application   | Characteristics important for the design                 | Technologies used or envisaged   |
|----------|---|--|--|
| SLI      | Automobiles, electrogen groups, etc.                                      | Cost, W/kg<br>no maintenance                             | Fine-plates flooded lead-acid  |
|          | Trucks, tractors, etc.  | Cost, W/kg, Wh/kg  | Flooded lead-acid  |
|          | Boat engines  | Cost, W/kg, Wh/kg  | Sealed lead-acid.<br>Lithium-ion   |
| Traction | Handling machinery, wheelchairs, electrically-assisted pedal cycles, etc. | Cost, Wh/kg  | Tubular-plate flooded lead-acid.<br>Reinforced flat plate flooded lead-acid.<br>VRLA <sup>11</sup> . Lithium polymer |
|          | Electric vehicles: cars, scooters, golf buggies, go-karts                 | Wh/kg, Wh/L, W/kg, cyclability, little or no maintenance | Flooded lead-acid or VRLA.<br>NiCd, NiMH.<br>Lithium-ion   |
|          | Hybrid vehicles   | Wh/kg, W/kg, no maintenance                              | NiMH   |
|          | “Plug-in” hybrid vehicles   | Wh/kg, W/kg, no maintenance                              | NiMH.<br>Lithium-ion   |
|          | “All-electric” vehicles   | Wh/kg, Wh/L, W/kg, little or no maintenance              | (Lead).<br>Lithium-ion.<br>Lithium metal polymer   |

**Table 1.1.** *Certain storage requirements and the appropriate technologies*

---

<sup>11</sup> Valve-Regulated Lead–Acid battery.

|                       |   |  |   |
|-----------------------|---|--|---|
| Stationary            | Inverters for grid support<br>Emergency lighting  | W/kg, lifetime in a floating regime                | Sealed lead.<br>NiCd  |
|                       | Storage for autonomous energy systems (solar, wind, telecommunications, pleasure boating) | Wh/kg, cyclability with no maintenance             | Open-circuit lead.<br>VRLA.<br>NiCd.<br>Lithium-ion             |
|                       | Storage for grid-connected energy systems   | Cost   | VRLA.<br>Sodium-sulfur.<br>Lithium-ion.<br>Redox flow batteries |
| Mobile                | Mobile devices<br>Wireless tools<br>Autonomous vacuum cleaners<br>Memory preservation     | W/kg, Wh/kg, Wh/L, cyclability with no maintenance | (NiCd <sup>12</sup> ).<br>NiMH.<br>Lithium-ion                  |
| Aeronautics and space | Autonomous onboard grid   | Wh/kg, cyclability with no maintenance             | NiCd.<br>Lithium-ion  |

**Table 1.1.** (Continued) Certain storage requirements and the appropriate technologies

## 1.4. Conclusion

Electricity storage requirements are extremely varied, both because of the applications and the amount of energy stored and because of the ways in which that charge is exploited. From data-saving in an electronic device which requires a few mWh with very slow discharge; to grid support which requires storing dozens or even hundreds of MWh<sup>13</sup>; to mobile telephones

<sup>12</sup> Replaced by NiMH batteries, and now, increasingly often, by lithium-ion technology.

<sup>13</sup> Gravity-based hydraulic storage (pumped storage (hydroelectric) power plants: PSP), is capable of storing an even greater quantity of energy (several tens of GWh). Although this is the device which is capable of storing the largest amount of electrical energy, the principle behind its operation is not electrochemical. Therefore, it will not be discussed in this book. Nor will this book deal with flywheel storage or SMES: Superconducting Magnetic Energy Storage, which – besides capacitors – is practically the only device for quasi-direct electricity storage.

By way of indication, the following figures recorded in 2012 reflect the installed powers the world over for the different storage technologies:

PSP: 140,000 MW;

Compressed Air Energy Storage (CAES): 477 MW;

NaS batteries: 400 MW;

Lead batteries: 45 MW;

Lithium batteries: 45 MW;

Nickel-cadmium batteries: 40 MW;

Redox flow systems: 3 MW.

(a few Wh), portable computers (a few tens of Wh), batteries for combustion-engine cars (a few hundred Wh and very intense peaks of current); electric vehicles (a few kWh to several tens of kWh) – there is no single form of technology that is capable of serving such a vast range of applications. Today, there are many different families of batteries coexisting. Lead and nickel technologies were examined in a previous book.<sup>14</sup> This book deals with recently-introduced technologies such as lithium batteries (Chapters 4–10), hot cells and redox flow systems (Chapter 12). Electricity storage by an “electrolyzer + hydrogen storage + fuel cell” system is not dealt with in this book, because another book<sup>15</sup> is devoted to the topic.

Before going on to give quantified real-world examples of applications using batteries (Chapter 3), it is necessary to lay down a number of definitions and measuring methods. This is the aim of the next chapter.

---

<sup>14</sup> Lead and nickel-based electrochemical secondary batteries are described in detail in: C. GLAIZE & S. GENIÈS, *Lead and Nickel Electrochemical Batteries*, ISTE Ltd, London, John Wiley & Sons, New York, 2012.

<sup>15</sup> M.C. PERA, D. HISSEL, H. GUALOUS, C. TURPIN, *Electrochemical Components*, ISTE Ltd, London, John Wiley & Sons, New York, 2013.

## Chapter 2

# Definitions and Measuring Methods

### 2.1. Introduction

This chapter defines the most commonly-used terms to express the electrical characteristics of secondary batteries. These terms will be employed very frequently in the following chapters, so it is helpful to master them. Professionals in the domain use them so often that they have become part of their everyday speech. However, it is by no means unimportant to recap them and specify their meaning.

Beyond definitions, we shall also present methods for measuring these characteristics – particularly those stemming from testing techniques and standards.<sup>1</sup>

### 2.2. Terminology

Before going into technical considerations, with a view to preventing all ambiguity later on, it is necessary to clearly define the objects with which we are going to be working. It is crucial to properly grasp the difference between terms such as primary and secondary batteries or anodes and cathodes.

---

<sup>1</sup> Citations from standards are deliberately simplified to give the principle of the measurements. It is vital that readers consult each standard in order to gain an accurate picture of the actual test procedures which give us the measurement.

### 2.2.1. *Accumulator*

An “accumulator” stores (accumulates) energy, converting electrical energy<sup>2</sup> into a form of chemical energy, and then gives it back at any moment, as required. Thus, an accumulator can be viewed as a reversible generator. In English, it is usually called a secondary battery, as opposed to a primary battery which, with certain exceptions, is not rechargeable.

### 2.2.2. *Element, elementary cell, electrolyte*

A battery element or elementary cell comprises two electrodes immersed<sup>3</sup> in an electrolyte.<sup>4</sup> <sup>5</sup> For instance, in a very common lithium-ion secondary battery, these two electrodes are made of a lithiated metal oxide and carbon.

Usually, the electrodes are in the solid state and the electrolyte is in the liquid<sup>6</sup> or gelled state. Conversely, in sodium-sulfur secondary batteries

---

2 The term “energy” covers two physically distinct notions:

- potential energy, kinetic energy (and many other forms of energy) which are state variables. For example, the level of water behind a hydraulic dam can be used to calculate the potentially transformable energy;

- for electricity, as well as the energy which can be stored in an inductor or a capacitor and which is of the same nature as the previous definitions, the term “energy” also refers to the integration of electrical power over a given period of time. For instance, it is represented by the difference between two readings taken from an electricity meter. Thus, it is no longer a state variable. Rather, this would be referred to as the work of the electricity vector.

Confusion often arises, because these two entities are expressed in terms of the same unit: the Joule (or, more commonly, the kWh).

3 The term “immersed” is used for historical reasons because, in the first secondary battery (lead secondary battery introduced by Gaston Planté in 1859) and all those for almost a century afterward, the electrodes were immersed in a liquid electrolyte (dilute sulfuric acid or potassium, for instance). Nowadays, the electrolyte can also impregnate a solid matrix, or be solid itself.

4 Electrolyte: substance or compound which facilitates the passage of an electric current by the movement of ions. This term was coined by British physicist Michael Faraday in 1834 (“many bodies are decomposed directly by the electric current... these I propose to call electrolytes”), from the particle “*electro*” + *lyte* from the Greek *λύτος* [*lytos*], meaning “that which can be split”). See [www.cnrtl.fr/etymologie/%C3%A9lectrolyte](http://www.cnrtl.fr/etymologie/%C3%A9lectrolyte).

5 More generally, the space between the electrodes could be referred to as the “ion exchange zone”, which – depending on the technology in question – is given the name “electrolyte” or “membrane”.

6 In lithium secondary batteries, the liquid electrolyte impregnates a porous separator. If the enclosure is broken, there is a danger of the liquid leaking.

(see Chapter 9), the electrodes are liquid and the electrolyte is a ceramic (solid). In lithium-air batteries (Chapter 10), one of the two electrodes is a gas. In a redox flow system (Chapter 12), the electrolyte and electrodes are combined as one: the materials for the electrodes are diluted in the electrolyte and separated by a solid separating membrane. In the interests of exhaustivity, note also that there are some secondary batteries wherein all the components are in liquid phase.<sup>7</sup> Such secondary batteries were introduced by D. Sadoway and his team at MIT (Massachusetts Institute of Technology, USA). The negative electrode is molten magnesium, the electrolyte is a mixture of magnesium-, potassium- and sodium chlorides ( $\text{MgCl}_2$ ,  $\text{KCl}$  and  $\text{NaCl}$ ) and the positive electrode is made of antimony, also molten. This secondary battery operates at high temperature ( $700^\circ\text{C}$ ). The immiscibility of these three substances gives rise to a natural stratification into three distinct layers. The tests are carried out with current densities in the cells ranging from 50 to  $200\text{ mA/cm}^2$ , and show an energy efficiency of 69%. The advantage of this system is the low cost of the materials. On the other hand, antimony is toxic.

### 2.2.3. *Electrode, half-element, half-cell*

The two electrodes are respectively qualified as *positive* and *negative*.<sup>8</sup> We shall avoid using the terms anode and cathode (see section 2.2.4 onwards) because each electrode changes its role depending on whether the secondary battery is being charged or discharged (see Table 2.1). A laboratory-scale electrode is frequently studied in an electrochemical cell versus metal lithium.<sup>9</sup> In electrochemical jargon, such a cell is often qualified as a half-element or a half-cell.<sup>10</sup>

---

7 D. J. BRADWELL, H. KIM, A. H. C. SIRK, D. R. SADOWAY, Magnesium-antimony liquid metal battery for stationary - energy storage, *J. Am. Chem. Soc.*, vol. 134, pp. 1895–1897, 2012.

8 “*Positive*” and “*negative*” are adjectives. However, for simplicity’s sake, people in the field use them as nouns to speak of the electrodes. For instance, one might say “at the positive” rather than “at the positive electrode”.

9 Metal lithium is chosen because it is the material with the lowest potential and which therefore serves as a reference point (origin of potentials in comparison to lithium). Any material which is compared to it will be a positive electrode in comparison to lithium. In other cases, we use the normal hydrogen electrode (NHE) (defined more precisely in footnote 56) as a reference, whose potential in relation to lithium is  $+3.05\text{ V}$ . It is in comparison to the NHE that redox potentials tend to be quoted (see the list in section 4.4.1).

10 Although it is incorrect, we often use the label “battery” because test cells are often made in a button-battery casing (see photo of coin-cell in Figure 6.28).

### 2.2.4. Oxidation, reduction, anode, cathode

Regarding the electrodes, it is important to recap certain definitions.

Oxidation is a reaction in which an atom or an ion loses one or more electrons. The “actor” in oxidation is an electron donor, which is a reducer.<sup>11</sup>

Reduction is a reaction in which an atom or ion gains one or more electrons. The “actor” in a reduction is an electron acceptor, which is an oxidant.

An oxidation/reduction reaction (redox reaction) can be generically formulated as:



where  $a$ ,  $n$  and  $b$  are coefficients used to balance the two sides of the equation. They depend on the species which are present. Numerous examples are given in Chapters 4–10.

The anode is the electrode where the oxidation reaction takes place.

The cathode is the electrode where the reduction reaction takes place.

Thus, an electrode will switch from playing the role of the cathode to playing that of an anode depending on the direction of the current, i.e. depending on whether the secondary battery is being charged or discharged. Conversely, a positive electrode (or respectively a negative one) will always remain positive (or respectively negative) whether the secondary battery is being charged or discharged. The behavior of the two electrodes is detailed in Table 2.1.

|                    | Charge  | Discharge |
|--------------------|---------|-----------|
| Positive electrode | Anode   | Cathode   |
| Negative electrode | Cathode | Anode     |

**Table 2.1.** Behavior of the electrodes in a charge and discharge process

<sup>11</sup> The concepts of electrochemistry are to be found in: M.C. PERA, D. HISSEL, H. GUALOUS, C. TURPIN. *Electrochemical Components*, ISTE Ltd, London, John Wiley & Sons, New York., 2013.



Electrochemists very often incorrectly employ the term “cathode” for the positive electrode and “anode” for the negative electrode because, in the earliest days of electricity generation by electrochemical reactions (the early 19<sup>th</sup> Century), there were only primary batteries (and here, the terms are indeed synonymous) and not yet secondary batteries (the earliest secondary batteries only emerged in the mid-19<sup>th</sup> Century).

### 2.2.5. *Active material*

The chemical products involved in the charge and discharge reactions constitute active material. For lithium secondary batteries, the active matter is contained in the electrode<sup>12</sup>: we speak of positive active matter at the positive electrode and negative active matter at the negative electrode. For instance: metal oxide at the positive and graphite at the negative for a lithium-ion element, or transition metal oxide at the positive and metal lithium at the negative for a lithium metal polymer cell.

We shall use the term “inactive material” for the casing, the electrical connections, the insulators, the separator, etc., that is, all the components which are not involved in the electrochemical reactions for charging/discharging of the battery.

### 2.2.6. *Voltage*

A battery element provides a voltage of around 1 volt or a few volts. The approximate values for this voltage, which depends on the charge or discharge current, are as follows for operation in a “normal” operating current:

– 1.2 V for a Nickel-Cadmium (NiCd) or Nickel-Metal Hydride (NiMH) element;

---

<sup>12</sup> Note that in lead secondary batteries, the electrolyte is considered to be active material, because it takes part in the electrochemical reactions. In lithium secondary batteries, however, the role of the electrolyte is to transport the lithium ions from one electrode to the other. In the electrolyte, the concentration of lithium ions therefore remains constant, even down to the consumption of lithium over time to reconstitute the interface layer between the electrolyte and the carbon of the electrodes. This interface layer is called the SEI (*Solid-Electrolyte Interphase*). It is a passivation layer, whose role is explained in section 4.1.

- between 1.5 and 1.8 V for a bromine or vanadium redox flow element;
- 2 V for a lead element or a sodium-sulfur element;
- 2.6 V for a nickel chloride element;
- depending on the choice of electrodes, from 1.8 V to nearly 4 V (and even 5 V in research laboratories – see section 7.1.3) for the couples used for lithium-based elements. The nominal voltage is usually between 3.6 V and 3.8 V for the elements used in nomadic devices such as graphite–lithium cobalt nickel aluminum. It is closer to 3.2 V for graphite–iron phosphate elements (detailed in section 6.1.3) but only 1.8 V for lithium titanate–iron phosphate elements (detailed in section 6.1.5).

The voltage of a cell is notated as  $V_{pc}$  (*per cell*) or V/element.

### 2.2.7. Battery of accumulators, modules, packs, BMS

With the notable exception of cellphones and small digital cameras which function with a single lithium-ion element which generally delivers 3.7 V, these voltages are usually too low for most applications, such as the supply of electronic devices and, *a fortiori*, energy storage for an electrical vehicle or for electricity distribution grids. Therefore, secondary battery elements are rarely used alone. They tend to be connected in series to obtain the desired operating voltages, with the increased capacity able to be obtained by connecting elements in parallel. This connection of elements in series and in parallel constitutes a battery of accumulators or a *pack*. To define a pack, we might use abbreviations such as “4s2p”, which means that the ensemble comprises two parallel branches of 4 elements connected in series.

Thus, a secondary battery may be available:

- either in the form of a unique element;
- or in the form of a combination of several elements connected in parallel in the same container, called a module. They can be separated by disconnecting the metal bars or cables which link the positive and negative terminals of the elements.

A combination of several elements or modules connected in series and/or in parallel is a battery pack or an energy pack which often also contains a BMS: *Battery Management System* (which gauges the autonomy and the

state of health (section 2.4.4)), balances the voltage between the elements, etc.).

## 2.3. Definitions of the characteristics

The choice of a secondary battery (or a battery of accumulators) requires knowledge of its characteristic data. These characteristics are primarily its nominal voltage, its energy or the charge that it can store (capacity) or, for certain applications, its maximum current or maximum power. The definitions of these characteristics are given below.

### 2.3.1. *Nominal voltage*

The nominal voltage is a value indicative of the operational voltage, usually in a discharge current with medium amplitude, which discharges the secondary battery in the space of a few hours. The nominal voltage represents the value of the average voltage of the voltage profile observed in a discharge current for the above current (therefore outside the zone of significant variation in voltage at the start and end of discharge). Apart from the specific case of a car battery for which the usage voltage of the power-consuming components is defined in periods of charge by the alternator, the nominal voltage is less than the electromotive force (emf).

### 2.3.2. *Voltage under current*

With a current running through the component, the measured voltage  $U$  corresponds to the sum of various contributions: the emf  $\Delta E$ , the overvoltages<sup>13</sup> of the electrodes ( $\eta_+$  and  $\eta_-$ ) and the (algebraic) ohmic voltage drop<sup>14</sup>  $R.I$ :

$$U = \Delta E + \eta_+ + \eta_- + R.I \quad [2.2]$$

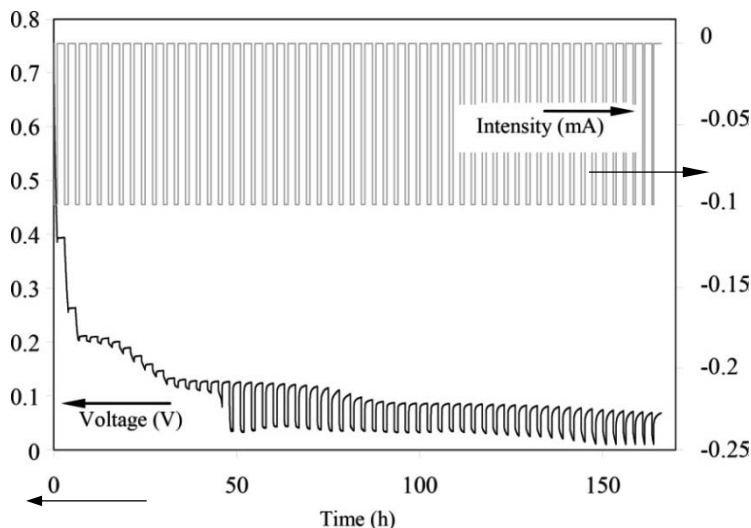
---

<sup>13</sup> When a secondary battery is traversed by a current (either charging or discharging), the voltage between the electrodes is different from the no-load emf (or open-circuit voltage). These differences in voltage are called “overvoltages” by electrochemists. This variation in voltage is different from the Ohmic loss of voltage.

<sup>14</sup> Electrochemists use the term “polarization” for the algebraic sum of the electrode overvoltages and the ohmic voltage drop.

Overvoltage or polarization as a difference between a potential difference when subject to a current and a potential difference in the absence of current.

Figure 2.1 illustrates the discharge of a lithium/graphite secondary battery (or “half-cell”)<sup>15</sup> with a C/50 current<sup>16</sup> where, every hour, a one-hour rest with no current is intercalated. We can see that the voltage increases when the current is absent, because the overvoltages and ohmic voltage drop are eliminated. The open-circuit voltage corresponds to the emf and is given by Nernst’s law.<sup>17</sup> We also note that the sum of the electrode overvoltages and the ohmic loss vary greatly depending on the state of discharge.



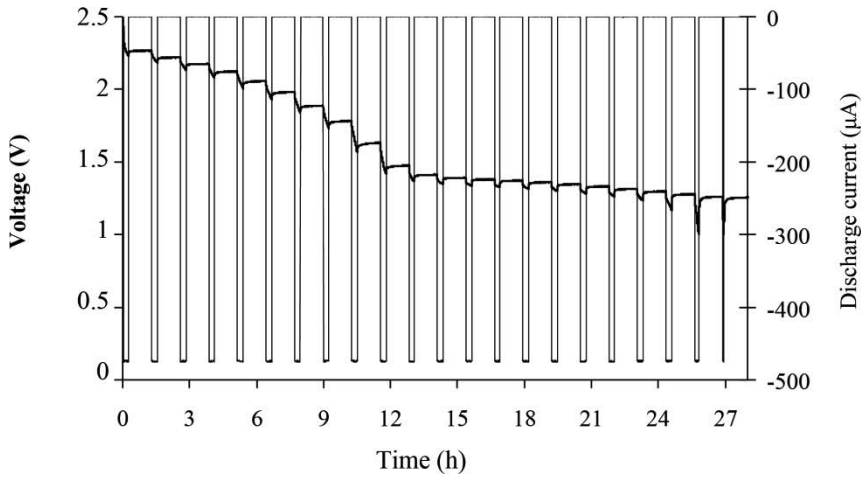
**Figure 2.1.** Discharge of a lithium-graphite secondary battery with a C/50 current with a one-hour pause with every 10% discharge

Figure 2.2 shows the discharge of a test secondary battery with capacity 2.5 mAh with a  $\text{Li}_2\text{Ti}_3\text{O}_7$  positive electrode facing a metal lithium negative electrode. Discharge takes place with a C/5 current with a one-hour pause every 4.76% of discharge.

<sup>15</sup> This is a laboratory experiment. Carbon was studied as a “half-cell” (section 2.2.3) with a metal lithium electrode as the counter electrode. The difference in voltage between these two electrodes is, naturally, very low. This is one of the reasons why carbon is often used as the negative electrode in lithium-ion secondary batteries instead of metal lithium, because it does not decrease the voltage of a cell too greatly. Such a decrease would lower the specific energy (defined in section 2.4.16.). It should be noted that in this “half-cell”, carbon is a positive electrode because it is used in conjunction with lithium.

<sup>16</sup> Defined in section 2.3.3.5.

<sup>17</sup> Explained in section 2.9.3.



**Figure 2.2.** Discharge of a lithium- $\text{Li}_2\text{Ti}_3\text{O}_7$  secondary battery with a C/5 current with a one-hour pause with every 4.76% discharge

From these measurements, we can deduce the emf as a function of time, and therefore of discharge, by measuring the voltage after each rest period without current (called “relaxation” by electrochemists). This emf is given as a function of the SOC in Figure 2.3.

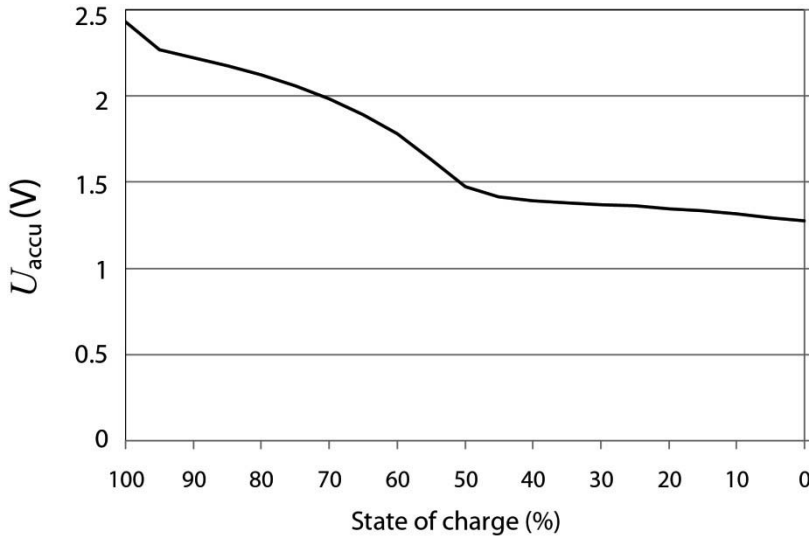


**Figure 2.3.** The emf of a lithium- $\text{Li}_2\text{Ti}_3\text{O}_7$  secondary battery versus SOC

From these measurements, we can also deduce the internal resistance of the element and see its variation with the changing SOC (Figure 2.4).

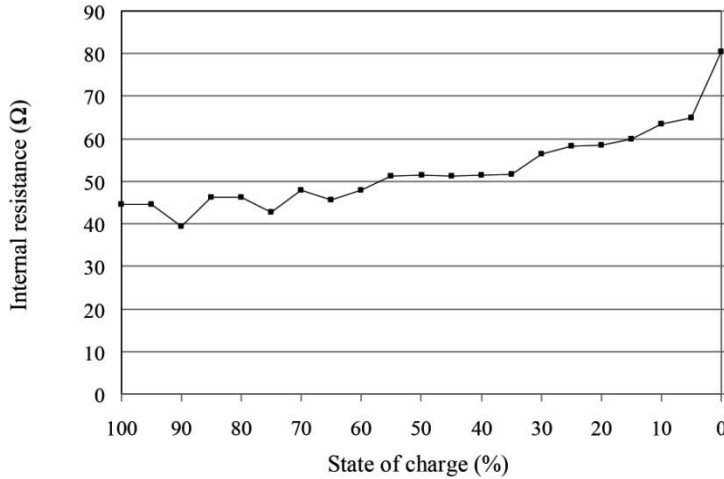


**Figure 2.4.** Internal resistance of a lithium- $\text{Li}_2\text{Ti}_3\text{O}_7$  secondary battery versus SOC

### 2.3.3. Capacities

#### 2.3.3.1. General definition

The term *capacity*<sup>18</sup> covers the idea of potentiality of the amount of electricity able to be released by a pre-charged secondary battery. The term can also be applied to the active material, to an electrode or to a battery.

The SI unit for measuring the amount of electricity is the coulomb (C). However, by requirement and by force of habit, we essentially use the product of an intensity (in A or mA) for a duration of a certain number of hours. Also, electrotechnicians and electrochemists prefer to use the ampere-hour (A.h or Ah) or, for small secondary batteries, the milliampere-hour (mAh).

REMINDER 2.1. –

$$1 \text{ Ah} = 1000 \text{ mAh} = 3600 \text{ As} = 3600 \text{ C}.$$

<sup>18</sup> Not to be confused with the capacitance of a capacitor, which is expressed in Farad and does not refer to the same physical value.

More specifically, this quantity of electricity is the integral of the current (be it constant or variable) over the duration of discharge. Its value is:

$$C = \int_0^t i(t) dt \quad [2.3]$$

From an electrochemical point of view, it is also  $n.N_A.e$  or  $n.F$ , where  $n$  is the number of moles<sup>19</sup> of electrons exchanged,  $e$  is the charge on the electron ( $1.6 \times 10^{-19}$  C in absolute value),  $N_A$  is Avogadro's number (or constant) ( $6.022 \times 10^{23}$  moles) and  $F$  is Faraday's constant<sup>20</sup> which is the product of the above two numbers, which is therefore 96485 C/mol (coulombs per mole) or 26.8 Ah/mol (ampere-hours per mole).

Depending on the conditions of discharge (intensity, temperature, end of discharge criterion, etc.) and the secondary battery's operational history (previous conditions of charge and discharge), this capacity may be variable or have changed in relation to an initial value. There are many definitions of capacity which are given from section 2.3.3.3 onwards.

#### 2.3.3.2. Faraday's law

Faraday's law indicates that the amount of electricity needed to change one mole of material is equal to 96485 coulombs (see section 2.3.3.1).

Its expression is:

$$m = R_F \cdot \frac{M.Q}{n.F} \quad [2.4]$$

where

$m$  is the mass of product formed at the electrode (g);

---

<sup>19</sup> One mole (mol) is the amount of material of a system containing the same number of elementary entities as there are atoms in 0.012 kg of carbon 12 – i.e.  $6.02217 \times 10^{23}$  atoms (Avogadro's number).

The notation "XM" is used for the quantity of moles in a solution: there are  $X$  moles per liter. For instance, 2.5 M means 2.5 moles per liter.

<sup>20</sup> For simplicity's sake, we often find the value 96500 C/mol for Faraday's constant. By definition, Faraday's constant is the product of the charge on the electron by Avogadro's number: that is,  $F = q.N$ . If  $q = 1.602192 \times 10^{-19}$  C and  $N = 6.02217 \times 10^{23}$  g/mol, then the value of Faraday's constant is 96485 C/mol.

$R_F$  the faradaic efficiency (see section 2.5) which is considered to be equal to 1;

$M$  the molar molecular mass (g/mol);

$Q$  the past quantity of electricity (in C);

$n$  the number of moles of electrons exchanged per mole<sup>21</sup> of product formed during the electrochemical process in question (quite simply it is the coefficient in front of “e<sup>-</sup>” in a chemical formula);

$F$  Faraday’s constant (96485 C/mol).

The theoretical capacity can be deduced from Faraday’s law.

In order to determine the theoretical gravimetric capacities  $C_{th}$  (in mAh/g or Ah/kg, see the definition in section 2.4.7.), Faraday’s law can be transformed:

$$\text{Theoretical gravimetric capacity: } C_{m.th} \text{ (C/g)} = \frac{n \times F}{M} \quad [2.5]$$

By transforming the coulombs into Ah and the grams into kilograms (or the amperes into milliamperes), we get:

$$\text{Theoretical gravimetric capacity: } C_{m.th} \text{ (mAh/g or Ah/kg)} = \frac{1000 \times n \times F}{3600 \times M} \quad [2.6]$$

$$\text{or indeed: } C_{m.th} \text{ (mAh/g)} = \frac{1000 \times n \times 96485}{3600 \times M} = 26801 \cdot \frac{n}{M} \quad [2.7]$$

We shall apply Faraday’s law only to the active material.

---

<sup>21</sup> A mole is a set of molecules, the number of which is given by Avogadro’s number ( $6.022 \times 10^{23}$  moles). A molecule is a collection of atoms whose composition is given by its chemical formula. The term “molecule” comes from the Latin “*molecula*”, which denotes a small mass of material or a grain of material.

An atom (from the Ancient Greek *ατομος* [*atomos*], meaning “that which cannot be divided”) is the smallest part of a simple substance that can chemically combine with another. Atoms are, themselves, composed of a nucleus comprising protons and neutrons, around which electrons orbit; electrons are the particles that are shared with other atoms to form molecules. The diameter of an atom is roughly a tenth of a nanometer (nm), i.e.  $10^{-10}$  m, but most of the mass of the atom is concentrated in the nucleus, which occupies a very small volume indeed (dimensions of around  $10^{-15}$  m).



In actual fact, it is extremely difficult to exploit all of the active material. In addition, for this to happen, all the active materials would need to be in a perfectly stoichiometric<sup>22</sup> ratio (as required by the redox equations involved at the electrodes) so that they are totally transformed during the process of discharge (or charge) at the electrodes. In reality, this is difficult to achieve. Finally, certain technologies require the oversizing of one of the components. For instance, for a cobalt electrode (as described in section 5.3.1), only half the lithium ions contained in the positive electrode can be used, for fear of collapse of the crystalline insertion structure and, consequently, definitive breakdown of the device. The capacity of the negative electrode therefore has to be twice that which is stoichiometrically necessary, in order to avoid this collapse. Another example: the capacity of the negative electrode will often be greater than the usable capacity of the positive so as to facilitate the formation of the passivation layer (SEI, solid electrolyte interphase – see section 4.1). This formation may consume around 10% of the lithium initially present, thereby decreasing the available capacity by the same amount (this loss of capacity is irreversible).<sup>23</sup> The initial stoichiometry therefore does not precisely reflect the primary redox equations, but needs to be adapted to these reactions of formation of interfaces during the initial charging process (see sections 5.4.1 and 6.2.10) and to the intrinsic characteristics of the materials.

#### 2.3.3.3. *Theoretical capacity*

The theoretical capacity  $C_{th}$  of a secondary battery is the amount of charge which would be delivered by that secondary battery, pre-charged to its full capacity, during a complete discharge which consumes all of the active material. The theoretical capacity therefore depends not on the conditions of discharge but solely on the amount of active material.

---

22 A perfectly stoichiometric ratio means that the proportions of each of the reagents (substances used in a chemical reaction) are in the exact proportion given by that reaction's formula.

23 This irreversible consumption of lithium can be optimized by adding adjuvants into the electrolyte. The use of an adjuvant such as VC (*Vinylene Carbonate*) is often cited in the composition of the electrolyte. It is, like other molecules, considered to be a precursor of the SEI, because it decomposes early on (at high potential), before the other solvents in the electrolyte, forming a fine, homogeneous film on the surface of the graphite particles. The number of lithium ions involved in its decomposition is therefore low, and the irreversible capacity reduced.

This notion has the advantage of revealing the maximum limit of a battery's capacity and, therefore, its maximum mass- and volumetric capacities (defined in sections 2.4.7 and 2.4.8 respectively).

#### 2.3.3.4. *Effective capacity*

The effective capacity (also known as the real or practical or usable or available or released or measured capacity) is the amount of electricity released by a fully-charged battery during a complete discharge, with a given discharge current rate, end voltage and temperature. This amount of electricity  $C_{eff}$  is the integral of the current throughout the duration of the discharge. If the discharge rate exhibits constant current, it is simply the product of the current strength by the duration of the discharge.

For example, a battery delivering 2 A for 5 hours has an effective capacity of 10 Ah.

The effective capacity is necessarily less than the theoretical capacity.

The effective capacity depends essentially on the conditions of discharge. For this reason, we need to introduce the notion of nominal capacity (definition given in section 2.3.3.5 below).

#### 2.3.3.5. *Nominal capacity*

A battery's effective capacity depends on the conditions of discharge, which include:

- the discharge current<sup>24</sup>;
- the temperature;
- the history of the battery's operation (and in particular its degree of aging);

---

<sup>24</sup> For certain lithium-ion secondary battery technologies such as cobalt, the capacity is only very slightly dependent on the discharge current. With other technologies such as lead or LiAl/MnO<sub>2</sub> (lithium-aluminum/manganese dioxide alloy), designed for very slow discharges (e.g. lasting over 300 hours), the capacity will decrease by 40% for a discharge in 10 hours (with the same threshold voltage and the same temperature). In addition, the lifetime in cycling for this type of secondary battery, including metal alloys at the negative electrode, is strongly linked to the depth of discharge applied.

- the charge/discharge stop conditions (usually a threshold level of voltage<sup>25</sup>);
- etc.

Thus, for the same battery and depending on the usage conditions, we can define a number of different capacity values, which may become a source of confusion. Therefore, we introduce the notion of nominal capacity, which is intended to represent the value of the capacity for a new secondary battery and for clearly-determined conditions of discharge (see the list above). In order to ensure compatibility with the different conditions of discharge, manufacturers often give certain capacity values, specifying the conditions applied during charge and discharge.

This *nominal capacity* (or *rated capacity*), notated as  $C_n$ , appears in manufacturers' manuals and on the identification plate on the primary or secondary battery. It is given for a duration of discharge fixed by international standards, depending on the domain of application. The subscript  $n$  represents this reference time-period (in hours).

With lithium secondary batteries for mobile applications, paragraph 3.5 of the European Standard EN 61960 (2004)<sup>26</sup> defines a discharge over 5 hours. For an electric road vehicle<sup>27</sup>, a 3-hour discharge capacity is defined. We could also include the indication of the capacity in 5 hours, 3 hours and ½ hour.

When the discharge is faster, the capacity may, depending on the technology, remain constant or fall (see section 6.2.12).

A battery with nominal capacity  $C_{20}$  of 15 Ah (manufacturer's indications) in a  $C_{20}/20$  current therefore needs to be able to provide a current of 15 Ah/20 h = 0.75 A for 20 hours until the set stop voltage threshold is reached.

The charge or discharge current for a battery is often written in reference to its capacity. For instance, one might speak of a  $C/5$  discharge,

---

<sup>25</sup> Unlike lead or nickel secondary batteries, for which it is easy to suggest realistic end of charge/end of discharge voltages, with lithium secondary batteries, the values of these voltages are heavily dependent on the technology.

<sup>26</sup> Secondary Cells And Batteries Containing Alkaline or Other Non-acid Electrolytes – Secondary Lithium Cells And Batteries For Portable Applications.

<sup>27</sup> IEC 61982-1:2006 or EN 61982-1 (2007) – Secondary batteries for the propulsion of electric road vehicles – Part 1: Test parameters.

corresponding to a current  $I=C/5$  (meaning  $C/5$  h, but the “hours” symbol is usually omitted and the capacity  $C$  corresponds to a nominal value). For a battery whose capacity  $C=C_{10}=15$  Ah, this denotes a current of  $C_{10}/5=15$  Ah/5 h=3 A. For rapid discharges, one might speak of a 2C discharge, i.e. for a current (always kept constant)  $I=2.C$ . With the above example ( $C=15$  Ah), this gives us a discharge with a 30 A current.

#### 2.3.3.6. *Assigned capacity*

Instead of nominal capacity, the European standards define the assigned capacity, notated as  $C_r$ . This is the minimum amount of electricity, indicated by the manufacturer, that a battery is capable of delivering in specific conditions after a complete recharge.<sup>28</sup> It is this capacity which is indicated on a battery. However, in practice, documentation usually employs the term *nominal capacity*.

It is noteworthy that the initial and nominal capacities of lithium devices are generally very close (in the nominal conditions specified by the manufacturer). The initial capacity is expected to be greater, if only slightly, than the nominal capacity in order to conform to the standard on capacity.

#### 2.3.3.7. *Aging. Residual capacity. End-of-life criteria. Lifetime.*

The *aging* of a secondary battery results in a decrease of its capacity and an increase of its internal resistance. When these parameters reach a certain level of degradation, the secondary battery can no longer fulfill the function for which it was intended. We then say that it is at *end of life* – *EOL* – even if it is still functional. We also speak of its *lifetime*.<sup>29</sup>

This aging is all the more significant when the secondary battery is used in an extreme or abusive manner, i.e. beyond the bounds of its normal operational domain. There are many different causes of aging, such as, e.g.:

- loss of active material such as the consumption of lithium by natural degradation of the SEI or to recreate this passivation layer after an excessive discharge;

---

<sup>28</sup> For lithium secondary cells for portable applications, paragraph 3.5 of European Norm EN 61960 (2004) defines a 5-hour discharge.

<sup>29</sup> This notion must not be confused with that of autonomy (the duration of operation of a battery-powered device, conferred by its complete discharge), which is sometimes incorrectly called the lifetime.

- modification of the crystalline structure of the materials of the electrodes, particularly during excessive charging;
- degradation of the electrolyte after excessive charging;
- decohesion of the particles, which lose contact with the others because of the contraction and expansion of the active material depending on the SOC and/or because of degradation of the binder (surrounding polymer) ensuring the mechanical cohesion of the particles to one another;
- secondary reactions to the electrochemical reactions, involving pollutant species or species released by the electrodes over time (e.g. traces of water<sup>30</sup>, metal cations from positive active materials). These compounds, which are involved in secondary reactions, lead to the degradation of the electrode/electrolyte interfaces (changed chemical composition of the SEI, pore-blocking, gas evolution/formation) and the current collectors (corrosion).

There are also other parameters which influence the lifetime of a secondary battery:

- high storage- and operating temperatures, which shorten the lifetime;
- the end-of-charge or floating voltage. For lithium secondary batteries, there is therefore a compromise between capacity and lifetime. For instance, if we increase the end-of-charge voltage during the final phase at constant voltage (e.g. 100 mV/element), the recharged capacity (and therefore the capacity which will then be discharged) is slightly greater, but the aging will be increased and therefore the lifetime shortened;
- the depth of the charge/discharge cycles. The greater this depth, the more quickly the secondary battery will degrade. More specifically, it is the extreme limits of the state of charge (the highest and lowest SOC's) of the

---

<sup>30</sup> The presence of water is often due to the actual components of the device which have not been sufficiently dried prior to the assembly of the cell, or which it is difficult to dry because of the morphology of nanometric-scale particles (as are being increasingly used to increase the exchange surface areas). For instance, we could cite lithiated iron phosphate  $\text{LiFePO}_4$  (abbreviated to LFP, described in section 5.3.3) which – in order to compensate its poor electrical conductivity – is synthesized in the form of nanoparticles upon which carbon is deposited. During its synthesis, traces of water may become trapped in the nanoparticle architecture. If heat treatments are not carried out or do not succeed in completely eliminating it, this residual water will be released little by little during the secondary battery's operation, contaminating the carbon negative electrode, for instance, and/or degrading the lithium salt.

cycles which are important factors for the lifetime of secondary batteries. In such operating conditions (full charge, full discharge), the demand placed on the active materials, either fully lithiated or fully de-lithiated, causes a mechanical stress which causes loss of capacity, therefore decreasing the cycling lifetime.

A secondary battery can therefore be seen as a reservoir of energy, whose capacity (maximum storable energy) decreases with aging, and the internal resistance increases. On this final point, staying with the analogy of a reservoir, we can say that the maximum flowrate decreases (lower maximum power) and the friction losses increase.

Determining the effective capacity enables us to work out the moment of EOL of a secondary battery. Generally a secondary battery, for stationary applications and for electric vehicles, is considered to be out of service when its measured capacity is less than 80% of its nominal capacity. This is a commercial or contractual notion, which does vary (e.g. 70% for stationary secondary batteries). This end-of-life capacity is called the *residual capacity*.

For “individual portable sealed” lithium devices, the EOL is defined for a ratio of measured capacity to nominal capacity less than 60% (EN 61960:2004<sup>31</sup> which replaces IEC 61960:2003).

Regardless of the form of technology used, this 60 or 80% constitutes a contractual given. There is nothing preventing a secondary battery being used below this capacity, given the significant cost of replacing batteries (in cellphones or portable computers) – users will keep their batteries as long as they deem them to have sufficient range. Note, however, that when the capacity is reduced, the relative stress is more intense (unchanged power requirement and therefore unchanged current requirement, but in relation to a reduced capacity which is usually accompanied by an increase in internal resistance), which tends to accelerate the loss of autonomy still further.

EXERCISE 2.1.– A mobile telephone is supplied by a Li-ion secondary battery whose capacity (in the fresh state) is 1200 mAh. The technology used means that this capacity is practically unchanged regardless of the discharge current rate. Standby mode consumes 1.7 mA. Conversation mode

---

31 Secondary Cells And Batteries Containing Alkaline or Other Non-acid Electrolytes – Secondary Lithium Cells And Batteries For Portable Applications.

consumes 65 mA in GSM operation and 220 mA in 3G operation. For each of these modes of operation, we shall take the consumption to be constant.<sup>32</sup>

What is the range of such a telephone in GSM operation and then in 3G operation if it is in “conversation” mode for 5% of the total time?

*Solution on page 82*

#### 2.3.3.8. *Calendar aging*

Secondary batteries will also degrade even if they are not being used (are completely unplugged). This phenomenon is known as *calendar aging*. Above all, it is the temperature and the average SOC which exert the greatest influence on this type of degradation. From this point of view, not all secondary battery technologies are entirely alike. For instance, lithium-ion secondary batteries for portable devices degrade far more quickly (often in 2–3 years) than certain NiCd elements, which may exhibit an effective lifetime of over 20 years or lithium-ion industrial technologies.

#### 2.3.3.9. *Cycle endurance*

The cycle endurance of a secondary battery is defined by the number of discharge/recharge cycles that it can withstand in conditions specified by published standards until it reaches the imposed limit of loss of capacity. The amplitude of the cycles and the temperature are the factors which have the greatest impact on the aging in terms of cycles.

#### 2.3.3.10. *Amount of electricity discharged*

The number of Ah discharged or the amount of electricity discharged (or released or consumed or supplied) is obtained by integrating the current supplied as a function of time.

#### 2.3.3.11. *Amount of electricity still available*

The amount of electricity still available is not a state variable. With different lithium secondary battery technologies, it may vary depending on various parameters. For technologies using insertion materials (this mechanism is explained in section 4.3.1), the capacity, and consequently the

---

<sup>32</sup> In reality, the current required in conversation mode depends on the power necessary for transmission; this power depends on how far the phone is from the nearest *Base Transceiver Station* (BTS).

amount of electricity still available, are not heavily influenced by the discharge currents. This is true to a far lesser extent when the (negative) electrodes are made of alloys or conversion materials (as is the case with lead-acid technology). In these secondary batteries, whilst it is easy to determine the amount of electricity delivered, it is more difficult to evaluate the amount of available electricity remaining (this notion is equivalent to “the amount of electricity that remains to be discharged” or “the amount of electricity still available” or “the amount of electricity still releasable”). Indeed, over the course of discharge, the amount of electricity remaining or still available depends on the past conditions (the conditions in which the amount of electricity already discharged (and therefore consumed) was furnished), but also and above all on the future conditions of discharge (essentially the amplitude, which is often variable, of the discharge current and the temperature). It also depends on whether or not there are rest periods (called relaxation periods). Therefore, the amount of electricity still available may not be the same depending on the discharge currents. It may also increase if we switch from an intense current to a less punishing one.

The relation between the amount of electricity still available and the amount of electricity already discharged is simply written as:

$$Q_{\text{still available}} = C_{\text{effective}} - Q_{\text{already discharged}} \quad [2.8]$$

The amount of electricity still available is complementary to the amount of electricity already discharged in relation to the effective capacity.

## 2.4. States of the battery

### 2.4.1. Depth of discharge

The *Depth of Discharge* (DOD or DoD) is an indication of the amount of electricity already extracted from a battery (section 2.3.3.10) in relation to its capacity. Thus, it is the ratio of the integral of discharge current  $i_{\text{disch}}$ , whether constant or variable, to the capacity. Consequently:

$$DOD = \frac{\int_0^t i_{\text{disch}}(t) dt}{\text{Capacity}} \quad [2.9]$$

This is a dimensionless value, usually expressed as a percentage. For example, a DOD of 90% corresponds to a deep discharge, as the theoretical maximum is 100%.



### 2.4.2. State of charge

The *State of Charge* (SOC) is an indication of the amount of electricity still available in the secondary battery (see section 2.3.3.11) in relation to its capacity in given conditions (discharge current amplitude) of discharge past and future:

$$SOC = \frac{\text{Amount of charge remaining}}{\text{Practical capacity of the accumulator}} \quad [2.10]$$

$$SOC = \frac{\text{Capacity} - \int_0^t i_{\text{disch}}(t) dt}{\text{Capacity}} \quad [2.11]$$

The SOC is associated with a chemical energy. Therefore, it can be used to evaluate the remaining range.

It is also a dimensionless value, which is usually expressed as a percentage:

$$SOC = 1 - DOD, \text{ so therefore } DOD = 1 - SOC \quad [2.12]$$

This relation can be compared to that given by equation [2.8] by dividing each of its terms by the capacity.

### 2.4.3. State of energy

Similarly, we can replace the concept of the “amount of electricity” in our discussion above with the notion of energy.<sup>33</sup> Thus, we define the *State of Energy* (SOE), which is the ratio of the amount of energy still available to the total amount of energy stored.<sup>34</sup>

### 2.4.4. State of health

The *State of Health* (SOH) is an indication of the state of aging or failure of a secondary battery. It can be evaluated as the amount of electricity

---

<sup>33</sup> The energy densities in the secondary batteries are defined in section 2.4.13. However, we have placed this notion here because it is very similar to that of the SOC.

<sup>34</sup> K. MAMADOU, Prévisions de la disponibilité énergétique des accumulateurs électrochimiques par estimation d'états d'énergie (SoE), Doctoral Thesis, INP-Grenoble, 2010.

measured during a complete discharge in relation to the nominal capacity<sup>35</sup> or maximum capacity attained or initial (determined in a current amplitude coherent with the current(s) to which the battery will be subject) during its lifetime.

$$\text{SOH} = Q_{\text{discharge}}/C_{\text{nominal}} \quad [2.13]$$

Thus, this parameter characterizes its degradation over the course of its use. The SOH is usually expressed as a percentage. It is this parameter which indicates the contractual EOL for a secondary battery (see section 2.3.3.7). One of the functions of the BMS is to identify the SOH.

It is noteworthy that the initial and nominal capacities of lithium devices are generally very similar (in the nominal conditions specified by the manufacturer). The initial capacity is expected to be greater, if only slightly, than the nominal capacity in order to conform to the standard on capacity.

Two examples of the curves of decreasing capacity with an increasing number of cycles are shown below, for two different lithium-ion technologies used in cycled applications for portable computers and power supply to mobile devices.

Figure 2.5 shows the evolution of the SOH of a lithium-ion device comprising two insertion materials (graphite for the negative electrode and mixed cobalt/nickel oxide for the positive electrode). Cycling was performed to a DOD of 75% for a C/5 charge/discharge current amplitude.

The SOH after 1500 cycles is 85%.

Figure 2.6 shows the evolution in the SOH for a lithium-ion device comprising a lithium-aluminum alloy for the negative electrode and a manganese oxide for the positive electrode. Cycling was performed to a DOD of 100% for a C/20 charge/discharge current.

Under such conditions, the SOH worsens very quickly. After only 15 cycles, the capacity falls to 85% of the initial capacity. Indeed, the behavior of this lithium-ion technology is very sensitive to the DOD because, when it is completely lithiated and de-lithiated, the alloy experiences significant

---

<sup>35</sup> With this first definition, we may have a state of health which is greater than 1, because the practical capacity may actually be greater than the nominal capacity.

volumetric expansion (greater than 200%) which drastically reduces its cycle tenacity. This type of secondary battery is obviously not designed for deep discharges: if the depth of discharge were limited to 10%, its lifetime would be 1000 cycles.

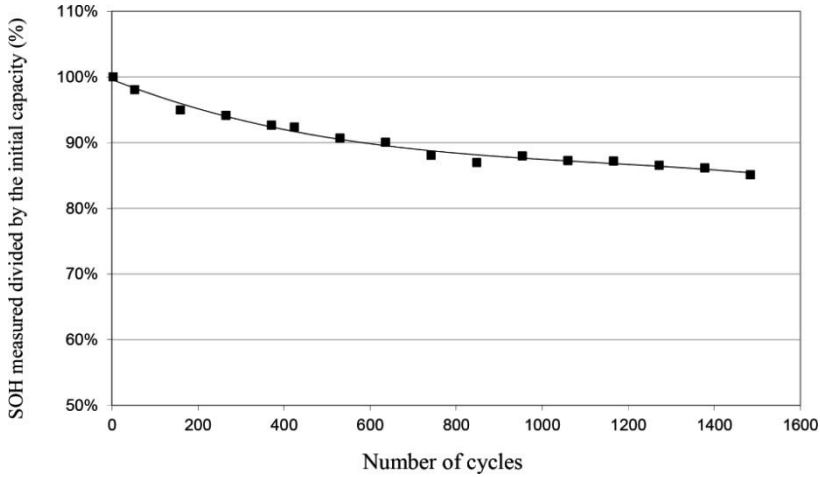


**Figure 2.5.** Evolution of the state of health of a Graphite/NCA lithium-ion device (cycling to DOD = 75%, C/5 currents for charge and discharge)

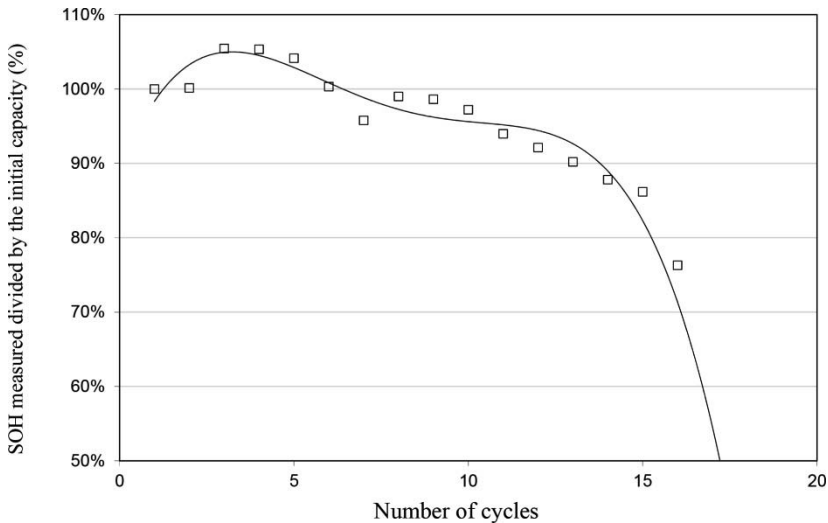


**Figure 2.6.** Evolution of the state of health of a Graphite/NCA lithium-ion device (cycling to DOD = 100%, C/20 currents for charge and discharge)

We can also define a state of health at the level of the available power. This notion is an important one for an electric vehicle (EV) or a hybrid electric vehicle (HEV). It can be determined by looking at the internal resistance, which inevitably increases with time and the cycling of the secondary battery.

Figure 2.7 shows the evolution of the internal resistance of a lithium-ion device comprising two insertion materials (graphite for the negative electrode and mixed cobalt- and nickel oxide for the positive electrode) in cycling with DODs of 75%. Measurements of the internal resistance are taken throughout complete charge/discharge cycles, so we are able to quantify the capacity of the device (the capacity and resistance are measured every 100 cycles). An initial measure of the resistance is taken at 50% DOD and another at 75% DOD (25% SOC). The resistances are measured by applying a C/2 pulse in the discharge current for a few seconds. The internal resistance is calculated as explained in section 2.4.10.

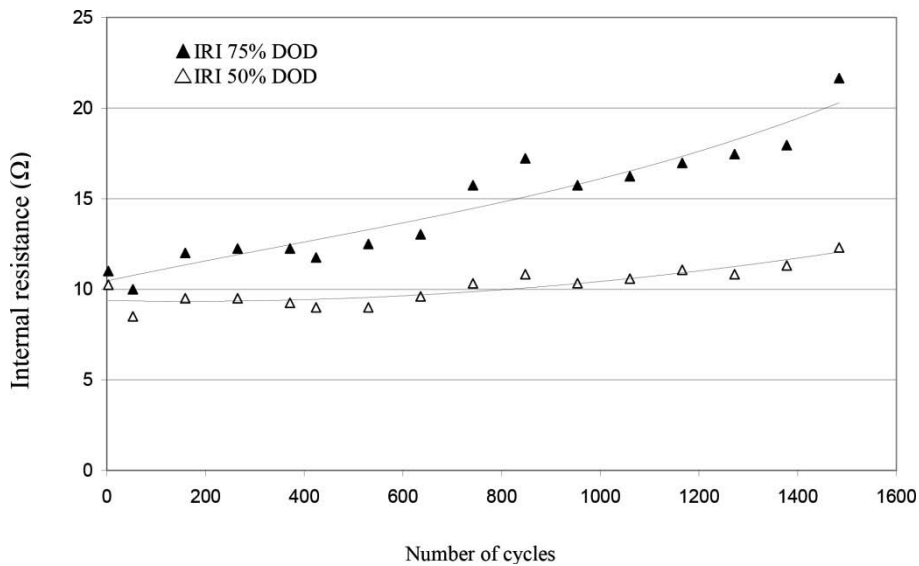


**Figure 2.7.** Evolution of the internal resistance (IR) of a Graphite-NCA lithium-ion device (cycling to DOD = 75%, C/5 currents for charge and discharge)

Note the different evolution of the internal resistance measured at 50% and 25% SOC. The resistance at 25% SOC (DOD = 75%) increases more

rapidly, which shows that, as the battery undergoes cycles, the maximum power decreases at the low levels of SOC.

#### **2.4.5. *State of function***

The state of charge and state of health of a secondary battery, as defined above, may not always be the most pertinent criteria to use for the purposes of the application. It is for this type of reason that the notion of the *State of Function* (SOF) has been introduced more recently. The SOF gives an account of the ability to render the service for which the secondary battery was intended. This state needs to be defined on the basis of the application. Depending on the application, the definition may be binary or “analog”.

For the same battery, the SOF may be different depending on the application. A secondary battery may no longer be able to properly drive an electric vehicle (EV) because of an increase in its internal resistance (which limits the maximum deliverable power) and/or a decrease in its capacity (which decreases the range), but may be given a second lease of life in domestic storage, with or without photovoltaic generation. Indeed, the EV application requires significant power peaks which are not required by domestic storage to smooth the energy demand on the grid and/or to stagger the production of photovoltaic (PV) energy in relation to the requirements.

#### **2.4.6. *Theoretical gravimetric capacity***

The theoretical gravimetric capacity is the ratio of the amount of electricity which can theoretically be released by using all of the active material of an electrode or a secondary battery, to the mass of that active material. This value has to be calculated. For this reason, we sometimes find extremely high values, having nothing whatsoever to do with the reality of the situation, as is sometimes the case with lithium-air secondary batteries (see Chapter 10).

The gravimetric capacity is expressed in Ah/kg. Calculations for determining theoretical gravimetric capacities are to be found in the chapters corresponding to the different technologies examined (sections 5.8, 6.3, 9.4 and 10.7).

#### 2.4.7. *Practical gravimetric capacity*

The practical gravimetric capacity is the ratio between the amount of electricity generatable with a given current to the total mass of the secondary battery. It is necessary to specify the discharge current in which the secondary battery is discharged.

This notion is particularly useful for the sizing of a primary battery in on-board systems. It is also interesting with a view to comparing different storage devices in a given discharge current and for a given operational voltage.

#### 2.4.8. *Volumetric capacity*

The volumetric capacity is the ratio between the nominal amount of electricity deliverable in a given current or the maximum stored electricity to the volume of the secondary battery. The volumetric energy is expressed in  $\text{Ah/m}^3$  or  $\text{Ah/dm}^3$ . Again, here, it is necessary to specify the discharge current in which the secondary battery is discharged. The dimensions in question are the overall dimensions, i.e. including the terminals, connections, fixing or handling devices, etc.

This concept is useful for the sizing of a stationary battery because, in these applications, the volume is often a more important criterion than the mass. It is also interesting with a view to comparing different storage devices in a given discharge current and for a given operational voltage.

#### 2.4.9. *Specific capacity*

The term *specific capacity* (or *related capacity*) is used indiscriminately to speak of gravimetric capacity and volumetric capacity. The density of the materials is not the same for all secondary battery technologies or for all electrodes, so the two quantities are not really linked. Depending on the applications, it is the consideration of one or other of these two values which is meaningful. The ambiguity can be resolved by looking at the unit associated with the values quoted. This term can easily be avoided by using the term *ad hoc*.

The notions of gravimetric capacity, volumetric capacity and specific capacity may apply to a single electrode, an element or indeed a whole battery pack. The gravimetric capacity of an electrode is an important point when choosing the components for a lithium secondary battery.

#### **2.4.10. Direct-current internal resistance and short-circuit current**

The term “DC internal resistance” is used to denote the sum of the real resistances (connections, electrodes, electrolyte, etc.) and the “resistances” due to the reaction sites. In the following sections (2.4.11 and 2.4.12), this value will be extended to the notion of AC impedance.

Of course, in a battery, the internal resistance is proportional to the number of elements (which must, of course, be identical) in series.

Given the very low internal resistance values of high-power secondary batteries, it is practically impossible to directly measure the short-circuit current, except perhaps with pulsed currents, but the short-circuit device itself needs to have a resistance far lower than that of the secondary battery in question. However, it may be advantageous to discover the amplitude of current that could be reached in the case of an accidental short-circuit directly at the terminals of a secondary battery.

For a portable lithium secondary battery, the norm EN 61960 [2004] suggests measuring the DC resistance on the basis of two measurement points. For the first point, the voltage is measured after 10 seconds of discharge at 0.2 times the discharge current  $C_5/1h$ . This discharge is immediately followed by another discharge of 1 second at  $C_5/1h$ , after which the voltage is measured.

These two points (respectively  $(U_1, I_1)$  and  $(U_2, I_2)$ ) enable us to trace a line on the voltage/current plot and thereby to simply deduce the internal resistance  $R_{int}$  and the short-circuit current  $I_{sc}$  by the relations:

$$R_{int} = \frac{U_1 - U_2}{I_2 - I_1} \quad [2.14]$$

$$I_{sc} = \frac{U_1 I_2 - U_2 I_1}{U_1 - U_2} \quad [2.15]$$

This so-called short-circuit current<sup>36</sup> is in fact simply an extrapolated current. If we measure the true short-circuit current, we note that it varies over time, if only for thermal reasons.

EXERCISE 2.2.– On the voltage/current plot, draw the line passing through the two measured points and find the above expressions of the internal resistance  $R_{\text{int}}$  and the short-circuit current  $I_{\text{sc}}$ .

*Solution on page 82*

For the secondary batteries used for the propulsion of electric road vehicles, the standard EN 61982-3 (April 2002) suggests a procedure for determining the internal resistance, which again is based on two measured points but after specific microcycling.<sup>37</sup>

#### 2.4.11. AC internal resistance

It is also possible to measure the AC internal resistance for a given frequency.

For a portable secondary battery, the standard EN 61960 [2004], on secondary lithium cells and batteries for portable applications, proposes to determine the AC resistance by applying a sinusoidal voltage at a 1 kHz frequency, of less than 20 mV peak value for 1–5 seconds and measuring the current. The resistance is then the ratio of this imposed effective voltage to the measured effective current.<sup>38</sup> Thus, in reality, it is a measurement of the modulus of the impedance.

---

36 Remember that when a true short-circuit occurs, there is no energy delivered to the outside of the secondary battery, and all the energy dissipates inside the cell. In reality, the short-circuit resistance itself, and the resistance of the contacts, are non-null. The very intense current circulating in the cell may lead to the melting of the current collectors and/or the connecting devices, possibly with the spraying of molten metal droplets. It is for this reason that the wearing of protective eye goggles and the use of insulated tools (in conformity with IEC/EN 60 900) are obligatory when handling batteries.

37 IEC 61982-3 or EN 61982-3 (April 2002): Secondary batteries for the propulsion of electric road vehicles – Part 3: performance and life testing (traffic compatible, urban use vehicles).

38 The standard speaks of alternating current resistance, whereas electrotechnicians know that this relation gives the modulus of the impedance.



### 2.4.12. Impedance, impedancemetry, impedance spectroscopy

We can go further still and measure the complex impedance (comprising both the real and imaginary parts) presented by a battery (or an electrode in relation to a reference electrode) on the basis of the frequency. This characteristic measurement uses the technique of *electrochemical impedance spectroscopy (EIS)*.<sup>39, 40</sup> This consists of applying a sinusoidal disturbance around a point of operation, i.e. in a given SOC (Figure 2.8). In order to do so, we can:

- either apply a modulation of the voltage of peak value  $V_{\max}$  and pulsation  $\omega$  so  $v = V_{\max} \sin(\omega t)$  at the terminals of the element around its DC voltage at the desired point of operation. This is the potentiostatic method, which is primarily used in the laboratory. If the voltage is of low amplitude, this disturbance leads to a sinusoidal current response whose amplitude  $I_{\max}$  and phase shift  $\varphi$  depend on the frequency  $f = \omega/2\pi$ . The amplitude  $I_{\max}$  will only be proportional to the amplitude  $V_{\max}$  applied in the linear domain (small signals). This response can be written in the form  $I = I_{\max} \sin(\omega t - \varphi)$ ;

- or superpose the battery's current with a current of peak value  $I_{\max}$  and pulsation  $\omega$ , so  $i = I_{\max} \sin(\omega t)$ . This is the galvanostatic method, used in the laboratory and in real-life operation. If the current is of low amplitude, this disturbance leads to a sinusoidal voltage response whose amplitude  $V_{\max}$  and phase shift  $\varphi$  depend on the frequency  $f$ . The amplitude  $V_{\max}$  will only be proportional to the amplitude  $I_{\max}$  applied in the linear domain (small signals). This response can be written in the form  $v = V_{\max} \sin(\omega t + \varphi)$ .

From an experimental point of view, so as to remain in a linear domain, these applied stresses need to be low in amplitude (e.g. around 10% of the voltage or current). However, this amplitude needs to be significantly greater than the noise gate levels on the measuring device.

This characterization is often done by way of the galvanostatic method, because it is difficult to charge or discharge a battery to a given open-circuit voltage to obtain a given SOC. However, the SOC can be approximately calculated by integrating the current over time. In the case of lithium-ion

39 E. BARSOUKOV, J. R. MACDONALD (Eds), *Impedance Spectroscopy Theory, Experiment, and Applications*, Second Edition, John Wiley & Sons, Inc., 2005.

40 J.-P. DIARD, B. Le GORREC, C. MONTELLA, *Cinétique électrochimique*, Éditions Hermann, 1996.

technology, as the secondary reactions are practically non-existent, the galvanostatic method becomes more favorable than the potentiostatic method.

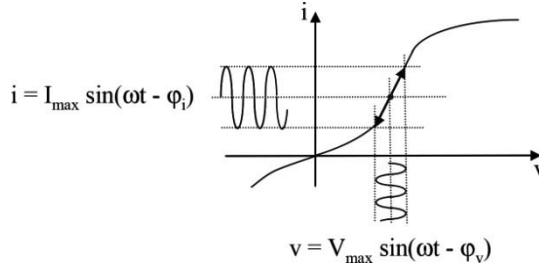


**Figure 2.8.** *Principle of electrochemical impedance spectroscopy at the level of an electrode*

Around the chosen point of operation, these two modes enable us to measure the impedance of the secondary battery for each frequency. For a given pulsation (or frequency), the impedance is defined by the formula:

$$Z(\omega) = |Z|e^{j\phi} \quad [2.16]$$

where  $|Z|$  is the modulus of the impedance and is given by the ratio  $\frac{V_{\max}}{I_{\max}}$  and  $\phi$  is the phase angle between the current and the voltage ( $\phi = \phi_i - \phi_v$ ).

We can also write:

$$Z(\omega) = |Z|(\cos \phi + j \sin \phi) \quad [2.17]$$

This impedance can be broken down into its real and imaginary parts, in the form:

$$Z(\omega) = Z_{\text{Re}} + jZ_{\text{Im}} \quad [2.18]$$

where:

$$Z_{\text{Re}} = \text{Re}(Z) = \frac{V_{\max}}{I_{\max}} \cdot \cos \phi \quad \text{and} \quad Z_{\text{Im}} = \text{Im}(Z) = \frac{V_{\max}}{I_{\max}} \cdot \sin \phi \quad [2.19]$$

Thus, the impedance is a complex value which depends on the frequency ( $f = \omega/2\pi$ ) and which is characterized either by a real and an imaginary part or by a module and a phase.

The complex impedance can be represented in two modes:

- on the Nyquist plot<sup>41</sup>, we represent  $-Im(Z)$  as a function of  $Re(Z)$ , using the pulsation or the frequency as a parameter (see Figure 2.9).

- on the Bode plot, we show the logarithm of the modulus  $|Z|$  and the phase  $\varphi$  as a function of the logarithm of the pulsation or frequency (Figure 2.10).

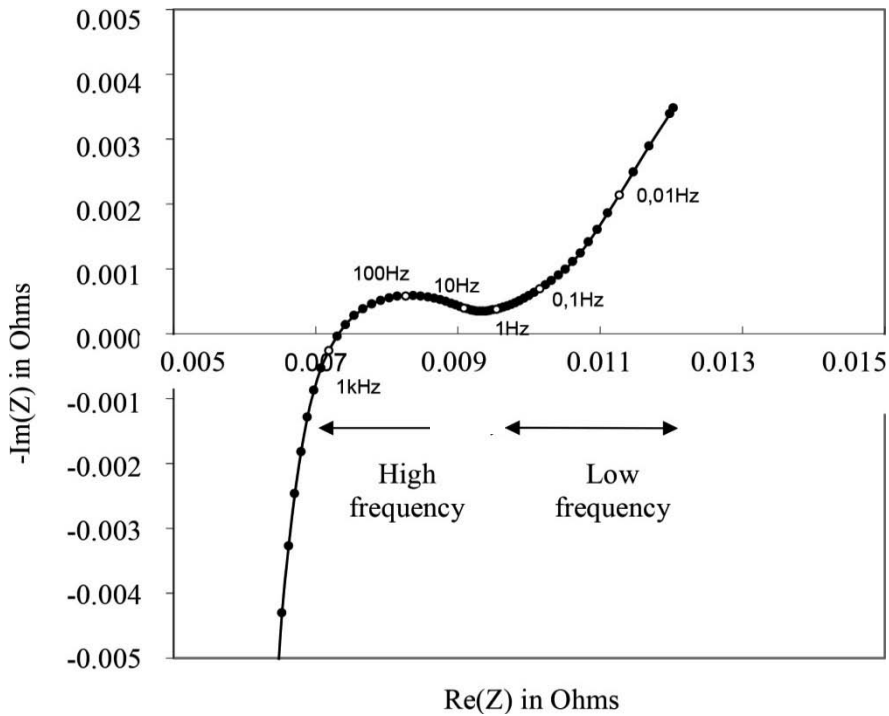


**Figure 2.9.** Impedance spectrum of a cylindrical lithium-ion graphite-NCA element with a 10 Ah capacity in the new and fully-charged state, represented on the Nyquist plot

<sup>41</sup> Electrochemists tend to represent this impedance on a Nyquist plot by changing the sign of the imaginary part.

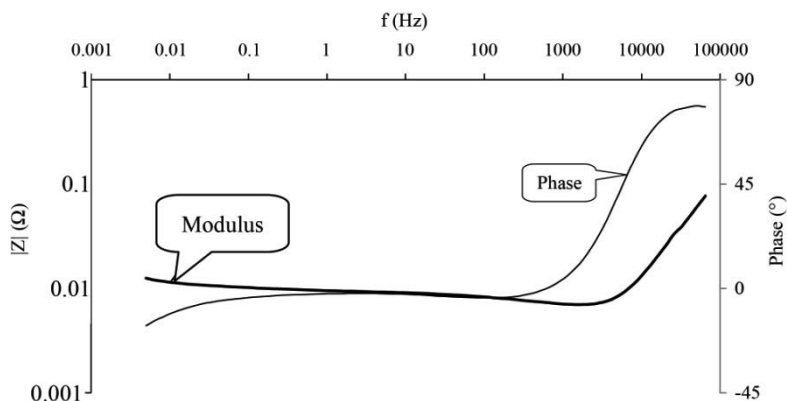


**Figure 2.10.** Impedance spectrum of a cylindrical lithium-ion graphite-NCA element with a 10 Ah capacity in the new and fully-charged state, represented on the Bode plot

The characteristic parameters of an impedance spectrum are determined by modeling the impedance spectrum as an equivalent electric circuit diagram. The complexity of the model is adapted, depending on the degree of precision sought.

#### 2.4.12.1. Simple model of an electrochemical cell

A simple model of an electrochemical cell, deduced from the theory of the double layer<sup>42</sup> at the electrode/electrolyte interface is represented in Figure 2.11. The resistance  $R$  represents the sum of the ohmic resistances of the electrolyte, the separators and the current collectors. The capacity  $C_{dl}$  represents the double layer capacity. The resistance  $R_{ct}$  is the charge transfer resistance.<sup>43</sup>

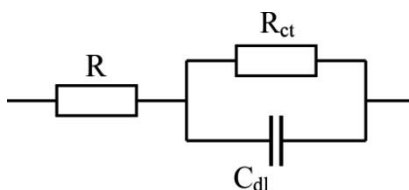


**Figure 2.11.** Simplified model of an electrochemical cell

<sup>42</sup> A double layer occurs at the electrode/electrolyte interface when the liquid carries electrical charges. A fuller explanation is given in section 2.10.

<sup>43</sup> More specifically, the values of these components depend on the polarization and on the amplitude of the “small” signals applied.

EXERCISE 2.3.— Calculate the impedance of the above circuit and represent it on a Nyquist plot (by inverting the sign of the imaginary part).

Indicate the frequencies for which we can determine the values of the two resistances.

*Solution on page 83*

On the Nyquist plot, the impedance of the dipole shown in Figure 2.11 can be represented as a semi-circle some distance apart from the origin (Figure 2.12).

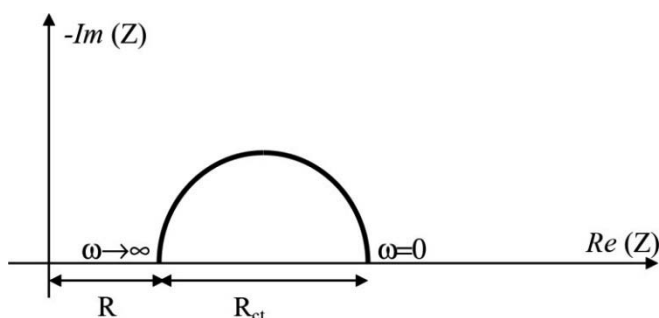


**Figure 2.12.** Representation of the impedance of an electrochemical cell

#### 2.4.12.2. Introduction of the Warburg impedance

Reality tells us that a simple model with two resistances and a capacitor is a long way from being capable of representing all of the phenomena observed. Indeed, experience shows that for very low frequencies, the curve does not stop at the point  $\{R + R_{ct}, 0\}$ . A line appears which symbolizes the phenomena of diffusion of ions in the materials of the electrodes (of the interfaces and/or the electrolyte). This is known as the Warburg line.<sup>44</sup> From an electrical point of view, we add a series impedance with  $R_{ct}$ . This impedance is determined using the laws of electrochemical diffusion. It is of the form  $A_W / \sqrt{j\omega}$ , where  $A_W$  is the Warburg coefficient.

Thus, it is a straight line at a  $45^\circ$  angle in an orthonormal framework (Figure 2.13).

<sup>44</sup> The Warburg resistance (and more generally the Warburg impedance) is explained clearly in the appendix to this chapter (section 2.11).

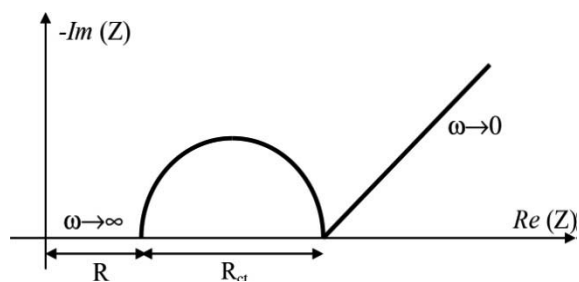


**Figure 2.13.** Representation of the impedance of an electrochemical cell with the Warburg line

Reality is often less simple. The transition between the semi-circle and the Warburg line may be more gentle (see the dashed line in Figure 2.14):

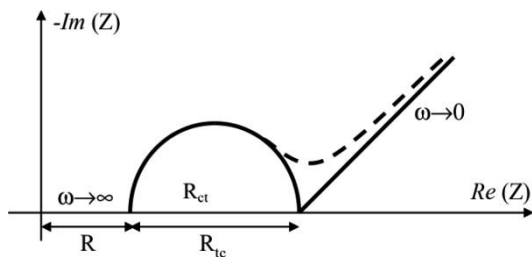


**Figure 2.14.** Representation of the impedance of an electrochemical cell with the deformed Warburg line

This is what we would see, for instance, on the real measurement of a fully-charged 10 Ah element (Figure 2.15).

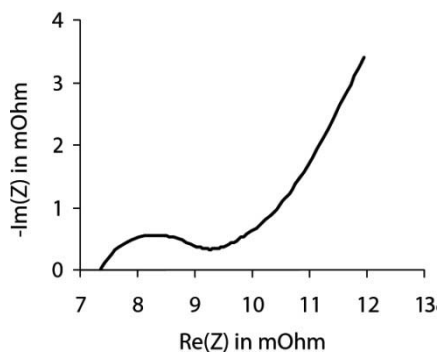


**Figure 2.15.** Measurement of the impedance of a Li-ion secondary battery with nominal capacity of 10 Ah

We also see the same shape trend of the complex impedance on smaller elements (Graphite/NMC with nominal capacity of 650 mAh) for SOC's greater than 20% (see Figures 2.16 and 2.17).

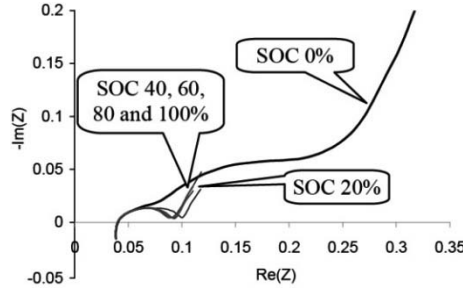


**Figure 2.16.** Real representation of the impedance of a lithium-ion Graphite/NMC element with nominal capacity 650 mAh in different states of charge (values in  $\Omega$ )

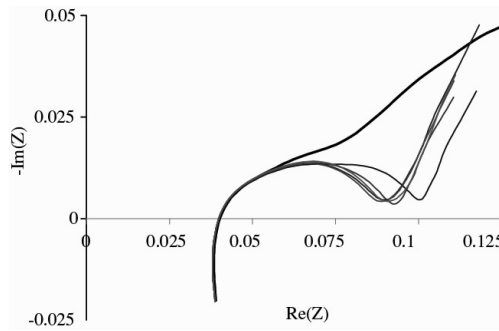


**Figure 2.17.** Extension of the impedance of a Graphite/NMC element with nominal capacity 650 mAh in different states of charge (values in  $\Omega$ )

Figure 2.16 shows that the impedance varies greatly when the secondary battery is almost fully discharged. Conversely, between 40 and 100% SOC, even on extended curves (Figure 2.17), these measurements are unable to serve as indicators of the SOC.<sup>45</sup>

<sup>45</sup> Smoothing of the impedance spectra, using an equivalent circuit model representative of the element, can help track the evolution of the electrical characteristics associated with these components on the basis of the SOC and the SOH, for instance. If this evolution is monotonous with the changing state of charge (or state of health), an indicator of the state of charge (or health) can be defined.

However, unlike other technologies, the impedance of a lithium-ion secondary battery using insertion materials (such as Graphite/NMC for instance, like the cell whose impedance is presented in Figure 2.16) does not vary significantly as a function of the SOC, except at the extremities of the SOC. Therefore it can only serve as an indicator of the end of charge or end of discharge.

This type of behavior in relation to the SOC limits the advantage to frequency analysis by impedance spectroscopy, as the charge and discharge can be monitored simply by measuring the voltage. However, the contribution of this technique is significant in terms of determining the state of health (SOH). A great deal of effort has been invested in developing effective indicators of SOH.

#### 2.4.12.3. Randles model

In order to further refine the simulation, we can choose more complex electrical models<sup>46</sup> interpreting the physico-chemical processes that take place on an electrode. Figure 2.18 illustrates the model put forward by Randles.<sup>47</sup>

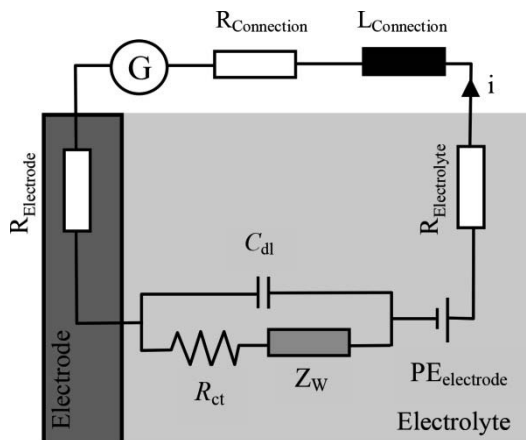


**Figure 2.18.** *Topology of the Randles model*

<sup>46</sup> The data given in this section are inspired by the doctoral thesis of K. DONG, Contribution à la modélisation dynamique des batteries lithium-ion pour l'application photovoltaïque et stockage connecté au réseau, INP Grenoble, 2010.

<sup>47</sup> J. E. B. RANGLES, "Kinetics of rapid electrode reactions", *Discuss Faraday Soc.*, 1, 11–19, 1947.



With this model, the equilibrium potential is represented by the ideal voltage source ( $PE_{\text{electrode}}$ ); the contribution of the electrolyte is represented by a resistance ( $R_{\text{electrolyte}}$ ); the behavior of the double layer (explained in Appendix 2.10) is associated with the capacity  $C_{\text{dl}}$ ; the kinetics of the electrochemical reaction is described by the charge transfer resistance ( $R_{\text{ct}}$ ); and finally the phenomenon of diffusion is modeled by the Warburg impedance ( $Z_{\text{W}}$ ). In order to take account of the connections, we introduce an ohmic resistance ( $R_{\text{connection}}$ ) and an inductance ( $L_{\text{connection}}$ ). The details of these elements are presented below:

- the equilibrium potential ( $PE_{\text{electrode}}$ ) is the difference between the potential of the electrode in question and that of a reference electrode with a open circuit. It is a function of the SOC;

- the ohmic resistance ( $R$ ) results from the contributions of the electrolyte ( $R_{\text{electrolyte}}$ ), the materials and their geometry ( $R_{\text{electrode}}$ ) and the electrical connections ( $R_{\text{connection}}$ ). Theoretically, this resistance could depend on the SOC, the history and the aging because of chemical and/or morphological changes in the active material, the electrode material and an altered concentration of electrolyte. It may also depend on the current circulating in the device. Its value can be determined quite simply by the intersection at high frequency between the measured impedance and the real axis;

- the inductance ( $L$ ) is due to the passage of the current through the electrical connectors, the electrodes and the electrolyte. This phenomenon is, of course, observable mainly at high frequencies. In the representation of the impedance on the Nyquist plot, it corresponds to a passage below the real axis which is visible in Figures 2.16 and 2.17;

- the element  $R_{\text{ct}}$  models the charge transfer resistance caused by the electrochemical reactions at the electrode/electrolyte interface;

- the element  $C_{\text{dl}}$  corresponds to the phenomena of charge and discharge of the double layer capacity;

- the Warburg impedance corresponds to the diffusion of the species. It has a noticeable effect only at very low frequencies (Figure 2.13) and is represented by a line at  $45^\circ$ ;

- finally,  $G$  represents a generator and/or a user charge.

The Warburg impedance is sometimes represented by the graphic shown in Figure 2.19.



**Figure 2.19.** Another symbol for the Warburg impedance

#### 2.4.12.4. Model with a constant-phase element

The double-layer capacity ( $C_{dl}$ ), which is a simple electrical capacity, is often represented by a nonlinear capacity or a *constant-phase element* ( $CPE_{dl}$ ) so as to adjust the difference of the electrochemical system from the ideal behavior of an electrical system. Indeed, the use of a simple capacity does not facilitate a perfect adjustment of the real and simulated spectra. The origin of this deviation from the ideal is essentially attributed to irregularities on the surface of the electrode (roughness, presence of impurities, variation in thickness or surface composition of the electrode).

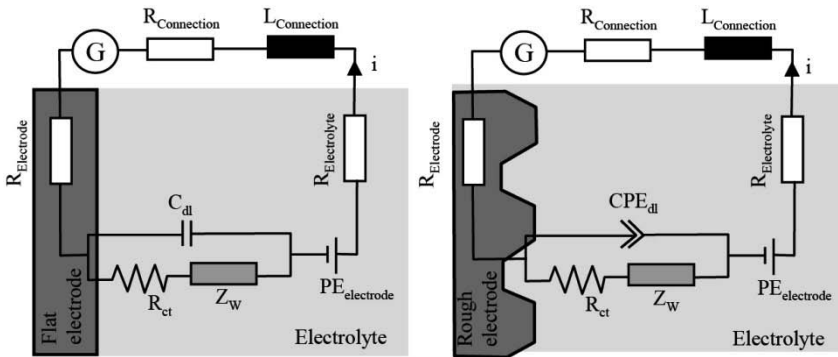


**Figure 2.20.** Topology of the Randles model with an ideal flat electrode (left) and a rough electrode (right)

A CPE is characterized by two parameters:  $Q$  and  $\alpha$ . Its impedance is written as:

$$Z_{CPE}(\omega) = \frac{1}{Q} \times \frac{1}{(j \cdot \omega)^\alpha} \quad [2.20]$$

Note that the CPE assumes a capacity of value  $Q$  when  $\alpha = 1$ .

On the Nyquist plot, the impedance of the circuit shown in Figure 2.18 is given in black in Figure 2.21. At high frequency, we again see the effect of

the inductance, and then the capacitor  $C_{dl}$  “short-circuits”  $R_{ct}$  and  $Z_W$ . The equivalent circuit can therefore be summed up as a simple resistance  $R$ , the sum of the resistances  $R_{electrolyte}$ ,  $R_{electrode}$  and  $R_{connection}$ . If we introduce a constant-phase element ( $CPE_{dl}$ ) instead of the capacity  $C_{dl}$ , the impedance is shown by the gray curve in Figure 2.21.

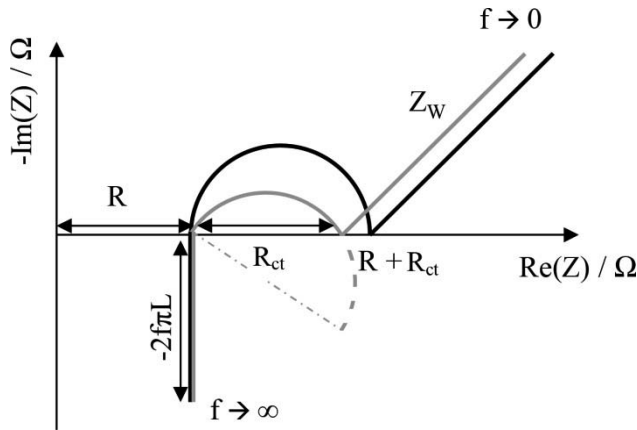


**Figure 2.21.** Nyquist impedance in the Randles model (model with  $C$  in black; model with  $CPE$  in gray)

#### 2.4.12.5. Example of how to measure the spectrum

An example of a real impedance spectrum obtained for a new, fully-charged Graphite-NCA coil element with 10 Ah is shown in Figure 2.22 in accordance with the Nyquist representation. This figure is identical to Figure 2.9 but with the addition of the components of the electrical model.

In a simplified manner, we again see:

- an inductive part for frequencies greater than 1 kHz;
- a high-frequency resistance  $R$  corresponding to the real part of the impedance for 900 Hz;
- a capacitive semi-circle between 1 kHz and 1 Hz corresponding to the electrochemical reactions usually linked to the charge transfer resistance;
- a line forming a  $45^\circ$  angle with the real axis corresponding to the diffusion for frequencies lower than 0.1 Hz.

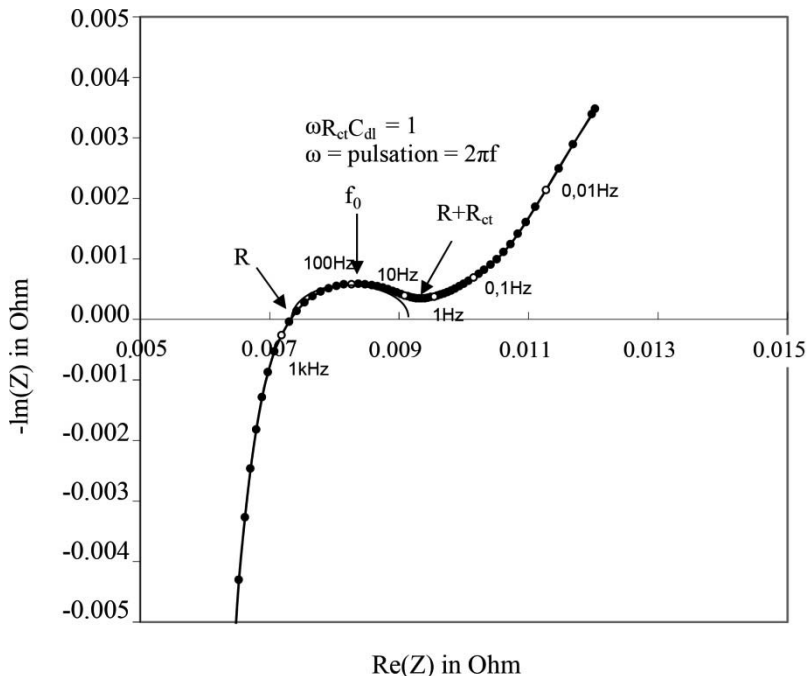


**Figure 2.22.** Impedance spectrum for a 10 Ah cylindrical graphite-NCA element in the new and fully-charged state, shown on the Nyquist plot

#### 2.4.12.6. Determination of the elements of the spectrum for a whole cell

Above, the models were applied to a single electrode. To model a complete cell (or element), we repeatedly use one of the above models, which is connected in a series as indicated in Figure 2.23. In this model, account has been taken of the fact that there are various sizes of particles in an electrode, by placing in parallel two circuits  $R_C$  and  $W_C$  in series at the cathode.

Measuring devices combined with software suites can be used to find the values of the elements in the model. Depending on the number of elements chosen, we can obtain a nearly-ideal *curve fitting* of the impedance spectra, but the electrochemical meaning of the electrical components integrated into the electrical circuit is not always obvious. An example of this is given in Figure 2.24, for which we have chosen a model of the following form:

$$L_0 + R_1 + Q_2/R_2 + Q_3/R_3 + Q_4/R_4 + Q_5/(R_5 + W_5) \quad [2.21]$$

where  $L_0$  and  $R_1$  represent the total inductance and resistance of the circuit,  $Q_x$  the constant-phase elements,  $R_2$ ,  $R_3$ ,  $R_4$  and  $R_5$  the resistances and  $W_5$  the Warburg impedance.

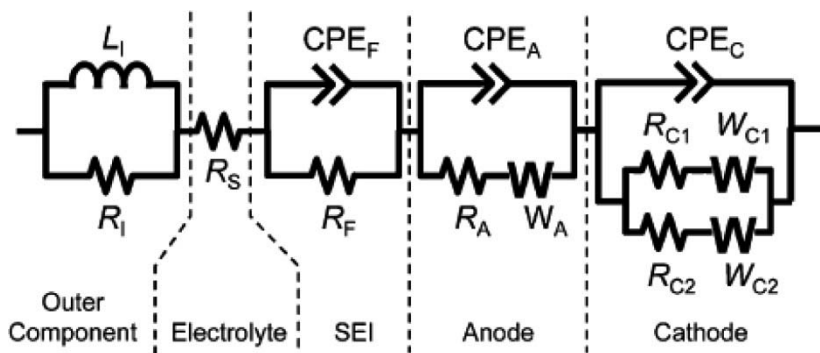


**Figure 2.23.** Example of an electrical model of the impedance of an electrochemical cell<sup>48</sup>  
 Symbols: F – passivation Film (SEI); A – Anode; C – Cathode

In Figure 2.24, the heavily-drawn curve is properly superimposed onto the measured points. The two points represented by the circles indicate the ends of the domain of variation in frequencies used for the fitting of the parameters of the model.

Once the frequency sweep has been carried out, the software iteratively calculates the values of the elements in the model. For the example shown in Figure 2.24, it finds:

$$\begin{aligned}
 L_0 &= 0.1144 \mu\text{H} \text{ and } R_1 = 19.72 \text{ m}\Omega \\
 R_2 &= 27.93 \text{ m}\Omega; Q_2 = 1.702 \text{ F}\cdot\text{s}^{\alpha-1} \text{ and } \alpha_2 = 0.4184 \\
 R_3 &= 32.01 \text{ m}\Omega; Q_3 = 0.1081 \text{ F}\cdot\text{s}^{\alpha-1} \text{ and } \alpha_3 = 0.3695 \times 10^{-9} \\
 R_4 &= 24.73 \text{ m}\Omega; Q_4 = 1.942 \text{ F}\cdot\text{s}^{\alpha-1} \text{ and } \alpha_4 = 0.9223 \\
 R_5 &= 289.6 \text{ m}\Omega; Q_5 = 244.1 \text{ F}\cdot\text{s}^{\alpha-1} \text{ and } \alpha_5 = 0.7364 \\
 s_5 &= 519.2 \Omega\cdot\text{s}^{-1/2}
 \end{aligned}$$

48 D. MUKOYAMA, T. MOMMA, H. NARA, T. OSAKA, “Electrochemical impedance analysis on degradation of commercially available lithium ion battery during charge/discharge cycling”, *Chem. Lett.*, 41, 444–446, 2012.

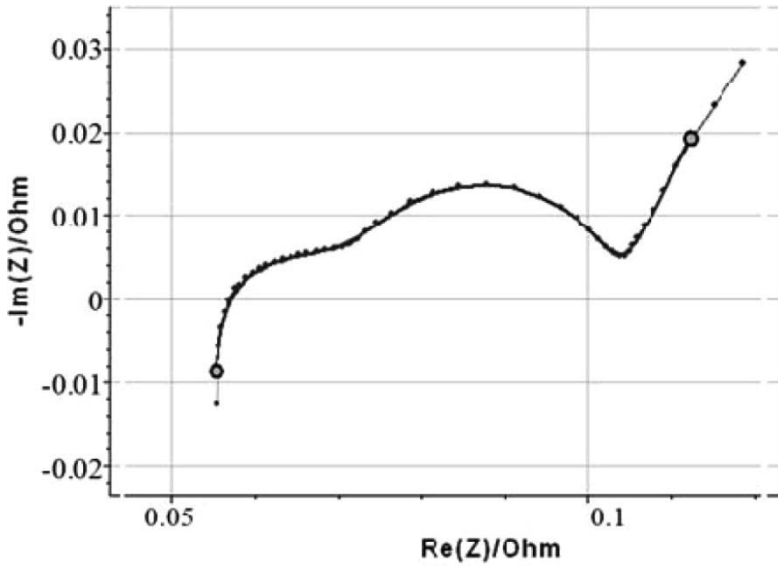


**Figure 2.24.** Example of curve fitting for an impedance spectrum of a Graphite/NMC element with nominal capacity 650 mAh at 20% SOC obtained by the software, fed into the VMP3 testing array made by the company Bio-logic

#### 2.4.13. Stored energy and deliverable energy

The theoretical stored energy is that which is determined only on the basis of the active material. Due to its definition, stored energy does not depend on the discharge current amplitude. Given that not all the active material is fully “delithiable” or electrically accessible (poor conductivity of certain materials such as lithium iron phosphate, LFP), this theoretical stored energy is not fully recoverable.

From the point of view of a user, the stored energy that we consider is that which is delivered by a battery during a complete discharge. It depends on the discharge conditions both in terms of the level of capacity and the losses associated with the discharge. It is referred to as the deliverable energy or the practical stored energy, or quite simply the stored energy. It is equal to the integral of the product  $u \cdot i$ , applied here over the total duration of the discharge:

$$W_{\text{deliverable}} = \int_{(\text{total duration of discharge})} u \cdot i \, dt \quad [2.22]$$

Although the SI unit of energy is the Joule (J), electrotechnicians and electrochemists prefer to use the Wh or kWh because they work in W or kW over durations of discharge which are usually expressed in hours.

REMINDER 2.2.-

$$1 \text{ Wh} = 3600 \text{ Ws} = 3600 \text{ J.}$$

We can, of course, look at the energy already discharged during a partial discharge. In this case it will be the integral of the product  $u \cdot i$  applied over the duration in question:

$$W_{\text{already discharged}} = \int_{(\text{duration in question})} u \cdot i \, dt \quad [2.23]$$

If the voltage at the terminals of the secondary battery is constant (which is a commonly-used hypothesis to switch from a capacity value to an energy value) and the value  $U$ , the expression of the energy can be written as:

$$W_{\text{deliverable}} = \int_{(\text{total duration of discharge})} U \cdot i \, dt = U \int_{(\text{total duration of discharge})} i \, dt \quad [2.24]$$

The term  $\int_{(\text{total duration of discharge})} i \, dt$  represents the capacity of the secondary battery.

Therefore, we can write that the energy is the product of the voltage at the terminals of the secondary battery by its capacity. For instance, a secondary battery with nominal voltage 11.1 V and capacity 5 Ah stores 55.5 Wh of energy.

#### 2.4.14. Gravimetric energy density

The gravimetric energy density is the ratio of the energy deliverable with a given current to the mass of the secondary battery. The gravimetric energy density is expressed in Wh/kg. It is of course necessary to specify the discharge current in which the secondary battery is discharged.

Using the same hypothesis of constant voltage as in the previous section, we can write that the gravimetric energy density is the product of the voltage at the terminals of the secondary battery by its gravimetric capacity.

This notion is particularly useful for the sizing of a battery in on-board systems where the mass is a crucial design criterion. It can also be used to compare different electrochemical storage technologies between themselves, or even totally different storage technologies, in a given discharge current.<sup>49</sup>

#### 2.4.15. *Volumetric energy density*

The volumetric energy density is the ratio of the energy deliverable with a given current to the volume of the secondary battery. The volumetric energy density is expressed in Wh/m<sup>3</sup> or Wh/dm<sup>3</sup>. Here, again, it is necessary to specify the discharge current in which the secondary battery is discharged.

This notion is useful for the sizing of a stationary battery because, in these applications, the volume is often a more important criterion than the mass. It can also be used to compare different storage technologies in a given discharge current.

#### 2.4.16. *Specific energy*

The term *specific energy* is used indiscriminately for gravimetric energy density and volumetric energy density.<sup>50</sup> Similarly, as with the specific

---

<sup>49</sup> Electrochemical secondary batteries exhibit a greater gravimetric energy density (in Wh/kg) than do supercapacitors, but the gravimetric power (in W/kg, see the definition in section 2.4.17) of supercapacitors is greater than that of secondary batteries. It is possible to design batteries so that they perform better in terms of power, but this is done at the expense of their gravimetric energy density (section 6.2.2). In general, therefore, secondary batteries are better suited to long discharges whereas powerful supercapacitors are better adapted for rapid discharges. Thus, there is the possibility of complementarity of the storage (short term/long term). Note that the operational behavior of a capacitor (or supercapacitor) and a secondary battery are different. During discharge (or respectively charge), the voltage at the terminals of a capacitor decreases (or respectively increases) when we extract (or respectively inject) energy, because it is expressed in  $\frac{1}{2} CV^2$ . In a secondary battery, the voltage is much more constant.

<sup>50</sup> The term “energy density” is also used indiscriminately to speak of the gravimetric energy density and volumetric energy density.



capacity, the density of the materials is not identical for all secondary battery technologies, so the two quantities are not really connected. Depending on the applications, it is the consideration of one or other of these two values which is meaningful. This ambiguity can be overcome by looking at the unit associated with the quoted figures. This term can easily be avoided by using the term *ad hoc*.

#### 2.4.17. Gravimetric power and volumetric power

The gravimetric (or respectively volumetric) power is the power per unit mass (or respectively volume) that can be supplied by the secondary battery under certain conditions. It may be a question of the maximum power (e.g. that achieved in starter batteries for a short duration) or the maximum acceptable power over a certain duration for reasons of heat, for instance.

The gravimetric power is expressed in W/kg. The volumetric power is expressed in W/m<sup>3</sup> or W/dm<sup>3</sup>.

Behind these notions, the basic idea is to determine a device's ability to withstand for a predefined duration, when subjected to the current indicated by the manufacturer specifications. The maximum volumetric and gravimetric powers are therefore linked to the internal resistance.

Depending on the applications, these definition conditions may be very different. For instance, we can specify the amplitude of current and the duration<sup>51</sup>, i.e. the percentage capacity (or discharge) with which this power is obtained. We can also define a pulsed gravimetric power or volumetric power over, say, 2 seconds or 30 seconds. In these tests, it is also necessary to specify which SOC (defined in section 2.4.2) the element is in at the beginning of the test (e.g. half-charged) and if this SOC has been reached after a charge or a discharge, etc.

We may also be interested in a gravimetric or volumetric power over a complete discharge. These values will be labeled as "average" because the power varies throughout the course of that discharge.

---

<sup>51</sup> The current and the time are values which are directly accessible, whereas the amount of electricity and, *a fortiori*, the percentage capacity, require calculations to be performed.

We can also specify a minimum discharge voltage or a percentage of the no-load voltage.

As one might imagine from the previous sections, this maximum power is heavily dependent upon the measuring conditions. It is not a notion which is as characteristic of a technology as, say, the capacity.

## 2.5. Faradaic efficiency

The faradaic efficiency (sometimes referred to as the coulombian efficiency or coulombic efficiency) over a charge/discharge cycle is the ratio between the number of electrons delivered (or the amount of electricity delivered) and the number of electrons (or amount of electricity) injected into the secondary battery.

From the user's point of view, the faradaic efficiency is the product of a discharge efficiency by a charge efficiency. Without some means of internal analysis, there is no way of separating the two.

The faradaic efficiency must be considered over a discharge/charge cycle. If, by a rapid discharge, less electricity is extracted than by a slow discharge, less electricity will need to be injected during the next recharge.

For lithium elements functioning normally, there is neither electrolysis nor any other secondary reactions. Thus, for a lithium secondary battery in such a case, the faradaic efficiency is almost equal to 1 both during charging and discharging, if the element is in a good state.<sup>52</sup> When the faradaic efficiency becomes less than 1, it may be a sign of an irreversible consumption of current. Many reactions may be involved, which are caused by the imbalance between the capacities of the two electrodes in terms of aging. For instance, at the end of charge, if the negative electrode presents a capacity deficit, the derivative of the potential of the negative electrode may reach the domain of potential where metallic deposition of lithium becomes possible. This deposition of metal lithium may not be re-oxidized during the next discharge (very dispersed deposition, loss of electrical contact between

---

<sup>52</sup> Here, we are indeed dealing with an element with no associated electronics. In reality, this situation is rare with lithium technologies because, usually, the elements are connected in a pack including a battery management system (BMS) which consumes current and degrades the faradaic efficiency as seen by an outside observer.

metal grains). Conversely, at the end of discharge, the voltage of the negative electrode may veer toward potentials where the dissolution of the SEI can occur. Some of the recharging current will be used to re-form the SEI.

## 2.6. Self-discharge

After a charge, even if the secondary battery is not subjected to a forced discharge, the fully-charged state is never completely reached. Indeed, the secondary batteries experience self-discharge phenomena. Independently at each electrode, these self-discharge phenomena are associated with redox reactions (parasitic reactions), which are fed by the discharge reaction of the electrode itself. Given that this is a chemical reaction, the higher the temperature, the greater the self-discharge.

In the case of lithium secondary batteries using a graphite negative electrode, self-discharge occurs all the more quickly when the SOC is high, because it is essentially due to the reactivity of the negative electrode in relation to the electrolyte. In the charged state, the negative electrode is lithiated and therefore presents a very high reductive potential (nearly 0 V versus<sup>(53)</sup>  $\text{Li}^+/\text{Li}$ ). There is oxidation/reduction of the inserted lithium, reacting with the molecules of solvent (or lithium salt). Some of the lithium will be irretrievably lost, which – in addition to the self-discharge – leads to an irreversible decrease in the capacity of the element.

The supply of a BMS consumes an electrical current, which discharges the secondary battery. An outside observer will also perceive this consumption as a self-discharge.

---

53 The potential of an electrode can only be defined in relation to that of another electrode. In chemistry, it is often measured in relation to the NHE (the Normal Hydrogen Electrode, defined in footnote 58). For lithium secondary batteries, we rather take a reference electrode of metal lithium. Therefore we use the notation  $XV \text{ versus } \text{Li}^+/\text{Li}$ , which denotes a difference of potential of  $X$  volts versus (*versus*) a metal lithium electrode. Alternatively, we use  $YV \text{ versus NHE}$ , which means a difference of potential of  $Y$  volts *versus* a normal hydrogen electrode. We also find the notation  $YV/\text{NHE}$ .

Lithium is  $-3.05V \text{ versus the NHE}$ .

## 2.7. Acceptance current

During the process of charge, the current that a secondary battery can accept for its recharge *per se* is limited by the kinetics<sup>54</sup> of the internal electrochemical reactions.

The notion of acceptance is not used in the same way for all types of secondary batteries. For a lithium secondary battery, there is no secondary reaction in the normal operational domain of potential. Similarly, the electrolyte is not involved in the main electrochemical reactions. Therefore, the notion of acceptance current does not hold as much interest as the case of lead-acid batteries, for instance, where we see problems of the diffusion of ions in the electrolyte around the active sites at which the electrochemical reaction is taking place. These secondary batteries are also characterized by the fact that electrolysis of water is in competition with the main charge/discharge electrochemical reactions. However, even for a lithium battery, this notion may be useful if it is linked to an initial operating temperature. In certain use conditions, the application of too strong a current may lead to significant increases in the temperature in the secondary battery, and excess potential at the level of the electrodes, with lithium deposition, for example. Exceeding the current acceptable to the element may, in extreme cases, lead to a temperature surge or an explosion. To avoid this risk, the charge voltage is limited so as to reduce the current being injected. We then note that the charging current at an imposed voltage decreases as the secondary battery is recharged.

Therefore, the acceptance current is, for a given voltage imposed on the secondary battery, this maximum effective charging current.

This acceptance current assumes a different meaning for lithium-ion elements with an alloy-based negative electrode. Indeed, at the beginning of the charging process, the alloy is de-lithiated and the diffusion of lithium into the metal is very slight, so it is preferable to apply a weak current. Then, as the amount of lithium increases, the diffusion also increases and the element becomes capable of accepting a stronger current. The risk of too rapid a charge, compounded by low operating temperatures (low diffusion

---

<sup>54</sup> Kinetics denotes the rate of the chemical reactions, knowing that they are limited because the reactions cannot be instantaneous.

coefficients at low temperature) is the deposition of metal lithium and the formation of dendrites (see section 4.4.2).

It should also be noted that the very design of the electrodes can have an influence on the acceptance current of the element. For the same electrochemical couple, the acceptance current will be different if the cells are designed to deliver energy (lesser acceptance current) or power (greater acceptance current).

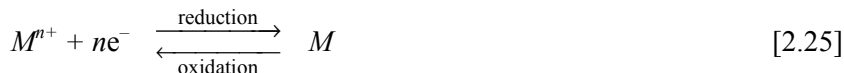
## 2.8. Conclusion

The characteristics defined above are illustrated and quantified in the following chapters for each of the secondary battery technologies being examined. Therefore, we have defined the majority of terms specific to secondary battery. When other technical terms relating to materials chemistry or organic/inorganic chemistry are employed, they will be explained in a footnote with a view to pedagogy and comprehension. We have also made references to scientific publications so that the reader can refer to these works if further or more in-depth explanations are required. We have attempted to cite the most significant references in the various domains touched upon, but certain major references may have been overlooked in spite of this intention, given the diversity of the topics and technologies discussed. We apologize to those authors for that oversight.

## 2.9. Appendix 1: Nernst's law

### 2.9.1. Redox potential of an electrode<sup>55</sup>

When we introduce a metal  $M$  into a solution containing  $M^{n+}$  ions, a thermodynamic equilibrium is established which involves an oxidation reaction between the metal  $M$  and a reduction reaction with the electro-active species  $M^{n+}$  in solution:




---

<sup>55</sup> More detailed electrochemical discussions can be found in J. ROBERT, J. ALZIEU, "Accumulateurs. Considérations théoriques", *Techniques de l'ingénieur*, D 3 351, 2005.

which is a particular case of the more general redox equation:



This reaction is characterized by the thermodynamic potential for oxidation-reduction (also known as the redox potential) notated  $E$  (in volts). This value enables us to predict the reactivity of the chemical species with one another. The thermodynamic potential of an Ox/Red couple ( $E_{\text{Ox/Red}}$ ) is expressed in volts versus a reference value, often given by the potential of a Normal Hydrogen Electrode (NHE), which gives the unit V/NHE used in electrochemical publications. By convention, the potential of the NHE (the proton/hydrogen  $\text{H}^+/\text{H}_2$  couple) has been chosen as the origin of the potentials<sup>56</sup> and is therefore equal to 0 ( $E_{\text{NHE}}^0 = 0 \text{ V}$ ) in standard conditions (represented by the exponent<sup>0</sup>) of temperature (298 K or 25°C), concentration (1 mol/L) and pressure (101325 Pa or 1 atm). Chemists use tables which give the standard potentials  $E_{\text{Ox/Red}}^0$  measured in standard pressure and temperature conditions in relation to this Normal Hydrogen Electrode (examples are given in section 4.4.1).

Finally, by convention, the choice is made to associate the negative sign with the redox potential of reduction reactions.

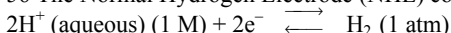
### 2.9.2. Electromotive force of an electrochemical cell

The voltage of an electrochemical cell is a thermodynamic order of magnitude: it is the difference in potential which is established, with a current of strictly zero, between the two electrodes. The absolute value (i.e. regardless of the sign) is called the electromotive force of the cell (emf) and is notated as  $\Delta E$ :

$$\Delta E = E_1 - E_2 \text{ where } E_1 > E_2 \text{ by convention} \quad [2.27]$$

---

<sup>56</sup> The Normal Hydrogen Electrode (NHE) corresponds to the following redox reaction:



It corresponds to the cell:  $\text{Pt}/\text{H}_2 (\text{gaseous})/\text{H}_3\text{O}^+$  with a concentration of hydronium ions  $\text{H}_3\text{O}^+$  equal to 1 mol/L.

Its potential is taken as a reference in standard conditions: temperature 298 K (25°C) and pressure 101,325 Pa (1 atm).

In standard conditions, the electromotive force measured is called the standard electromotive force standard and notated at  $\Delta E^\circ$ .

### 2.9.3. Nernst's law

We have just defined the electromotive force of an electrochemical cell for standard conditions. Yet these conditions are not very realistic, or at least are very limited in terms of a chemical reaction during which the concentrations of the reagents are different from standard conditions or change.

Nernst's law enables us to express the emf as a function of the concentrations of the species, and of the temperature outside of standard conditions.

Consider the electrochemical half-reaction:



The determination of Nernst's law involves thermodynamic notions. We use the free enthalpy<sup>57</sup> (Gibbs function) notated as  $\Delta G$ . Taking  $n$  moles of electrons to be involved in the chemical reaction, we get:

$$\Delta G = -n.F.E_{\text{Ox1/Red1}} \quad [2.29]$$

where  $\Delta G$  is the free enthalpy [J],  $n$  the number of moles of electrons exchanged,  $F$  Faraday's constant ( $F = 96,485 \text{ C.mol}^{-1}$  calculated in section 2.3.3.2) and  $E_{\text{Ox1/Red1}}$  the thermodynamic redox potential of the reaction with no current (in V or  $\text{J.C}^{-1}$ ).

---

<sup>57</sup> The free enthalpy is the most appropriate energetic function for examining the chemical equilibria established at constant temperature and pressure. The free enthalpy is an energy. Its unit is, naturally, the joule.

We can show (1<sup>st</sup> and 2<sup>nd</sup> principles of thermodynamics) that, for a thermodynamically reversible reaction,  $dG = V.dP - S.dT + \delta W$ , where  $T$  is the absolute temperature (in K),  $S$  is the entropy (in J/K),  $P$  is the pressure (in  $\text{N/m}^2$ ),  $V$  is the volume (in  $\text{m}^3$ ) and  $\delta W$  is the external work (in J), which in this case is the electrical energy delivered to the external circuit. For a finite, reversible transformation, therefore with zero or near-zero current (the voltage that then needs to be considered is the emf), at constant temperature and pressure, we then get  $\Delta G = -E.i.dt = -W_{\text{electrical delivered}} = -n.F.E$ .

If standard conditions of pressure, temperature and concentration are fulfilled, we write:

$$\Delta G^0 = -n.F. E_{\text{Ox1/Red1}}^0 \quad [2.30]$$

Nernst's law is given by the relation:

$$\Delta G = \Delta G^0 + RT.\ln(K) \quad [2.31]$$

where  $R$  is the ideal gas constant ( $R = 8.314 \text{ J.mol}^{-1}.\text{K}^{-1}$ ),  $T$  is the absolute temperature (in Kelvin) and  $K$  is the thermodynamic equilibrium constant of reaction [2.28] given by the relation:

$$K = \frac{a_{\text{Red1}}^b}{a_{\text{Ox1}}^a} \quad [2.32]$$

where the  $a_x$  represent the activities of the species, which will be explained in detail later on (section 2.9.4).

By combining the previous relations, we can write:

$$nFE = nFE^0 - RT.\ln K \quad [2.33]$$

$$E = E^0 - \frac{RT}{nF} \ln K \quad [2.34]$$

This gives us:

$$E = E^0 - \frac{RT}{nF} \ln \frac{a_{\text{Red1}}^b}{a_{\text{Ox1}}^a} \quad [2.35]$$

For  $T = 298 \text{ K}$  ( $T = 25^\circ\text{C}$ ):

$$\frac{RT}{F} = \frac{8.314 \times 298}{96485} = 0.0257 \text{ V} \quad [2.36]$$



After transformation of the natural logarithm into a decimal logarithm [ $\ln(x) = 2.3 \log(x)$ ], we obtain the following expression:

$$E = E^0 - \frac{0.059}{n} \log \frac{a_{\text{Redl}}^b}{a_{\text{Oxl}}^a} \quad [2.37]$$

This Nernst equation is given for the simplest of electrochemical reactions (equation [2.28]). In general, the electrochemical reactions involve other species, so we have to include their activities in the calculation.

#### 2.9.4. Activity of the species

The activity  $a_i$  of a species  $i$  is expressed as a function of the nature of the species under discussion. It is a dimensionless value.

– in the case of a compound in a gaseous mixture, the activity is expressed in the form:

$$a_i = \gamma_i \frac{P_i}{P^0} = \frac{f_i}{P^0} \quad [2.38]$$

where  $\gamma_i$  is the dimensionless activity coefficient ( $0 < \gamma_i < 1$ ) of the species  $i$ ,  $P_i$  is the partial pressure of the gas and  $P^0$  standard pressure (both pressures will be expressed in the same unit. By convention,  $P^0 = 1 \text{ atm}$ ). The quantity  $f_i = \gamma_i \cdot P_i$  has the dimension of a pressure and is called the fugacity.

In the case of an ideal solid or liquid solution, the activity of the compound belonging to that solution is expressed by:

$$a_i = x_i \quad [2.39]$$

where  $x_i$  is the molar fraction of the compound. Consequently, the activity of a pure, monophasic compound is equal to one unit, with its molar fraction being equal to 1. By extension, the activity of the solvent in a dilute solution is taken to be equal to the unit, because its molar fraction is approximately 1. If the solution is concentrated (dissolved species = solute at a concentration greater than 0.05 mol/L), the molar fraction is not equal to the unit and therefore needs to be calculated.

When, in a solution, the compound is not in a single phase, its activity  $a_i$  is expressed by:

$$a_i = \gamma_i \cdot x_i \quad [2.40]$$

In the case of a dissolved species (in low concentration), the activity is normally expressed by:

$$a_i = \gamma_i \frac{C_i}{C^0} \quad [2.41]$$

where  $C^0$  is the standard molarity of the species (1 mol/L) and  $C_i$  is the concentration of the species  $i$  (in mol/L).

When the concentration of the compound in its phase is low (a solute in a solvent in the case of a liquid solution), its activity coefficient  $\gamma_i$  is near to 1. This means that the activity becomes equal to the ratio of its concentration to the reference concentration. For an electrolyte, as long as the concentrations are greater than 0.05 mol/L, the expression as a function of the concentrations involves too high a degree of approximation. Therefore we need to take account of the activity coefficient.

It should be noted that, in the literature, we often see confusion between  $a_i$  and  $C_i$ , because  $C^0$  is 1 (mol/L). In fact, instead of writing a logarithm of a concentration, we should – strictly speaking – write  $\log(C_i/C^0)$  so that the argument of the logarithm becomes a dimensionless number.

### **2.9.5. Example of the application of Nernst's law to a lithium secondary battery using the insertion mechanism<sup>58, 59</sup>**

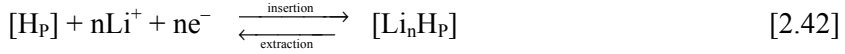
Nernst's law, which we discussed above, refers to an electrode. In the case of an entire secondary battery, we look first at one electrode and then at the other. The emf will be deduced from the element  $\Delta E$  by an algebraic sum of the values obtained on each of the two electrodes  $E_{(+)}$  and  $E_{(-)}$  in accordance with equation [2.27].

---

58 S.A. HASHIM ALI, "Thermodynamic analysis of lithium ion cells", *Ionics*, 11, pp. 410-413, 2005.

59 D. K. KARTHIKEYAN, G. SIKHA, R.E. WHITE, "Thermodynamic model development for lithium intercalation electrodes", *Journal of Power Sources*, 185, 1398-1407, 2008.

In a lithium-ion secondary battery, the electrochemical reactions take place in the solid compound within which the phenomenon of insertion/extraction occurs. Thus, we need to introduce the notions of sites available in the host material and of intercalated species:



where  $[\text{H}_p]$  is the vacant insertion site available for intercalation into the host material and  $[\text{Li}_n\text{H}_p]$  are the intercalated species.

Nernst's law can be formulated on the basis of expression [2.37]:

$$E = E^0 - \frac{0.059}{n} \log \frac{a_{[\text{Li}_n\text{H}_p]}}{a_{[\text{H}_p]}} \quad [2.43]$$

We are dealing with a solid solution with two compounds present. Their reactivity is expressed by:

$$a_{[\text{Li}_x\text{H}_p]} = \gamma_{[\text{Li}_x\text{H}_p]} \cdot x_{[\text{Li}_x\text{H}_p]} \quad [2.44]$$

$$a_{[\text{H}_p]} = \gamma_{[\text{H}_p]} \cdot x_{[\text{H}_p]} \quad [2.45]$$

Thus:

$$E = E^0 - \frac{0.059}{n} \log \frac{\gamma_{[\text{Li}_n\text{H}_p]} \cdot x_{[\text{Li}_n\text{H}_p]}}{\gamma_{[\text{H}_p]} \cdot x_{[\text{H}_p]}} \quad [2.46]$$

$$E = E^0 - \frac{0.059}{n} \log \frac{x_{[\text{Li}_n\text{H}_p]}}{x_{[\text{H}_p]}} - \frac{0.059}{n} \log \frac{\gamma_{[\text{Li}_n\text{H}_p]}}{\gamma_{[\text{H}_p]}} \quad [2.47]$$

The deviation from ideal behavior is associated with the last term in the above equation, which represents the interaction between the lithium ions and the host matrix during the processes of insertion/extraction. Indeed, in the ideal case, the activity is equal to the molar fraction (considering the activity coefficient  $\gamma_i = 1$ ) and we again see the classic representation of Nernst's law with  $x_{[\text{Li}_n\text{H}_p]}$  being the molar fraction of  $[\text{Li}_n\text{H}_p]$  and  $x_{[\text{H}_p]}$  the molar fraction of  $[\text{H}_p]$ :

$$E = E^0 - \frac{0.059}{n} \log \frac{x_{[Li_nH_p]}}{x_{[H_p]}} \quad [2.48]$$

where  $E^0$  is the standard electrochemical potential and  $x_{[H_p]}$  and  $x_{[Li_nH_p]}$  are the molar fractions of vacant sites available for intercalation into the host material  $[H_p]$  and of the intercalated species  $[Li_nH_p]$  such that:

$$x_{[H_p]} + x_{[Li_nH_p]} = 1 \quad [2.49]$$

$$\text{where } x_{[H_p]} = \frac{n_{[H_p]}}{n_{[H_p]} + n_{[Li_nH_p]}} \quad \text{and} \quad x_{[Li_nH_p]} = \frac{n_{[Li_nH_p]}}{n_{[H_p]} + n_{[Li_nH_p]}} \quad [2.50]$$

$$E = E^0 - \frac{0.059}{n} \log \frac{x_{[Li_nH_p]}}{1 - x_{[Li_nH_p]}} \quad [2.51]$$

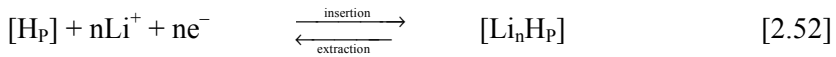
Considering:

$n_{[H_p]}$ : number of moles of sites available at time  $t = 0$ ;

$n_{[Li_nH_p]}$ : number of moles of intercalated sites at time  $t_1 > 0$   
(corresponding to the progression of the reaction);

$n_{[H_p]} - n_{[Li_nH_p]}$ : number of sites vacant at time  $t_1$

and taking reaction [2.42] (rewritten below):



we can write for both times  $t_0 = 0$  and  $t_1 \neq 0$ :

|           |                             |  |                 |
|-----------|-----------------------------|--|-----------------|
| $t_0 = 0$ | $n_{[H_p]}$                 | $\xrightleftharpoons[\text{extraction}]{\text{insertion}}$ | 0               |
| $t_1$     | $n_{[H_p]} - n_{[Li_nH_p]}$ | $\xrightleftharpoons[\text{extraction}]{\text{insertion}}$ | $n_{[Li_nH_p]}$ |

$$\text{At } t_1, x_{[H_p]} = \frac{n_{[H_p]} - n_{[Li_nH_p]}}{n_{[H_p]}} : x_\beta = \frac{n_\beta - n_\alpha}{n_\beta} \text{ and } x_\alpha = \frac{n_\alpha}{n_\beta} x_{[Li_nH_p]} = \frac{n_{[Li_nH_p]}}{n_{[H_p]}} \quad [2.53]$$

On the basis of expression [2.51], we can write:

$$E = E^0 - \frac{0.059}{n} \log \frac{\frac{n_{[Li_nH_p]}}{n_{[H_p]}}}{\frac{n_{[H_p]} - n_{[Li_nH_p]}}{n_{[H_p]}}} \quad [2.54]$$

and considering the degree of insertion notated  $Xi$  (with an uppercase  $X$  to differentiate it from the molar fraction  $x_i$ ):

$$Xi = \frac{n_{[Li_nH_p]}}{n_{[H_p]}} \quad (0 < Xi < 1) \quad [2.55]$$

$$E = E^0 - \frac{0.059}{n} \log \frac{Xi}{1-Xi} \quad [2.56]$$

However, in most lithium-ion secondary batteries, the system is non-ideal because of the mixture of solid species. In order to take account of this non-ideality, specific expressions for the activity coefficients need to be used. There are various different models which we can use to calculate the activity coefficients  $\gamma$  of the species  $[H_p]$  and  $[Li_nH_p]$ . For instance:

$$\ln(\gamma_{[Li_nH_p]}) = A(1 - x_{[Li_nH_p]})^2 \quad [2.57]$$

$$\ln(\gamma_{[H_p]}) = Ax_{[Li_nH_p]}^2 \quad [2.58]$$

If we replace the natural logarithm with the decimal logarithm  $\ln(x) = 2.3 \log(x)$ , we get:

$$\log(\gamma_{[Li_nH_p]}) = \frac{A}{2.3} (1 - x_{[Li_nH_p]})^2 \quad [2.59]$$

$$\log\left(\gamma_{[H_p]}\right) = \frac{A}{2.3} x_{[Li_n H_p]}^2 \quad [2.60]$$

and again working on the basis of equation [2.47], recapped below:

$$E = E^0 - \frac{0.059}{n} \log \frac{x_{[Li_n H_p]}}{x_{[H_p]}} - \frac{0.059}{n} \log \frac{\gamma_{[Li_n H_p]}}{\gamma_{[H_p]}} ,$$

we get:

$$E = E^0 - \frac{0.059}{n} \log \frac{x_{[Li_n H_p]}}{x_{[H_p]}} - \frac{0.059}{n} \left[ \log \gamma_{[Li_n H_p]} - \log \gamma_{[H_p]} \right] \quad [2.61]$$

$$E = E^0 - \frac{0.059}{n} \log \frac{x_{[Li_n H_p]}}{1-x_{[Li_n H_p]}} - \frac{0.059}{n} \left[ A \left( 1-x_{[Li_n H_p]} \right)^2 - A \left( x_{[Li_n H_p]} \right)^2 \right] \quad [2.62]$$

$$E = E^0 - \frac{0.059}{n} \log \frac{x_{[Li_n H_p]}}{1-x_{[Li_n H_p]}} - \frac{0.059}{n} \left[ A \left( 1-2x_{[Li_n H_p]} \right) \right] \quad [2.63]$$

This latter term describes all the interactions relating to the intercalated ions, which includes, for instance, the repulsion between the electrons and ions. The coefficient  $A$  has been modeled, for instance, as a linear equation for the absolute temperature  $T$ :

$$A = 0.0154 T - 2.211 \quad [2.64]$$

As an example, below we have given the simulation of the discharge curve for a graphite electrode (where  $E^0=0.10606$  V) with  $A$  as defined above.

## 2.10. Appendix 2: Double layer<sup>48</sup>

According to Helmholtz (1879), when a metal is immersed in a solution, it will tend to be charged negatively on the surface because of an excess of electrons. This surface in turn attracts positive ions from its vicinity to create an (internal) positive layer. For reasons of equilibrium, an (external) layer of ions with the opposite sign will also form almost instantaneously alongside

the first layer. Later on, Gouy and Chapman (1910 and 1913) made significant improvements to this model by separately developing the theory of a diffuse double layer linked to thermal excitation. In this extended model, the surface potential decreases exponentially because of a layer of counterions from the solution, which are adsorbed<sup>60</sup> to the surface. The model used today is the Gouy-Chapman-Stern model including Helmholtz's two dense layers (internal and external) and the diffuse layer of the Gouy-Chapman model.

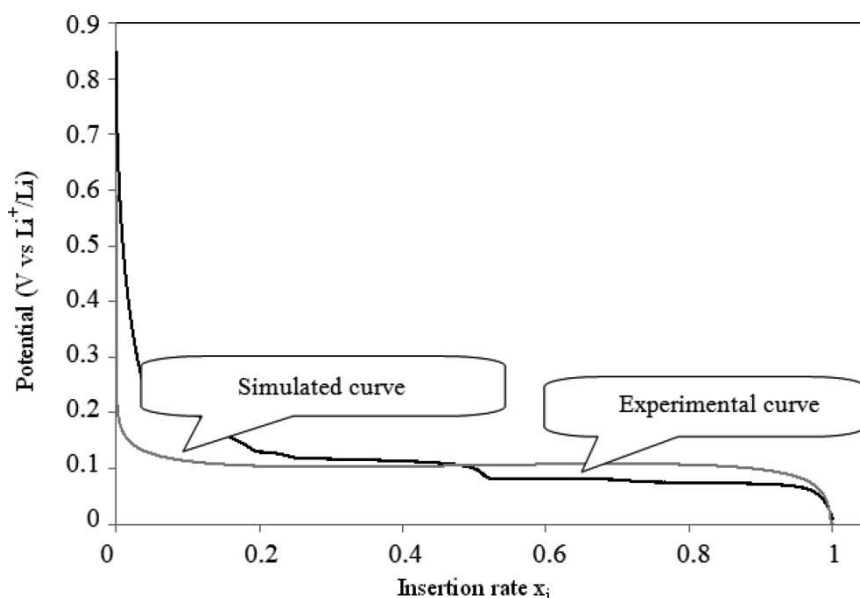


**Figure 2.25.** Comparison of experimental data with the model presented for the electrochemical potential of graphite  $U^0 = 0.10606 \text{ V}$

## 2.11. Appendix 3: Warburg impedance<sup>37</sup>

Transport by diffusion is the movement of material under the influence of the gradient of chemical potential, from more concentrated media toward less concentrated ones. Its limitation can be expressed in terms of electrochemical impedance, which is often called the Warburg impedance.

<sup>60</sup> In chemistry, the term “adsorption” refers to a surface phenomenon whereby atoms or molecules of gases or liquids affix to a solid surface. Adsorption must not be confused with absorption, whereby atoms, molecules or ions enter into the pores of a solid.

Three scenarios are generally to be considered, depending on the thickness of the diffusion layer: semi-infinite thickness, finite thickness in the presence of convection (or Nernst's hypothesis) and finite thickness through a thin film in an open circuit.

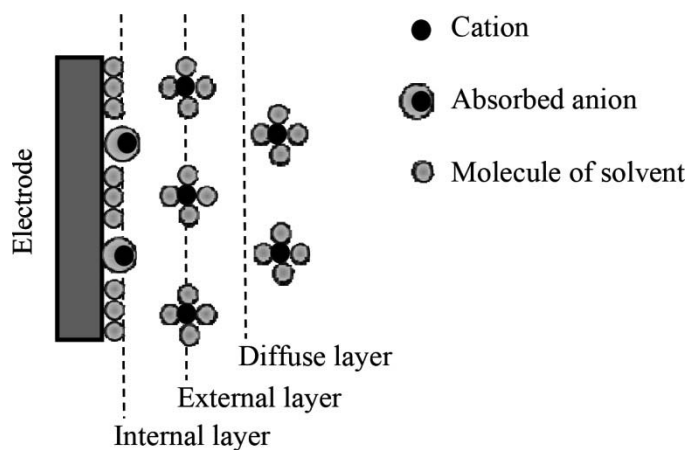


**Figure 2.26.** Gouy-Chapman-Stern model of the double layer  
(from T. Dong's thesis<sup>48</sup>)

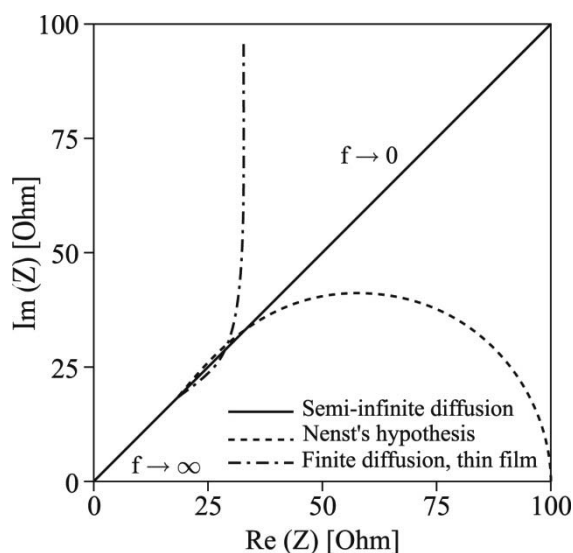


**Figure 2.27.** Three hypotheses for calculating the Warburg impedance



Depending on the case in question, the diffusion impedance can be calculated in different ways:

– semi-infinite diffusion can be represented by a constant-phase element (CPE, see section 2.4.12.4, and impedance in accordance with equation 2.20 with  $\alpha = 1/2$  and  $A_w$  the Warburg coefficient) so that:

$$Z_w = A_w \cdot \frac{1}{\sqrt{j\omega D}} \quad [2.65]$$

– finite diffusion in accordance with Nernst's hypothesis is generally expressed by:

$$Z_w = A_w \cdot \frac{\tanh(\sqrt{jT\omega})}{\sqrt{jT\omega}} \quad [2.66]$$

Note that at very low frequencies, the Warburg impedance behaves like a resistance (Figure 2.27). For this reason, we speak of a “closed circuit”, by contrast to the following case;

– finite diffusion through a thin film is generally expressed by:

$$Z_w = A_w \cdot \frac{\coth(\sqrt{jT\omega})}{\sqrt{jT\omega}} \quad [2.67]$$

Equations [2.66] and [2.67] are deduced from the boundary conditions of the diffusion equations.<sup>61</sup>  $T$  represents the time constant  $T = L^2/D$  where  $L$  is the thickness of the diffusion layer and  $D$  is the diffusion coefficient.

Note that the imaginary part then tends toward infinity for the lowest frequencies, which corresponds to the impedance of a capacity or to an “open circuit” state.

In Figure 2.27, we see that the three impedances are similar at high frequencies, but are very different at very low frequencies. Measuring the

---

61 M.E. ORAZEM and B. TRIBOLLET, *Electrochemical Impedance Spectroscopy*, John Wiley & Sons, 2008.

J.-P. DIARD, B. Le GORREC & C. MONTELLA, *Cinétique électrochimique*, Éditions Hermann, 1996.

spectra of batteries right down to these low frequencies is a very long, drawn-out process. For example, it takes 20 minutes to cover a range from 100 kHz to 10 mHz.

## 2.12. Solutions to the exercises in Chapter 2

### Solution to exercise 2.1:

Autonomy in GSM mode: over one hour, the average consumption is  $1.7 \times 0.95 + 65 \times 0.05 = 4.865$  mAh. With a secondary battery whose capacity is 1200 mAh, the autonomy in this mode is therefore  $1200/4.865 = 247$  hours, which is a little over 10 days.

Autonomy in 3G mode: over one hour, the average consumption is  $1.7 \times 0.95 + 220 \times 0.05 = 12.615$  mAh. With a secondary battery whose capacity is 1200 mAh, the autonomy in this mode is therefore  $1200/12.615 = 95$  hours, which is essentially 4 days.

### Solution to exercise 2.2: Determination of the short-circuit current

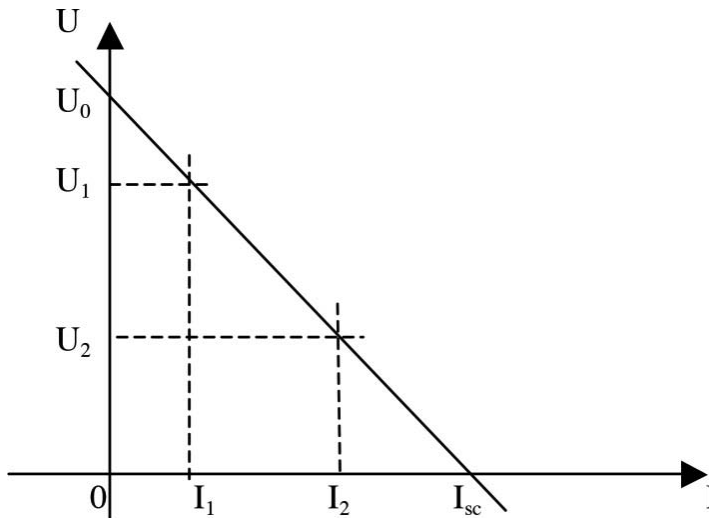


Figure 2.28. Line for calculating the short-circuit current

The equation of the line is written:  $U = a.I + b$ , or indeed  $U = U_0 - R.I$ .

The direction coefficient (slope)  $a$  is:  $\Delta y/\Delta x$ , so here  $\Delta U/\Delta I = (U_1 - U_2)/(I_1 - I_2)$ .

From this, we deduce the internal resistance (equal to  $-a$ ):  $R_{\text{int}} = \frac{U_1 - U_2}{I_2 - I_1}$ .

We can return to the equation of the line  $U = a.I + b$  for the point  $U_1, I_1$  in order to determine  $b$ .

Hence,  $b$  is equal to  $U_1 - a.I_1$

To determine  $I_{sc}$ , we write the equation of the line  $U = a.I + b$  and take  $U = 0$ , so that  $0 = a.I_{sc} + b$ , from which we draw the conclusion that  $I_{sc} = -b/a = I_1 - U_1/a$ .

Thus, with all the calculations having been performed:  $I_{sc} = \frac{U_1 I_2 - U_2 I_1}{U_1 - U_2}$

We could also have plotted  $I$  as a function of  $U$ , which would simplify the calculations, but in that case they would have been less intuitive.

### Solution to exercise 2.3: impedance of the dipole $R_S, R_P, C$

The aim here is to calculate the impedance of the dipole shown below (for the sake of ease of calculation, the notation of the elements has been simplified:  $R_S$  is the series resistance and  $R_P$  is the parallel resistance).

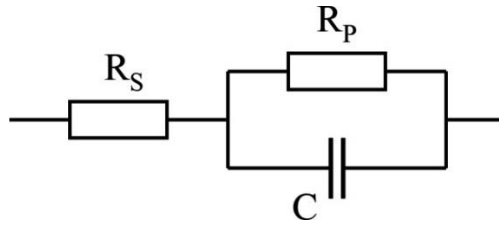


**Figure 2.29.** Simplified model of an electrochemical cell

The admittance of the part  $R_P C$  is the sum of the admittances of the two elements, so  $Y_1 = (1/R_P) + jC\omega$ , so indeed  $(1 + jR_P C\omega)/R_P$ . This gives us an impedance  $Z_1$  equal to  $R_P/(1 + jR_P C\omega)$ .

Separate out the real and imaginary parts by multiplying the numerator and the denominator by the conjugate expression of the denominator  $(1-jR_pC\omega)$ . We then obtain  $Z_1 = R_p(1-jR_pC\omega)/(1+jR_pC\omega)(1-jR_pC\omega) = (R_p-jR_p^2C\omega)/(1+R_p^2C^2\omega^2)$ .

We now need to add the series resistance  $R_s$ . The total impedance  $Z_t$  is written:

$$Z_t = R_s + \frac{R_p}{1+R_p^2C^2\omega^2} - j\frac{R_p^2C\omega}{1+R_p^2C^2\omega^2} \quad [2.68]$$

For  $\omega=\infty$ , this impedance can be summarized as  $R_s$ . Thus, it is a point on the real axis.

For  $\omega=0$ , this impedance can be summarized as  $R_s+R_p$ . Hence, again, it is a point on the real axis.<sup>62</sup>

We now need to draw the impedance as a function of  $\omega$  in the complex plane.

The real part has the expression:

$$\text{Re}(Z_t) = R_s + \frac{R_p}{1+R_p^2C^2\omega^2} \quad [2.69]$$

As this expression comprises only positive terms, its value will always be positive.

We can also write it as:

$$\text{Re}(Z_t) - R_s = \frac{R_p}{1+R_p^2C^2\omega^2} \quad [2.70]$$

---

<sup>62</sup> The frequency limits can also be determined very simply by examining the electrical diagram. At low frequency, the impedance of the capacitor is high: the dipole is equivalent to the two series resistances. At high frequency, the capacitor “short-circuits” the resistance  $R_p$ . The dipole is equivalent only to the resistance  $R_s$  (see Figure 2.27).

or indeed:

$$1 + R_P^2 C^2 \omega^2 = \frac{R_P}{\operatorname{Re}(Z_t) - R_S} \quad [2.71]$$

and, if we introduce  $\omega^2$ :

$$\omega^2 = \frac{1}{R_P^2 C^2} \left( \frac{R_P}{\operatorname{Re}(Z_t) - R_S} - 1 \right) \quad [2.72]$$

The opposite of the imaginary part has the expression:

$$\operatorname{Im}(-Z_t) = \frac{R_P^2 C \omega}{1 + R_P^2 C^2 \omega^2} \quad [2.73]$$

As it comprises only positive terms, this value is always positive.

We can also write it as:

$$(1 + R_P^2 C^2 \omega^2) \cdot \operatorname{Im}(-Z_t) = R_P^2 C \omega \quad [2.74]$$

By squaring this expression:

$$(1 + R_P^2 C^2 \omega^2)^2 \cdot \operatorname{Im}(-Z_t)^2 = R_P^4 C^2 \omega^2 \quad [2.75]$$

By eliminating  $\omega$  between the real and imaginary parts, we get:

$$\left( \frac{R_P}{\operatorname{Re}(Z_t) - R_S} \right)^2 \cdot \operatorname{Im}(-Z_t)^2 = R_P^4 C^2 \left( \frac{1}{R_P^2 C^2} \left( \frac{R_P}{\operatorname{Re}(Z_t) - R_S} - 1 \right) \right) \quad [2.76]$$

or indeed, successively:

$$\left( \frac{R_P}{\operatorname{Re}(Z_t) - R_S} \right)^2 \cdot \operatorname{Im}(-Z_t)^2 = R_P^2 \left( \frac{R_P}{\operatorname{Re}(Z_t) - R_S} - 1 \right) \quad [2.77]$$

$$\left( \frac{R_P}{\operatorname{Re}(Z_t) - R_S} \right)^2 \cdot \operatorname{Im}(-Z_t)^2 = R_P^2 \left( \frac{R_P - \operatorname{Re}(Z_t) + R_S}{\operatorname{Re}(Z_t) - R_S} \right) \quad [2.78]$$

$$R_P^2 \cdot \operatorname{Im}(-Z_t)^2 = R_P^2 (R_P - \operatorname{Re}(Z_t) + R_S) (\operatorname{Re}(Z_t) - R_S) \quad [2.79]$$

$$\operatorname{Im}(-Z_t)^2 = (R_P - \operatorname{Re}(Z_t) + R_S) (\operatorname{Re}(Z_t) - R_S) \quad [2.80]$$

$$\operatorname{Im}(-Z_t)^2 = (R_P - \operatorname{Re}(Z_t) + R_S) \operatorname{Re}(Z_t) - (R_P - \operatorname{Re}(Z_t) + R_S) R_S \quad [2.81]$$

It is interesting to develop the right-hand side of the equation:

$$\operatorname{Im}(-Z_t)^2 = R_P \operatorname{Re}(Z_t) - \operatorname{Re}(Z_t)^2 + R_S \operatorname{Re}(Z_t) - R_P R_S + \operatorname{Re}(Z_t) R_S - R_S^2 \quad [2.82]$$

$$\operatorname{Im}(-Z_t)^2 + \operatorname{Re}(Z_t)^2 - 2R_S \operatorname{Re}(Z_t) + R_S^2 - R_P \operatorname{Re}(Z_t) + R_P R_S = 0 \quad [2.83]$$

which can be written by placing  $x$  instead of  $\operatorname{Re}(Z_t)$  and  $y$  instead of  $\operatorname{Im}(-Z_t)$ :

$$y^2 + x^2 - 2R_S x + R_S^2 - R_P x + R_P R_S = 0 \quad [2.84]$$

Hence:

$$y^2 + x^2 - (2R_S + R_P)x + R_S^2 + R_P R_S = 0 \quad [2.85]$$

Remembering the equation of a circle with center  $\{x_C, y_C\}$  and radius  $R$ :

$$(x - x_C)^2 + (y - y_C)^2 = R^2 \quad [2.86]$$

which can be developed to become:

$$y^2 + x^2 - 2xx_C + x_C^2 + y_C^2 - 2yy_C - R^2 = 0 \quad [2.87]$$

By identification between equations [2.85] and [2.87], we get:

$$x_C = R_S + R_P/2 \text{ and } y_C = 0 \quad [2.88]$$

Therefore:

$$R_S^2 + R_P R_S = x_C^2 - R^2 \quad [2.89]$$

Thus, if we replace  $x_C$  with the value found in equation [2.88], we can easily find the radius of the circle  $R_P/2$ .

The impedance sought is represented by a semi-circle (because  $-Im(Z)$  is always positive, as indicated in equation [2.73]), whose center is on the real axis at the abscissa  $R_S + R_P/2$  and whose radius is  $R_P/2$  (Figure 2.30).

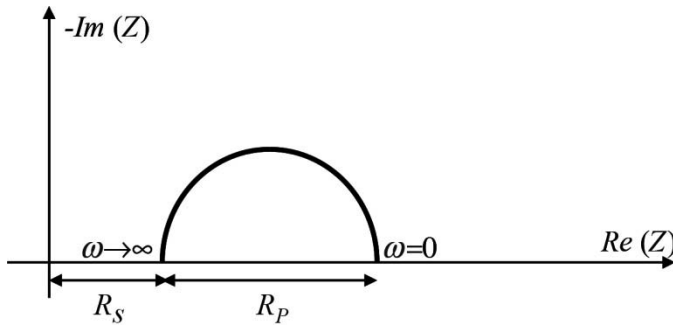


**Figure 2.30.** Representation of the impedance of an electrochemical cell

It is simple to determine the values of the two resistances. At high frequency, the capacitor “short-circuits” the resistance  $R_P$ . The measured impedance is  $R_S$ . At low frequency, the impedance of the capacitor is high: the dipole is equivalent to both series resistances. The resistance  $R_P$  is that diminished measurement of the value of  $R_S$ .





## Chapter 3

# Practical Examples Using Electrochemical Storage

### 3.1. Introduction

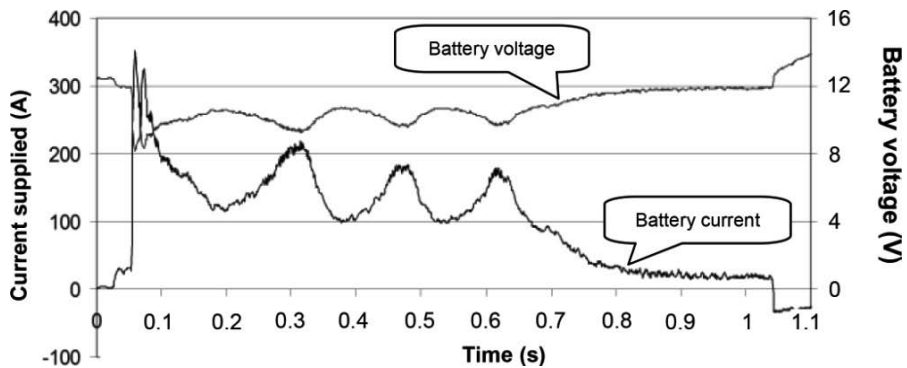
The following pages offer numerous examples of the use of electrochemical batteries. It is more important to focus on the demands made on the batteries in each application than on the technology used today for each purpose, because this technology is ever-changing. We have seen applications (such as electronic camera flashes or electric cars) which began using lead-acid batteries, then moved on to nickel and then to lithium batteries. The user requirements have not changed, but the need for increasingly small on-board weight for a given range of functions has caused the storage solutions to evolve on the basis of the availability of new couples with ever-increasing gravimetric energy levels.

#### 3.1.1. *Starter currents for internal combustion engines in cars*

The figures presented in this section are real currents and voltages measured in winter in starter batteries (SLIs) for internal combustion engines in cars.

Figure 3.1 shows the current supplied by the battery and the voltage at its terminals during cold start of a 1.4-liter cylinder gasoline engine in a car made in 1988. The peak current supplied by the battery is 352 A. We can see

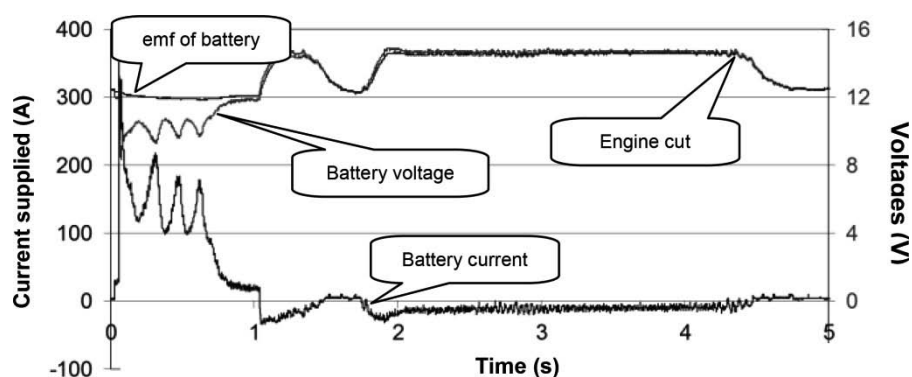
the effect of the compression in the cylinders which causes the irregular current corresponding to the torque provided by the electric starter. After 0.75 s, the engine ignites: the alternator begins providing power. At 1.05 s, the supply of the electric starter is cut off and the direction of the current is reversed to flow back into the battery. The voltage at the terminals of the battery (right-hand scale) drops to 8 V at the moment when the current peaks. We can very easily calculate the amount of electricity being summoned by the electric starter by time-integrating the current. Its value is 30 mAh, or 1% less than the specified battery capacity<sup>1</sup> of 40 Ah. We can indeed see that in this usage, the battery is designed for the peak power (or peak current) that it has to supply rather than for the energy that it needs to store. However, to provide a high level of power or a strong current requires a significant surface area of the electrodes and, consequently, given that for mechanical reasons the electrodes cannot be infinitely thin, their volume means that a large amount of energy can be stored. In an internal combustion vehicle, the need for a large amount of energy to be stored will only be critical if energy-hungry applications are left to run when the engine is off (e.g. headlights, forgetting to turn off the sidelights or an interior light and, in particular, the hazard-warning signals, which need to function for several hours in case of breakdown), or if the vehicle is left parked for months at a time (even with the contact cut off, modern cars consume a small amount of current: e.g. to run the dashboard clock, warning lights, anti-theft mechanisms, etc.).



**Figure 3.1.** *Cold start of a gasoline engine*

<sup>1</sup> The international standards on batteries speak of assigned capacity (see section 2.3.3.6).

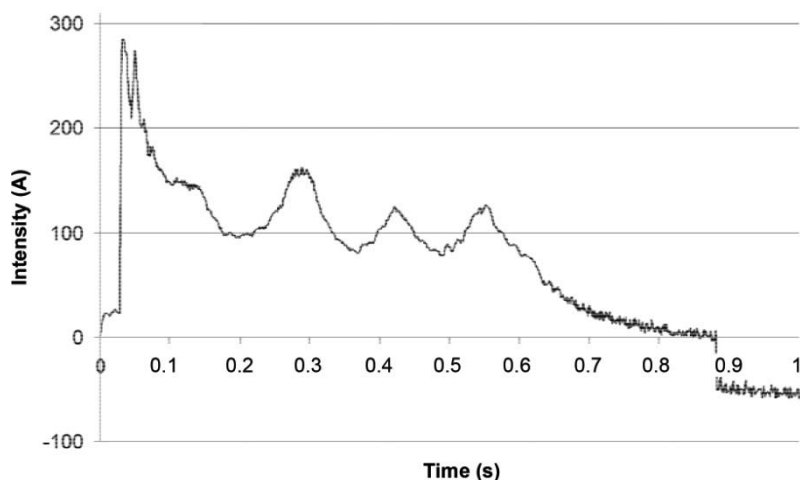
Figure 3.2 shows the evolution of the voltage at the terminals of the battery after startup of the combustion engine and its recharge by the alternator. It also shows the emf of the battery. These two values are different when a strong current is being summoned by the electric starter (the sum of the internal resistance of the battery and the line resistance is  $12.5\text{ m}\Omega$ ). After that, they mimic each other closely, because the current supplied by the alternator is far less intense than that demanded by the electric starter. We note that as soon as the battery begins charging, its emf immediately goes up to  $14.6\text{ V}$ . When the engine is cut, the battery voltage drops to around  $12\text{ V}$ .



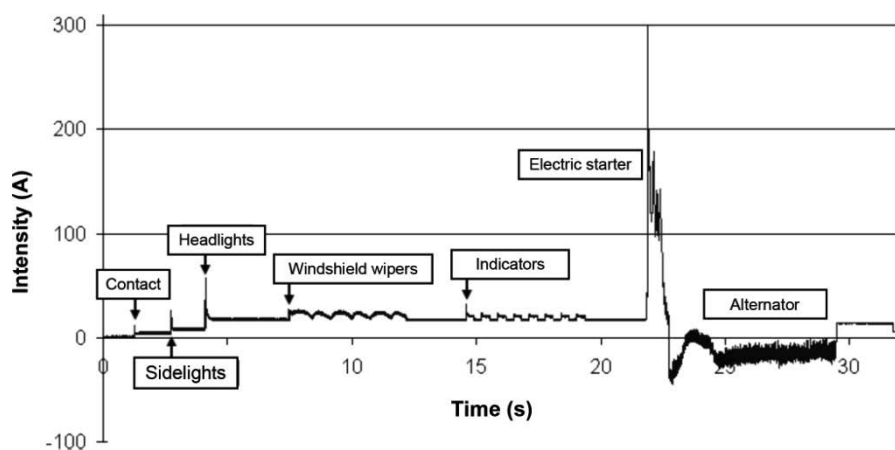
**Figure 3.2.** Cold start of a gasoline engine followed by recharging of the battery by the alternator

Figure 3.3 shows the current supplied by the battery when starting the same 1.4 L-cylinder gasoline engine, but after it has already been running for some time. Hence, the oil is hotter, and therefore more fluid. The peak current supplied by the battery is therefore less: it is  $284\text{ A}$ . The trend exhibited by the current absorbed is the same (effect of compression in the cylinders and then charging by the alternator).

Figure 3.4 shows the current supplied by the battery to run various auxiliary components. It is noteworthy that the amount of electricity (proportional to the surface below the curve) summoned during startup is slight in comparison to the amount of electricity required by the different auxiliaries.



**Figure 3.3.** *Startup of a hot gasoline engine followed by recharging of the battery by the alternator*



**Figure 3.4.** *Currents absorbed from the battery by different auxiliaries when the engine is stopped, followed by recharging of the battery by the alternator*

Figure 3.5 illustrates the current supplied by the battery and the voltage at its terminals during cold start on a different 1.4 L-cylinder gasoline engine which has not been used for several weeks. The peak current supplied by the battery (which is more powerful, specified at 50 Ah 400 A, with internal resistance 7.5 m $\Omega$ ) is 392 A. The duration of the starting process is far

longer (around 4 seconds as compared to less than one second) because the starter motor first has to allow the gas pump to fill the chamber of the carburetor. The voltage at the terminals of the battery (right-hand scale) drops to around 10 V. The amount of electricity summoned by the starter motor is 182 mAh, which is less than 0.4% of the battery's capacity.

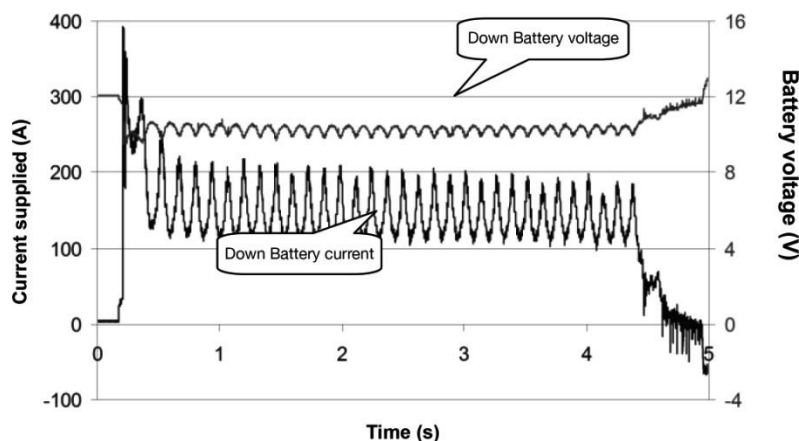


**Figure 3.5.** Cold start of a gasoline engine which has not been used for several weeks

Figure 3.6 illustrates the current supplied by the battery and the voltage at its terminals during cold startup of a 2 L-cylinder diesel engine. The peak current supplied by the battery (which is more powerful, specified at 61 Ah 600 A, with internal resistance 6 m $\Omega$ ) is 685 A. The voltage at the terminals of the battery (right-hand scale) drops to 7.7 V at the moment of the peak current. The amount of electricity summoned by the starter motor in 125 mAh, which is around 0.2% of the battery's capacity.

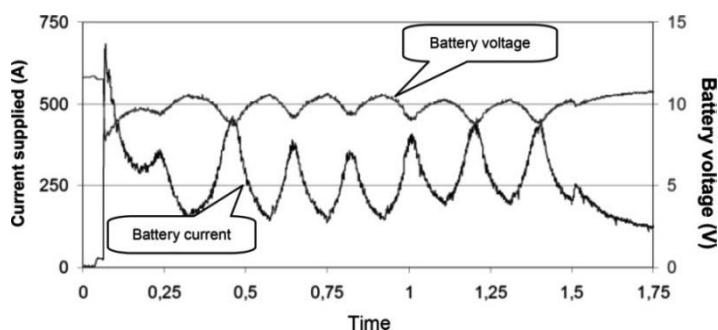


**Figure 3.6.** Cold start of a diesel engine

### 3.1.2. Power required by a telecommunications transceiver in an isolated site

In order to make a wireless telecommunications network (GSM: *Global System for Mobile Communications*) available in a site isolated from any electrical distribution grid, we can use a photovoltaic (PV) generator, possibly supplemented by an electrogen group.

The following example is taken from the power supply to a *Base Transceiver Station* (BTS) in western Africa, near to the equator.<sup>2</sup>

The electronics require a maximum power of 2.6 kW and an average power of 2.2 kW. The power<sup>3</sup> of the PV generator is 9 kW<sub>p</sub>. The battery (“sealed” lead<sup>4</sup>) stores 130 kWh. Its nominal voltage is 48 V.

We are going to study the behavior of the system over three consecutive days of average sunshine in January 2013.

The solar irradiation over these three days never went above 560 W/m<sup>2</sup>. The average ambient temperature was approximately 31°C. The temperature in the modules was far higher – around 65°C. Thus, the PV generator

---

<sup>2</sup> The data given here were provided by Benoît Connes and Matthieu Prigent from Phaesus France ([www.phaesun.com](http://www.phaesun.com)). The author would like to extend their gratitude to these two for the highly interesting discussions that they have had.

<sup>3</sup> A PV generator is characterized by its peak power (notated  $W_p$ ) which corresponds to the electrical power produced under a given level of solar irradiance (referred to as the AM1.5 spectrum) of 1000 W/m<sup>2</sup> and a temperature of 25°C. In reality, the power supplied by the PV generator is often less, or even far less than this, because the solar irradiance only rarely reaches 1000 W/m<sup>2</sup>, and the temperature of the modules is much higher than 25°C (the power provided by PV modules decreases when the temperature increases. Around 10% of the power is lost with a 25°C increase in temperature). Despite what one might assume from the term “peak power”, a PV generator is able to supply a higher level of power than the stated peak power, e.g. when it is installed high on a mountain, where the solar irradiation may be greater than 1000 W/m<sup>2</sup> and the temperature may be negative.

<sup>4</sup> So-called “sealed” batteries are not actually hermetically sealed. In conditions of significant overcharging, the recombination of the gases produced by electrolysis is insufficient, and we have to be able to evacuate them. Therefore, this type of battery has safety valves to prevent an explosion. The term “VRLA”, for “*Valve-Regulated Lead-Acid*”, is therefore more meaningful. The major advantage to these batteries is that they do not require maintenance. Further details about the constitution and operation of these batteries are to be found in:

C. GLAIZE and S. GENIÉS, *Lead and Nickel Electrochemical Batteries*, ISTE Ltd, London, John Wiley & Sons, New York, Ltd 2012.

naturally supplies far less than its peak power. Over the period in question, the maximum power delivered was established at 3.6 kW.

EXERCISE 3.1.– Taking the PV production at the site where the BTS is installed, in winter, to be represented by a half-sinusoid with a duration of  $9\frac{1}{4}$  hours and with peak intensity of 70 A, what is the amount of electricity produced over the course of a day?

*Solution page 110*

EXERCISE 3.2.– Per day, what is the maximum amount of electricity necessary to run the electronics of the BTS?

*Solution page 111*

EXERCISE 3.3.– Is the PV production sufficient to cover the installation's energy requirements?

*Solution page 111*

In the conditions of irradiation and temperature quoted above, the PV generator provides only a third of the electricity needed by the installation. More sunny days would nearly double the amount of photovoltaic electricity produced. In any case, the amount of electricity provided by the PV generator is less than that which is required. Therefore, an electrogen group (EG) is added to complete the charging of the battery and supplement the energy in the case of more than 2 days without sun. In reality, the sizing actually tends to be based on electricity production by the EG. As we want the EG to function at around its nominal power for reasons of efficiency, and we do not need it to function 24 hours a day, we install batteries. If we do not want the EG to be operational for more than 8 hours a day, we need to supply a level of power four times greater than the needs of the electronic components (in view of the efficiency of the battery). The PV generator is then installed to decrease fuel consumption. Its size is limited, either for reasons of weight or economic reasons.

EXERCISE 3.4.– In a completely autonomous functional regime (i.e. only using the battery), what is the range of the system in days?

*Solution page 111*

The curves in Figure 3.7 show the currents produced by the PV generator and the electrogen group and those absorbed by the electronics. In this figure

and the rest of the figures in this section, the time (on the horizontal axis) is counted in hours from the first day at 0 hours.

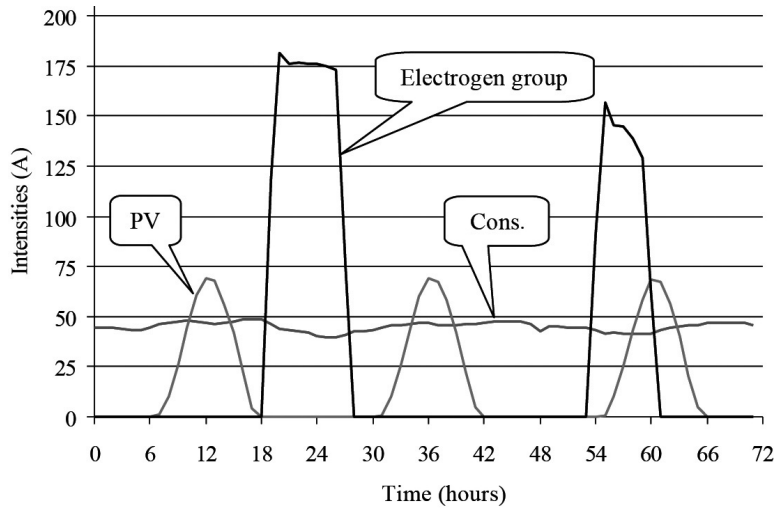


**Figure 3.7.** Currents produced by the PV generator and by the electrogen group, and absorbed by the consumers (Cons.) of a BTS

By algebraic addition of the currents, we can deduce the current flowing into the battery, plotted in Figure 3.8.

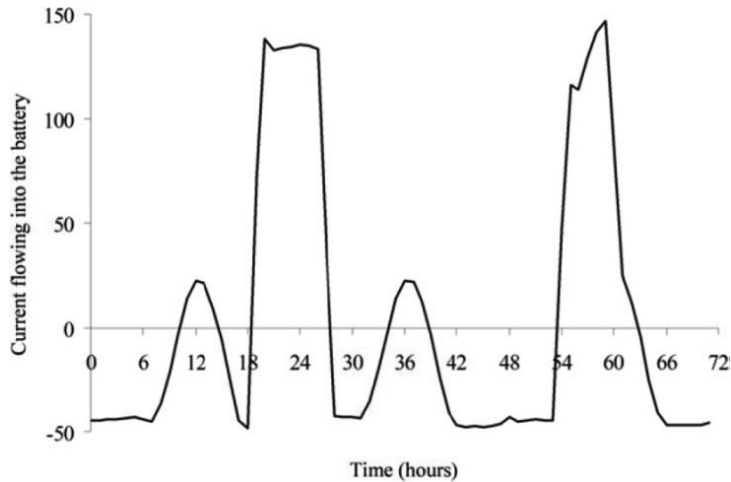


**Figure 3.8.** Current flowing into the battery of a system to supply electricity to a BTS



The voltage at the output terminals from the regulator to the battery is shown in Figure 3.9. The rapid rise in voltage is due to the charging of the battery by the EG, which takes place at a far greater intensity than that delivered by the PV generator. We note that the electrogen group is started up when the voltage at the terminals of the battery (to which the algebraic drop in voltage in the conductors must be added) is around 47 V, and is shut down when the battery voltage climbs back to around 54 V.

EXERCISE 3.5.— What is the power delivered by the electrogen group? Compare this to the power of the PV generator.

*Solution page 112*

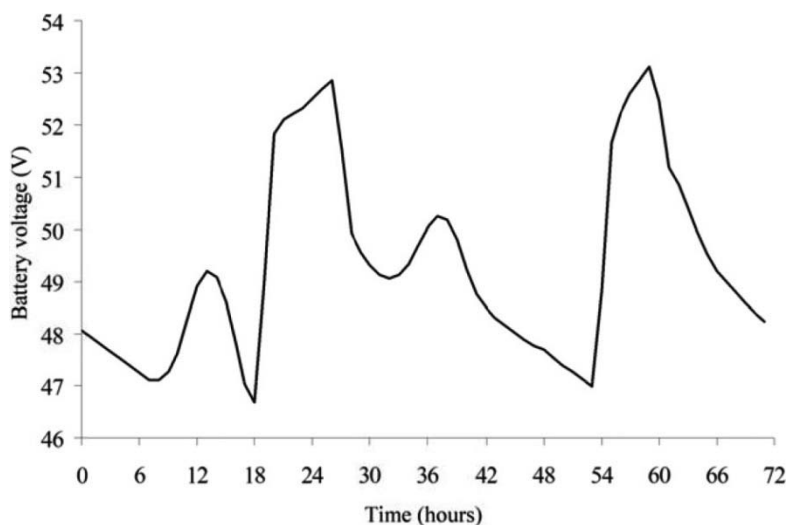


**Figure 3.9.** *Voltage at the terminals of the battery of a system to supply electricity to a BTS*

If we know the resistance of the connecting conductors between the regulator and the battery, we can work back to find the emf of the battery. We can also show the shape of the trend in the amount of electricity discharged<sup>5</sup> (Figure 3.10). Note the similarity between the variation in emf and the state of charge (SOC) of the battery.

<sup>5</sup> For the battery, we use receiver convention. This means that the discharge current and the amount of electricity discharged are counted negatively.

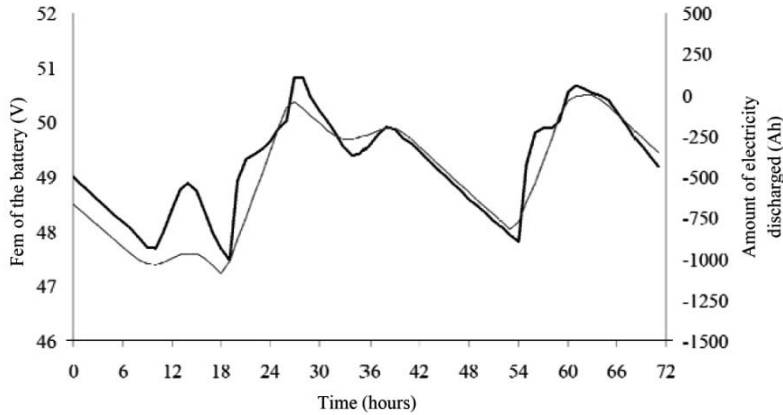


**Figure 3.10.** *The emf (heavy line) and the amount of electricity discharged (light line) for the battery of a system to supply electricity to a BTS*

### 3.1.3. House in an isolated site

The following example relates to a house in the south of France whose owners have decided to be as autonomous as possible in terms of energy.<sup>2</sup> The predicted average consumption is 10 kWh per day.<sup>6</sup> The installation includes a 5.44 kWp PV generator, storage by an array of 48V lead batteries with a nominal capacity of 2350 Ah and a 7.5 kVA inverter to supply the user loads at 230 V. A 230 V, 30 kVA electrogen group can be used periodically to supplement the PV production in winter. Because of its power, it can supply the user loads whilst recharging the batteries. Note that the angle of inclination of the PV modules (directed due south) is 60° to aid production in winter.<sup>7</sup>

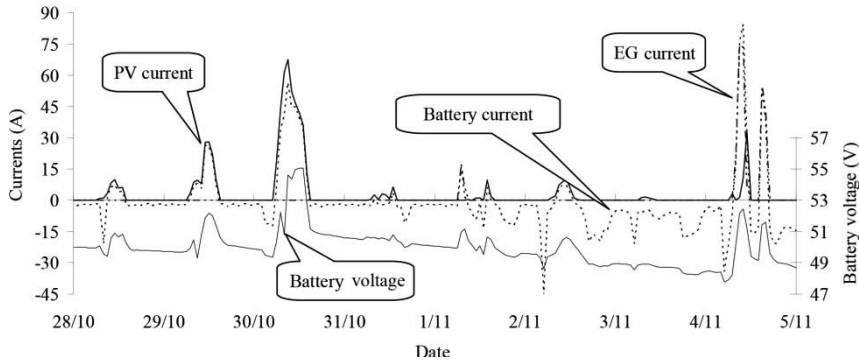
**EXERCISE 3.6.**— Based on the data above, what is the autonomy of this installation in days? In other words, how long can the batteries supply the loads with no PV production and no input from the electrogen group?

*Solution page 112*

<sup>6</sup> By way of indication, 1 kWh is consumed, for instance, by one cycle of the washing machine or an hour of ironing, to say nothing of the more powerful energy-hungry functions because, of course, in such an installation, the heating could not be electric.

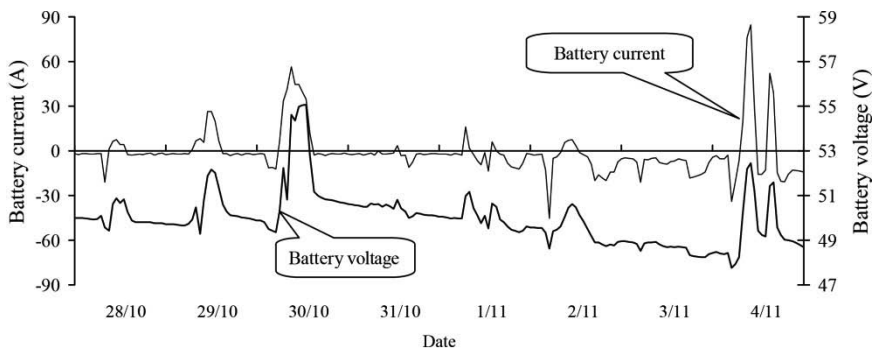
<sup>7</sup> For a photovoltaic installation injecting power into the grid, we wish to maximize the amount of energy produced throughout the year, so we incline the panels 30° from the horizontal (in the south of France).

Unlike in the previous case (section 3.1.2), the power consumed is very variable over the course of a day. Figure 3.11 illustrates the behavior of the installation over 8 days in October-November. The current which (algebraically) charges the battery is the sum of the currents supplied by the PV generator and the electrogen group (EG), from which we need to take away the current demanded by the user loads.



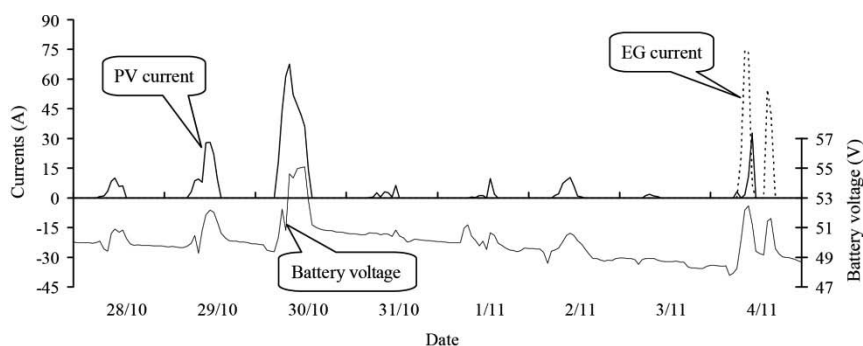
**Figure 3.11.** Currents produced by the PV generator (solid line above the horizontal axis) and the electrogen group (EG, dash-dot line). Current absorbed by the battery (dotted line). Voltage at the terminals of the battery (right-hand scale)

Figure 3.12 shows the correlation between the voltage at the terminals of the battery and the current running through it. The stronger the current supplied, the more the voltage at its terminals decreases because of the internal resistance, but also because of the decrease in SOC, to which the electromotive force is sensitive.



**Figure 3.12.** Current absorbed by the battery and voltage at its terminals

Also we note a regular decrease in the voltage at the terminals of the battery on 28 and 29 October. This decrease is due to a lack of sunshine. On 30 October the sun is shining once more and the battery is charged: its voltage climbs back up. Over the next five days, we again see the battery voltage decline, until it becomes sufficiently low to trigger the start of the electrogen group on the morning of 4 November.<sup>8</sup> There is a little sunshine in the morning, so the EG is stopped, but the irradiation drops away and the EG is started again in the afternoon.



**Figure 3.13.** *Currents produced by the PV generator (solid line above the horizontal axis) and the EG (dotted line). Voltage at the terminals of the battery*

Over a 5-month period in winter (October to February), the EG provided less than 10% of the total energy consumed by the house.

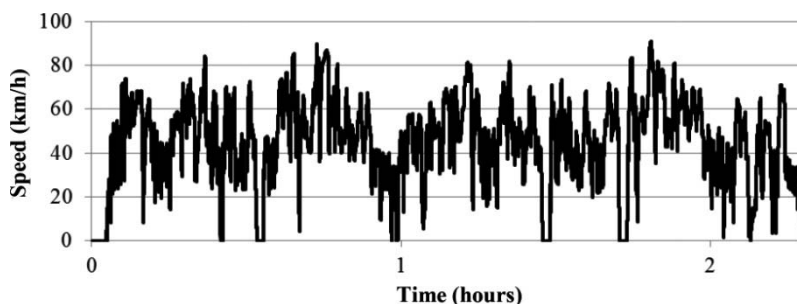
The energy efficiency of the battery (energy supplied/energy to charge) is established at 85%. This is fairly high for this type of secondary battery. This is due to the fact that the battery is rarely completely charged. The phenomenon of electrolysis of water therefore occurs only infrequently, which also minimizes the need for maintenance to readjust the levels of water (little more than a liter of water needed to be replaced for the whole of the battery array over the five months in question). This also limits the oversizing of the PV generator: little of the energy which is produced by the PV generator is “lost” in the battery. However, this does mean that we need to use batteries specific to photovoltaic usage, which are able to remain incompletely charged over long periods of time.

<sup>8</sup> In order to avoid too low a state of charge of the battery and damage to it, the electrogen group is started when the battery voltage dips below a value set by the regulator.

Nearly ten years after its installation, this system is still functioning very well. The batteries are the same ones that were originally installed. Their impressive longevity is undoubtedly due to the fact that they have not been subjected to intense charges or discharges. Over the period in question, the charge current never rose above 100 A (which represents a C/25 current<sup>9</sup>) and the discharge current 55 A (a C/50 current).

### 3.1.4. Currents in an operational electric car battery

The following example<sup>10</sup> relates to a 104 km journey made by a pure-electric car (the Citroën AX). This distance was covered in 2 hours 20 minutes with a top speed of 91 km/h (limitation due to the Highway Code). The profile of the vehicle's speed is shown in Figure 3.14.



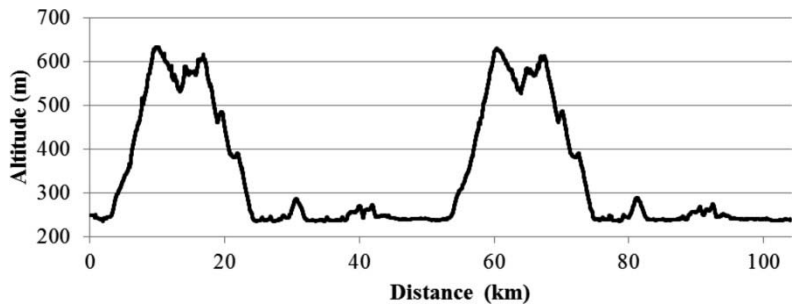
**Figure 3.14.** *Profile of the speed of the electric car*

Figure 3.15 shows that the journey (made twice) is over fairly uneven ground. The range of altitude covered is 400 m.

We cannot see any particular drop in speed when going uphill, which shows that the power of the engine is sufficient. The maximum power provided by the battery is around 30 kW. During regenerative braking, approximately 20 kW of power are recovered and injected into the battery. The algebraic form of the current supplied by the battery is shown in Figure 3.16. It reaches up to 210 A during traction and attains nearly 150 A during energy recovery.

<sup>9</sup> Defined in section 2.3.3.5.

<sup>10</sup> Many thanks to Marion Perrin from the CEA, who kindly provided us with the data in this section.



**Figure 3.15.** *Profile of the journey*

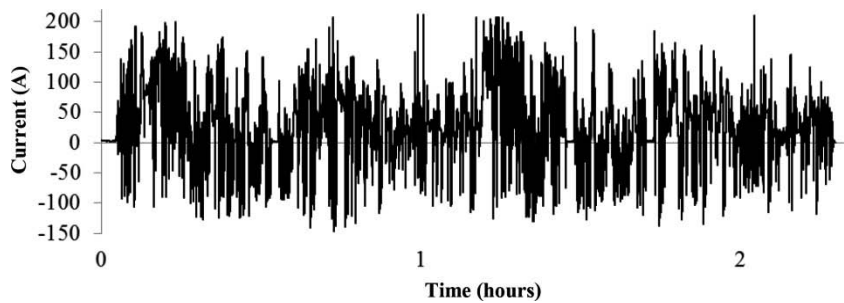


**Figure 3.16.** *Current supplied by the battery during the journey*

It may be helpful to separately represent the power supplied by the battery (see Figure 3.17) and the power injected into the battery (Figure 3.18). Although this division is artificial (there is no discontinuity between these two currents), it enables us to show the amount of electricity consumed during traction and the amount that is recovered during braking.

The energy injected back into the battery during recovery phases (regenerative braking) seems fairly significant in relation to the energy supplied for traction. The measurements show that the energy required during traction is equal to 13.22 kWh, and the energy recovered is 3.44 kWh which is 26% of the energy consumed for traction. In total, the journey will have used 9.78 kWh from a battery whose nominal capacity is 14 kWh. Without energy recovery, the battery would be empty following this journey. Thanks to the regenerative braking, the final SOC is established at 28%. The evolution of the SOC is shown in Figure 3.19.

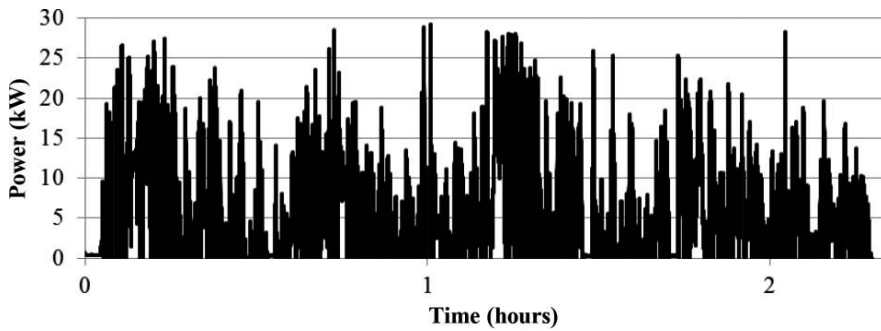


**Figure 3.17.** *Power delivered by the battery during traction*

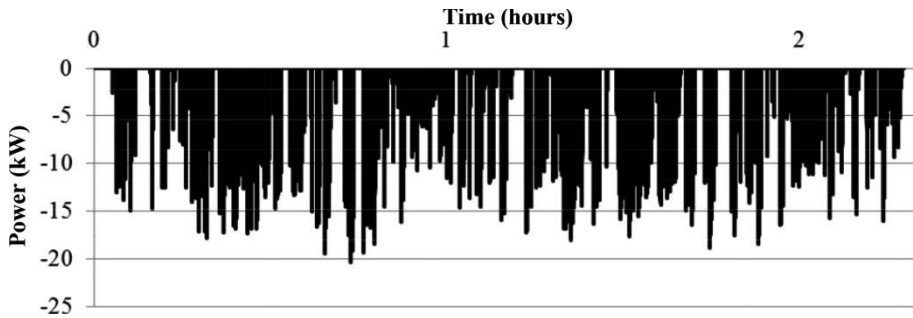


**Figure 3.18.** *Power injected into the battery during regenerative braking*

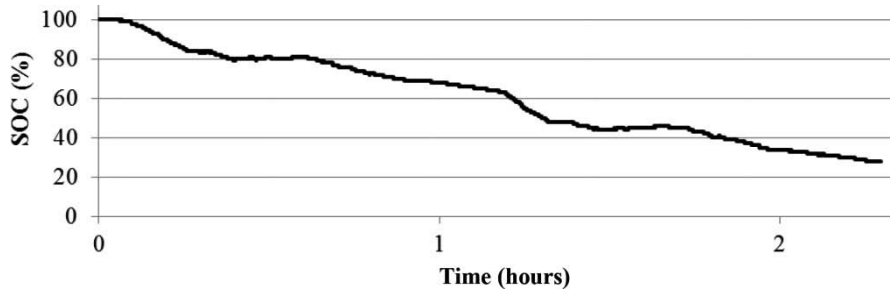


**Figure 3.19.** *Evolution of the SOC*

Figure 3.20 show the evolution of the voltage at the terminals of the battery. We can indeed see a correlation between this voltage and the SOC.

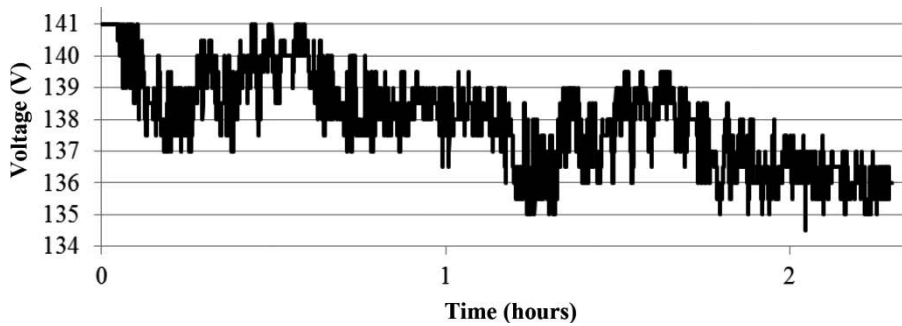


**Figure 3.20.** *Evolution of the voltage at the terminals of the battery*

### **3.1.5. Currents during the phase of recharging of batteries in electric cars**

The battery of a purely electric vehicle is recharged either by an on-board charger or by charge points. The following pages present the profiles of charge measured<sup>11</sup> on four electric vehicles (three are purely electric; the fourth is a rechargeable “plug-in” hybrid vehicle).

On-board chargers or domestic chargers are intended to be plugged into a standard outlet delivering at most 16 A, which is around 3.5 kVA at 230 V. Charge points, which are installed in parking lots, public spaces, business premises, etc., have higher powers than this (several tens of kW). They are capable of delivering a swift (though often incomplete) recharge; for instance, an 80% SOC can be regained in less than 30 minutes.

In the examples below, the electrical architecture is a mix between the two cases presented above. These vehicles are charged in photovoltaic parking sheds. The on-board charger of the vehicle is plugged in to a charge point which can modulate the power delivered to the charger (between 0.7 and 2.4 kW) depending on the potential for PV production and the predicted journey range for each of the vehicles being charged. This modulation can quite clearly be seen in Figure 3.24.

<sup>11</sup> The data in this section were supplied by Marion Perrin and Mathieu Quéard from the CEA. We are very grateful to them for this.



### 3.1.5.1. Electric car with a NiCd battery

The NiCd battery in this Peugeot 106 has a nominal capacity of 12 kWh. The power injected and the SOC are shown in Figure 3.21.

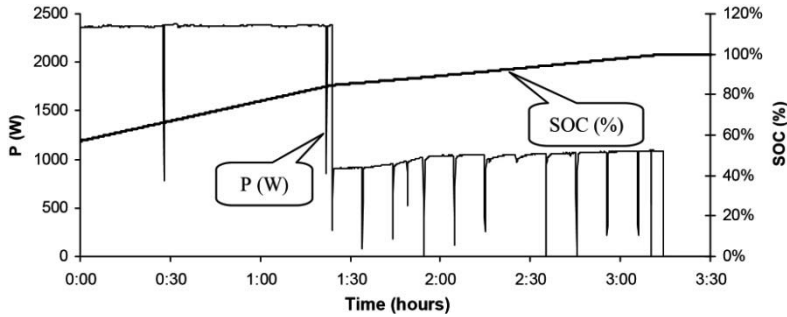


**Figure 3.21.** Charging power and SOC for the NiCd battery of the Peugeot 106 (source CEA)

The charger delivers the maximum power (approximately 2.4 kW) until an 85% SOC is reached. Beyond this SOC, it reduces the power to around 1 kW. The increase in current during the second phase is due to the increase in PV production during the morning. The gaps in the current enable us to measure the no-load voltage.

### 3.1.5.2. Electric car with a lithium-ion battery

The C-LMO (graphite–lithium manganese oxide) lithium-ion battery in the Nissan Leaf has a nominal capacity of 24 kWh. The power injected and the SOC are shown in Figure 3.22.

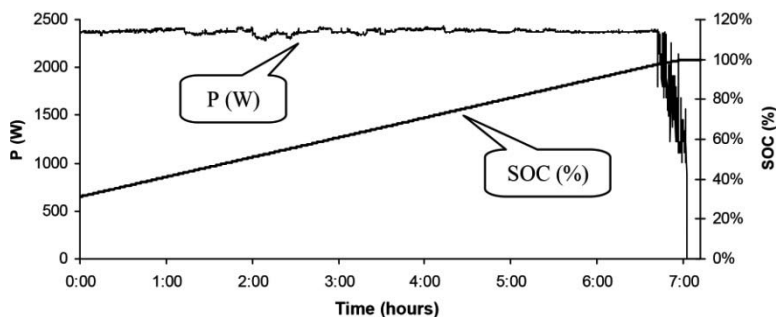


**Figure 3.22.** Charging power and SOC for the C-LMO lithium-ion battery in the Nissan Leaf (source CEA)

### 3.1.5.3. Small electric car with a lithium-ion battery

The lithium-ion battery in the Renault Twizy has a nominal capacity of 6 kWh. The power injected and SOC are shown in Figure 3.23.

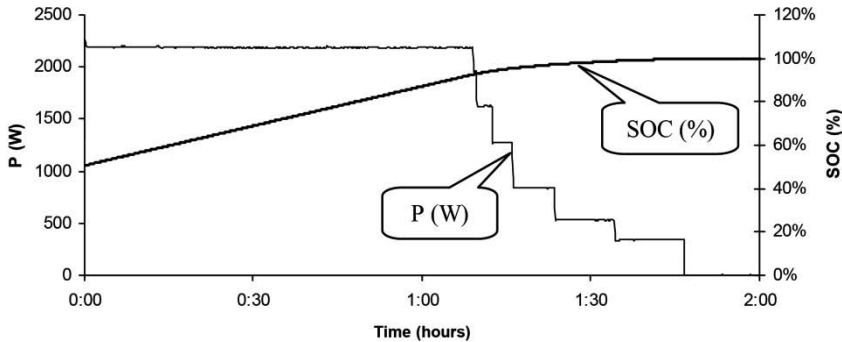


**Figure 3.23.** Charging power and SOC for the lithium-ion battery in the Renault Twizy (source CEA)

### 3.1.5.4. Plug-in hybrid electric car with a lithium-ion battery

In a plug-in hybrid electric car, the battery has a smaller storage capacity (4.4 kWh) than in a purely electric vehicle, because this type of vehicle has another energy source which is its combustion engine. With charger powers comparable to the previous cases, the charge is therefore much quicker. This is illustrated in Figure 3.24 on the basis on measurements taken in the case of a plug-in Toyota Prius.

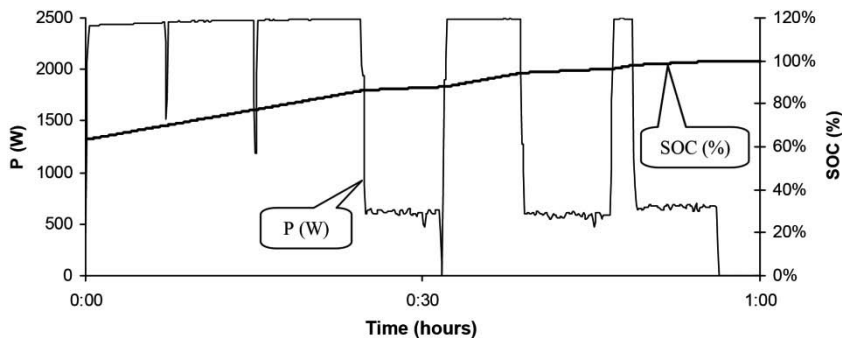


**Figure 3.24.** Charging power and SOC for the lithium-ion battery in a plug-in Toyota Prius using PV production multiplexed over several chargers (source CEA)

The charger delivers either its maximum power (around 2.4 kW) or a reduced power (0.7 kW). In part, it is the overall management algorithm in the vehicles charging under the roof of the parking shed which imposes these two levels of power to distribute the PV power between the different vehicles charging simultaneously. In spite of spells with reduced power, a battery at 64% SOC is raised to its fully-charged state in less than one hour.

### 3.1.5.5. Remark about the chargers of batteries of electric vehicles

The examples given above demonstrate that there is not really a “standard” charge profile for the batteries in electric vehicles. Even with the last three cases, which all use a lithium-ion battery, the end-of-charge periods are dealt with differently. However, we can compare the end-of-charge periods for the Leaf (Figure 3.25) and the Twizy (Figure 3.26) which exhibit classic decrease: the charger in the Leaf reduces the power beyond an SOC of around 98%, whereas the Twizy’s charger begins charging at reduced power at a 92% SOC. The reduced-power phase lasts around 20 minutes for the Leaf but 40 minutes for the Twizy, although the Twizy’s capacity is quarter of that of the Leaf.

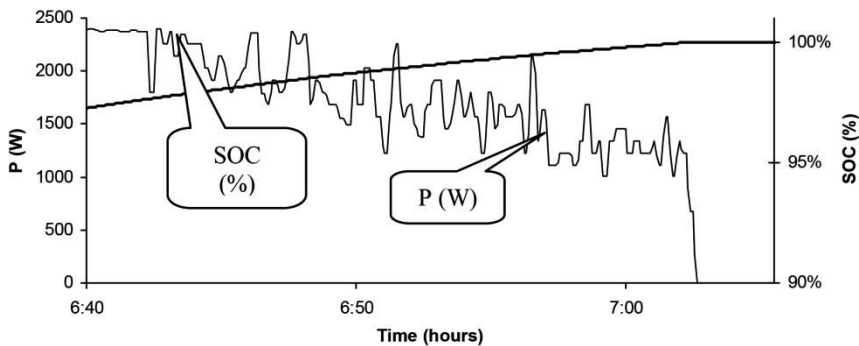


**Figure 3.25.** Charging power and SOC at end of charge for the lithium-ion battery in the Nissan Leaf (source CEA)

### 3.1.6. Autonomous urban lighting

In order to limit installation and operational costs, increasingly often we are seeing street furniture with autonomous power supplies, such as parking meters or streetlamps. This limits the need for trench-digging, sidewalk-resurfacing and electricity meter rental.

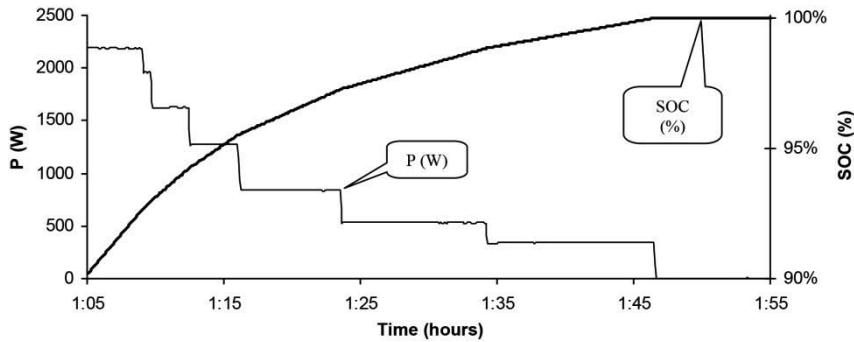


**Figure 3.26.** Charging power and SOC at end of charge for the lithium-ion battery in the Renault Twizy (source CEA)

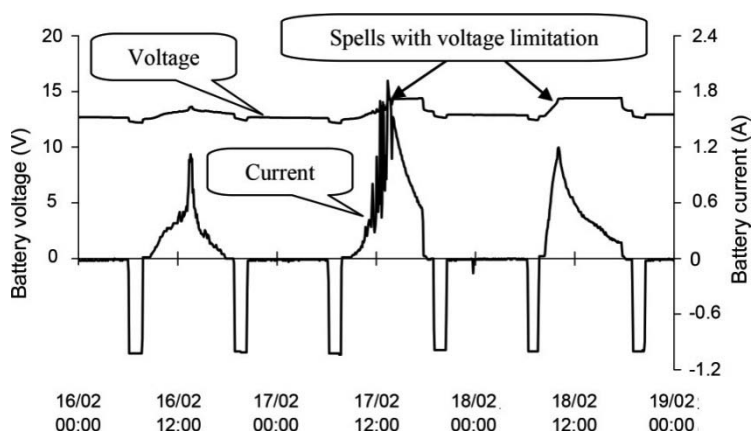
The following example is based on measurements taken in February 2013 on streetlamps developed and commercialized by the company NOVEA Energies ([www.novea-energies.com](http://www.novea-energies.com)).<sup>12</sup> These lamps use powerful LEDs. This light source is chosen for its high energy efficiency<sup>13</sup> (in lumens per watt) to minimize the size of the battery (and thereby minimize the installation cost) and/or increase the range so as to limit maintenance.

Figure 3.27 presents the current (algebraic and averaged over 5 minutes) injected into the battery and the voltage at its terminals. On 16 February, the battery is not completely charged by the PV production: all the PV energy produced is used. Over the next two days, the battery reaches a level of charge such that the voltage at its terminals is limited (14.8 V). The charging current decreases. Some of the energy that can be produced by the PV generator is not used.

From the point of view of consumption, the streetlamp is programmed to deliver full lighting power for 1 hour 30 minutes at the beginning and end of the hours of darkness. In addition, it illuminates at full power for 45 seconds every time the passage of a user is detected.

<sup>12</sup> The authors would like to thank Jean-Pierre Belliard, the founder and CEO of the company NOVEA Energies, and Jérémie Jousse, a doctoral candidate at NOVEA/CEA, for all the data and explanations they kindly supplied.

<sup>13</sup> The LED also has the longest lifetime of all possible light sources, which minimizes the need for the costly operation of *relamping* (changing of the lamp).



**Figure 3.27.** Current injected and voltage for the battery of a LINEO 2 solar streetlamp from NOVEA Energies ([www.novea-energies.com](http://www.novea-energies.com))

EXERCISE 3.7.– Calculate (in Ah) the amount of electricity required of the battery during the periods of illumination at the beginning and end of the hours of darkness (at full power, the current summoned by LEDs will be taken to be 1 A).

*Solution page 112*

EXERCISE 3.8.– Calculate (in Ah) the amount of electricity required from the battery each time the passage of a user is detected.

*Solution page 112*

Assume that there are 20 occurrences during the night of the passage of a user being detected. Then calculate the amount of electricity required from the battery for the total number of passages during the night.

EXERCISE 3.9.– With the above data, calculate the battery capacity needed to obtain a range of 5 days without the sun.

*Solution page 113*

### 3.2. Conclusion

This chapter has illustrated some of the very numerous applications in which batteries are crucial. Even today, we find secondary batteries of very different generations (flooded lead–acid batteries, VRLAs, NiCd, lithium).

However, the tendency is toward the introduction and promulgation of the most recent technologies – take for instance all the variants of lithium batteries for a very broad range of power and stored energies, or indeed hot batteries or redox flow batteries for large-scale storage. It is these modern secondary batteries which we are going to discuss in the coming chapters.

### 3.3. Solution to the exercises in Chapter 3

#### *Solution to exercise 3.1: amount of electricity produced in one day*

If we assimilate the PV production to a half-sinusoid of duration 9.25 hours and peak intensity 70 A, the quantity  $Q$  of electricity produced over the course of a day is written:

$$Q = \int_{\text{over 24hrs}} i \cdot dt = \int_0^{9.25\text{h}} I_{\text{MAX}} \cdot \sin\left(\frac{t}{9.25} \cdot \pi\right) \cdot dt = 70 \cdot \frac{9.25}{\pi} \cdot \left(-\cos\left[\frac{t}{9.25} \cdot \pi\right]\right)_0^{9.25}$$

$$Q = 70 \cdot \frac{9.25}{\pi} \cdot [-\cos(\pi) + \cos(0)] = 70 \cdot \frac{9.25}{\pi} \cdot 2 = 417\text{Ah} \quad [3.1]$$

The half-sinusoidal model is justified by Figure 3.28:

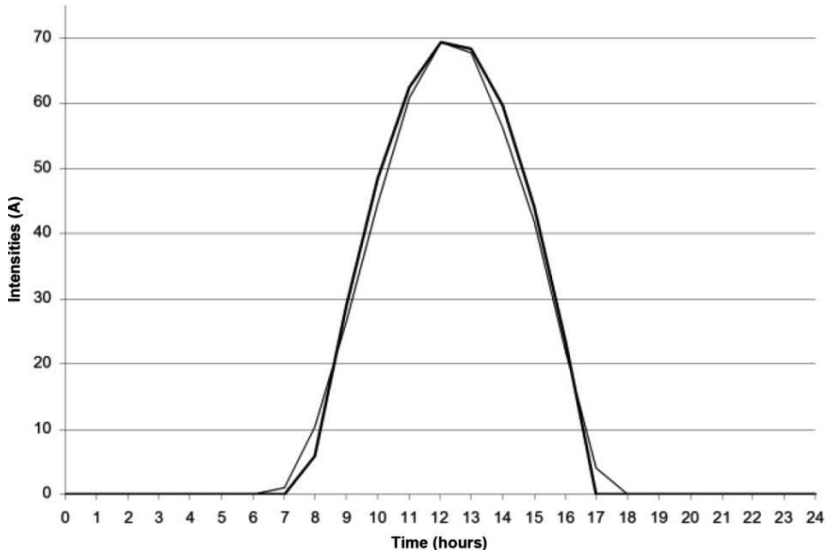


**Figure 3.28.** PV production (thin line) and half-sinusoidal model (thick line).  
The curves are drawn using one point per hour

The half-sinusoidal model shows a quantity of electricity equal to 417 Ah, whereas the actual PV production is 404 Ah, so there is an error of around 3%. This error is acceptable in view of the simplicity of the model.

***Solution to exercise 3.2: maximum amount of electricity needed to run the electronics***

The maximum power absorbed by the electronics is 2.6 kW. This requires a maximum daily amount of electricity of  $2600 \text{ W} \times 24 \text{ hrs}/48 \text{ V} = 1300 \text{ Ah}$ .

In reality, the average power is 2.2 kW at an average voltage of 49 V, which gives us an average current demand<sup>14</sup> of  $2200/49 = 45 \text{ A}$  and a daily amount of electricity of  $2200 \text{ W} \times 24 \text{ hrs}/49 \text{ V} = 1078 \text{ Ah}$ .

***Solution to exercise 3.3: the installation's energy requirements***

The maximum daily amount of electricity (1300 Ah) and the real daily amount of electricity (1078 Ah) are both greater than the photovoltaic production (by approximately 400 Ah), even if we suppose that the energy producible by the PV generator is indeed produced, meaning that the battery is never fully charged, the result of which would be that the difference between the power produced by the PV generator and that consumed by the BTS is lost.

***Solution to exercise 3.4: range of the system***

The stored energy is 130 kWh. However, not all of this energy can be used, because with a lead–acid battery, the DOD should not exceed 80%. The maximum power required is 2.6 kW. Thus, the range is at least  $130 \text{ kWh} \times 0.8/2.6 \text{ kW}$ , which is 40 hours. If we look at the average power absorption (2.2 kW), the range increases to  $130 \text{ kWh} \times 0.8/2.2 \text{ kW}$ , which is 47 hours. Therefore, we can estimate the range of the system when running on the battery alone as being nearly two days.

---

<sup>14</sup> Strictly speaking, we cannot write that the average power is the product of the average current and the average voltage. This calculation is performed here because the values of current and voltage are relatively constant.

***Solution to exercise 3.5: power supplied by the photovoltaic system and the electrogen group***

The maximum power delivered by the electrogen group is  $180 \text{ A} \times 53 \text{ V} = 9.5 \text{ kW}$ . Its label indicates 15 kVA. It is more powerful than the PV generator, which is specified as having a  $9 \text{ kW}_p$  power. It is noteworthy that, unlike with a PV generator, the power supplied by the electrogen group is not dependent on solar irradiation, and depends only, to a secondary degree, on the temperature.

***Solution to exercise 3.6: range of the system***

The battery stores 2350 Ah at 48 V, which gives us an energy value equal to 113 kWh. As the battery being used employs lead technology, it is not discharged below an 80% DOD. The usable energy, therefore, is  $113 \times 0.8 = 90 \text{ kWh}$ . With an average daily consumption of 10 kWh, the range is therefore 9 days.

***Solution to exercise 3.7: amount of electricity required during the periods of illumination at the beginning and end of the hours of darkness***

The amount of electricity corresponding to an intensity of 1 A for 1.5 hours is 1.5 Ah. The total amount of electricity required over the course of a night is therefore 3 Ah.

***Solution to exercise 3.8: amount of electricity required when the passage of a user is detected***

The amount of electricity corresponding to an intensity of 1 A for 45 seconds is  $1 \times (45/3600) \text{ Ah} = 0.0125 \text{ Ah}$ .

For 20 such illuminations, the amount of electricity required is equal to  $20 \times 0.0125 = 0.25 \text{ Ah}$ . This is much less than the amount of electricity needed for the illumination after dusk and before dawn. Thus, in order to decrease the sizing of the battery, it is advantageous to have the streetlamp only illuminate when it is necessary.



***Solution to exercise 3.9: battery capacity***

The amount of electricity needed for 24 hours is  $3 + 0.25$  Ah. For 5 days, we need  $5 \times (3 + 0.25) = 16.25$  Ah.

If we are using a lead–acid battery, we need to avoid having the SOC go below 20%. The required capacity would therefore be  $16.25/(1-0.2) = 20$  Ah. Finally, the standards stipulate that an industrial battery reaches end-of-life when its capacity is no longer more than 80% of its nominal capacity. Hence, we shall choose a battery with at least  $20/0.8$ , which is 25 Ah.



## PART 2

# Lithium Batteries



## Chapter 4

# Introduction to Lithium Batteries

### 4.1. History of lithium batteries

At present, lithium batteries are still in the full throes of development, irrespective of the component in question (electrodes, electrolyte, design, etc.). Although the first experiments on electrochemical generators using lithium began in 1912 (with G.N. Lewis), research really began in earnest in the 1960s. The very high electronegativity<sup>1</sup> of this material (in electrochemistry, we more usually speak of the highly reductive nature of the  $\text{Li}^+/\text{Li}$  couple:  $-3.05 \text{ V/NHE}^{(2)}$ ) when combined with another more oxidative couple<sup>3</sup>, indeed renders it very attractive for making generators with a “high” voltage, and therefore which *a priori* offer a high energy density – all the more so as this material has a particularly low density<sup>4</sup>

---

1 The  $\text{Li}^+/\text{Li}$  couple exhibits the lowest redox potential. Used in combination with a different redox couple involving the lithium ion, it will always have a lower potential and will therefore always be the negative electrode.

2 The Normal Hydrogen Electrode (NHE) is defined in footnote 56 in Chapter 2.

3 A table of oxidant/reducer couples is given in section 4.4.

4 This increase in gravimetric energy density is, however, accompanied by a decrease in volumetric energy density. Indeed, for a given capacity, a given mass of lithium is needed, which means a more significant volume of it, when compared to another denser electrochemical couple. This implies using electrodes with a greater volume, a larger quantity of electrolyte and consequently a larger container. Finally, the mass of the secondary battery increases and the gravimetric energy density decreases.

(0.534). One of the difficulties with its use lies in the formulation of an electrolyte that is compatible with the electrode voltages, particularly in the higher ranges of voltage (beyond 4 V), so mainly toward the end of a charge cycle.<sup>5</sup> Unless particular caution is exercised (see section 10.2.1), aqueous electrolytes are precluded in lithium batteries, because lithium oxidizes spontaneously on contact with water. Indeed, it is impossible for the same medium (the electrolyte) to contain both the oxidant  $\text{H}_2\text{O}$  from the couple  $\text{H}_2\text{O}/\text{H}_2$ , which has the highest possible potential<sup>6</sup>, and the reducer  $\text{LiC}_6$  from the couple  $\text{C}/\text{LiC}_6$  or lithium from the couple  $\text{Li}^+/\text{Li}$ , which have the lowest possible potentials, as this would cause a spontaneous reaction whereby the water would be reduced and the graphite lithiated or the lithium would be oxidized. These organic solvents also spontaneously react with metallic lithium, as soon as they are brought into contact, but form insoluble lithium salts at the interface and which then passivize (i.e. chemically insulate) the electrode. This layer (sometimes referred to as the passivation film) is commonly called the *Solid-Electrolyte Interphase* (SEI). However, it is permeable to  $\text{Li}^+$  ions – a condition which is of crucial importance for the operation of the battery. Hence, it plays a fundamental role in the operation and the lifetime of the lithium battery.

Chemically speaking, the general operational principle of lithium batteries is based on charge, on the side of the negative electrode, on the reduction of the lithium ion by capture of an electron from the external electrical circuit:



In the case of lithium-ion batteries based on the principle of insertion (explained in section 4.3.1), the lithium ions, even when they are inserted, retain a significant positive charge, and the sites of insertion of the intercalation material retain a negative charge.<sup>7</sup>

---

<sup>5</sup> When there is no more lithium to be extracted from the positive electrode, the electrode degrades, as does the electrolyte. The negative, which is often present in excess capacity in comparison to the positive electrode, does not present such dangers, at least at the beginning of its life.

<sup>6</sup> 4.28V versus  $\text{Li}^+/\text{Li}$  (case of a metal lithium negative electrode) or 4.18V versus  $\text{C}/\text{LiC}_6$  (case of a lithiated carbon negative electrode in lithium-ion secondary batteries).

<sup>7</sup> M. WINTER, K.-C. MOELLER, J.O. BESENHARD, Chapter 5 “Carbonaceous and graphitic anodes”, section 5.3.2.3 “Nature of the bond in Li-graphite intercalation compounds”, in G.-A. NAZRI, G. PISTOIA (Eds) *Lithium-ion Battery, Science & technology*, 2009.

On the positive side, the electrode is the site of the oxidation (see section 2.2.4) of the reduced form LiRed of the active matter, with the release of an electron into the external electrical circuit:



To begin with (in the mid-1970s<sup>8</sup>), the positive electrode was made of intercalation materials such as  $\text{TiS}_2$  (titanium disulfide) whose lamellar structure contained inserted lithium, the negative electrode being made simply of metal lithium, with the difficulties inherent to that electrode, which we shall recap below. These difficulties remain with lithium-metal polymer technology as described in Chapter 8.

During discharge, the reactions are reversed: the lithium is oxidized and the positive material Ox is reduced:



Very early on, it was shown that electro-deposition of lithium does not occur homogeneously all over the active surface but rather in a divided form, forming outgrowths called dendrites (see section 4.4.2 at the end of this chapter) – all the more so when the current densities are high. The surface areas developed by these deposits are very significant, and react with the electrolyte, becoming passivated. Hence, some of the electrolyte which is in contact with these surfaces is consumed during each cycle. These irregular, “foamy” deposits may also break off, forming isolated micro-aggregates: this phenomenon results in the loss of active material at each cycle, which causes a charge efficiency of less than one. In order to compensate for this loss of capacity, the element is manufactured with an excess quantity of lithium (and of electrolyte), so there is more lithium (and electrolyte) than is strictly necessary. However, this is done to the detriment of the gravimetric energy density. In addition, these outgrowths cause another major disadvantage: they have a significant effect on the battery’s capability to undergo cycles because they “grow” through the separator and cause internal short-circuits, thereby shortening the lifetime of the battery. Furthermore, the

---

8 M.S. WHITTINGHAM (from Exxon), “Electrical energy storage and intercalation chemistry”, *Science*, vol. 192, no. 4244, pp. 1126–1127, 1976.

operational safety of the battery is damaged by this dendritic phenomenon, because the re-deposited lithium is very divided, is extremely reactive and may burst into flame if there is a local increase in temperature (micro short-circuits) or the casing of the battery is accidentally ruptured. These devices therefore have limited recharge power densities so as to reduce the danger of dendrite formation (by limiting the current density applied to charge the element).

These constraints account for the fact that the earliest electrochemical generators using lithium and an organic liquid electrolyte were simple primary batteries (non-rechargeable), commercialized in the 1970s: in a non-rechargeable cell, the absence of recharge process means there is no deposition of lithium, and therefore no danger of dendrite formation. The first rechargeable systems endured only until the early 1980s, after immense and fruitless research into how to address the issue of lithium deposition and two abandoned attempts at commercialization. Researchers then turned their attention to another material for the negative electrode into which lithium could be inserted, and whose structure would be equivalent to that of the positive electrode made of  $\text{TiS}_2$ . The choice was based on a graphite host matrix with a flat two-dimensional structure, into which the lithium could be inserted. This reversible introduction of lithium into the graphite was demonstrated in an electrochemical cell with a polymer electrolyte by R. Yazami and Ph. Touzain<sup>9</sup> in 1983. It became apparent that the choice of electrolytic solvents, the nature of the original carbonaceous materials and the heat treatments to graphitize these carbon materials are crucial to ensuring the reversibility of the intercalation reaction, which is possible only with the formation of a passivation film at the interface between the carbon and the electrolyte (SEI). Once again, these investigations commanded the attention of a great many researchers.

It is this idea of the insertion/extraction of lithium ions into/from the electrodes which Sony Energitech (Japan) exploited, to develop and commercialize (since 1991) the technology it called “lithium-ion” (Li-ion), in order to serve applications where the volumetric and particularly the gravimetric energy densities are very important criteria. Such applications

---

9 R. YAZAMI, Ph. TOUZAIN “A reversible graphite-lithium negative electrode for electrochemical generators”. *Journal of Power Sources*, vol. 9, no 3, pp. 365–371, 1983.



relate essentially to power supply to mobile systems such as portable computers, cellphones, digital cameras, etc. Nowadays, the fields of application are broader and lithium-ion batteries are tending to replace other electrochemical couples such as NiMH for mobile devices, for instance.

## 4.2. Categories of lithium batteries

The term “lithium battery” is a generic umbrella term which covers two broad categories:

- lithium-ion<sup>10</sup> technologies, in which lithium ions are exchanged, e.g. by way of insertion/extraction mechanisms (see section 4.3.1), from one electrode to the other. For this to happen, both electrodes have to be made of two materials capable of accepting lithium, as reversibly as possible. The next section (4.3) goes into greater detail about the different materials for electrodes which are currently used commercially or are in the development phase. The electrolytes used are either organic (liquids or polymers) or ionic liquids, which are not yet at the stage of commercial viability (see section 5.5). Lithium-ion technology will be described from an electrochemical point of view in Chapters 5 to 7.

- lithium metal polymer technology, in which the negative electrode is made of a foil of metal lithium, with the electrolyte being a polymer film based on poly(ethylene oxide) (PEO) with lithium salt and the positive electrode an intercalation material. This technology will be described from an electrochemical point of view in Chapter 8.

In the category of metal-lithium-based batteries, we must also cite lithium-sulfur and lithium-air batteries, which we shall discuss in Chapters 9 and 10. The negative electrode is composed of metal lithium; the positive electrode, which is the innovative component in these two systems, is oxygen for lithium-air and liquid sulfur with the formation of lithium polysulfide  $\text{Li}_2\text{S}_x$  during discharge for lithium-sulfur technology. Their performances in terms of gravimetric energy density are very promising with potential values of over 500 Wh/kg.

---

10 M. BROUSSELY, “Les accumulateurs lithium-ion - état de l’art”, *La Revue 3EI*, no. 48, pp. 36–45, 2007.

### 4.3. The different operational mechanisms for lithium batteries

The variety of nature, composition and structure of the compounds available as active materials causes a diversity of lithiation/de-lithiation electrochemical reactions. A classification can be established on the basis of the nature of the redox reaction that occurs in the active material to accommodate the lithium. This is what is done below.

#### 4.3.1. *Intercalation (or insertion) materials*<sup>11</sup>

According to IUPAC (International Union of Pure and Applied Chemistry), an intercalation reaction is a generally-reversible reaction which involves the introduction of a species into a host structure without major alteration of that structure, be it in terms of dimensions or of chemistry. This term applies more specifically in the case of insertion of a species into a one, two- or three-dimensional structure. The inserted species is not randomly distributed but rather occupies chosen positions within the host structure. These 1D, 2D or 3D networks are represented diagrammatically in Figure 4.1. The spaces available in these structures are the preferred positions to receive the lithium.

The materials for electrodes present in lithium-ion batteries and corresponding to this definition are (Figure 4.1):

- lamellar graphites or oxides  $\text{LiMO}_2$  (where  $\text{M} = \text{Co}, \text{Ni}, \text{Mn}$ ) in which the lithiation/de-lithiation reaction occurs by insertion of lithium between planes or layers (1D structure);
- the compounds  $\text{LiMn}_2\text{O}_4$  or  $\text{Li}_4\text{Ti}_5\text{O}_{12}$ , whose 2D structure facilitates the reversible occupation of lithium ions in the vacant accessible sites (cavities);

---

<sup>11</sup> We can consider that the terms “intercalation” and its opposite, “de-intercalation”, apply only in the case of a crystalline network whose structure remains unchanged (presence of preferred sites within the crystalline network where the intercalated species is placed). Hence, these are very restrictive terms.

The terms “insertion” and its opposite, “extraction” are also frequently found, but apply more generally to any reaction which leads to the introduction of one species into a host structure, whether or not there is a structural or chemical alteration (e.g. breaking of a covalent bond) to the host structure. Hence, the definition is broader than that of intercalation.

– lithiated phosphates ( $\text{LiFePO}_4$  or  $\text{LiFe}_y\text{M}_{(1-y)}\text{PO}_4$ , where  $\text{M} = \text{Mn}, \text{Co}$ , etc.), which have a 3D structure.

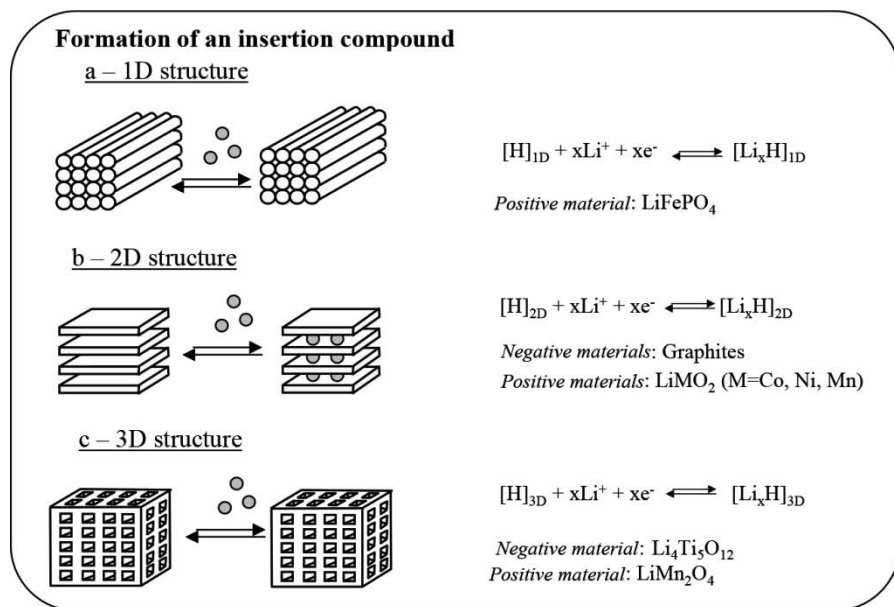


**Figure 4.1.** Diagrammatic representation of the spaces available in 1D, 2D and 3D crystalline structures and illustration of the insertion mechanisms

The specific capacities of these types of compounds are limited by the number of vacant sites in the host structure. The very slight variations in volume (5-10% alteration of the crystal lattice between the de-lithiated and fully lithiated states) mean that they exhibit very significant cycle lifetimes.

#### 4.3.2. Alloys

Pure metals and metal compounds (metal oxides, intermetallic compounds) which are capable of forming alloys with lithium constitute another category of electrode materials versus the insertion materials seen previously. They are used for the negative electrode in lithium-ion batteries because their redox potential versus lithium is less than 2 V. They are cited in the following four sections:

#### 4.3.2.1. Alloys of pure metals

Alloys of pure metals such as silicon, tin, aluminum, antimony, germanium (and others) offer great interest, because the amount of lithium that can be dissolved in the metal is very high (as demonstrated by the gravimetric capacities obtained: for instance, 4200 mAh/g for  $\text{Li}_{22}\text{Si}_5$  and 991 mAh/g for  $\text{Li}_{22}\text{Sn}_5$  – these values are much higher than those obtained with conventional negative electrodes ( $< 400$  mAh/g, as indicated by Table 5.2), but this can only be achieved at the cost of non-reversibility of the lithiation/de-lithiation mechanism. Indeed, when the lithium is introduced into the crystal structure of the metal, we see a reorganization with a consequent increase in volume of the crystal lattice, up to three times its initial volume in certain cases with complete lithiation. This volumetric expansion leads to significant mechanical stresses, which result in the cracking of the surface and loss of integrity of the electrode.<sup>12</sup> Thus, the capacity falls after a few cycles. This phenomenon is not seen with insertion materials for which the volumetric expansion after lithiation is less than 11%, for instance (this is the value of the change in distance between layers of graphene (shown in Figure 5.6) between graphite and lithiated graphite  $\text{LiC}_6$ ).

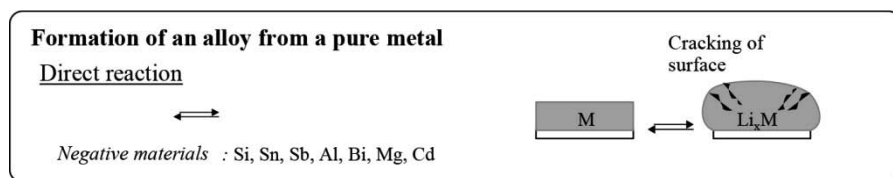


**Figure 4.2.** Diagrammatic representation of the lithiation of an alloy of pure metal

In order to minimize the impact of volumetric expansion, nanoparticles are used. However, the first cycle presents a significant irreversible capacity<sup>13</sup> due to the formation of a passivation layer on the surface of the nanoparticles, creating a very significant specific surface area. In spite of this, the cyclability during subsequent cycles is enhanced by this approach (see section 4.3.2.4).

<sup>12</sup> A microphone is able to pick up the acoustic sound of this cracking, whereas with insertion materials, no perceptible noise is emitted.

<sup>13</sup> Note that, for certain technologies, not all of the electricity injected during the first charge process is released during the first discharge. This difference in the amount of electricity is called the irreversible capacity.

#### 4.3.2.2. Alloys formed from a metal oxide

In alloys formed from a metal oxide (e.g. SnO), the electrochemical process that occurs takes place in two stages. Only the second stage is reversible. Stage 1 consists of the formation *in situ* of metallic nanoparticles in the inert Li<sub>2</sub>O matrix which plays the role of a “buffer”, minimizing the volumetric expansion of the active metal species M<sup>0</sup> (14) during its lithiation (stage 2) and preventing the clustering of small M<sup>0</sup> particles to form larger particles.

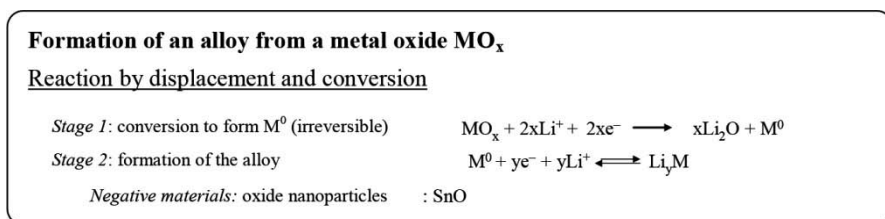
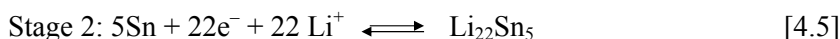


**Figure 4.3.** Representation of the mechanisms of lithiation of an alloy formed from a metal oxide

The reactions leading to the formation of the lithiated alloy Li<sub>22</sub>Sn<sub>5</sub> are shown below:



The gravimetric capacity of Li<sub>22</sub>Sn<sub>5</sub> is 994 mAh/g, with an insertion potential of approximately 0.5 V versus Li<sup>+</sup>/Li, but the irreversible capacity during the first cycle is very significant and the cyclability remains to be improved.

#### 4.3.2.3. Intermetallic compounds

Intermetallic compounds (solid solution of several metals such as Cu<sub>6</sub>Sn<sub>5</sub>) again obey the principle of dispersion of the active species, as seen with lithium in a matrix comprising metallic elements which play the part of an inactive support. In this type of alloys, MM', the inactive metal versus lithium plays the role of a “buffer” and limits the consequences of the volumetric expansion of the active metal.

14 The notation M<sup>0</sup> represents a metal with a zero degree of oxidation, so a pure metal.

As shown by Figure 4.4<sup>15</sup>, we speak of a reaction by conversion, or displacement and conversion, because it is a question of introducing lithium into the lattice, which leads to the displacement of the inactive species.

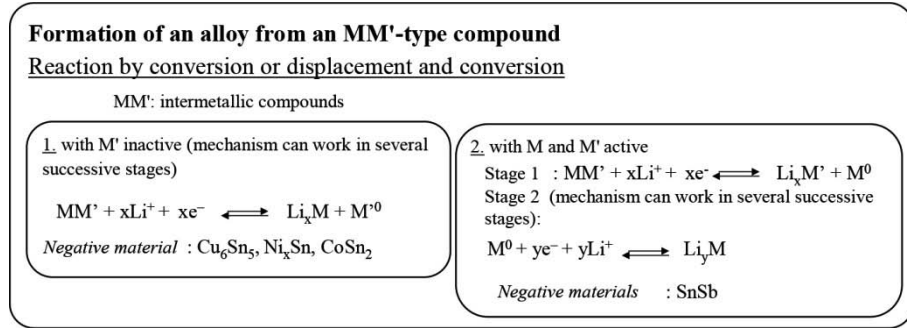


**Figure 4.4.** Representation of the lithiation of an alloy formed from an intermetallic compound

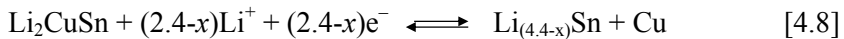
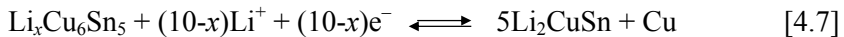
This type of mechanism is often limited by the number of atoms of lithium which can be inserted into the host structure MM', which prevents us from achieving particularly significant capacities. Conversely the cycle resistance is excellent.

For case 1, we can give the example of the bi-metallic compound Cu<sub>6</sub>Sn, for which the insertion of lithium occurs in two steps:

Step 1: Formation of a solid solution Li<sub>x</sub>CuSn

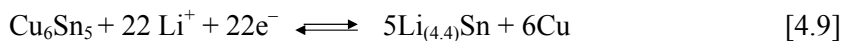


Step 2: Decomposition by displacement of the Cu outside the lattice and formation of the Li<sub>x</sub>Sn phase.



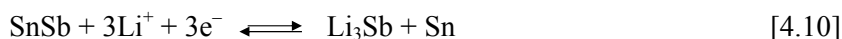
15 M. MOUYANE, Nouveaux matériaux composites pour électrodes négatives à base d'étain, Doctoral thesis, Université Montpellier II, 11 December 2008.

Balance:

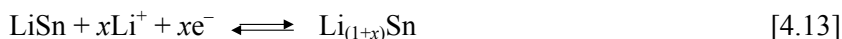


The reversible capacity of this material is around 300 mAh/g with a good cycle behavior.

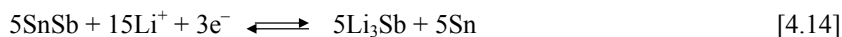
For case 2, we cite the example of the compound SnSb, for which the lithium interacts as shown in the following steps:



Then:



Balance:



The reversible capacity of this material is around 600 mAh/g with a good cycle behavior.

#### 4.3.2.4. Alloys formed in a matrix

In order to prevent the irreversible capacity loss during the first cycle and to reduce the volumetric expansion of the crystal lattice, the active element can be dispersed, not *in situ* as above, but *ex situ* in a electrochemically-inactive matrix. This is a promising technique, because it reduces the phenomenon of clustering of the active species. In order to do this, two methods have been developed: embedding of the particles within the support matrix and adhesion to the surface of the particles of the matrix. Various composites have been studied, but generally always we see the presence of particles of silica (Si/C) or tin: Sn/C, Sn-Fe/C, Sb/CNT, SnSb<sub>0.5</sub>/CNT. For the latter two compounds, Sb or SnSb<sub>0.5</sub> is deposited on the surface of carbon nanotubes (CNTs).

Synthesis of the composite Sn/C can be performed by the chemical reduction of a salt of tin ( $\text{SnCl}_2$  for instance) in solution in an organic medium in the presence of carbon in an inert atmosphere (argon). This mode of synthesis facilitates the formation of nanoparticles of tin finely dispersed on the surface of the carbon particles, whose structure is able to absorb the volumetric variations of the tin. The active particle can also be dispersed through an oxide-type inactive matrix, such as  $\text{Al}_2\text{O}_3$ .

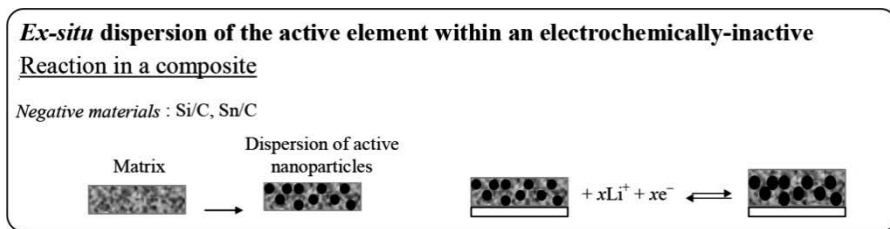


**Figure 4.5.** Representation of the mechanisms of lithiation of an alloy from metallic particles dispersed ex-situ in an inactive matrix

#### 4.3.3. Direction conversion materials

We speak of a direct conversion when there is an alteration of the chemical structure of the material in the wake of a reaction of decomposition of the original material,  $\text{MX}$ , in a composite electrode comprising nanoparticles of metal  $\text{M}^0$  encapsulated in a  $\text{LiX}$  matrix. There is no formation of a lithiated metal alloy as before, but rather of metal particles which are inactive in comparison to lithium. The reaction leads to the formation of a metastable compound  $\text{LiX}$  (essentially  $\text{Li}_2\text{O}$ ). In theory, this compound which is formed is not stable, but it is considered to be so because of its very slow rate of transformation. Many transition-metal oxides are involved: oxides of cobalt  $\text{CoO}$  and  $\text{Co}_3\text{O}_4$ , of copper  $\text{CuO}$ , of nickel  $\text{NiO}$  and of iron  $\text{FeO}$  and  $\text{Fe}_2\text{O}_3$ . Other compounds such as  $\text{NiP}_3$  and  $\text{FeS}_2$  can also be considered.

#### **Conversion reaction with the formation of a metastable compound**



Negative materials:  $\text{CoO}$ ,  $\text{Co}_3\text{O}_4$ ,  $\text{CuO}$ ,  $\text{NiO}$ ,  $\text{FeO}$ ,  $\text{Fe}_2\text{O}_3$ ,  $\text{NiP}_3$ ,  $\text{FeS}_2$

**Figure 4.6.** Representation of the mechanisms of direct conversion



Some examples of conversion reactions are given below:

For the compound CoO:

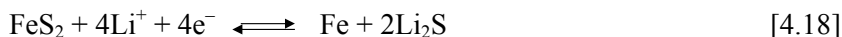


Electrochemical tests performed on simple cobalt oxides demonstrate specific capacities between 700 and 1100 mAh/g and an excellent cycle behavior. The formation of nanoparticles of cobalt dispersed in a  $\text{Li}_2\text{O}$  matrix occurs because of the reduction of the cobalt in CoO.  $\text{Li}_2\text{O}$  is often inactive in electrochemistry, but its formation *in situ* in the material means it is able to be electrochemically active. However, the cost of cobalt reduces the commercial prospects of this type of compound.

For the compound  $\text{NiP}_3$ :



For the compound  $\text{FeS}_2$ :



These last two reactions are highly interesting because the resultant gravimetric capacity is very high: 1590 mAh/g for  $\text{NiP}_3$ , for instance. These types of conversion materials have potentials of less than 2 V versus  $\text{Li}^+/\text{Li}$ . Therefore, they are used for the negative electrode in lithium-ion elements.

Many other examples (approximately fifty) are to be found in the publication by Cabana *et al.*<sup>16</sup>

#### **4.3.4. Differences of voltage profiles between intercalation materials, alloys and conversion materials**

We can see significant hysteresis of the voltage between the process of charge and discharge with materials for which the processes occurring involve the formation and breakage of covalent bonds between atoms. The

---

<sup>16</sup> J. CABANA, L. MONCONDUIT, D. LARCHER and M. R. PALACÍN “Beyond intercalation-based Li-ion batteries: State of the art and challenges of electrode materials reacting through conversion reactions”. *Advanced Materials*, 22, E170-E192, 2010.

conversion energies required in both senses are significant. Such hysteresis is not seen with intercalation phenomena:  $\text{LiCoO}_2$ , C (in the case of graphite, the layers of graphene hardly move at all when the lithium is inserted).

#### ***4.3.5. Properties of the electrode materials***

Regardless of the nature of the materials and the type of reaction involved, the electrode materials need to satisfy a certain number of requirements such as:

- a high Gibbs free energy with lithium (i.e. the facility for the compound to accommodate lithium);
- the aptitude to incorporate as much lithium as possible;
- reversibility of the reaction;
- high diffusivity of lithium;
- good electrical conductivity;
- insolubility in the electrolyte;
- a process of synthesis from available, affordable compounds, and the process itself must not be costly.

Intercalation compounds fulfill most of these requirements, with the exception of the aptitude to accept a large amount of lithium, because the number of vacant sites within the crystal lattice is low. Intercalation compounds are presents in most batteries sold the world over, unlike other types of materials. These other materials are also more recent and are still at the stage of development with a view to improving their performances in terms of cycling. Pure alloys are not widely present in the world of commerce as negative materials, except in certain “coin cell” elements intended for the backup of information in electronic circuits (see section 1.2.3.4) – an application for which the DODs are usually slight and therefore the volumetric expansions on the scale of the material are reduced, thereby facilitating a large number of cycles.

## 4.4. Appendices

### 4.4.1. Appendix 1: Examples of redox couples

The table below shows the redox potentials (in volts) of a number of redox couples used in lithium batteries, quoted versus the normal hydrogen electrode (NHE):<sup>17</sup>

|   |       |
|---|-------|
| $\text{MnO}_4^- / \text{MnO}_2$                   | +1.69 |
| $\text{MnO}_4^- / \text{Mn}^{2+}$                 | +1.51 |
| $\text{MnO}_2 / \text{Mn}^{2+}$                   | +1.23 |
| $\text{O}_2 / \text{H}_2\text{O}$                 | +1.23 |
| $\text{O}_2 / \text{O}^{2-}$                      | +1.12 |
| $\text{Mn}_2\text{O}_4 / \text{LiMn}_2\text{O}_4$ | +1.0  |
| $\text{Li}_{0.5}\text{CoO}_2 / \text{CoO}_2$      | +0.9  |
| $\text{NiO}_2 / \text{LiNiO}_2$                   | +0.8  |
| $\text{Fe}^{3+} / \text{Fe}^{2+}$                 | +0.77 |
| $\text{Cu}^{2+} / \text{Cu}$                      | +0.34 |
| $\text{H}^+ / \text{H}_2$                         | +0.00 |
| $\text{Sn}^{2+} / \text{Sn}$                      | -0.14 |
| $\text{Ni}^{2+} / \text{Ni}$                      | -0.23 |
| $\text{Fe}^{2+} / \text{Fe}$                      | -0.44 |
| $\text{S} / \text{S}^{2-}$                        | -0.45 |
| $\text{Zn}^{2+} / \text{Zn}$                      | -0.76 |
| $\text{Al}^{3+} / \text{Al}$                      | -1.66 |
| $\text{Mg}^{2+} / \text{Mg}$                      | -2.37 |
| $\text{Na}^+ / \text{Na}$                         | -2.71 |
| $\text{C} / \text{LiC}_6$                         | -2.9  |
| $\text{Li}^+ / \text{Li}$                         | -3.05 |

### 4.4.2. Appendix 2: Dendrites

Dendrites – the word deriving from the Greek *δενδρίτης* (*dendrites*, “relating to trees”), which itself derives from *δένδρον* (*dendron*, “tree”) – are non-uniform deposits which form outgrowths on the active surfaces at the electrodes. A dendrite might be, for example, a non-uniform lithium deposit caused during its electrochemical reduction. Dendrites which cross through

---

<sup>17</sup> The Normal Hydrogen Electrode (NHE) is defined in footnote 56 in Chapter 2.

the space separating the electrodes (separator + electrolyte) can short-circuit the cell by establishing direct electrical contact between the electrodes and cause the destruction of the element. This phenomenon has meant metal lithium batteries are not able to use liquid electrolyte, because the separators used did not have sufficient mechanical strength to resist dendrite penetration. This phenomenon occurs similarly in lithium metal polymer batteries, but the polymer electrolyte, which contains mineral loads (magnesium oxide  $\text{MgO}$ , which is thermodynamically stable in comparison to lithium), is capable of limiting these dendritic growths (the dendrites are blocked by particles of  $\text{MgO}$ ). In such batteries, we observe dips and then sharp recoveries of the voltage, linked to a short-circuit of one or more dendrites which self-destruct (melting effect) by the temperature increase linked to the passage of current through a very small surface area. A true short-circuit only occurs with the breakthrough of a large number of dendrites, thus reducing the intensity of the current. In order to limit the formation of dendrites, lithium metal polymer batteries are subjected to stresses with low current densities in order to facilitate a more uniform deposition of lithium.

Figure 4.7 shows the formation of dendrites in the inter-electrode space in a symmetrical lithium/PEO/lithium element: the lithium accumulates, forming a cluster which grows through the electrolyte until it causes the destruction of the battery element by an internal short-circuit.

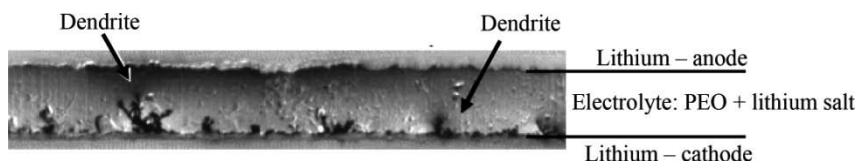


**Figure 4.7.** Formation of dendrites (source: Thesis, Anna Teyssot, *Étude de l'interface lithium métal/électrolyte polymère fondu et gélifié*. École Polytechnique, Paris, 2005)

#### 4.4.3. Appendix 3: Transition metals

A transition metal is one of the 38 chemical elements from periods 4 to 7 (rows) and groups 3 to 12 (columns) in the Periodic Table of the Elements (also called Mendeleev's Table or the Periodic Classification of the Elements), an extract of which is shown in Figure 4.8:

|   |    |    |    |    |    |    |    |    |    |    |    |    |    |    |    |    |    |    |
|---|----|----|----|----|----|----|----|----|----|----|----|----|----|----|----|----|----|----|
|   | 1  | 2  | 3  | 4  | 5  | 6  | 7  | 8  | 9  | 10 | 11 | 12 | 13 | 14 | 15 | 16 | 17 | 18 |
| 1 | H  |    |    |    |    |    |    |    |    |    |    |    |    |    |    |    |    | He |
| 2 | Li | Be |    |    |    |    |    |    |    |    |    |    | B  | C  | N  | O  | F  | Ne |
| 3 | Na | Mg |    |    |    |    |    |    |    |    |    |    | Al | Si | P  | S  | Cl | Ar |
| 4 | K  | Ca | Sc | Ti | V  | Cr | Mn | Fe | Co | Ni | Cu | Zn | Ga | Ge | As | Se | Br | Kr |
| 5 | Rb | Sr | Y  | Zr | Nb | Mo | Tc | Ru | Rh | Pd | Ag | Cd | In | Sn | Sb | Te | I  | Xe |
| 6 | Cs | Ba |    | Hf | Ta | W  | Re | Os | Ir | Pt | Au | Hg | Tl | Pb | Bi | Po | At | Rn |
| 7 | Fr | Ra |    | Rf | Db | Sg | Bh | Hs | Mt | Ds | Rg | Cn |    |    |    |    |    |    |

**Figure 4.8.** Extract from the Periodic Table of the Elements

Thus, the transition metals are the following (Table 4.9):

|    |           |          |           |           |           |           |           |           |    |
|----|-----------|----------|-----------|-----------|-----------|-----------|-----------|-----------|----|
| Sc | <b>Ti</b> | <b>V</b> | <b>Cr</b> | <b>Mn</b> | <b>Fe</b> | <b>Co</b> | <b>Ni</b> | <b>Cu</b> | Zn |
| Y  | Zr        | Nb       | Mo        | Tc        | Ru        | Rh        | Pd        | Ag        | Cd |
|    | Hf        | Ta       | W         | Re        | Os        | Ir        | Pt        | Au        | Hg |
|    | Rf        | Db       | Sg        | Bh        | Hs        | Mt        | Ds        | Rg        | Cn |

**Figure 4.9.** Transition metals

Unlike alkali metals (column 1 of the Periodic Table) and alkali earth metals (column 2), the transition metals (particularly those in groups 4-11) can form ions with a wide variety of degrees of oxidation. It is this property which is exploited in batteries. In practice, only those metals on the first row (in bold) in Figure 4.9 are usable today, because of the existence of high degrees of oxidation: they are titanium  $\text{Ti}^{4+}/\text{Ti}^{3+}$ ; vanadium  $\text{V}^{1.5+}/\text{V}^{1.8+}$ ; manganese  $\text{Mn}^{3+}/\text{Mn}^{4+}$ ; iron  $\text{Fe}^{2+}/\text{Fe}^{3+}$ ; cobalt  $\text{Co}^{3+}/\text{Co}^{4+}$ ; nickel  $\text{Ni}^{3+}/\text{Ni}^{4+}$ ; with the exception of scandium (Sc) which is rare, chromium (Cr) which is toxic, copper (Cu) for which oxidation reactions occur at too low a potential and zinc (Zn) which does not have a high-enough degree of oxidation. These materials have a sufficiently low molar mass, of around 80 g/mol, but which increases for materials from row 5 to 180 g/mol, which disqualifies them from being used as electrode materials. The metals which form alloys with lithium are Al, Si and Sn.



## Chapter 5

# The Basic Elements in Lithium-ion Batteries: Electrodes, Electrolytes and Collectors

### 5.1. Introduction

Unlike many other secondary batteries, lithium-ion batteries are not linked to a single electrochemical couple. In fact, any material which is able to reversibly accommodate lithium ions can be considered as an active material in a lithium-ion battery. Hence, this implies a great diversity of types of materials for the electrodes, each of which has different properties in terms of gravimetric and volumetric energies, nominal voltage, lifetime, safety, cost, etc.

Thus, lithium-ion battery technology is far from being fixed. Numerous university-based researchers and industrialists are working on ways to improve lithium batteries, which involves better awareness of the properties of each of the two electrodes, the electrolyte, current collectors and the interactions between them. The domain is so complex that there are research teams specializing in the study of positive electrodes, whereas others specialize solely in the study of negative electrodes.

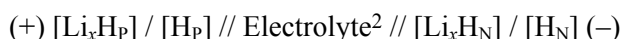
Ultimately, at present, there is no one electrode which is excellent for all the objectives sought for the “best” battery, because compromises must be sought. Thus, a very high specific energy is, as yet, still usually synonymous with a short lifetime. Also, better operational safety is obtained to the detriment of specific energy.

This chapter looks at different electrodes that are used or are under investigation, taking an interest in their properties: first positive electrodes, then negative electrodes, then electrolyte and finally current collectors. In order to work on an electrode, electrochemists often combine it with a counter-electrode made of metal lithium. They refer to this setup as a half cell<sup>1</sup> (although the cell is complete, with both of its electrodes), because it is assembled in a coin-cell-type casing, which is easy to use in the laboratory.

## 5.2. Operation of lithium-ion technology

The operation of lithium-ion technology is based on the reversible exchange of a lithium ion between the positive and the negative electrode. The insertion/extraction mechanism has often been referred to as a “*rocking-chair*” mechanism, referring to the back-and-forth movement of the lithium ion from one electrode to another. During charging, lithium is inserted into the negative electrode (which then plays the role of the cathode) in an ionic state with a higher potential than that of the metallic deposit, thereby preventing the formation of metallic deposits in the form of dendrites (see section 4.4.2). The formation of dendrites is at the root of the safety problems caused by an internal short-circuit (piercing of the separator) which are well known in metal lithium batteries, but which may also be encountered with lithium-ion batteries in certain conditions of current and temperature.

In a lithium-ion battery, the electrochemical sequence involved is:



where:  $[\text{H}_\text{P}]$ : positive host structure: insertion material functioning at a high potential<sup>3</sup> of approximately +3 to +5 V/Li<sup>+</sup>/Li;

$[\text{H}_\text{N}]$ : negative host structure: electrode material functioning at a low potential, less than +2 V/Li<sup>+</sup>/Li.

---

<sup>1</sup> We can quickly implement a test device using *Swagelok*<sup>TM</sup> screw cells.

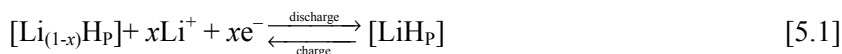
<sup>2</sup> Electrolyte = organic solvent(s) + lithium salt(s) + adjuvants.

<sup>3</sup> In electrochemistry, the voltage of an electrode is defined versus a reference electrode (see section 2.9.1: Redox potential of an electrode). The voltage between the two electrodes in a battery is therefore equal to the difference between the voltages of those two electrodes versus the reference electrode.

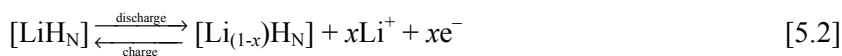


The reactions at the electrodes lead to the exchange of a lithium ion via the internal circuit (electrolyte, ionic solution) and an electron via the external electric circuit, as described by the following general principle of operation of a lithium-ion battery<sup>4</sup>:

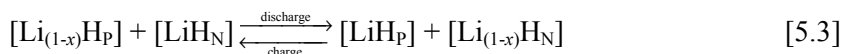
### Positive electrode



### Negative electrode



### Balance equation



These relations are illustrated in Figure 5.1 and are explained later on for the materials which are actually used in the most recent batteries.

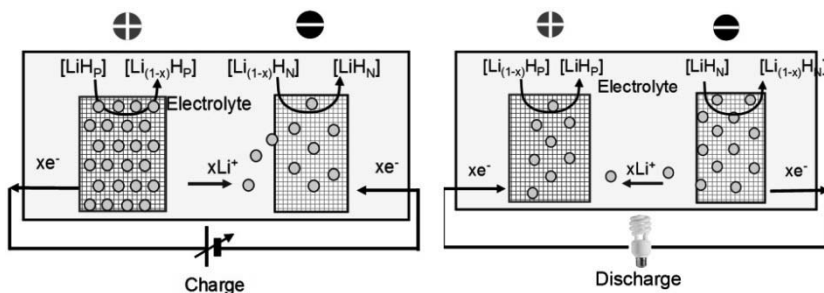


**Figure 5.1.** Principle of operation of a lithium-ion battery  
(the arrows represent the direction of movement of the charges)

As indicated in the introduction to this chapter, quite unlike the electrochemical couples discussed previously (lead, nickel, etc.), both for the positive and the negative electrode, the choice of materials is vast. Here, we

<sup>4</sup> We have chosen to use the notation  $\text{Li}_{(1-x)}\text{H}$  rather than  $\text{Li}_x\text{H}$  for an insertion material. In this latter case,  $x$  corresponds to the number of electrons exchanged. The degree of insertion, notated  $x_i$ , is such that  $x_i = 1 - x$ .

shall discuss those that are most commonly used, and which are most typical in terms of their function in an electrode (positive or negative).<sup>5</sup>

### 5.3. Positive electrodes

#### 5.3.1. *Lithiated transition metal oxides*

Lamellar oxides of lithiated transition metals  $\text{Li}_{(1-x)}\text{MO}_2$  (where M represents one or more metals such as Co, Ni, etc. – see section 4.4.3, on transition metals) possibly doped with aluminum or manganese, spinels<sup>6</sup> of manganese in the form  $\text{Li}_{(1-x)}\text{Mn}_2\text{O}_4$  or indeed lithiated iron phosphates  $\text{Li}_{(1-x)}\text{FePO}_4$ , are generally used as the positive material. These materials exhibit a crystallized host structure, which offers one-, two- or three-dimensional paths for diffusion into which the lithium can be inserted. Figure 5.2 compares the ranges of potentials for electrochemical insertion of several of these materials versus the potential of metal lithium (left-hand scale). These potentials cover a range of voltage between approximately 3 to 5 V versus  $\text{Li}^+/\text{Li}$ . The right-hand scale represents these same electrochemical potentials versus the normal hydrogen electrode (NHE). The vertical line indicates the variation of these potentials on the basis of the fraction  $x$  of lithium ions inserted.

Historically the first material to have been used, and still the most commonplace today, is Lithium Cobalt Oxide  $\text{Li}_{(1-x)}\text{CoO}_2$  (LCO, whose function is detailed in section 6.1.2), because it has a stable lamellar crystalline structure. However, this stability is obtained only if the degree of lithium insertion is no lower than 0.5, i.e. with a value of  $x$  greater than 0.5. Put differently, in case of an excess charge, if more than half the lithium is extracted, an irreversible structural alteration occurs, rendering the insertion

---

<sup>5</sup> A material may have the role of the positive or negative electrode depending on the nature of the material in conjunction with which it is being used. In the laboratory, we study materials for both positive and negative electrodes (when they are in a complete-cell arrangement), characterized versus metal lithium which always acts as the negative electrode, because its redox potential is the lowest of all.

<sup>6</sup> Spinel is a 3D arrangement (octahedral and tetrahedral cavities) in which the lithium is inserted or from which it is removed. They were introduced as an alternative to lamellar structures (transversal molecular planes, layers) which, at first, had seemed most appropriate for the easy insertion of lithium. The term “spinel” was originally the denomination of magnesium aluminum oxide  $\text{MgAl}_2\text{O}_4$ , a precious stone used in jewelry. By extension, the term was used for isomorphic crystalline structures of  $\text{MgAl}_2\text{O}_4$ , including  $\text{Li}_{(1-x)}\text{Mn}_2\text{O}_4$ .

of lithium during the next charge cycle impossible: the material, and therefore the battery, is degraded. This structural alteration consists of the compression of the lamellar structure, with a decrease in the inter-layer distance which no longer affords sufficient space for the lithium to be inserted. This is accompanied by a release of oxygen. For this reason, the uppermost limit of the charge voltage in a  $\text{Li}_{(1-x)}\text{CoO}_2$  device needs to be carefully regulated at 4.1–4.2 V<sup>7</sup>, because beyond this, the amount of lithium extracted exceeds the threshold value of 0.5. Thus, as long as  $x \leq 0.5$ , the process of insertion/extraction of lithium in the structure has a high degree of reversibility.

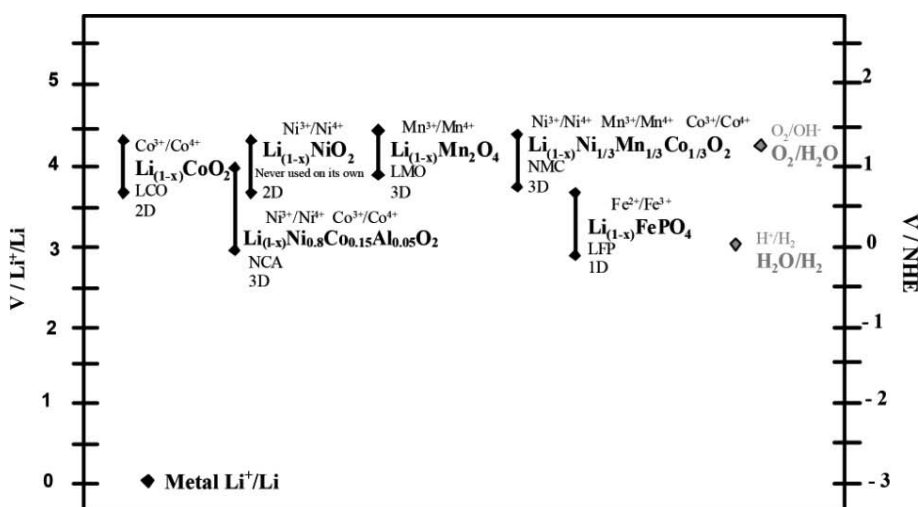


Figure 5.2. Potentials for electrochemical insertion of some positive insertion materials

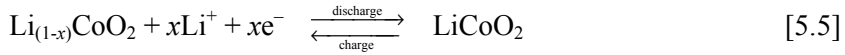
The general chemical formula for this type of electrode is:



(with  $M = \text{Co}$ ;  $x = \text{lithium exchanged}$ ;  $0 < x \leq 0.5$ ) (for  $M = \text{Ni}$  and other materials such as  $\text{Mn}$ , phosphate;  $x = \text{lithium exchanged}$ ;  $0 < x \leq 1$ )

<sup>7</sup> Limiting the charge voltage to 4.1 V extends the lifetime of the cell, to the detriment of its capacity, which is decreased by approximately 10%.

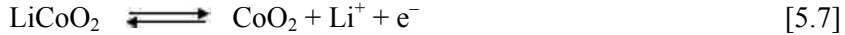
Hence, for compounds of cobalt oxide, it is written as:



The theoretical mass capacity  $C_{th}$  (in mAh/g or Ah/kg) is determined using Faraday's law (see section 2.3.2.2), which is expressed as follows in the form adapted for the calculation we wish to carry out:

$$C_{m.th} \text{ (mAh/g)} = \frac{1000 \times n \times 96485}{3600 \times M} = 26801 \cdot \frac{n}{M} \quad [5.6]$$

For  $\text{LiCoO}_2$ , the reaction to consider, deduced from equation 5.4, is given below:



This equation shows that a mole of lithium and a mole of electrons can be liberated for each mole of  $\text{LiCoO}_2$ .

With a molar mass of 6.9 g/mol for lithium, 58.9 g/mol for cobalt and 16 g/mol for oxygen (which needs to be multiplied by two because there are two atoms of oxygen in the molecule in question  $\text{LiCoO}_2$ ) and a single electron exchanged, we can write:

$$C_{m.th} = \frac{1}{6.9 + 58.9 + 2 \times 16} \times 26801 = 274 \text{ mAh/g} \quad [5.8]$$

This theoretical mass capacity is that of the material. In its use in a secondary battery element, we must remember that at most, around half of the lithium can be extracted. The operational theoretical mass capacity will therefore be approximately half of that quoted above, so will be approximately 137 mAh/g.

Figure 5.3 represents the voltage of a  $\text{Li}_{(1-x)}\text{CoO}_2$  electrode versus  $\text{Li}^+/\text{Li}$  as a function of the degree of lithium insertion representative of the SOC of the electrode (lower horizontal axis), lithium insertion/extraction occurring jointly with the capture/release of an electron, as indicated in the reaction below. For a battery in the charged state ( $x = 0.5$ ), the electrode is made of  $\text{Li}_{0.5}\text{CoO}_2$  (mechanism of extraction during charging, with the lithium released being transferred to the negative electrode). In the discharged state,

it is composed of  $\text{LiCoO}_2$  (mechanism of lithium insertion during discharging): when completely discharged, all of the insertable lithium is in the positive electrode. The second (upper) horizontal axis represents the amount of electricity charged or discharged in comparison to the mass of active material of the positive electrode, given in mAh/g.<sup>8</sup> In order to further clarify the upper axis used, we have simply compared the number of Ah injected during charge and then delivered during discharge at the terminals of the battery to the active mass of  $\text{LiCoO}_2$  present. We see the value of the practical mass capacity of the electrode  $\text{Li}_{(1-x)}\text{CoO}_2$  of 120 mAh/g, which is slightly less than the theoretical value (137 mAh/g).

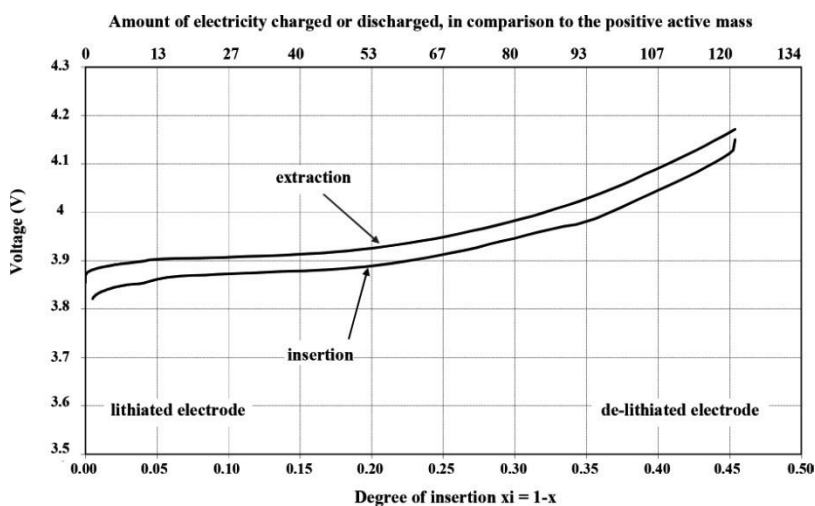


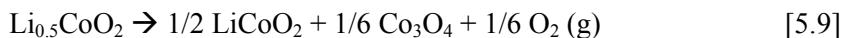
**Figure 5.3.** Voltage curves for charge and discharge of a  $\text{LiCoO}_2$  positive electrode depending on the degree of insertion  $\xi$  (lower axis) or the amount of electricity in comparison to the positive active mass (upper axis)

Unfortunately, because of the very limited worldwide reserves and its strategic nature<sup>9</sup>, cobalt is extremely expensive. It is also toxic. In addition,

<sup>8</sup> Electrochemists tend to use the mAh/g (definition given in section 2.4.7) to characterize the materials used for electrodes. The same numerical value could be expressed in Ah/kg – these units are more closely related to the practices of electrotechnicians. The values are always high: >100 Ah/kg. However, this is a measure of the performances of the material used for the electrode. In order to work out the mass capacity of an element, we must remember that there are two electrodes, but also the electrolyte, the current collectors, the casing, etc.

<sup>9</sup> Africa has most of the cobalt resources on the planet: the Democratic Republic of Congo (DRC) alone possesses almost half the known reserves.

if the amount of lithium extracted becomes lower than  $\text{Li}_{0.5}\text{CoO}_2$  ( $x \geq 0.5$ ), it proves to be unstable at high temperature, releasing oxygen:



The oxygen released reacts with the electrolytic organic solvents, with significant risks of fire and explosion.

More recently, by substitution of the Co in  $\text{LiCoO}_2$  with Ni, Mn or Al, we have been able to compensate for the high cost of Co (nickel is also an expensive material, but less so than cobalt) and the relatively poor thermal stability of de-lithiated  $\text{Li}_{(1-x)}\text{CoO}_2$ . Materials such as  $\text{Li}(\text{Ni}_x\text{Co}_y\text{Mn}_z)\text{O}_2$ , called *lithium-Nickel-Manganese-Cobalt-oxide* (NMC for the compound  $\text{LiNi}_{1/3}\text{Mn}_{1/3}\text{Co}_{1/3}\text{O}_2$ ) or  $\text{Li}(\text{Ni}_x\text{Co}_y\text{Al}_z)\text{O}_2$ , called *lithium-Nickel-Cobalt-Aluminum-oxide* (NCA for the compound  $\text{LiNi}_{0.8}\text{Co}_{0.15}\text{Al}_{0.05}\text{O}_2$ )<sup>10</sup> have thus been developed, with a lower cost, a high mass capacity and a good heat tolerance. For example, the Saft Group uses  $\text{LiNi}_{0.8}\text{Co}_{0.15}\text{Al}_{0.05}\text{O}_2$  for its industrial batteries.

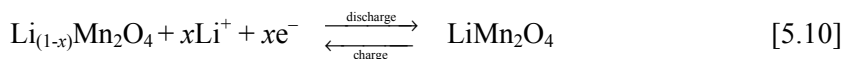
### 5.3.2. Manganese oxide

In parallel, spinels of manganese oxide  $\text{Li}_{(1-x)}\text{Mn}_2\text{O}_4$  have been developed, so the lithium can be de-intercalated over a range of voltage between 3 and 4.2 V versus  $\text{Li}^+/\text{Li}$  for a theoretical faradaic capacity of the material of 148 mAh/g and of the electrode of 74 mAh/g (see exercise 5.1 and its solution on section 5.8) comparable to that of  $\text{LiCoO}_2$ . The spinel  $\text{Li}_{(1-x)}\text{Mn}_2\text{O}_4$  (LMO for *Lithium-Manganese-Oxide*) offers the advantages of lower cost and “non-toxicity”. In addition, methods for recycling are well known, because manganese oxide is also used in alkaline batteries. However, for a long time, it was not used because of its mediocre performances in terms of storage and cycling at 55°C – the temperature at which a phenomenon of dissolution of the manganese begins to occur. Research has found solutions to these disadvantages by a twofold partial substitution of manganese with aluminum and of oxygen with fluorine. Coupled with a passivation of the surface, it has thus been possible to considerably improve the temperature resistance of this compound, but the procedures for manufacturing such a material are thereby made more complicated, which is still a penalizing factor from the point of view of commercialization.

---

<sup>10</sup> With NCA, we can extract up to 0.65 of the Li, which gives us a higher specific energy than  $\text{LiCoO}_2$ , whose structure limits extraction to 0.5 Li.

The general chemical formula for this type of electrode is:



( $x$  = lithium exchanged;  $0 < x \leq 1$ )

EXERCISE 5.1.— Using Faraday's law (see section 2.3.2.2), calculate the theoretical mass capacity of the manganese oxide electrode.

*Solution page 162*

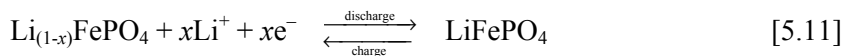
### 5.3.3. Lithiated iron oxyphosphate

In comparison to the current conventional couple with a lithium-nickel-oxide- and/or lithium-cobalt-oxide based positive electrode and a negative electrode made of low-cost natural-graphite – which, in cylindrical batteries, has demonstrated excellent cyclability and a long lifetime – a new couple is now becoming a commercial presence. The positive electrode is made of transition metal phosphates, and particularly lithiated iron oxyphosphate  $\text{Li}_{(1-x)}\text{FePO}_4$ , more commonly called simply iron phosphate (LFP for *Lithium-FerroPhosphate* with *F* (Ferrous) referring to Iron). Its crystalline structure is isomorphic to that of olivine<sup>11</sup>  $\text{LiMgFeSiO}_4$  and facilitates the reversible insertion of lithium. However, also for this type of compound, the manufacturing process and the surface treatments have a significant influence on the capacity delivered. Their poor conductivity necessitates the synthesis of nanopowders (grains of 20–50 nm) with carbon deposits on their surface. These are highly attractive materials, because in spite of a nominal voltage lower than that of other materials, 3.2 or 3.3 V versus  $\text{Li}^+/\text{Li}$  as compared to 3.6 V versus  $\text{Li}^+/\text{Li}$  for LCO, they are less dangerous in case of abusive operation. Also, these materials are not very costly and are non-toxic.

---

<sup>11</sup> The name olivine was originally given to a mineral in the silicates group which is olive green in color. By extension, the name olivine is applied to isomorphic crystalline structures of  $\text{LiMgFeSiO}_4$ .

The general chemical formula for this type of electrode is:



( $x$  = lithium exchanged;  $0 < x \leq 1$ )

For a charged battery, this positive electrode is composed of  $\text{LiFePO}_4$  ( $x=0$ ). In the discharged state, we have  $\text{FePO}_4$ .

EXERCISE 5.2.– using Faraday's law (see section 2.3.2.2), calculate the theoretical mass capacity of the LFP electrode.

*Solution page 163*

In the olivine structure of  $\text{LiFePO}_4$ , the de-intercalation of lithium ions follows a two-phase process between a lithium-rich phase ( $\text{Li}_{(1-x)}\text{FePO}_4$ ,  $x \rightarrow 0$ ) and a lithium-poor phase ( $x \rightarrow 1$ ) with two domains of solid solution at both ends of the charge and discharge curves.<sup>12</sup> This type of process can be seen in the curve of cycling at constant current by a plateau of potential: the potential remains relatively constant and no longer depends on the chemical composition. The complete extraction of the lithium ions (and therefore the oxidation of  $\text{Fe}^{2+}$  ions into  $\text{Fe}^{3+}$  ions) causes the formation of  $\text{FePO}_4$ , whose crystalline structure is identical to  $\text{LiFePO}_4$ . This similarity between the two structures is the reason for the very good reversibility of the cycling process. Today, the origin of this biphasic reaction is explained as a “domino-cascade” mechanism.<sup>13</sup> This phenomenon manifests itself as soon as stresses occur at the interface between the discharging and already-discharged material. Electronic and ionic conduction then take place extremely rapidly in the interface area: it propagates step by step, like dominos, as the de-intercalation front is displaced. This novel reaction process, which resembles a wave sweeping through the crystal, explains why, in spite of the presence of two insulating materials  $\text{LiFePO}_4$  and  $\text{FePO}_4$  whose properties of ionic and electronic conduction are poor, the electrode is still able to function.

12 A. YAMADA, M. YONEMURA, Y. TAKEI, N. SONOYAMA & R. KANNO, “Fast Charging  $\text{LiFePO}_4$ ”, *Electrochemical Solid State Letters*, 8 (1) A55–A58, 2005.

13 C. DELMAS, M. MACCARIO, L. CROGUENNEC, F. Le CRAS, F. WEILL, “Lithium de-intercalation in  $\text{LiFePO}_4$  nanoparticles via a domino-cascade model”, *Nature Materials*, 7, 665–671, 2008.



### 5.3.4. Crystalline structures

Figure 5.5 represents the three types of crystalline structure which characterize the insertion materials presented herein:  $\text{LiMO}_2$  ( $M=\text{Co}, \text{Ni}$ ),  $\text{LiMn}_2\text{O}_4$  and  $\text{LiFePO}_4$ . The structures are drawn by linking the atoms to form planes, thereby helping to visualize the available spaces, the cavities, in which the lithium ions (represented by little spheres) can position themselves. At each vertex of the polyhedra there is an oxygen atom; the iron or phosphorus are at the center of the polyhedron.

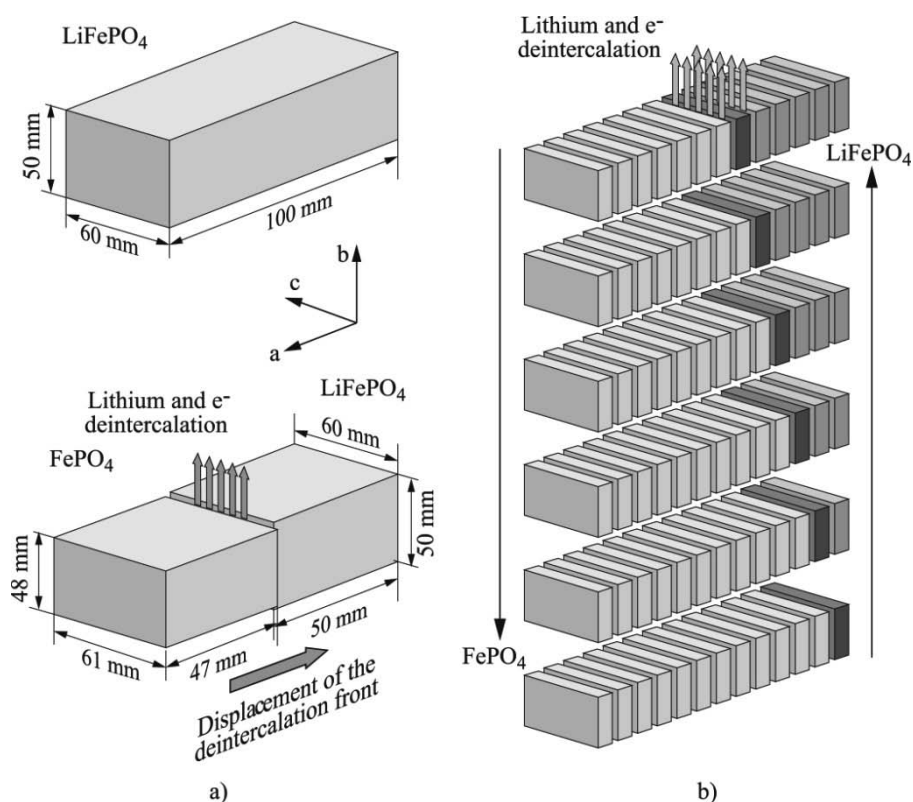


**Figure 5.4.** Representation of the “domino-cascade” mechanism in a  $\text{LiFePO}_4$  crystallite.

a) View of the stresses occurring because of lithium de-intercalation.

b) Change of the two-phase state by the operation of lithium de-intercalation/intercalation.

Figure taken from Delmas et al.<sup>13</sup>

### 5.3.5. Mass capacities

Table 5.1 gives the theoretical and practical mass capacities for the most widely-used positive materials.

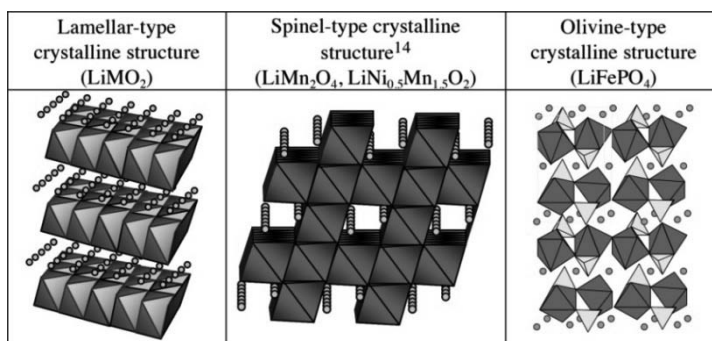


**Figure 5.5.** Crystalline structure for each of the 3 types of insertion materials

| Materials  | Theoretical gravimetric capacity (mAh/g) | Theoretical gravimetric capacity (mAh/g) with account taken of the degree of insertion | Average practical gravimetric capacity (mAh/g) | Cost   |
|--|--|--|--|--------|
| $\text{LiCoO}_2$   | 274                                      | 137  | 120  | High   |
| $\text{LiNiO}_2$   | 275                                      | 275  | 220  | Medium |
| $\text{LiMn}_2\text{O}_4$                                    | 148                                      | 148  | 120  | Low    |
| $\text{LiCo}_{0.2}\text{Ni}_{0.8}\text{O}_2$ <sup>(15)</sup> | 274                                      | 247  | 180  | Medium |
| $\text{LiFePO}_4$  | 170                                      | 170  | 150  | Low    |

**Table 5.1.** Gravimetric capacities of usual positive active materials

## 5.4. Negative electrodes

### 5.4.1. Carbonaceous materials

To date, negative electrodes have always essentially been composed of carbonaceous compounds such as graphites or cokes, with varying natures

<sup>14</sup> This is the same crystalline structure for  $\text{Li}_4\text{Ti}_5\text{O}_{12}$  that is used as a negative electrode.

<sup>15</sup> The theoretical mass capacity of  $\text{LiCo}_{0.2}\text{Ni}_{0.8}\text{O}_2$  is calculated on page 31.

and degrees of graphitisation, capable of reversibly accepting lithium insertion between 0 and 0.3 V versus  $\text{Li}^+/\text{Li}$  or between  $-3.0$  and  $-2.7$  V versus NHE, which retains a very low potential at the electrode (as provided by metal lithium in Li-metal batteries). Today, graphite is used by most battery manufacturers for a variety of reasons: low cost, very low electrochemical potential for insertion (see section 4.4) leading to a very high element voltage, high mass capacity (372 mAh/g if we only take account of the mass of the graphite; see exercise 5.3) and good reversibility.



( $x$  = degree of insertion,  $0 < x \leq 1$ )

In a discharged element, the carbon electrode (as the negative electrode) is entirely delithiated: we can consider the presence of carbon on its own, with no inserted lithium. In a charged battery, the carbon electrode (again as the negative electrode) is  $\text{LiC}_6$ . Note that  $\text{LiC}_6$  represents a stoichiometric composition rather than a molecule. There is no covalent bond (no exchange of electrons between atoms) but only electrostatic forces between the layers of carbon and the inserted lithium. This is also demonstrated by formulations such as  $\text{Li}_x\text{C}_6$ . Such is also the case for positive electrodes  $\text{Li}_{(1-x)}\text{CoO}_2$ ,  $\text{Li}_{(1-x)}\text{FePO}_4$ , etc.

EXERCISE 5.3.— using Faraday's law (see section 2.3.2.2), calculate the theoretical mass capacity of the graphite electrode, taking account only of the host structure. Compare this with the mass capacity of a metal lithium electrode. This latter value needs to be calculated using the following equation (given previously by equation [4.1]):



What mass of lithium is needed to store 1 Ah of energy?

*Solution page 164*

Figure 5.6 represents the voltage of a graphite electrode as a function of the degree of lithium insertion (lower horizontal axis), which correlates to the SOC, and as a function of the amount of electricity charged or

discharged in comparison to the mass of active material of carbon C, given in mAh/g (upper horizontal axis).

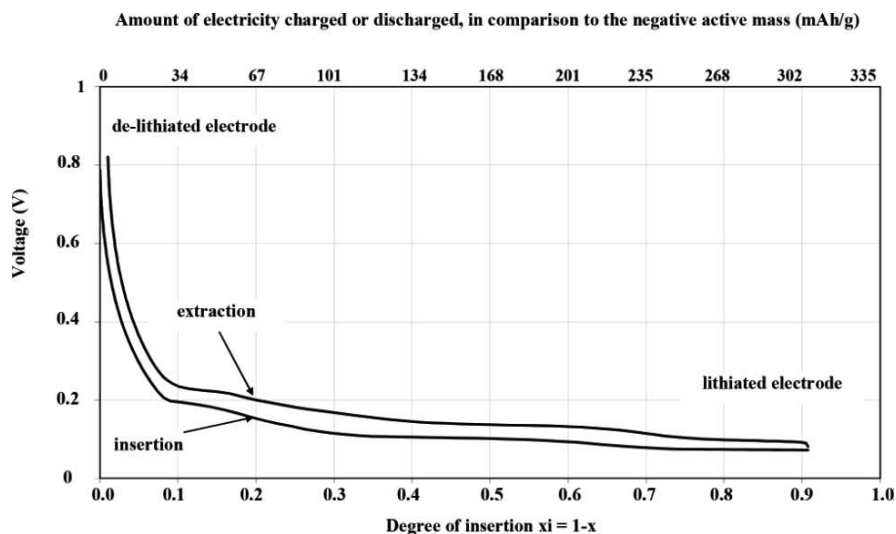


**Figure 5.6.** Voltage curves for charge and discharge of a graphite negative electrode depending on the degree of insertion  $\xi$  (lower axis) or the amount of electricity in comparison to the negative active mass (upper axis)

We note that the effective mass capacity delivered by the negative electrode, for this experimental example (type of graphite used, formulation of the electrode, electrical characterization protocol applied) is 300 mAh/g, which is below the practical value of 350 mAh/g given by the literature.

The high reversibility of the lithium insertion into graphite is linked to the typical structure of the graphite, which comprises layers of graphene placed 0.335 nm apart. When lithium is inserted, this distance increases only very slightly, becoming 0.370 nm in  $\text{LiC}_6$ . This separation is sufficiently slight for the planar structure of the graphite to be preserved. The structure of  $\text{LiC}_6$  is presented below (Figures 5.7 and 5.8).

This inter-layer separation remains slight (which is an essential condition for the battery to work) because the lithium is inserted without its solvation shell formed by the organic molecules from the electrolyte. This phenomenon of desolvation takes place when lithium ions are diffused in an interfacial passivation layer present between the electrode and the

electrolyte. This layer at the interface between the carbon electrode and the electrolyte is called the passivation film, or more commonly the Solid Electrolyte Interphase (SEI), by analogy with the passivating layer formed on the surface of the metallic lithium. However, unlike this latter layer, chemically formed by contact between the metal lithium and the electrolyte, the SEI on the carbon is electrochemical in nature. It is formed during the first charge, called the “activation charge”, or also referred to as the initial charging process, performed in the factory by the manufacturer before commercialization, by decomposition on the surface of the grains of carbon from the electrolyte, which plays a very important role for the stability of the electrode itself. Without this film and its “desolvation capability”, lithium would be inserted along with its solvation shell, causing the complete destruction of the structure of the graphite, called exfoliation. The choice of solvents used for the electrolyte conditions the nature and stability of this surface layer. With successive charge/discharge cycles, the carbon matrix is sufficiently stable in terms of dimensions so as not to damage the SEI.

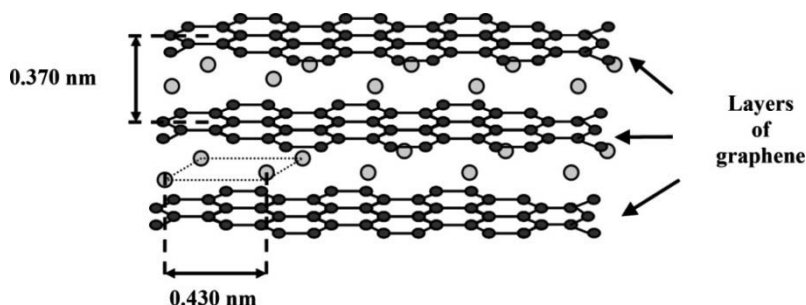


**Figure 5.7.** *Lithium insertion into a carbon matrix: layers of graphene between which lithium is inserted*

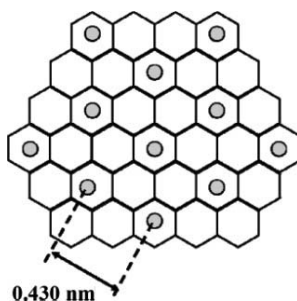


**Figure 5.8.** *Lithium insertion into a carbon matrix: bird's-eye view showing the position of the lithium atoms to form  $\text{LiC}_6$*

The formation of the SEI is modeled by the diagram below (Figure 5.9), put forward by J. Vetter, P. Novak and M.R. Wagner<sup>16</sup>:

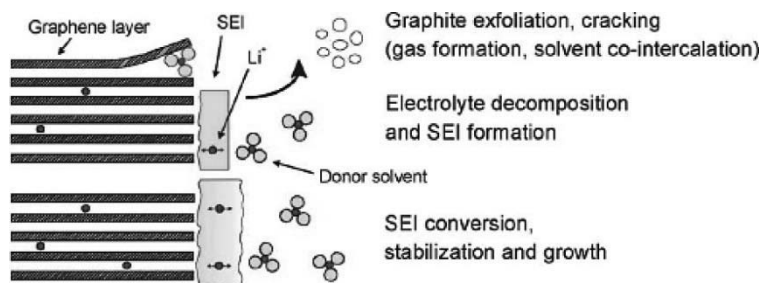


**Figure 5.9.** Diagrammatic model of the mechanism of SEI formation on graphite

#### 5.4.2. Other carbonaceous materials

A great deal of effort is currently being invested in the development of “high-capacity” carbon materials. These materials tend to be synthesized at low temperatures, ranging from 500°C up to 1000°C. They exhibit reversible mass capacities between 400 and 2000 mAh/g (with a degree of insertion  $1.2 < x < 5$  in  $\text{Li}_x\text{C}_6$ ), depending on the temperature of the heat treatment, the original organic starting material and the electrolyte used.

To explain these high specific capacities, a variety of models (some of which are highly controversial) have been put forward:

- arrangement of lithium in faults in the crystalline structure or between two adjacent crystallites;
- formation of  $\text{Li}_2$  molecules in neighboring hexagonal sites (Figure 5.10a);
- arrangement in nanometric cavities (Figure 5.10b);
- storage at the edge or on the surface of small particles of carbon, in addition to the lithium intercalated between the graphene layers (Figure 5.10c). It has been suggested that, in one way or another, the lithium could be connected with hydrogen, although hydrogen is no longer present in graphites because it is eliminated by the heat treatments;

<sup>16</sup> “Ageing mechanisms in lithium-ion batteries”, *Journal of Power Sources*, 147, 269–281, 2005.

– adsorption of lithium on both sides of the graphene layers. This ultimately corresponds to the storage of lithium in micropores, the size and opening of these pores being sufficiently small to prevent the lithium from reacting with the electrolyte (Figure 5.10d).

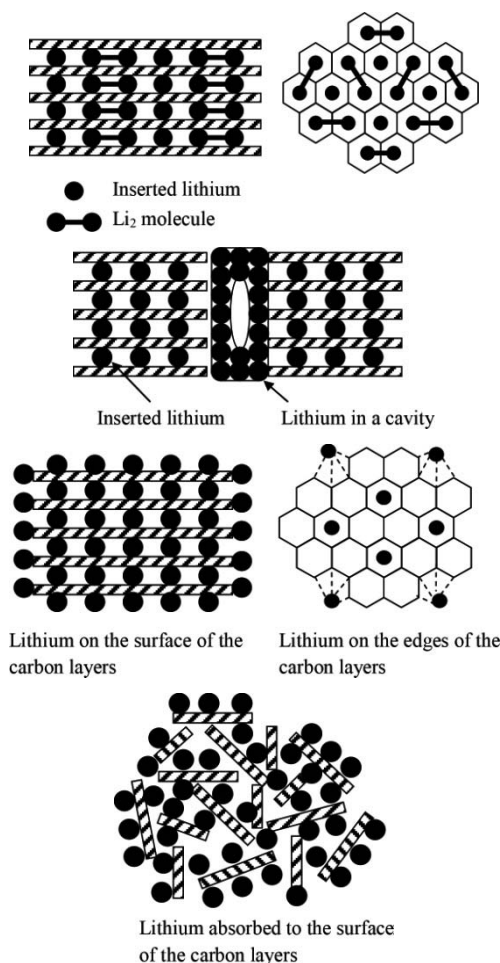


**Figure 5.10.** Diagrammatic models of the suggested mechanisms for reversible lithium storage in high-capacity carbon materials

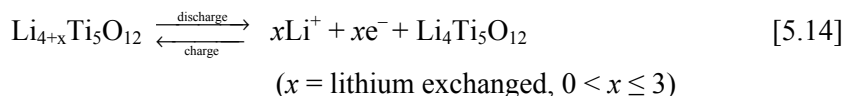
These carbons, however, present serious drawbacks, such as significant irreversible capacities during the first cycle but also during subsequent cycles. The irreversible capacity indicates the amount of irreversibly inserted

lithium, which is quantified in practice by the difference in capacity discharged between two successive cycles. They may also exhibit a significant degree of hysteresis in terms of their voltage profile during discharge and charge, typically around  $1\text{ V} \pm 1\text{ V}$ , i.e. a range of voltage between 0 and 2 V. In addition, in certain cases in a battery configuration and at the end of charge, the negative electrode can reach negative values versus lithium, in which case deposition of metal lithium may occur. The same is not true for graphite, which exhibits a very low voltage hysteresis, with a difference in potential between  $\text{LiC}_6$  and lithium deposition from 0.1 V.

In order to resolve these drawbacks, research is now turning toward the production of high-capacity carbons with characteristics equivalent to those of graphite.

#### 5.4.3. *Lithium titanate oxide*

Today, lithium-titanate-oxide<sup>17</sup> (LTO) seems to be a negative electrode material which could be used as an alternative to graphite.<sup>18</sup> For this material, lithium insertion occurs with electrochemical potentials greater than the electrochemical potential of deposition of metal lithium (1.55 V versus  $\text{Li}^+/\text{Li}$ ). It is therefore capable of accepting high charge currents, even at low temperature, without the risk of metal lithium forming at the interface, unlike graphite, with which the insertion potential is close to the potential for lithium reduction and charge transfer limited by the SEI.



LTO has proved to be an effective material for negative electrodes, thanks to its high chemical and thermal stability, its non-toxicity and its electrochemical performances in terms of lifetime.

---

<sup>17</sup> Also called lithium titanate.

<sup>18</sup> Note: lithium titanate can be used as a positive electrode, with lithium (e.g.) being used as the negative electrode. This is primarily the case when we look at it as a half-cell.

It also plays the role of a positive electrode when combined with a carbon negative electrode, as happens in the Maxell TC920S battery (coin cell format) used in Seiko Kinetic<sup>®</sup> watches. In this case, the nominal voltage is low: 1.5 V.



The reaction of lithium insertion/extraction in LTO takes place by way of a two-phase process similar in nature to that seen with LFP. For a so-called biphasic insertion reaction, there is no domain of stable solid solution, but rather there is coexistence of two phases of definite compositions within the electrode during electrochemical insertion. This mechanism is different to that which is observed for a so-called monophasic insertion reaction (such is the case for  $\text{LiMO}_2$  with M being Co, Ni, Mn or indeed  $\text{LiMn}_2\text{O}_4$ ), where a new phase with homogeneous composition is stabilized at each (infinitesimal) step of the insertion, such that a domain of solid solution is defined as the reaction progresses. To represent the advancement of the reaction which leads to the formation of a homogeneous compound (in terms of lithium concentration in this particular case), we have borrowed the idea of using the image of a die, with a progressive increment of the number of dots.

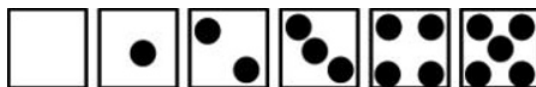


**Figure 5.11.** Image of the progression of the reaction  
(from Jérôme Bernardi's doctoral thesis<sup>19</sup>)

The equilibrium potential of the electrode, in this case, obeys the standard form of Nernst's law (ignoring the interactions between the charged species in the electrode) and the voltage changes throughout the process of charge or discharge (Figure 5.12). In addition, the kinetics of the reaction is primarily limited by ion diffusion.

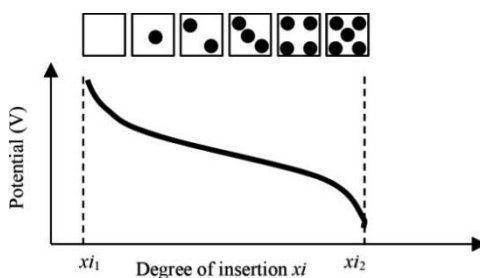


**Figure 5.12.** Plot of a potential curve for a mechanism of monophasic lithium insertion  
(from Jérôme Bernardi's doctoral thesis<sup>19</sup>)

19 J. BERNARDI, Etude théorique de matériaux de conversion pour le stockage de l'énergie, Doctoral thesis, Université Montpellier II, 12 December 2008.

In this case of two-phase (or biphasic) insertion, the electrode consists of a proportional mixture of two phases throughout the duration of the reaction, which therefore imposes that the equilibrium potential of the half-cell be constant throughout the biphasic domain defined by the limits  $xi_1$  and  $xi_2$  (Figure 5.13). This time, to represent the advancement of the reaction with the presence of two “compounds” or two phases with two different concentrations (of lithium, in this case), we show two different dice coexisting throughout most of the progression of the reaction.

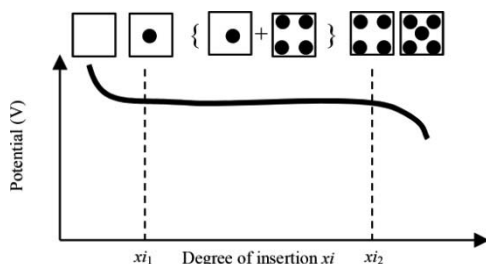


**Figure 5.13.** Plot of a potential curve for a mechanism of biphasic lithium insertion (from Jérôme Bernardi's doctoral thesis<sup>19</sup>)

Of course, both types of reactions may be observed successively during the course of the same discharge, with each one being associated with a particular domain of composition.

Thus, we can write:



The  $\text{Li}_4\text{Ti}_5\text{O}_{12}$  insertion structure is a spinel-type structure<sup>20</sup> (Figure 5.14): the octahedral sites formed by the oxygen atoms (dark gray) are occupied by all of the titanium atoms and  $\frac{1}{4}$  of the lithium atoms; the tetrahedral sites (light gray) are filled by the remaining lithium atoms.

Lithium insertion occurs in the vacant cationic octahedral sites around each occupied tetrahedral site. Migration of ions through the structure occurs in three dimensions, and does not alter the anionic arrangement and therefore the lattice parameters, which accounts for the very slight volumetric

<sup>20</sup> Lithium titanate oxide  $\text{Li}_4\text{Ti}_5\text{O}_{12}$  has a crystalline structure which is isomorphic to that of the mineral  $\text{MgAl}_2\text{O}_4$  (magnesium aluminum oxide) called spinel (central column in Figure 5.5).

expansion and therefore the very high mechanical stability of the structure during cycling. It presents excellent lithium ion conductivity. The lithium reversibility is therefore very high.

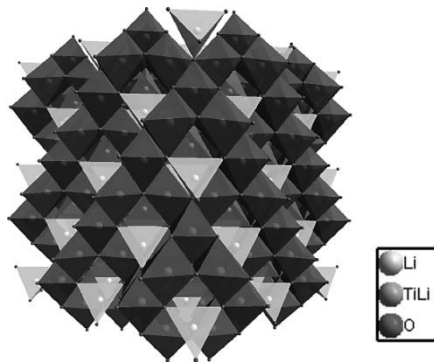


**Figure 5.14.** Representation of the structure of spinel  $\text{Li}_4\text{Ti}_5\text{O}_{12}$   
(Figure taken from Adrien Soares' doctoral thesis<sup>21</sup>)

EXERCISE 5.4.– using Faraday's law (see section 2.3.2.2), calculate the theoretical mass capacity of lithium titanate oxide.

*Solution page 165*

Hence, this material exhibits numerous advantages, and is in the process of replacing current graphite-based electrodes in spite of its poor volumetric capacity (its theoretical gravimetric capacity is 175 mAh/g, but in practice it is less than this – around 160 mAh/g. These values should be compared to those for graphite – theoretically 372 mAh/g, and 350–372 mAh/g in practice – see Table 5.2). However, basically, it has certain faults, such as its electrically insulative nature, preventing the use of high current densities, at the risk of greatly decreasing the electrochemical performances and increasing polarization. This disadvantage has been circumvented by the use of new means of synthesis – e.g. the replacement of the strictly-solid method, whereby it is impossible to control the size of the particles, the morphology and the homogeneity of the material, by a sol-gel or solvothermal process, which facilitates control of the textural parameters. The insertion of ionic or non-ionic elements into the structure or the

21 A. SOARES, Batteries Lithium-ion innovantes, spécifiques pour le stockage de l'énergie photovoltaïque, Doctoral thesis, Université de Montpellier II, 22 October 2012.

incorporation of additional elements or phases, coating with metallic (Ag, Cu) or non-metallic (carbon,  $\text{SnO}_2$ ,  $\text{TiN}$ , etc.) conductive layers, are other techniques which help obtain better electrical conductivity. Thus, it has been possible to improve the performances obtained with a greatly dispersed active material (nanometric particle size) and/or “doping”/coating.

The chemistry of titanate and the techniques of careful coating/doping therefore open the way to a broad spread of morphologies (texture, size, etc.), which helps compensate for its poor intrinsic electron conductivity. Such modifications may facilitate a quick insertion/extraction, and therefore a use for high-powered applications. This compound is promising for “electric vehicle” applications because of its aptitude for rapid charging, and research is currently being done on the validation of its performances in the long term. This advantage compensates for the decrease in specific energy of a complete  $\text{Li}_4\text{Ti}_5\text{O}_{12}/\text{LiFePO}_4$  battery (section 6.1.5), which is penalized by the lower voltage (around 1.8 V) of this combination in relation to, e.g., a Graphite/ $\text{LiFePO}_4$  battery (around 3.2 V) or graphite/cobalt battery (3.6 V).

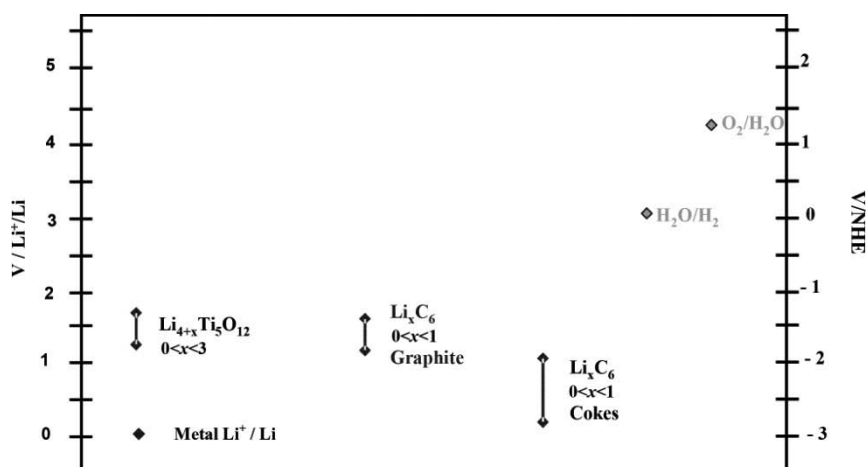
#### 5.4.4. *Electrochemical potentials*

Figure 5.15 compares the ranges of electrochemical insertion potentials of these two categories of materials versus metal lithium (left-hand scale). These potentials cover a range of voltage between 0 and 1.8 V versus  $\text{Li}^+/\text{Li}$ . The right-hand scale represents the same electrochemical potentials versus the NHE. The vertical line indicates the variation of these potentials depending on the fraction  $x$  of lithium inserted. The notation  $\text{Li}_{(1-x)}\text{C}_6$  with  $0 \leq x \leq 1-\varepsilon$  means that the active material of the electrode varies between carbon with or without a small quantity  $\varepsilon$  of lithium  $\text{Li}_6\text{C}_6$  and  $\text{LiC}_6$ . For lithium titanate, it varies between  $\text{Li}_4\text{Ti}_5\text{O}_{12}$  and  $\text{Li}_7\text{Ti}_5\text{O}_{12}$ .

The electrochemical potential of the couple  $\text{H}_2\text{O}/\text{O}_2$  is higher than that of the negative materials used for lithium-ion batteries. For this reason, these batteries are reactive to water and decompose in the presence of water or humidity.

#### 5.4.5. *Mass capacities*

To recap, the theoretical and practical mass capacities of these materials are given in Table 5.2.



**Figure 5.15.** *Electrochemical insertion potentials of some negative insertion materials*

| Materials                             | Theoretical gravimetric capacity (mAh/g) | Average practical gravimetric capacity (mAh/g) | Cost   |
|---------------------------------------|--|--|--------|
| Graphites                             | 372                                      | 350 to 372                                     | Medium |
| Cokes                                 | 372                                      | 300  | Low    |
| $\text{Li}_4\text{Ti}_5\text{O}_{12}$ | 175                                      | 160  | High   |

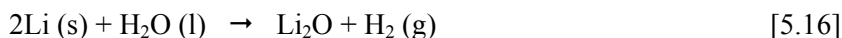
**Table 5.2.** *Gravimetric capacities of typical negative active materials*

As we can see from Table 5.2, the practical mass capacity of graphite is fairly close to its theoretical mass capacity. However, electrodes using coke exhibit a poorer practical mass capacity than graphite, because certain planes are not appropriately oriented and therefore do not allow the insertion of lithium. That said, they are less costly to produce.

Here, we shall not give the mass capacities of “high-capacity” carbonic materials – whose theoretical capacities may be, e.g., twice as great as those of graphite (for instance,  $\text{Li}_2\text{C}_6$ , 740 mAh/g) or even greater – because they are not currently used in commercial batteries. The major problem with these materials remains the significant irreversible capacity obtained with the first lithium insertion (formation process).

## 5.5. Electrolyte

Aqueous electrolytes cannot be used, because the lithium oxidizes spontaneously into lithium monoxide  $\text{Li}_2\text{O}$  and then into lithine  $\text{LiOH}$  if enough water is present, by way of the two successive reactions:



By combining the two reactions, we get the balance equation:



Therefore, we have to use non-aqueous electrolytes. Two families of electrolyte are presents on the market today: liquid electrolytes in combination with inert porous separators and gelled polymer electrolytes in combination with liquid electrolytes. In addition, research is being conducted to define a new, ionic type of electrolyte which is more thermostable. Thus, on a commercial level, today's lithium-ion technology can be subdivided into two subsets:

- liquid electrolyte lithium-ion (see section 5.5.1);
- polymer electrolyte lithium-ion (see section 5.5.2).

### 5.5.1. Liquid electrolyte

Liquid electrolyte lithium-ion technology uses mixtures of aprotic organic solvents (which are not likely to donate a proton) because the graphite-lithium electrode is very unstable in the presence of compounds with labile hydrogen.<sup>22</sup> The solvents used are alkyl carbonates (carbonates of ethylene, propylene, dimethyl, etc.)<sup>23</sup>; ethers, in which a lithium salt that

---

<sup>22</sup> In chemistry, lability is the capacity of an atom or group of atoms to be able to detach more or less easily from a molecule. The easier a group can detach, the more labile it is said to be. In the particular case whereby the departing group is the  $\text{H}^+$  ion (called a "proton", because a hydrogen atom which loses its one and only electron is reduced to its nucleus, comprising one proton), the lability of that proton will determine the protic or aprotic nature of the molecule which does or does not release it.

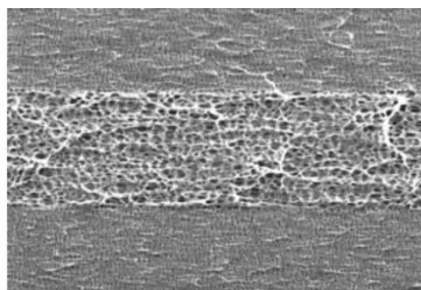
<sup>23</sup> Alkyl carbonates are often referred to by abbreviations, including: EC: ethylene carbonate; DEC: diethyl carbonate, DMC: dimethyl carbonate, EMC: ethyl methyl carbonate, PC: propylene carbonate.

serves to transfer<sup>24</sup> the lithium cation  $\text{Li}^+$  is solubilized. These salts are  $\text{LiPF}_6$  (lithium hexafluorophosphate, dissociated into  $\text{Li}^+$  and  $\text{PF}_6^-$ ) or  $\text{LiN}(\text{SO}_2\text{CF}_3)_2$  (lithium bis(trifluoromethanesulfonyl)imide, dissociated into  $\text{Li}^+$  and  $\text{N}(\text{SO}_2\text{CF}_3)_2^-$ ), commonly called LiTFSI (lithium bistrifluoromethanesulfonamide). Today, the electrolyte present in commercial batteries comprises an equivolumic mixture of ethylene carbonate (EC) and dimethyl carbonate (DMC), which are highly stable versus graphite with  $\text{LiPF}_6$  in a molar solution.

The separating membrane between the two electrodes is a mono- or multi-layer microporous film of polypropylene (PP) and polyethylene (PE), an example of which is Celgard<sup>®</sup> film (Figure 5.16). Safety constraints also weigh in favor of this latter type of separator, termed a “shutdown” separator, because in case of an increase in temperature, the polyethylene, which has a low melting point, begins to plug its own pores at around 110°C as it begins to melt, which considerably increases the resistance of the electrolyte and acts as a “chemical circuit-breaker”. The polypropylene, which is more thermostable, maintains the physical separation between the electrodes. The element can no longer deliver or receive any current.



Microporous separator



Scanning Electron Microscope (SEM)  
image of a triple-layer Celgard separator  
(PP/PE/PP)

**Figure 5.16.** *Celgard microporous separator* ([www.celgard.com](http://www.celgard.com))

<sup>24</sup> In reality, as the electrolyte is a collection of anions and cations, a lithium ion is not passed directly from one electrode to the other, but there is an exchange of ions between the two electrodes.

### 5.5.2. *Polymer electrolyte*

Polymer lithium-ion technology is also known commercially by the name LiPo. It has been commercialized more recently, particularly to serve the needs of model-making, and the need to have very varied formats of batteries, particularly in a flat pouch. LiPo technology is also to be found in electrically-assisted pedal cycles. More recently, it has been envisaged for electric vehicles or mobile devices.

The basic principle of a jellified (or gelled) polymer electrolyte was put forward in the mid-1970s. It is based on the ability of a polymer film to combine two main properties:

- a high affinity in relation to the liquid electrolyte chosen in order to ensure the formation of a so-called “jellified” film, with a high ionic conductivity (polymer/solvent interactions are favored). The polymers most widely used for this purpose are poly(ethylene) oxide (PEO), polyacrylonitrile (PAN) and methyl polymethacrylate (MPMA);

- good mechanical strength, meaning that the film is able to play the role both of a physical separator between the two electrodes, and of an electrolytic matrix imbibing the liquid electrolyte (polymer/polymer interactions are favored). In this case, only a few molecules of solvent are intercalated between the macromolecular chains. These films are said to be “plasticized”. They are composed of fluoride polymers based on Polyvinylidene fluoride (PVDF) or polystyrene (PS) and mineral content which can absorb liquid electrolyte and swell up.

Once the composition of the polymer matrix has been defined, the choice of liquid electrolyte needs to be carefully considered, because in particular it affects not only the mechanical strength of the membrane, but also the nature of the passivation layer which is formed on the surface of the lithium or of the graphite.

Originally, it was the company Bellcore (Bell Communications Research, USA) which, in 1994, demonstrated the feasibility of operation of such a fluoride polymer-based separator. Today, the technology is commercialized by the South Korean company Dow Kokam which, like other companies (Sony, Toshiba, Panasonic, Samsung, SAFT, Valence, etc.) in 1994 purchased the license to exploit the patent filed by Bellcore. However, it seems that only Kokam has succeeded in solving the technical difficulties



that this type of separator presents in terms of manufacture by rolling of the electrodes, by developing a stacked production-line technology and buying up all of the patents in the domain so as to have complete mastery of the process from start to finish. Kokam has also improved the ion conductivity of PVDF by adding a plasticizing agent; its published data states that its LiPo technology can provide discharges at 20 C. We can therefore say that today, it represents so-called “plasticized” technology.

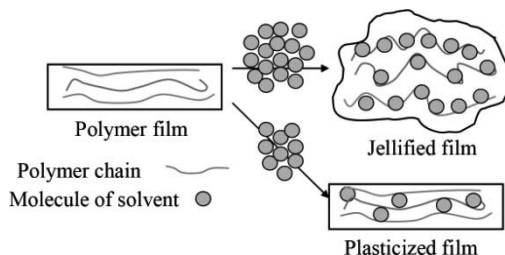


**Figure 5.17.** Diagrammatic representation of a gelled and a plasticized polymer film (taken from Lucas Sannier's doctoral thesis<sup>25</sup>)

Using this type of electrolyte, it is possible to make flat and flexible batteries, without the risk of the electrolyte leaking if the external casing is broken. This casing is a pouch which is metalized on the outside and covered on the inside surface with a heat-sealable polymer. This type of battery is also lighter, because there is no solid metal casing.

## 5.6. Current collectors

It is necessary to collect or supply electrons from or to the external electrical circuit. This is the role of current collectors.

Except in specific cases<sup>26</sup>, it may be very advantageous for this purpose to use aluminum (which is not only an excellent electricity conductor but is also a very light metal) for all the positive electrodes and those based on  $\text{Li}_4\text{Ti}_5\text{O}_{12}$ .

<sup>25</sup> L. SANNIER, Mise au point d'un électrolyte gélifié pour accumulateur au lithium fonctionnant à température ambiante, Doctoral thesis, University of Picardie Jules Verne (Amiens), 2003.

<sup>26</sup> Aluminum can become de-passivized below a certain value which depends on the electrolyte: 4.5 V for  $\text{LiPF}_6$  or less (3.5 V) for LiTFSI.

We can also use copper (which is also a very good electrical conductor) for graphite- or silicon-based electrodes.

However, we cannot use copper if the voltage is greater than approximately 3.2 V versus  $\text{Li}^+/\text{Li}$ , because beyond this value, copper becomes oxidized. Similarly, aluminum would not be used if the voltage were less than 0.7 V versus  $\text{Li}^+/\text{Li}$ , because below this value, aluminum accommodates lithium insertion.

## 5.7. Conclusion

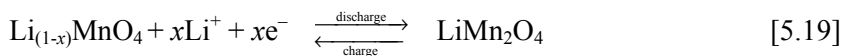
This chapter has discussed a sample of some of the electrodes used in commercialized batteries, or batteries which are in the process of beginning to be commercialized. Essentially, commercialized materials use the mechanism of lithium insertion (described in section 4.3.1), because these were the first materials to have been studied. Other materials seem potentially promising; these materials were mentioned in Chapter 4. Yet more materials will be discussed in Chapter 7, which deals with future developments of lithium-ion batteries.

The next chapter (Chapter 6) discusses the assembly of the electrodes to form a complete battery. Readers can also consult the article by Robert and Alzieu.<sup>27</sup>

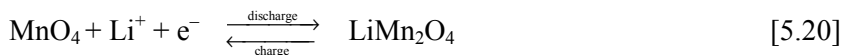
## 5.8. Solution to exercises in Chapter 5

### Solution to exercise 5.1 – Theoretical mass capacity of the $\text{LiMn}_2\text{O}_4$ electrode

Let us recap the reaction that we are dealing with (equation [5.10]):



To begin with, suppose that  $x = 1$  for complete extraction of the inserted lithium with one electron exchanged. Equation 5.19 is transformed into:




---

<sup>27</sup> J. ROBERT, J. ALZIEU, “Accumulateurs au lithium”, *Techniques de l'ingénieur*, D 3 354, 2005.

Using the transformed Faraday law (section 2.3.3.2):

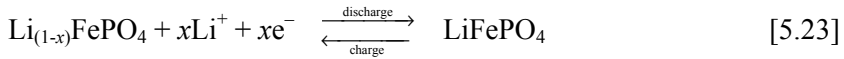
$$C_{m.th} \text{ (mAh/g)} = 26801 \cdot \frac{n}{M} \quad [5.21]$$

we get:

$$C_{m.th} = \frac{1}{6.9 + 2 \times 54.9 + 4 \times 16} \times 26801 = 148 \text{ mAh/g} \quad [5.22]$$

### **Solution to exercise 5.2 – Theoretical mass capacity of the LiFePO<sub>4</sub> electrode**

Let us recap the reaction that we are dealing with (equation [5.11]):

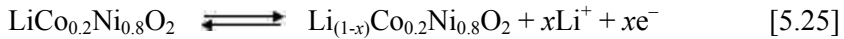


Suppose that  $x = 1$ , for complete extraction of the inserted lithium, with one electron exchanged.

$$Q_{th} = \frac{1}{6.9 + 55.8 + 30.97 + 4 \times 16} \times 26801 = 170 \text{ mAh/g} \quad [5.24]$$

### **Theoretical mass capacity of the LiCo<sub>0.2</sub>Ni<sub>0.8</sub>O<sub>2</sub> electrode**

The reaction we are dealing with is:



Suppose that  $x = 1$ , for complete extraction of the inserted lithium, with one electron exchanged. The theoretical mass capacity is written as:

$$C_{m.th} = \frac{1}{6.9 + 58.9 \times 0.2 + 58.7 \times 0.8 + 16 \times 2} \times 26801 = 274 \text{ mAh/g} \quad [5.26]$$

However, the maximum allowable degree of extraction for Li<sub>(1-x)</sub>CoO<sub>2</sub> is equal to  $x = 0.5$ . Thus, for the mixture of oxide 0.2 Li<sub>(1-x)</sub>CoO<sub>2</sub> + 0.8 Li<sub>(1-x)</sub>

NiO<sub>2</sub>, the maximum degree of extraction is  $0.2 \times 0.5 + 0.8 \times 1 = 0.1 + 0.8 = 0.9$ , giving us a theoretical mass capacity of:

$$C_{m.th} = \frac{0.9}{6.9 + 58.9 \times 0.2 + 58.7 \times 0.8 + 16 \times 2} \times 26801 = 247 \text{ mAh/g} \quad [5.27]$$

### **Solution to exercise 5.3 – Theoretical mass capacity of the graphite electrode**

Remember the reaction to take into account [5.12]:



Using the transformed Faraday law (section 2.3.3.2), the theoretical mass capacity for  $x = 1$  is:

$$C_{m.th} = \frac{1}{6 \times 12} \times 26801 = 372 \text{ mAh/g} \quad [5.29]$$

By way of comparison, we can calculate the theoretical mass capacity of the lithium electrode.

### **Theoretical mass capacity of the lithium electrode**

The reaction to consider is (equation [5.13]):



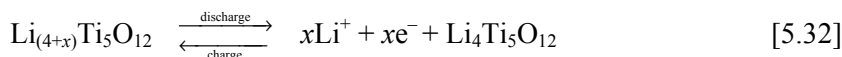
Using the transformed Faraday law (section 2.3.3.2), the theoretical mass capacity is:

$$C_{m.th} = \frac{1}{6.9} \times 26801 = 3884 \text{ mAh/g} \quad [5.31]$$

In a lithium battery, therefore, we need  $1000/3884 = 0.26$  g of lithium per stored Ah. The standard EN 62281, Safety of primary and secondary lithium cells and batteries during transport, gives 0.3 g of lithium per Ah.

### Solution to exercise 5.4 – Theoretical mass capacity of the $\text{Li}_4\text{Ti}_5\text{O}_{12}$ electrode

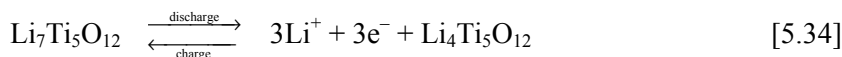
The reaction in question is equation [5.14], recapped below:



The maximum insertion capacity of a mole of  $\text{Li}_4\text{Ti}_5\text{O}_{12}$  is 3 moles of lithium with the exchange of 3 electrons. For  $x = 3$ , the theoretical mass capacity is:

$$C_{m.th} = \frac{3}{4 \times 6.9 + 5 \times 47.8 + 12 \times 16} \times 26801 = 175 \text{ mAh/g} \quad [5.33]$$

We note that the theoretical mass capacity is usually calculated by taking the minimum amount of lithium to be inserted into the material. This way of proceeding maximizes the theoretical mass capacity of the electrode in question. If, for the same electrode, we consider it in its lithiated state ( $x = 3$ ), the reaction is written:



and the theoretical mass capacity is now only:

$$C_{m.th} = \frac{3}{7 \times 6.9 + 5 \times 47.8 + 12 \times 16} \times 26801 = 168 \text{ mAh/g} \quad [5.35]$$

The difference is not overly great in this example. It may be greater with other electrodes, when the amount of lithium inserted is large or when the host structure has a low molar mass. While this difference may be perceptible with one electrode, it is no longer so with a complete element, because the lithium is transferred from one electrode to another: its mass is constant in the complete battery.

The same omission is found, for example, in the lithium-air battery (Chapter 10), for which there may be more than a tenfold difference between the theoretical values published and the actual performances expected in the real-world examples.



## Chapter 6

# Usual Lithium-ion Batteries

This chapter presents some lithium battery technologies that are among those most frequently encountered and made by combining the basic components examined in the previous chapter.

### 6.1. Principle of operation of conventional assemblies of electrodes

On the basis of the characteristics of the positive and negative electrodes described previously, we are going to construct different types of batteries. We shall begin with the generic couple C-LiMO<sub>2</sub><sup>(1)</sup>, which we shall first discuss in the form of the flagship technology C-LiCoO<sub>2</sub>, before going on to study couples such as C-LiFePO<sub>4</sub> and Li<sub>4</sub>Ti<sub>5</sub>O<sub>12</sub>-LiMn<sub>2</sub>O<sub>4</sub> and Li<sub>4</sub>Ti<sub>5</sub>O<sub>12</sub>-LiFePO<sub>4</sub>, which have been commercially introduced more recently.

---

<sup>1</sup> Throughout our discussion below, to refer to couples of electrodes, we shall use the order of international notation: negative electrode-positive electrode. However, in the existing body of literature, we often find the positive electrode cited first. In addition, we shall often abbreviate graphite as C, because graphite is carbon. Finally, regardless of the order of the electrodes, we shall first discuss the positive electrodes because, historically, they have been the subject of far more developments than the negative electrodes, which essentially comprise carbon for lithium-ion batteries (and metal lithium for lithium metal polymer batteries).

### 6.1.1. Principle of operation of a C-LiMO<sub>2</sub> element

The relations given previously in section 5.2 for two positive and negative matrices to accommodate lithium insertion can be transposed to a C-LiMO<sub>2</sub> element. The electrochemical chain that is then followed is:



The reactions at the electrodes are given below:

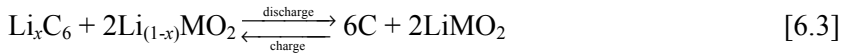
#### Positive electrode



#### Negative electrode



#### Balance equation



These equations are illustrated in Figure 6.1.

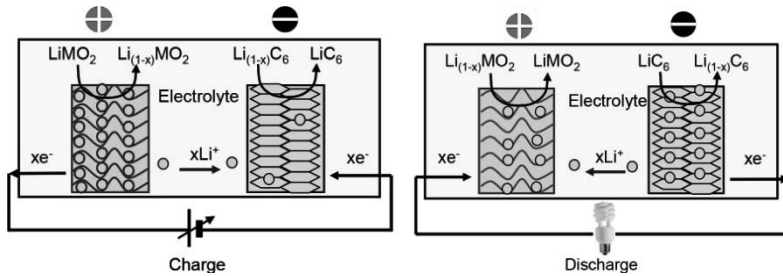


**Figure 6.1.** General principle of operation of a lithium-ion battery with a positive electrode made of a transition-metal oxide (the arrows represent the direction of displacement of the charges)

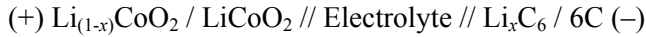
### 6.1.2. Principle of operation of a C-LiCoO<sub>2</sub> element

These equations and diagrams can be made clearer by specifying that the materials used for the positive electrode are those used in the type of battery



which has been most widely sold historically: C-LiCoO<sub>2</sub> (commonly notated C-LCO).

The electrochemical chain involved is simply rewritten as follows:



The reactions at the electrodes are given below:

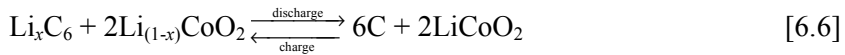
### Positive electrode



### Negative electrode



### Balance equation



As these equations show, during the charge process, lithium is inserted into the graphite. The reverse of this process occurs during discharge. Let us remember (section 5.3.1) that because the domain of stability of lithiated cobalt oxide  $\text{Li}_{(1-x)}\text{CoO}_2$  lies between  $x = 0$  and  $0.5$ , the element is designed so that the amount of negative material is limited, in order to ensure that the positive electrode receives at most a number of lithium ions corresponding to a maximum of  $x = 0.5$ .

These equations are illustrated in Figure 6.2, with the generic metal symbol M from Figure 6.1 being replaced with Co.

By algebraic addition of the curves for each of the two electrodes (Figures 5.3 and 5.5) obtained independently in a half-cell (section 2.2.3) thanks to the presence of a  $\text{Li}^+/\text{Li}$  reference electrode, we obtain the voltage for the whole element (Figure 6.3) represented as a function of the amount of electricity charged into the element or delivered by the element, and corresponding to its effective capacity. It is also the voltage obtained by

simply measuring the difference in potential at the terminals of the whole cellule.

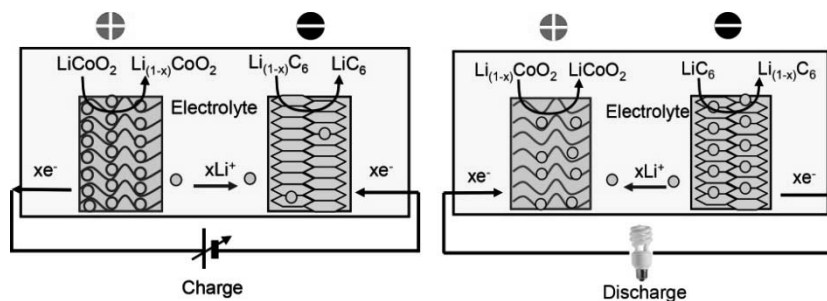


**Figure 6.2.** Principle of operation of the C-LiCoO<sub>2</sub> lithium-ion battery

The curve shows that the element in question is designed to deliver 4.25 mAh of electricity. This is its capacity. By setting this value against the total mass of the element (including active materials, electrolyte, collector and casing), we can calculate the real gravimetric capacity in mAh/g which, multiplied by its nominal voltage, gives us its real gravimetric energy density in Wh/kg and which is one of the most characteristic values of a battery.

**EXERCISE 6.1.**— Calculate the theoretical gravimetric capacity and the gravimetric energy density of a C-LiCoO<sub>2</sub> element.

*Solution page 230*

Figure 6.3 shows that the faradaic efficiency of charge/discharge (amount of electricity discharged/amount of electricity charged) is equal to 0.988 (the discharge curve does not return to zero). This efficiency is almost ideal. This faradaic efficiency of almost 1 is one of the major characteristics of lithium-ion technology.

Nowadays, this technology is no longer commercialized with a positive material of pure cobalt oxide. As indicated in section 5.3.1, because of its problematic behavior when overcharged, and because of the high cost of cobalt, this material is mixed with active materials such as nickel oxides LiNi<sub>0.8</sub>Co<sub>0.15</sub>Al<sub>0.05</sub>O<sub>2</sub> (NCA) or manganese and nickel oxides LiNi<sub>1/3</sub>Mn<sub>1/3</sub>Co<sub>1/3</sub>O<sub>2</sub> (NMC).

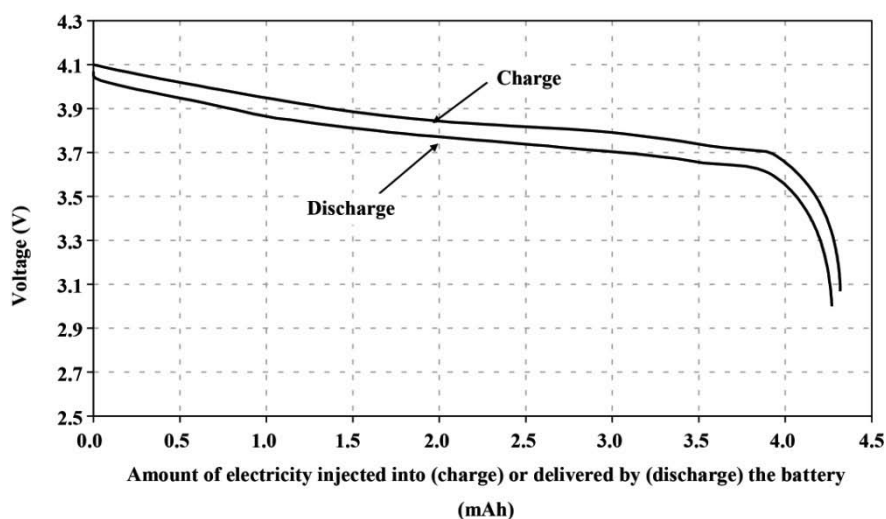


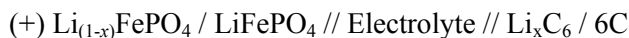
**Figure 6.3.** Voltage curves during charging and discharging of a  $\text{Li}_x\text{C}_6\text{-Li}_{(1-x)}\text{CoO}_2$  (C-LCO) element as a function of the charged or discharged capacity (currents = C/10)

Graphite- $\text{LiNi}_{0.8}\text{Co}_{0.15}\text{Al}_{0.05}\text{O}_2$  (NCA) technology, for instance, is commercialized by the company SAFT. Table 6.1 presents two models of elements made by that company, including the prismatic cell<sup>2</sup> from its MP range (which can be used, amongst other things, for applications in electrically-assisted pedal cycles (EAPCs) or portable devices). The third example is a battery with six cylindrical VLE elements connected in a series.




### 6.1.3. Principle of operation of a C- $\text{LiFePO}_4$ element

The couple graphite-iron phosphate (commonly notated C-LFP) is also widely available on the market.

The electrochemical chain involved is described below:



<sup>2</sup> The term “prismatic cell” is used for a cell which is not cylindrical in shape. Usually, it has a parallelepiped shape. We sometimes speak of flat batteries, which are in fact either flattened jelly-rolled batteries or “stacked” batteries, i.e. with electrodes which are stacked rather than jelly rolled.

| Range  | MP range  | VLE range   |  |
|--|---|---|--|
| Model  | Element<br>176065 HD  | Element<br>VLE45E   | Module<br>VLE 22–42  |
| Photo  |  |  |  |
| Nominal voltage  | 3.6 V   | 3.6 V   | 21.6 V   |
| Nominal capacity   | 3.6 Ah  | 45 Ah   | 42 Ah  |
| Mass   | 0.132 kg  | 1.07 kg   | 8 kg   |
| Dimensions (H: Height, W: Width, Ø: diameter, e: thickness)                  | H: 68.3 mm<br>W: 60 mm<br>e: 19.8 mm  | H: 222 mm<br>Ø: 54.3 mm   | H: 242 mm<br>W: 190 mm<br>e: 123 mm  |
| Gravimetric energy density   | 98.5 Wh/kg  | 149 Wh/kg   | 110 Wh/kg  |
| Volumetric energy density  | 160 Wh/L  | 313 Wh/L  | 158 Wh/L   |
| Specific powers up to 12.5 C   | 1200 W/kg<br>1950 W/L   | Not specified   | Not specified  |
| Specific powers (discharge for 30 s of 100–50% SOC, which is a 60 C current) | Not specified   | 664 W/kg<br>1392 W/L  | 533 W/kg<br>753 W/L  |

**Table 6.1.** Examples of NCA lithium-ion elements and modules using liquid electrolytes ([www.saftbatteries.com](http://www.saftbatteries.com))

The reactions at the electrodes are given below:

### Positive electrode



### Negative electrode



### Balance equation



These equations are illustrated in Figure 6.4.

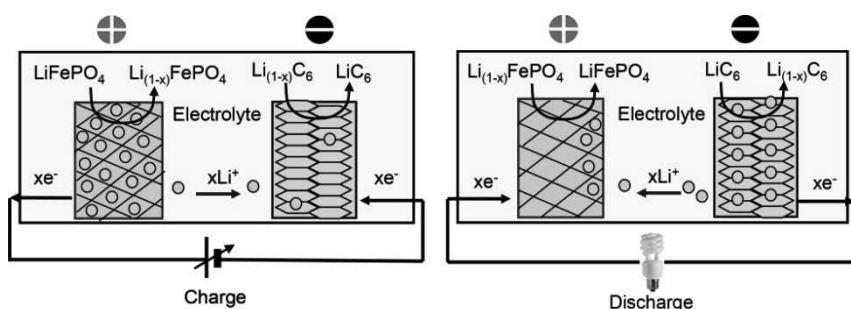




**Figure 6.4.** Principle of operation of the  $\text{Li}_{(1-x)}\text{C}_6\text{-LiFePO}_4$  lithium-ion battery

This technology is commercialized by many manufacturers (A123 Systems, Lifebatt, PHET, etc.). For example, at present, A123 Systems markets cylindrical elements with a 2.3 Ah capacity and flat-format elements with a 20 Ah capacity (see Table 6.2). A123 Systems has also made available a 5 kWh pack (“Hymotion L5 Plug-In Conversion Module”) compatible with the electrical system of the Toyota Prius plug-in.

#### 6.1.4. Principle of operation of a $\text{Li}_4\text{Ti}_5\text{O}_{12}\text{-LiMn}_2\text{O}_4$ element

Lithium titanate technology with a negative electrode of  $\text{Li}_{4+x}\text{Ti}_5\text{O}_{12}/\text{Li}_4\text{Ti}_5\text{O}_{12}$  (commonly notated as LTO) is currently being commercialized by a number of companies (including Toshiba, Altairnano, Enerdel, etc.). It is very much to be expected with applications where the needs for power and very quick recharging, combined with good operational safety, are significant, particularly in the area of electric vehicles.



| Model   | Nanophosphate <sup>®</sup> element<br>ANR26650M1-A                                | Nanophosphate <sup>®</sup> element<br>AMP20M1HD-A                                 |
|---|---|---|
| Photo   |  |  |
| Nominal voltage   | 3.3 V   | 3.3 V   |
| Nominal capacity  | 2.3 Ah  | 20 Ah   |
| Mass  | 0.07 kg   | 0.48 kg   |
| Dimensions (H: Height,<br>W: Width, Ø: diameter,<br>e: thickness) | H: 65 mm<br>Ø: 25.8 mm  | H: 200 mm<br>W: 152 mm<br>e: 7 mm   |
| Gravimetric energy density  | 108 Wh/kg   | 140 Wh/kg   |
| Volumetric energy density   | 236 Wh/L  | 315 Wh/L  |
| Specific powers at 10 s<br>(50% SOC)                              | 2250 W/kg<br>6000 W/L   | 3000 W/kg<br>6760 W/L   |

**Table 6.2.** Examples of C-LFP lithium-ion elements ([www.a123systems.com](http://www.a123systems.com))

As specified in the previous chapter (section 5.4.3), its ability to recharge in the space of a few minutes stems from the use of the negative electrode comprising nanocrystals of lithium titanate  $\text{Li}_4\text{Ti}_5\text{O}_{12}$ , creating an active surface area of approximately  $100 \text{ m}^2/\text{g}$  – as compared to the surface of carbon, which is around  $2 \text{ m}^2/\text{g}$  – and exhibiting an average insertion potential of 1.55 V versus  $\text{Li}^+/\text{Li}$ , which is therefore further than the potential for deposition of metal lithium than in the case of graphite (0.10 V versus  $\text{Li}^+/\text{Li}$ ). At the same time, this facility for quick recharging, combined with LTO's high insertion potential, is a disadvantage at the level of a single element, because the difference in potential between the two electrodes is reduced in comparison to elements with a graphite negative electrode. This battery is therefore disadvantaged by its low voltage and practical capacity in comparison to other, more conventional lithium-ion technologies.

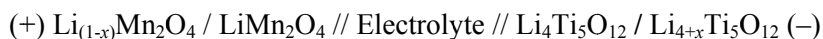
The example given in Table 6.3 is the Super Charge Ion Battery (SCiB), from Toshiba, whose positive electrode contains a manganese oxide

(commonly notated as LMO). Toshiba claims that the battery can be charged in the space of 10 min to 90% of its nominal capacity. However, SCiBs have a relatively poor energy density of around 67 Wh/kg, and thus are scarcely any better than NiMH batteries.

| Range   | Element   | Module   |
|---|---|--|
| Photo   |  |  |
| Nominal voltage                                     | 2.4 V   | 12 V   |
| Nominal capacity                                    | 4.2 Ah  | 4.0 Ah   |
| Mass  | 0.15 kg   | 1.0 kg   |
| Dimensions (H: Height, W: Width, e: thickness)      | H: 62 mm;<br>W: 95 mm; e: 13 mm   | H: 145 mm;<br>W: 109 mm; e: 48 mm  |
| Gravimetric energy density                          | 67 Wh/kg  | 48 Wh/kg   |
| Volumetric energy density                           | 132 Wh/L  | 63 Wh/L  |
| Specific powers with a pulsed 6 C current for 0.3 s | 400 W/kg<br>784 W/L   | 300 W/kg<br>395 W/L  |

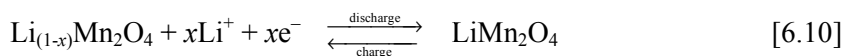
**Table 6.3.** Example of an element and module of LTO-LMO technology ([www.scib.jp/en/](http://www.scib.jp/en/))

In this battery, the electrochemical chain involved is described below:

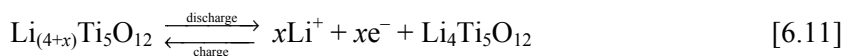


The reactions at the electrodes are given below:

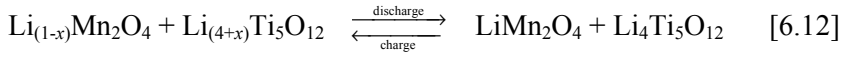
#### Positive electrode



#### Negative electrode



### Balance equation



These equations are illustrated in Figure 6.5.

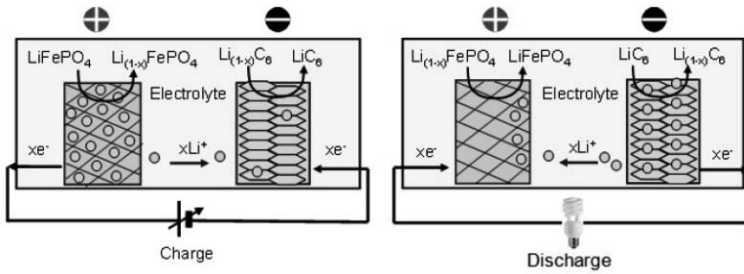


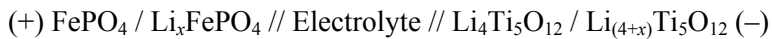
**Figure 6.5.** Principle of operation of the  $\text{Li}_4\text{Ti}_5\text{O}_{12}$ - $\text{LiMn}_2\text{O}_4$  (LTO-LMO) lithium-ion battery

Today, this battery is built into EAPCs (of the brand Schwinn Tailwind). Toshiba has stated its ambition to produce batteries for use in electric vehicles.

#### 6.1.5. Principle of operation of a $\text{Li}_4\text{Ti}_5\text{O}_{12}$ - $\text{LiFePO}_4$ element

Titanate-phosphate technology, which is a lithium-ion technology that is less advanced than other, more conventional technologies, is nevertheless very much to be expected with applications with significant needs for power and for very quick recharging (see section 5.4.3), combined with safe operation and high cyclability, particularly for electric vehicle applications. However, it falls down because of its lower gravimetric energy density than other technologies, owing to a smaller difference in potential between the two electrochemical couples present (2 V nominal voltage as opposed to 2.4 V for the  $\text{Li}_4\text{Ti}_5\text{O}_{12}$ - $\text{LiMn}_2\text{O}_4$  element presented above, or 3.7 V for the C- $\text{LiCoO}_2$  or C- $\text{LiMn}_2\text{O}_4$  element).

The electrochemical chain involved is simply rewritten as follows:



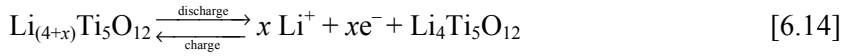


The reactions at the electrodes are given below:

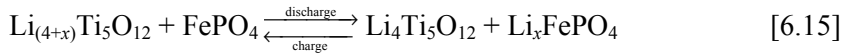
### Positive electrode



### Negative electrode



### Balance equation



These equations are illustrated in Figure 6.6.

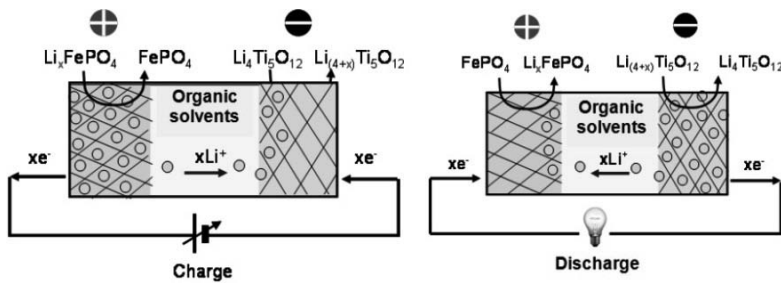


Figure 6.6. Principle of operation of the  $\text{Li}_4\text{Ti}_5\text{O}_{12}$ - $\text{LiFePO}_4$  lithium-ion battery

This couple is promising (inexpensive materials) but its long-term performances are still in the process of being validated. Indeed, dissolution of the iron, which is all the greater at higher temperatures, could decrease the cycling lifetime by poisoning the other electrode.

## 6.2. Major characteristics

The major characteristics of lithium-ion technologies (and lithium-ion polymer, LiPo, technologies) with a graphite-based negative electrode (except if a different electrode is mentioned and with the exception of those using ionic electrolytes) are listed below.

### 6.2.1. Voltage of an element

The voltage at the terminals of a lithium-ion element depends primarily on the choice of the two electrodes. This voltage is equal to the difference between the potentials of each of the two electrodes, which are shown individually in Figure 6.7 versus a  $\text{Li}^+/\text{Li}$  reference.

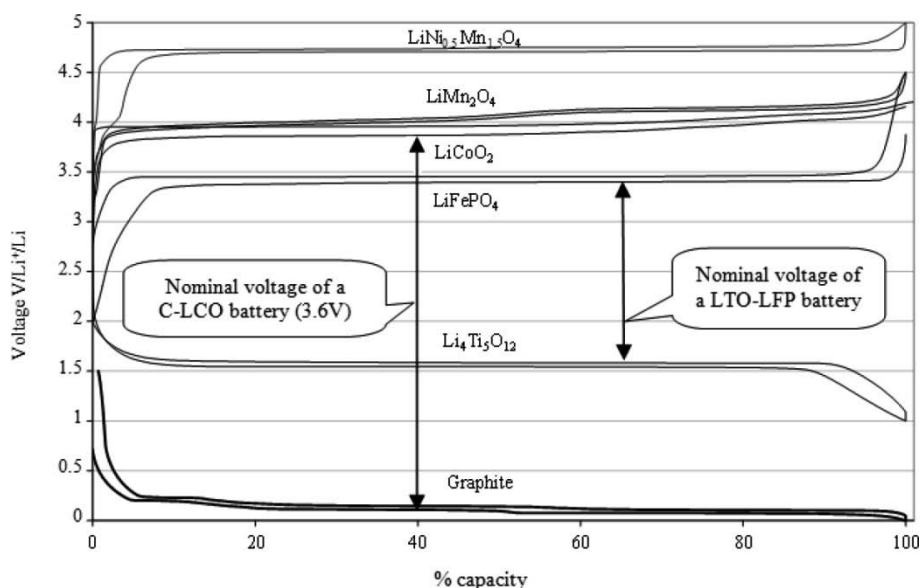


**Figure 6.7.** Evolution of the potentials during charge/discharge of different materials for positive and negative electrodes (source: Batteries – State of the Art – Presentation by F. Fusalba from the CEA at Journées “Electrotechnique” of the Club EEA in Belfort, 17 and 18 March 2010)

In this type of battery, the voltage increases with the degree of oxidation – either regularly, as happens with single-phase insertion mechanisms (such is the case for graphite, LCO and LMO electrodes) or in a more monotonous manner for biphasic insertion mechanisms (plateau of insertion for LFP and LTO) but still with a marked change at the end of charge or end of discharge. It is because of this that the criteria of end-of-charge or end-of-discharge voltage are meaningful. However, as with any technology, the evolution of the element’s voltage is different and is characteristic of the technology itself. This leads to the necessity to develop different indicators of state of charge (Ah) or energy (Wh) for each of the technologies used. These indicators are simpler to implement when the voltage evolves

regularly with the SOC (single-phase insertion mechanisms) because the voltage is then an indicator of the SOC in itself.

Table 6.4 shows the nominal voltages in standard conditions for different usual electrochemical couples.

| Negative electrode - Positive electrode | Nominal voltage (V) |
|---|---------------------|
| C-LCO                                   | 3.7                 |
| C-NCA                                   | 3.6–3.7             |
| C-LMO                                   | 3.7–3.8             |
| C-LFP                                   | 3.2–3.3             |
| LTO-LMN                                 | 2.4                 |
| LTO-LFP                                 | 2.0                 |

**Table 6.4.** *Nominal voltages for different typical electrochemical couples*

Thus, we can understand why the gravimetric energy density of a C-LFP element is higher than that of a LTO-LFP element in view of the difference in voltage between the two electrochemical couples, and considering the gravimetric capacity to be governed by the capacity of the positive electrode as is generally the case.

Considering the nominal potential of LFP ( $\text{LiFePO}_4$ ) to be approximately 3.5 V versus  $\text{Li}^+/\text{Li}$  and the nominal potential of LTO ( $\text{Li}_4\text{Ti}_5\text{O}_{12}$ ) to be 1.5 V versus  $\text{Li}^+/\text{Li}$ , the difference in potential (or difference in voltage) between the two electrodes is 2 V (as indicated in Table 6.4). Considering graphite, for which the nominal potential is 0.10 V versus  $\text{Li}^+/\text{Li}$ , the difference in voltage with LFP is greater: 3.3 V (Figure 6.8). Considering that the practical gravimetric capacity of LFP is 160 mAh/g, the gravimetric energy density (taking account only of the active material) for LTO-LFP will be 296 Wh/kg, and for Graphite-LFP 538 Wh/kg.

### 6.2.2. Usage for “energy” or “power”

With lithium-ion technology, we frequently hear the terms “energy-type battery” and “power-type battery”. This means that the internal design of the element is defined to serve:

- either energy needs, which requires stored capacity, i.e. a sufficient quantity of active material to deliver the intended autonomy. The typical

example of an application requiring a great deal of on-board energy is an electric vehicle (EV);

– or the need for significant instantaneous power, which requires an extensive exchange surface, i.e. large surface areas of the electrodes to the detriment of the active material. The typical example of an application requiring more power than on-board energy is a hybrid electric vehicle (HEV).

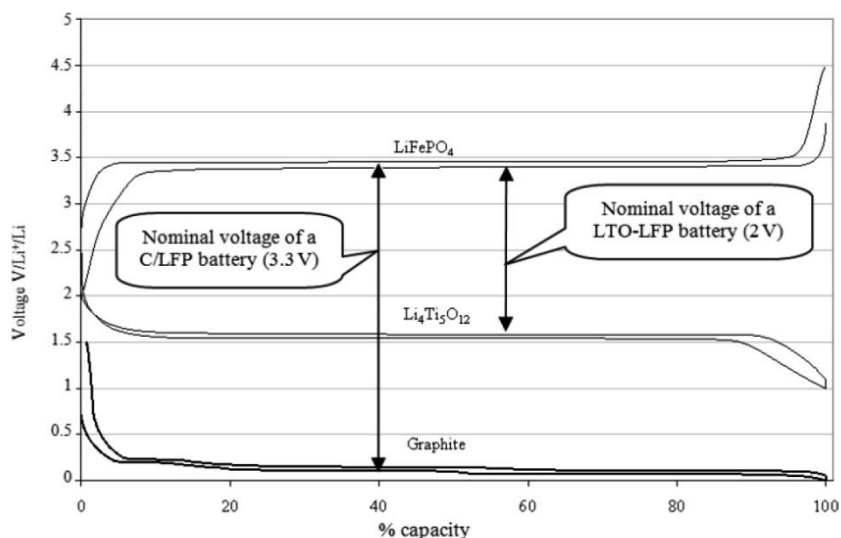


**Figure 6.8.** Comparison of the charge/discharge voltages for Graphite-LFP and LTO-LFP considering the profiles of potential of each material

These “energy” and “power”<sup>3</sup> elements use the same active materials, current collectors and separators in a similar jelly-roll design. However, differences in their internal design are necessary to serve the specific needs of each of these two applications. The distribution of the active material is different in each application. Power elements are often smaller than energy elements, in order to more easily dissipate the internal temperature increases related to the passage of strong currents. The internal connectics for current collection is specific. In addition, power elements often store less energy. Thus, packs for HEVs are usually smaller and lighter than those for EVs.

<sup>3</sup> This approximate classification is entirely associated with the maximum discharge regime.

Based on real data<sup>4</sup>, Table 6.5 reflects on the two opposing designs for elements, one for an EV and the other for a HEV (this latter application requires much more power than it does energy storage, so needs a greater gravimetric power density). Typically, 1,300 W/kg power elements have a specific energy of 60–70 Wh/kg, which is around two times less than energy elements. Plug-in HEVs (with the function of recharge from the electrical grid) present intermediary designs and are not detailed in Table 6.5. The characteristics shown in italics are calculated values.

These data enable us to clearly differentiate power-based and energy-based designs for a lithium-ion battery. In practice, on an industrial scale, a power-oriented electrode is made with a surface capacity (also called mass loading) of around 1.5 mAh/cm<sup>2</sup> or less. An energy-oriented electrode is made with a mass loading of 2.5 mAh/cm<sup>2</sup> (a small value) to 4 or 4.5 mAh/cm<sup>2</sup> (a large value). In the laboratory, electrodes with 7 or 8 mAh/cm<sup>2</sup> can be made in order to maximize the stored energy by increasing the ratio of active material to inert components (separator, packaging, etc.) but these electrodes cannot be discharged with currents stronger than C/10 and are also very fragile and breakable, and are therefore difficult to transpose to large surface areas to then be coiled.

In the case of an energy-oriented design, the mass of negative active material makes the greatest contribution to the mass of the element. In the case of a power-oriented design, the mass of the collectors contributes more to the mass of the element. Put differently, the surface capacity (mAh/cm<sup>2</sup>) of power-oriented elements is less for this configuration, as indicated by the calculation performed in Table 6.5.

### 6.2.3. *Window of voltage explored*

Figure 6.9 represents the window of voltage for the operation of a lithium-ion battery. The first charge is represented by a gray line, and shows the formation of the SEI which irreversibly consumes lithium on the side of the graphite and of the positive electrode, with the corresponding range of

---

<sup>4</sup> Values taken from GAINES L., CUENCA R., Costs of lithium-ion Batteries for Vehicles. AN/LESD-42, Center for Transportation Research, Energy Systems Division, Argonne National Laboratory, 9700 South Cass Avenue, Argonne, Illinois 60439, May 2000, reproduced in Florence Fusalba, CEA-Grenoble, Journées “Electrotechnique”, Club EEA – 18 March 2010, Belfort.

voltage no longer being exploited during the subsequent charge/discharge cycles in normal operation.

| Materials   | 5 Ah element for a<br>“power” application |      | 100 Ah element for<br>an “energy”<br>application |      |
|---|---|------|--|------|
|   | Mass (g)                                  | %    | Mass (g)   | %    |
| <b>C/Li<sub>x</sub>C<sub>6</sub> negative electrode</b>   |   |      |  |      |
| Active material   | 14.1                                      | 4.3  | 563.6  | 16.4 |
| <i>Practical gravimetric capacity</i>   | <i>5.3 Ah/kg</i>                          |      | <i>209.6 Ah/kg</i>                               |      |
| Binder (PVDF)   | 3.1                                       | 1.0  | 69.7   | 2.0  |
| Current collector (Cu foil)   | 41.6                                      | 12.8 | 151.9  | 4.4  |
| <i>Surface area (cm<sup>2</sup>) with <math>d_{Cu} = 8.92 \text{ g/cm}^3</math><br/>and thickness = 15 <math>\mu\text{m}</math></i> | <i>3109</i>                               |      | <i>11353</i>                                     |      |
| <i>Surface capacity</i>   | <i>1.72 mAh/cm<sup>2</sup></i>            |      | <i>18.47 mAh/cm<sup>2</sup></i>                  |      |
| Total   | 59.1                                      |      | 785.2  |      |
| <b>Li<sub>(1-x)</sub>CoO<sub>2</sub>/LiCoO<sub>2</sub> positive electrode</b>   |   |      |  |      |
| Active material   | 74.4                                      | 22.9 | 1408.6   | 41.0 |
| <i>Practical gravimetric capacity to be<br/>compared with theoretical capacity<br/>145 Ah/kg<br/>(for 50% material used)</i>        | <i>5.2 Ah/kg</i>                          |      | <i>98.6 Ah/kg</i>                                |      |
| Binder (PVDF)   | 6.3                                       | 1.9  | 92.9   | 2.7  |
| Current collector (Al foil)   | 19.4                                      | 6.0  | 63.0   | 1.8  |
| <i>Surface area with <math>d_{Al} = 2.74 \text{ g/cm}^3</math>, and<br/>thickness 15 <math>\mu\text{m}</math></i>                   | <i>4720 cm<sup>2</sup></i>                |      | <i>15328 cm<sup>2</sup></i>                      |      |
| <i>Surface capacity</i>   | <i>1.10 mAh/cm<sup>2</sup></i>            |      | <i>6.43 mAh/cm<sup>2</sup></i>                   |      |
| Conductive adjuvant (carbon black)  | 3.2                                       | 1.0  | 46.4   | 1.4  |
| Total   | 103.3                                     |      | 1610.9   |      |
| <b>Electrolyte</b>  |   |      |  |      |
| Solvents + salt   | 44.0                                      | 13.5 | 618.0  | 18.0 |
| Separator   | 16.4                                      | 5.0  | 60.5   | 1.8  |
| Total   | 60.4                                      |      | 678.5  |      |
| <b>Other</b>  |   |      |  |      |
| Internal connectics   | 32.2                                      | 9.9  | 66.2   | 1.9  |
| Core or mandrel   |   |      | 0.9  | 0    |
| Container   | 70.1                                      | 21.6 | 291.0  | 8.5  |
|   |   |      |  |      |
| <b>Total</b>  | 325                                       |      | 3433   |      |
| <i>Gravimetric energy density (for a<br/>nominal voltage of 3.8 V)</i>  | <i>63 Wh/kg</i>                           |      | <i>109 Wh/kg</i>                                 |      |

**Table 6.5.** Mass distribution in lithium-ion elements for “power” and “energy”

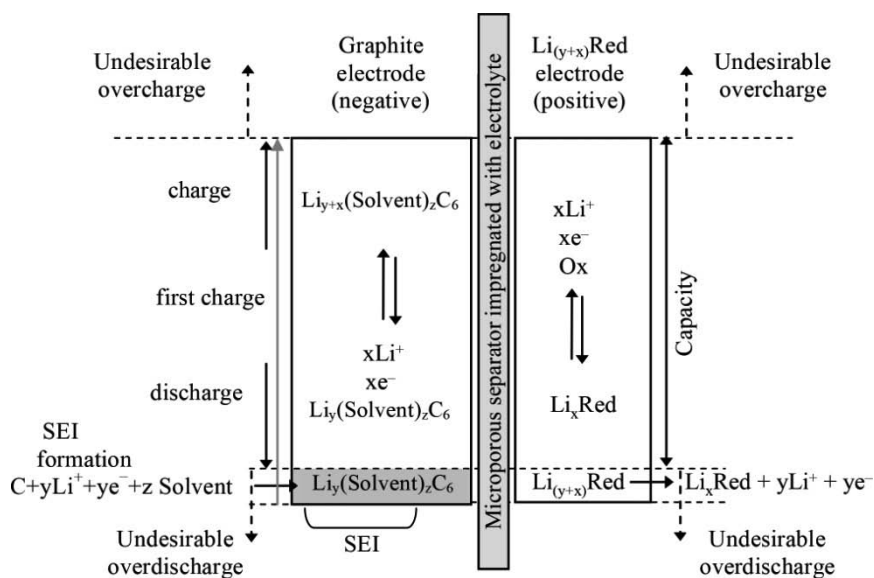


**Figure 6.9.** Range of electrochemical stability of a lithium-ion element for a C-LiCoO<sub>2</sub> electrochemical couple

Table 6.6 gives the charge and discharge voltages for four electrochemical couples: C-NCA, C-LMO, C-LFP and C-LMO/NCA.

| Electrochemical couple   | Threshold discharge voltage (V) | Threshold charge voltage (V) |
|--|---------------------------------|------------------------------|
| C-Li(Co,Ni,Al)O <sub>2</sub>   | 3.0                             | 4.2 / 4.0*                   |
| C-LiMn <sub>2</sub> O <sub>4</sub>                                   | 3.0                             | 4.3 / 4.0*                   |
| C-LiFePO <sub>4</sub>  | 2.0                             | 3.7 / 3.6*                   |
| C-LiMn <sub>2</sub> O <sub>4</sub> /Li(Co,Ni,Al)O <sub>2</sub> blend | 2.7                             | 4.2 / 4.0*                   |

\* voltage applied in a cycled regime

**Table 6.6.** Charge and discharge voltages for four electrochemical couples

### 6.2.4. Charge

The charge process is a complex issue even for a single element, and all the more so for an entire battery. It needs to be carefully managed, which

means we have to include additional electronic management systems for balancing and end of charge in the case of a combination of elements.

When the application permits (which, indeed, is not always, as exemplified by standalone photovoltaic systems), the charging of lithium-ion batteries is done by the method of constant current and then constant voltage (see Figure 6.10).

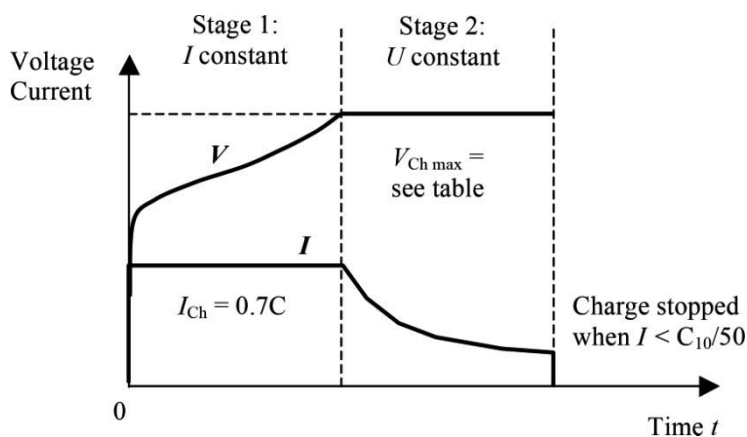


**Figure 6.10.** Profile of charge of a C-LiCoO<sub>2</sub> lithium-ion battery

The maximum charge voltage for a lithium-ion battery depends on the nature of the electrochemical couples present. Cobalt-based lithium-ion elements are generally charged with voltages between 4.0 and 4.2 V. The crystalline structure of the oxide LiCoO<sub>2</sub> is stable within this range of voltage, but blended oxides LiNi<sub>1-x</sub>Co<sub>x</sub>O<sub>2</sub> are more sensitive to the charge voltage, and to charge such batteries at 4.2 V, although it does enable us to obtain higher capacities, may affect their performances in terms of the number of cycles and the storage stability. For this reason, blended-oxide elements are usually charged at 4.1 V or 4.0 V. For phosphate-based lithium-ion elements (C-LiFePO<sub>4</sub>), the charge voltage is 3.6–3.7 V.

Table 6.7 recaps the nominal voltages of the different electrochemical couples and gives their charge voltage, when the negative electrode is made of graphite. These data are cited in the technical specifications associated with the element or battery or are written directly on the label (or on its packaging).



| Positive electrode            | Nominal voltage (V) | Charge with constant current / constant voltage |                        |
|-------------------------------|---------------------|---|------------------------|
|                               |                     | Threshold charge voltage (V)                    | Standard** current (A) |
| Cobalt (lamellar structure)   | 3.6                 | 4.0–4.2*  | 0.7 C                  |
| Manganese (spinel structure)  | 3.7–3.8             | 4.0–4.2*  | 0.7 C                  |
| Phosphate (olivine structure) | 3.2–3.3             | 3.6–3.7*  | 0.7 C                  |

\* For the higher value indicated, during the next discharge, the capacity discharged will correspond to the nominal value, but this will reduce the lifetime.

\*\* Maximum DC current.

**Table 6.7.** *Nominal voltages for different electrochemical couples*

For the first stage, with constant current, the optimal charge current recommended by manufacturers is usually equal to 0.7 C. However, if the battery is very heavily discharged, with a remaining voltage of less than 2.5 V, manufacturers recommend that it be recharged with weaker currents (less than 0.1 C). It should be noted that a weaker charge current would reduce the duration of the constant voltage phase, with complete charge being fully or nearly fully obtained during the constant current phase, because the phenomena of polarization linked to the overvoltages and the ohmic resistance are minimized. The threshold voltage at which the charging process switches from the constant current phase to the constant voltage phase is therefore delayed, meaning that during the application of constant current, a large amount of electricity, equal or almost equal to the capacity of the element can be stored. Conversely, a high charge current will drive the voltage up more quickly (significant polarization), and therefore the threshold voltage for the constant current charging will be attained earlier; hence the constant voltage phase will last longer before the element is fully charged. Thus, increasing the charge current does not significantly reduce the charge time, except of course if the actual design of the element facilitates it (power-oriented design, choice of materials).

During the constant voltage phase, the current decreases because the voltage is controlled as the element approaches the fully-charged state. End of charge is determined when the current reaches a threshold value. Typically this value is chosen between 0.03 C and 0.02 C.

The evolution of the voltage is different for cobalt-based or phosphate-based elements (Figure 6.11). For cobalt-based elements, the voltage

increases in an almost linear fashion until it reaches the threshold voltage of 4.0 V (end-of-charge voltage). For phosphate elements, the voltage evolves very little between 20 and 80% SOC. If the balancing of the SOC between the elements in the same pack is performed throughout the charging process, the actual management of that balancing will be more difficult for packs comprising phosphate-based elements.

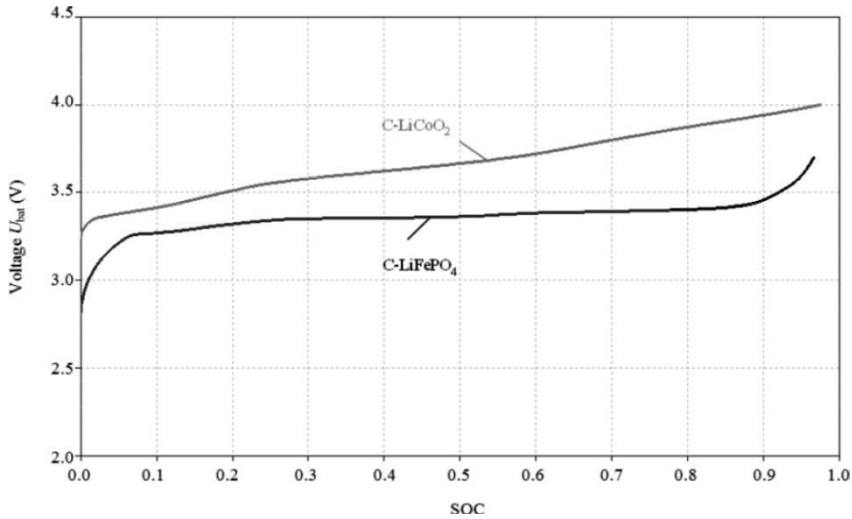


**Figure 6.11.** Charge voltage for a cobalt-based element and a phosphate-based element for a 0.2 C charge current

Unlike other secondary batteries such as lead–acid ones, no maintenance charge is needed, because lithium-ion batteries are not able to accept excess charge. However, in order to compensate for the (very slight) self-discharge and self-consumption of the balancing and safety circuits (BMSs), an additional short charge period with constant voltage can be carried out periodically or when the open-circuit voltage of the element falls below a predefined value until the charge voltage is once more equal to the threshold value.

We can apply much quicker charging (up to 60 C, with the limit being set by the battery's temperature control mechanism) to an element using a negative electrode made of titanium-oxide rather than graphite, because the insertion voltage of LTO is higher than that for graphite, so is a long way from the voltage for metal lithium deposition. Hence, there is no danger of

metal lithium deposition. However, this rapid charge can only be partial. Nevertheless, it is very advantageous and to be expected, e.g. to increase the autonomy of an electric vehicle. This is the concept of opportunity-charging, which involves performing partial recharges whenever the opportunity presents itself. Such is the case when parked in a lot which has an infrastructure for quick recharging (a parking lot for an electric car, a bus stop or terminus for an electric bus).

### 6.2.5. Safety management in cells

For reasons of safety, it is crucial that there be careful management of the energy in a cell and, *a fortiori*, in a battery of cells. It is essential to avoid excessive charges and excessive discharges by rigorous monitoring of the maximum and minimum voltages for the charge and discharge of each element.

To make batteries safe, many redundant protection devices are built into packs. We need to prevent the electrolysis of the electrolyte which would occur in case of an excessive charge. This release of gas causes excess internal pressure, which could lead to explosion or fire. Therefore, we include the following elements with the battery:

- pressure switch (deformation of a mechanical part causing the breakage of the electrical circuit) in each element, which definitively cuts off the passage of current if the safety threshold pressure value is exceeded (see Figure 6.12);

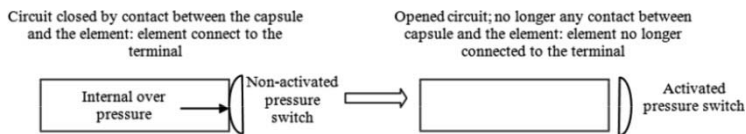


**Figure 6.12.** Diagram of the principle of operation of a pressure switch

- bi-metallic (two-strip) thermostats, which function as breakers, i.e. which can reset themselves and disconnect the charge if the temperature of the element goes above, say, 90°C;

- positive temperature coefficient (PTC) resistors or thermistors, which limit the current by increasing the resistance when the temperature of the cell

goes above the normal operating temperature (+30 to +50°C). This type of thermal component is cheap, is fairly simple to construct and is available for fairly varied ranges of current;

- electronic protection modules, which are connected to the battery like an additional module, and open the external circuit, thereby preventing any abusive usage of the battery.

In normal operation, the elements should not be discharged below 3 V. A safety device needs to intervene to ensure that the SOC does not go below 2.5 V per element.

In order to limit the dangers inherent to thermal runaway, these external safety devices are supplemented within the cell itself by internal protective mechanisms, such as “shutdown” separators (discussed in section 5.5.1), which are effective for temperature ranges from 135°C to 160°C; beyond this temperature, they become ineffective, because they lose their mechanical integrity, leading to the two electrodes coming into direct contact and an internal short-circuit. This type of separator tends to be found generally in high-capacity elements.

With regard to the danger of piercing or crushing, the solutions are to add an extra protective casing around the battery, but this is difficult to envisage for portable or on-board applications. Certain manufacturers use a polymerizing agent which forms a seal around the nail<sup>5</sup> at the moment of piercing, which ensures protection of the cell against thermal runaway.

### **6.2.6. *Internal failures***





Internal failures occur because of inadequate management of charging or discharging, operation at temperatures beyond the acceptable range: decomposition of the insertion materials, increase of the internal resistance which reduces the performances in terms of power or irreversible consumption of the lithium ions, the quantity of which becomes insufficient to provide the capacity of the element. These degradation phenomena are discussed in detail in section 6.2.21.

---

<sup>5</sup> For obvious reasons of safety, particularly in high-energy units such as those fitted to electric vehicles, batteries are tested to verify their resilience to certain extreme mechanical stresses such as crushing or piercing. The nail test consists of driving a nail into a battery and verifying that it does not catch fire and allows nothing to escape.

### 6.2.7. Operating temperatures

The ranges of operational and storage temperatures differ between the various technologies present on the market. Table 6.8 recaps the data quoted by manufacturers. We can distinguish the range of temperatures acceptable during charging and discharging, which may be different to that acceptable for storage.

| Technology                     | Elements or packs   | Charge         | Discharge      | Storage        |
|--------------------------------|---|----------------|----------------|----------------|
| SAFT      Graphite-NCA         |  | -20°C to +60°C | -50°C to +60°C | Not specified  |
| Kokam      Graphite-LMO        |  | -30°C to +60°C |                | Not specified  |
| A123 Systems      Graphite-LFP |  | -30°C to +60°C |                | -50°C to +60°C |
| Toshiba      LTO-LMO           |  | -30°C to +50°C |                | Not specified  |

**Table 6.8.** Operational and storage temperatures

Lithium-ion batteries for portable computers can withstand -20 to +60 or 65°C during discharge, but are limited to 50°C temperature during charge.

### 6.2.8. Self-discharge

The degree of self-discharge depends on the electrodes chosen: experimentally, we have obtained values of self-discharge of 0.6% per month to 1.2% per month (at 40°C) respectively for C-LiMO<sub>2</sub> and C-LiFePO<sub>4</sub> batteries. These values are extended for a single cell. However, in combinations of cells, the entirety of a battery system combined with its battery management system (BMS), may exhibit an “apparent” self-discharge which is far greater, because of the electricity consumption of the electronic circuits built into the BMS cards – e.g. up to 3% per month at

20°C for C-LiFePO<sub>4</sub>. This self-consumption causes a concomitant decrease in the faradaic and energy efficiencies.

### 6.2.9. *Memory effect*

No memory effect (as is observed in nickel-cadmium technologies<sup>6</sup>) has been demonstrated.

### 6.2.10. *Commercially available capacities*

Before the development of batteries for electric vehicles considerably changed the situation, the available lithium-ion batteries tended to have a small capacity: around 1 Ah to a few tens of Ah depending on the manufacturers. Therefore, it was necessary to connect the elements in series and in parallel to increase the voltage and capacity. These assemblies were made by intermediary companies, re-selling battery packs for portable equipment or for small autonomous systems. Today, manufacturers and companies specializing in connectics are working to develop methods of assembly and connection which offer the best performances of the pack. The assembly is of crucial importance to ensure the perennity of the performances over time (choice of connectors, management methods) and to make the battery safe (inclusion of fuses<sup>7</sup>, etc.).

### 6.2.11. *Dependency of the capacity on the discharge current and the temperature. Peukert's law*

So long as the discharge currents remain reasonable (around 1 C), the capacity depends only very little, if at all, on the regime of discharge, but appears to be more sensitive to temperature than is the case for a lead-acid battery. Peukert's law<sup>8</sup>, introduced for lead-acid batteries, describes the dependency of the capacity on the discharge current. It is expressed thus:

$$C_p = I^k t \quad [6.16]$$

---

6 C. GLAIZE & S. GENIÈS, *Lead and Nickel Electrochemical Batteries*, ISTE Ltd, London, John Wiley & Sons, New York, p. 243–245, 2012.

7 Protection devices described in section 6.2.5.

8 Although it is called a law, Peukert's law is in fact an empirically-determined expression and does not have the nature of a fundamental law.

where:

$C_p$  = Peukert capacity (Ah),

$k$  = Peukert exponent,

$I$  = discharge current (A),

$t$  = autonomy or duration of discharge (hours).

For lithium-ion batteries designed for power-oriented applications (i.e. the possibility of extracting strong currents), the Peukert exponent is very near to 1, because they are intended to be discharged rapidly, to the detriment of gravimetric capacity. On the other hand, with batteries designed for energy-oriented applications (maximization of the stored energy), the capacity is more sensitive to the discharge current.

To illustrate this analysis, we have given three results obtained with C-NCA elements in three very different formats: a 45 Ah element, a 10 Ah element designed for energy-oriented applications and a 700 mAh cylindrical element (see Table 6.9).

|                 | Range of discharge currents applied | Peukert exponent               |
|-----------------|-------------------------------------|--------------------------------|
| 45 Ah element   | $2 C_{10}$ to $C_{10}/5$            | 1.053 at 25°C                  |
| 10 Ah element   | $C_{10}/10$ to $C_{10}/3$           | 1.037 at 25°C<br>1.010 at 40°C |
| 700 mAh element | $C_{10}/100$ to $C_{10}/1$          | 1.010 at 25°C                  |

**Table 6.9.** *Examples of Peukert exponents for C-NCA elements*

This Peukert coefficient, close to 1, giving a capacity independent of the duration of discharge, may lead us to choose a linear model of the dependency of the capacity on the discharge current. For instance, for an NCA element with poor capacity, we find the following values at 25°C:  $C = 10.5 \text{ (Ah)} - 0.276.I \text{ (A)}$ .

For an NCA element with higher capacity, Thiaux<sup>9</sup> proffers the relation  $C = 49.7 \text{ (Ah)} - 0.38.I \text{ (A)}$  for currents ranging from 1 to 10 A (i.e. C/50 to C/5 currents) and at ambient temperature.

For C-LFP technology, values for Peukert coefficients are given in Table 6.10. It is difficult to establish a comparison between C-NCA and C-LFP technologies because the elements are not comparable in terms of their format or internal design.

|  | Range of discharge currents applied | Peukert exponent   |
|--|-------------------------------------|--|
| 2.2 Ah element for “power-oriented” applications               | C/10 to C/0.4                       | 1.000 at 0°C   |
| 10 Ah element<br>(see M. Dubarry <i>et al.</i> <sup>10</sup> ) | C/10 to C/2                         | 1.012 at 25°C for element n°1<br>1.015 at 25°C for element n°2 |

**Table 6.10.** Examples of Peukert exponents for C-LFP elements

The capacity is also dependent on temperature. We can see that the capacity increases when the temperature increases. Depending on the discharge current, this represents a gain in capacity of 2–6% when the temperature is increased from 25°C to 40°C. As we saw earlier, the capacity decreases with increasing current strength, but that decrease is far less pronounced at higher temperatures. For instance, with a 2 C discharge current, the capacity would decrease by 5–10% when the temperature drops from 40°C to 20°C, but would plummet by 70% for a drop from 20°C to 0°C.

### 6.2.12. Gauges

The role of a gauge is twofold: to show the SOC of a battery at a given time, but also to discover whether it has enough energy stored to complete a

<sup>9</sup> THIAUX Y., Optimisation des profils de consommation pour minimiser les coûts économique et énergétique sur cycle de vie des systèmes photovoltaïques autonomes et hybrides. Évaluation de la technologie Li-ion. Doctoral thesis, École Normale Supérieure de Cachan, 8 July 2010.

<sup>10</sup> DUBARRY M. *et al.*, “Identifying battery aging mechanisms in large format Li-ion cells”, *J. Power Sources*, 196, 3420–3425, 2011.



mission (e.g. for an electric vehicle, to carry out or complete the planned journey).

While it is easy to measure the amount of electricity and energy already provided by the battery, it is more difficult to evaluate the amount of electricity which is still available. Indeed, during the course of discharge, the amount of electricity remaining or still available depends not only on the past conditions (conditions in which the already-discharged electricity was provided, and therefore consumed), but also and above all on the future conditions of discharge (essentially the amplitude, which is often variable, of the discharge current and the temperature).

The amount of electricity and energy that a battery is still capable of delivering (respectively expressed in Ah and Wh) and the voltage at its terminals depend on its SOC (State of Charge, defined in section 2.4.2) but also on its SOH (State of Health, defined in section 2.4.4).

In order to define a gauge capable of giving an accurate indication of the SOC and/or SOE<sup>11</sup> (State of Energy, defined in section 2.4.3) of a battery, researchers are working to develop models of the capacity, the remaining amount of charge and/or voltage.

According to V. Pop *et al.*, it was in 1963 that the earliest gauges of SOC were developed for the automobile industry, based at the time on measurements of voltage.<sup>12</sup> Since then, many indicators have been developed to track the SOC<sup>13, 14</sup> and SOH<sup>15, 16</sup> of a battery: the coulometric

---

11 K. MAMADOU, Prévision de la disponibilité énergétique des accumulateurs électrochimiques par estimation d'états d'énergie (SoE), Doctoral thesis, University Grenoble, awarded by the Institut polytechnique de Grenoble, 3 December 2010.

12 V. POP, H. J. BERGVELD, P. H. L. NOTTEN, P. P. L. REGTIEN, "State-of-the-art of battery state-of-charge determination", *Meas. Sci. Technol.*, 16, R93–R110, 2005.

13 S. PILLER, M. PERRIN, A. JOSSEN, "Methods for state-of-charge determination and their applications", *J. Power Sources*, 96, 113–120, 2001.

14 L. LU, X. HAN, J. LI, J. HUA, M. OUYANG, "A review on the key issues for lithium-ion battery management in electric vehicles", *J. Power Sources*, 226, 272–288, 2013.

15 J. REMMLINGER, M. BUCHHOLZ, M. MEILER, P. BERNREUTER, K. DIETMAYER, "State-of-health monitoring of lithium-ion batteries in electric vehicles by on-board internal resistance estimation", *J. Power Sources*, 196, 5357–5363, 2011.

16 D. ANDRE, C. APPEL, T. SOCZKA-GUTH, D.U. SAUER "Advanced mathematical methods of SOC and SOH estimation for lithium-ion batteries", *J. Power Sources*, 224, 20–27, 2013.

method, measurement of the internal resistance or of another electrical parameter relating to the impedance of the battery, obtained at different frequencies<sup>17</sup>, a measure of the voltage at rest or under current (and comparison of the value obtained on voltage charts, with no current (open-circuit voltage), at different temperatures as a function of the SOC and the SOH if possible).

In practical terms, this involves modeling the available capacity using an SOC estimator in real time. In any case, the choice of an SOC indicator is complicated. To measure the open-circuit voltage necessitates relatively long relaxation times, depends on the temperature and is therefore difficult to apply to a vehicle. The electrical parameters obtained by impedance spectroscopy need to be sufficiently reactive to the SOC to facilitate an accurate evaluation of the SOC (on the other hand, with the SOH, the technique is more easily applicable).

Let us now discuss the operation and properties of the most commonplace estimators.

The simplest estimator to implement is to directly measure the voltage (under current or at rest) at the terminals of the battery. It can be used with electrochemical couples which exhibit monotonous decrease of the voltage as a function of the SOC (such as C-NCA, Figure 6.13), to the detriment of the integration of temperature in the measurement.

To measure the open-circuit voltage imposes relatively long relaxation times (rest periods). This voltage also depends on the temperature. It can therefore not be used in real time.

Conversely, other couples exhibit very extensive plateaus of voltage (see for instance LTO/LFP, illustrated in Figure 6.14), which means that the measured voltage cannot be used as an indicator of charge except in extreme SOC's.

---

<sup>17</sup> See section 2.4.12 on impedance spectroscopy.

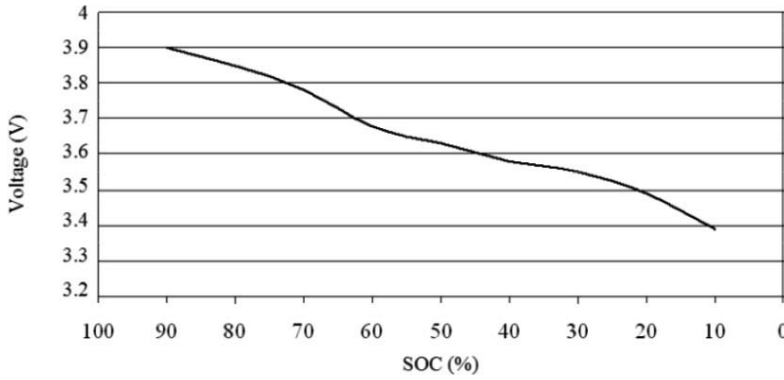


**Figure 6.13.** Profile of discharge voltage under current for a C-NCA element

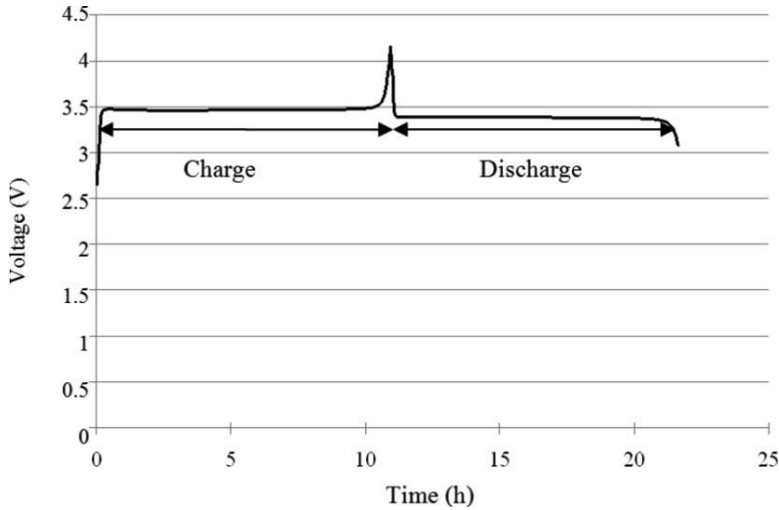


**Figure 6.14.** Profile of voltage under current for a LTO-LFP element, first charged and then discharged at constant current (C/10)

The most commonly used estimator is based on the coulometric method which consists, beginning with a capacity  $C_{\text{reference}}$  known and measured in reference conditions, of integrating the  $i$  (either for charge or discharge). The available capacity  $Q_{\text{available}}$  in the use conditions is then given by the relation:

$$Q_{\text{available}}(t) = C_{\text{reference}}(t_0) + \int_{t_0}^t i(t) dt \quad [6.17]$$

This measurement method is particularly advantageous with lithium technologies whose capacity depends very little on the charge/discharge current (see section 6.2.11.). For other technologies, we can apply coefficients on the basis of the amplitude and sign of the current.

The degree of precision of the estimator is therefore dependent on the reference capacity. Hence, it is necessary to evaluate it in<sup>18</sup> various usage conditions in order to use the appropriate value  $C_{\text{reference}}$  at each step of the calculation. Figure 6.15 shows a representation in the form of a tank whose capacity evolves over time as a function of the SOH.

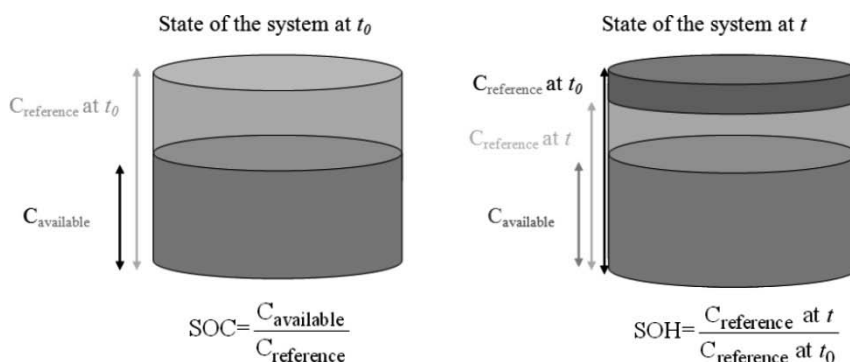


**Figure 6.15.** Diagrammatic representation of the SOC and SOH of an electrochemical system, viewed as a tank

The suggested models usually include errors which are corrected by recalibration parameters and methods. Thus, by way of example, tracking indicators based on coulometric methods require additional recalibration indicators, because of the integration of the current which may lead to errors if the measurement of the current is not sufficiently accurate. This recalibration might be performed, for instance, at the extreme states of charge. SOC indicators therefore need to be adapted to the application in terms of precision, frequency of measurement acquisition and also duration and frequency necessary for re-calibration.

<sup>18</sup> Remember that the best way to determine the capacity of a battery is to perform a complete discharge after a complete charge, with the discharge occurring with values of current and temperature that are representative of the application. The drawback to this method is that, besides the wastage of energy, the battery is no longer available for the entire duration of the complete charge/discharge/recharge cycle, which means several hours of immobilization.

More recently, techniques have been put forward that are based on fuzzy logic, neural networks or observation of parameters taken from electrical models by Kalman filtering.<sup>19, 20</sup>

In order to improve the accuracy of the result, we can also use several methods together, either by zones of SOC or simultaneously.

If, in addition to the instantaneous SOC, we wish to know the amount of energy remaining, we have to use more complex predictive models than those discussed previously. Indeed, on its own, knowledge of the capacity is insufficient to determine the available energy. We also need to know the voltage of the battery in each of its future states of charge. A number of models of voltage and energy have been developed, therefore, based on very different concepts<sup>21</sup>:

- “*black-box*”-type representative models, for which the battery is represented by a transfer function whose parameters are adjusted. This category includes all models such as Kalman filters<sup>22, 23</sup> or neural networks which require prior training;

- *physico-chemical models*, the goal of which is to describe the internal processes of the battery. These models are difficult to implement because of the very complicated computing codes and the many geometric data and parameters representing the different components of the battery;

- finally, *equivalent electrical circuit models*. These dynamic models are designed on the basis of temporal or frequential analyses. Frequential analyses help to show the different time constants of the internal processes in

---

19 M. MASTALI, J. VAZQUEZ-ARENAS, R. FRASER, M. FOWLER, S. AFSHAR, M. STEVENS, “Battery state of the charge estimation using Kalman filtering”, *J. Power Sources*, forthcoming.

20 D. V. DO, C. FORGEZ, K. EL KADRI BENKARA, G. FRIEDRICH, “Impedance Observer for a lithium battery using Kalman filter”, *Vehicular Technology*, IEEE Transactions, 58, 3930–3937, 2009.

21 T.-K. DONG., Contribution à la modélisation dynamique des batteries Lithium-ion pour l’application photovoltaïque et stockage connecté au réseau, Doctoral thesis, Institut National Polytechnique de Grenoble, 2010.

22 H. DAI, X. WEI, Z. SUN, J. WANG, W. GU, “Online cell SOC estimation of Li-ion battery packs using a dual time-scale Kalman filtering for EV applications”, *Applied Energy*, 95, 227–237, 2012.

23 M. MASTALI, J. VAZQUEZ-ARENAS, R. FRASER, M. FOWLER, S. AFSHAR, M. STEVENS, “Battery state of the charge estimation using Kalman filtering”, *J. Power Sources*, forthcoming.

the battery and thereby to obtain more detailed models of their dynamic behavior.<sup>24-25</sup>

Of these different modeling methods, the equivalent electrical circuit approach is the most widely used to serve the need for precision of the model without too high a degree of complexity of its implementation.

An example of a representation of the energy available in the form of a chart is given in Figure 6.16<sup>26</sup>, modeling the response of the battery when subjected to different conditions of discharge (currents, temperature, etc.).

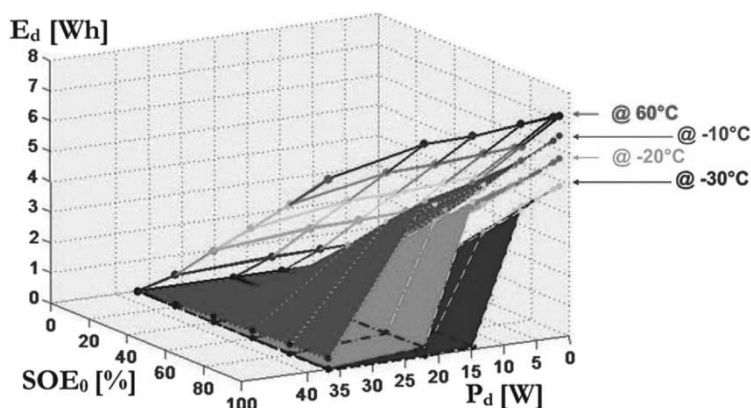


**Figure 6.16.** Chart of the energy available for different SOEs and different discharge powers at temperatures ranging between  $-30^{\circ}\text{C}$  and  $+60^{\circ}\text{C}$  (C-LiFePO<sub>4</sub> technology)

### 6.2.13. Practical gravimetric energy density








The gravimetric and volumetric energy densities will be very different depending on the nature of the electrodes. Also, we need to clearly distinguish between the gravimetric and volumetric energy densities of a cell

24 S. CHO, H. JEONG, C. HAN, S. JIN, J. H. LIM, J. OH, "State-of-charge estimation for lithium-ion batteries under various operating conditions using an equivalent circuit model", *Computers and Chemical Engineering*, 41, 1–9, 2012.

25 W. WAAG, C. FLEISCHER, D.U. SAUER, "On-line estimation of lithium-ion battery impedance parameters using a novel varied-parameters approach", *J. Power Sources*, forthcoming.

26 K. MAMADOU, E. LEMAIRE, A. DELAILLE, D. RIU, S. E. HING, Y. BULTEL, "Definition of a State-of-Energy indicator (SoE) for electrochemical storage devices: application for energetic availability forecasting", *J. Electrochem. Society*, 159 (8), A1298–A1307, 2012.

and those of a pack, which are necessarily lesser.<sup>27</sup> Examples of practical gravimetric energy densities calculated or stated by the manufacturers of elements or batteries are given in Table 6.11. The same values are used in Figure 6.17 to illustrate the decrease in gravimetric capacity when we switch from dealing with an element to dealing with a pack.

| Technology                    | Elements   | Modules  |
|-------------------------------|--|--|
| SAFT      Graphite-NCA        |  3.6 V / 45 Ah:<br>148 Wh/kg  |  21.6 V / 42 Ah:<br>110 Wh/kg |
| Kokam      Graphite-LMO       |  3.7 V / 100 Ah:<br>163 Wh/kg |  25.9 V / 31 Ah:<br>99 Wh/kg  |
| A123Systems      Graphite-LFP |  3.3 V / 20 Ah:<br>140 Wh/kg  | Not specified  |
| Toshiba      LTO-LMO          |  2.4 V / 4.2 Ah:<br>67 Wh/kg  |  12 V / 4 Ah:<br>48 Wh/kg     |

**Table 6.11.** Gravimetric energy density of elements and modules of different lithium-ion technologies

It is noteworthy that Graphite-NCA, Graphite-LMO and Graphite-LFP batteries exhibit unitary gravimetric energy densities between 140 and 160 Wh/kg, whether they are “stacked” (stacked arrangement of electrodes in a *mille-feuille*-type manner) or rolled, in an aluminum casing or a flexible sachet (or pouch). Assembly of these units into a pack reduces this criterion to a value between 100 and 110 Wh/kg. The LTO-LMO battery has a lower gravimetric energy density, with 67 Wh/kg for the 2.4 V element and 48 Wh/kg for the 12 V made by Toshiba.

Battery packs, including the BMS, are usually assembled using cylindrical elements (in the area of portable computers, we speak of cells), labeled “18650” (because their dimensions are standardized: 18 mm in diameter and 65 mm in length). We can now sometimes find so-called “26650” formats (26 mm in diameter and 65 mm in length) introduced by

<sup>27</sup> In order to valorize lithium-ion batteries in comparison to other less recent technologies, the gravimetric capacity of a cell is often quoted, rather than that of a pack.

A123 Systems, whose gravimetric energy density is higher – e.g. 190 Wh/kg for a laptop battery.

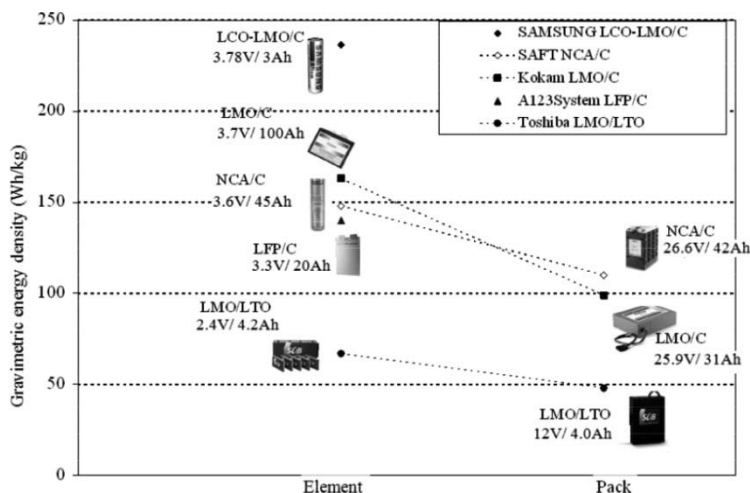


Figure 6.17. Gravimetric energy density: from the element to the pack

In spite of their small size, which means that the casing plays an important part, batteries for cellphones have high capacities (e.g. 190 Wh/kg) because they do not require any on-board electronics (there is only a temperature sensor) because there is no series connection of elements.

Remember that the theoretical gravimetric energy density for the C-LiCoO<sub>2</sub> element is 986 Wh/kg (section 6.1.2).

EXERCISE 6.2.– A portable computer battery pack commercialized in the 2,000 s comprises six 18650 Li-ion cells. The pack is specified as 11.1 V–3,600 mAh. Its volume is 312 cm<sup>3</sup>.

What is the amount of energy stored in this pack?

How are the cells interconnected electrically?

What is the capacity of each element?

The mass of an element is 40 g. What is the gravimetric energy density of a cell?



The total mass of the pack is 350 g. What is the gravimetric energy density of the pack?

In order to rationalize industrial-scale production, the same pack may contain nine 18650 Li-ion cells. In the six-cell assembly, the three absent cells are replaced by hollow tubes whose mass is 3.5 g. What is the gravimetric energy density of the nine-cell pack? How are the cells interconnected electrically?

*Solution page 231*

EXERCISE 6.3.– Thanks to progress, more recent portable computer battery packs integrated Li-ion cells, still in an 18650 format but of greater capacity: 2,350 and then 2,500 mAh. In the latter case, each cell weighs 46 g. The complete pack, still labeled as 11.1 V, has a mass of 350 g. Its volume is 168 cm<sup>3</sup>.

What is the amount of energy stored in such a pack?

What is the gravimetric energy density of a cell?

What is the gravimetric energy density of the pack?

*Solution page 232*

EXERCISE 6.4.– In 2010, a computer battery pack integrates nine Li-ion cells, still in an 18 650 format but with capacity 2,700 mAh. The complete pack, still labeled as 11.1 V, has a mass of 484 g. Its volume is 270 cm<sup>3</sup>.

What is the amount of energy stored in such a pack?

What is the gravimetric energy density of the pack?








What is the density of this pack?

*Solution page 232*

The solution of the exercises above demonstrates the significant evolution of gravimetric energy densities over those ten years: for an 11.1 V pack, the value rose from 114 to 186 Wh/kg, which represents a gain of over 60%.

### 6.2.14. Practical volumetric energy density

We shall look again at the same batteries to calculate their volumetric energy density (Table 6.12). The volumetric energy density of a cell is between 300 and 700 Wh/L for couples with a graphite negative electrode and approximately 130 Wh/L for LTO-LMO. Figure 6.18 shows how the volumetric energy density is more or less halved upon switching from a single cell to a module (or a pack).

| Technology   |              | Elements  | Modules   |
|--------------|--------------|---|---|
| SAFT         | Graphite-NCA |  3.6 V / 45 Ah:<br>304 Wh/L  |  21.6 V / 42 Ah:<br>158 Wh/L |
| Kokam        | Graphite-LMO |  3.7 V / 100 Ah:<br>355 Wh/L |  25.9 V / 31 Ah:<br>152 Wh/L |
| A123 Systems | Graphite-LFP |  3.3 V / 20 Ah:<br>315 Wh/L  | Not specified   |
| Toshiba      | LTO-LMO      |  2.4 V / 4.2 Ah:<br>132 Wh/L |  12 V / 4 Ah:<br>63 Wh/L     |

**Table 6.12.** *Volumetric energy density of elements and modules of different lithium-ion technologies*

**EXERCISE 6.5.**— What are the volumetric energy densities of the cells and packs for portable computers discussed in exercises 6.2 to 6.4?

*Solution page 233*

The solution to exercise 6.5 shows the substantial evolution of the volumetric energy density over those ten years: for an 18650 cell, the value has increased from 400 to 600 Wh/L, which is a proportion of 150%. In the same vein, for an 11.1 V pack, it increases from 114 to 186 Wh/kg. These values are higher than those quoted in Tables 6.11 and 6.12, because we have gone from dealing with a long-life industrial material to dealing with a material whose lifetime is much shorter (2–5 years).

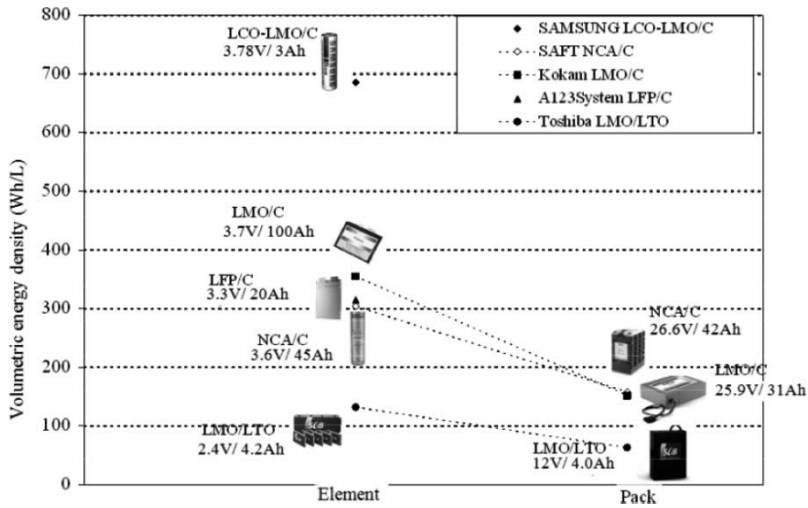


Figure 6.18. Volumetric energy density: from the element to the pack

#### 6.2.15. Plot of the gravimetric energy densities as a function of the volumetric energy densities

In order to compare lithium-ion technologies against older technologies (lead and nickel), we can represent the gravimetric energy density as a function of the volumetric energy density. This is what is done in Figure 6.19.

The plot shown in Figure 6.20 compares the specific energies of different technologies for portable or on-board applications. In this figure, we have deliberately chosen to consider only cylindrical batteries with a metal casing and a few amp-hours capacity so as not to skew the comparison by taking account of prism formats or envelope formats in a soft sachet. We can distinguish two ranges of lithium-ion batteries as a function of the nature of the materials used for the electrodes and the internal design which enables them to deliver energy (portable application) or power (HEV application). As a general rule, power-oriented elements are designed to provide high currents over short periods of time, whereas energy-oriented elements are not apt for delivering strong continuous currents. A Ragone plot (graphic representation of the gravimetric energy density versus the gravimetric power density, see sections 2.4.17 and 6.2.16) is easier to interpret on this point. However, such a plot is not easy to construct, because not all

manufacturers refer to the same testing procedure to characterize the power performances of their products (maximum current peaks over a predetermined time-period, maximum allowable current over a given range of SOC, etc.). Thus, unlike energy, power is not a characteristic which can be easily compared between batteries.

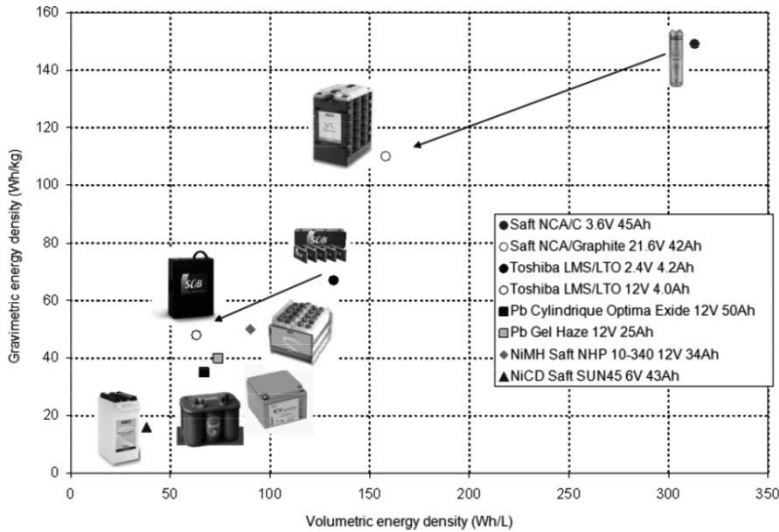


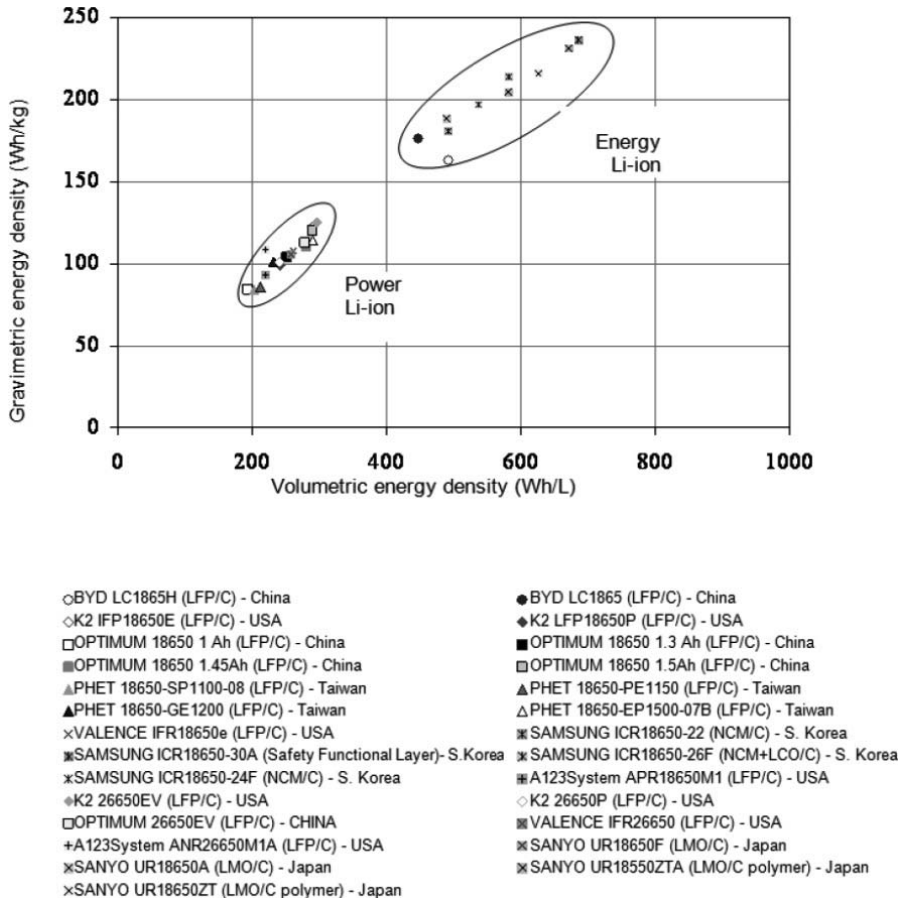
**Figure 6.19.** Comparison of technologies

We can consider that the electric vehicle (EV) application is on the boundary between a “power-oriented” and an “energy-oriented” application. Power is delivered in the form of peaks of current for a few seconds during the phases of acceleration or braking of the vehicle, but it is necessary to have sufficient energetic autonomy. For this type of application, the market is currently witnessing the apparition of elements with a prism format, which are easier to build into a pack and which have high capacities (e.g. Kokam 3.7 V–100 Ah or 123Systems 3.3 V–100 Ah).

#### 6.2.16. Gravimetric and volumetric power densities








Although this notion is more difficult to define, we can speak of a gravimetric power density, specifying the conditions of discharge in which that value was obtained. To date, no standard or specification prescribes

these test conditions, and it is therefore difficult to compare one technology to another. Table 6.13 quotes the data taken from the manufacturers' technical specifications for the models presented above. A123 Systems gives a far higher power value which is not comparable to the other models.



**Figure 6.20.** Gravimetric energy densities versus volumetric energy densities for different lithium-ion technologies

The same is true of the volumetric power density. The values given below are either calculated or read from the technical specifications where given. Once again, these values are difficult to compare because the conditions under which nominal power should be measured are not standardized.

| Technology   | Elements  | Packs  |
|--|---|--|
| SAFT Graphite-NCA<br>Pulses of 18 s (element) and 30 s (pack) – (50% DOD)  |  3.6 V / 45 Ah:<br>809 W/kg<br>1666 W/L  |  21.6 V / 42 Ah:<br>533 W/kg<br>753 W/L   |
| Kokam Graphite-LMO<br>Pulses at 3 C (element) and 10 C (pack)              |  3.7 V / 100 Ah:<br>478 W/kg<br>1042 W/L |  25.9 V / 31 Ah:<br>991 W/kg<br>151.7 W/L |
| A123 Systems Graphite-LFP/<br>HPPC <sup>28</sup> at 10 s (50 % SOC or DOD) |  3.3 V / 20 Ah:<br>3000 W/kg<br>6760 W/L | Not specified  |
| Toshiba LTO-LMO<br>Pulses at 6 C (0.3 s)                                   |  2.4 V / 4.2 Ah:<br>400 W/kg<br>784 W/L  |  12 V / 4 Ah:<br>300 W/kg<br>395 W/L      |

**Table 6.13.** Gravimetric and volumetric power densities

### 6.2.17. Faradaic efficiency of a charge/discharge cycle

After the first charge, carried out in the factory on the still-open element (i.e. before definitive sealing) – a charge which “shapes” the element<sup>29</sup> and during which we see gas releases relating to the formation of the SEI by electrochemical decomposition of the electrolyte – the faradaic efficiency (defined in section 2.5) of the lithium-ion technology is high. It should be noted that a value of faradaic efficiency needs to be quoted in combination with the experimental conditions in which it was measured (current strengths, temperature, range of SOC, charge protocol with or without application of the constant voltage phase, which is very important when the charge occurs with high current). At nominal currents, the faradaic efficiency of lithium-ion batteries is nearly 100% for charge/discharge cycles for which the current strengths and temperatures are identical during charge and discharge, for which the final SOC after a charge/discharge cycle is

<sup>28</sup> HPPC: Hybrid Pulse Power Characterization. The HPPC profile was designed to measure the aptitude for dynamic power during charge and discharge pulsed regimes.

<sup>29</sup> This is the activation phase, corresponding to the first charge/discharge cycles. An illustrative example of a similar nature is to be found in Figure 6.23.

identical to the initial SOC.<sup>30</sup> Such efficiency values of nearly 100% are possible only if there are no parasitic reactions – e.g. gas formation by electrolysis of water, which is unavoidable in any aqueous system (lead–acid, NiCd, NiMH, etc.), whose faradaic efficiencies will necessarily be lesser (often less or even a lot less than 90%).

However, the faradaic efficiency may decrease during the course of the life of a cell, because of the emergence of degradation phenomena, particularly relating to the passivation layer on the graphite electrode (such phenomena are described in section 6.2.21). This damage occurs by way of electrochemical reactions said to be irreversible, whereby electrons (and lithium ions) are consumed with no possibility of the reverse reaction occurring.

#### **6.2.18. Energy efficiency of a charge/discharge cycle**

The energy efficiency of a (repeated) charge/discharge cycle depends on the electrodes chosen and the operating conditions applied (current strengths, temperature, range of SOC, charging protocol with or without the application of the constant voltage phase), which therefore have to be specified when a value is quoted. In technologies using the mechanism of insertion or intercalation, it is high – around 95% for C-LiFePO<sub>4</sub> technologies, and 98% for C-Li(Co,Ni)O<sub>2</sub> in slow current regimes (C/10 during charge and discharge at 25°C) – because the faradaic efficiency is almost 100% and the voltage of the element, at a given SOC, is very similar during charge and discharge. We speak of a slight voltage hysteresis or a phenomenon of slight polarization<sup>31</sup>, linked only to the activation- and concentration overvoltages. This hysteresis relates to the nature of the mechanisms used by the lithium in electrode materials. It is very slight in insertion- or intercalation materials, because these mechanisms do not involve the breaking or forging of chemical bonds between atoms, but rather electrostatic interactions whereby lithium is inserted into or extracted from crystalline structures. This hysteresis appears to be lesser for C-Li(Co,Ni)O<sub>2</sub>

---

<sup>30</sup> Experimentally, we often find that the faradaic efficiency for a charge/discharge cycle is greater than 1. This is due to the fact that the conditions during charging and discharging are not perfectly identical. However, over a succession of several cycles, the average can of course not be greater than 1.

<sup>31</sup> Electrochemists use the term “polarization” to refer to this hysteresis, which is the difference in voltage between charge and discharge to a given SOC.

elements (Figure 6.22), which explains the fact that they have a greater energy efficiency than C-LiFePO<sub>4</sub> elements (Figure 6.21). The changes in voltage at a low SOC and a high SOC also have an impact on the final efficiencies. These values are valid for moderate regimes and temperatures. They are lower with strong currents (increase of the activation overvoltages) and at low temperature (increase of the concentration overvoltages) – conditions which degrade the internal resistance – but are unchanged throughout almost all the range of SOC.

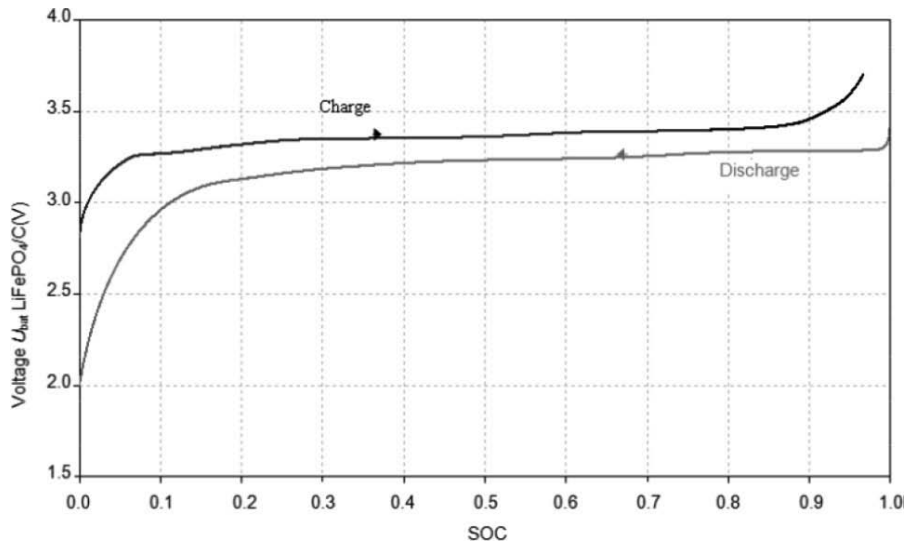


**Figure 6.21.** Voltage hysteresis between charge and discharge at constant current ( $C/10$  during both charge and discharge) of a 10 Ah C-LiFePO<sub>4</sub> element as a function of the SOC

For elements which employ the mechanism of conversion, the energy required to break and then reconstruct the covalent bonds during charge and discharge decreases the energy efficiency. From an electrical point of view, at a given SOC, the charge voltage is far greater than the discharge voltage, as is illustrated by Figure 6.23, which shows the first three cycles of a NiP<sub>3</sub> electrode in which lithium interacts by way of a conversion mechanism. The hysteresis cycle is much broader here because there is a rearrangement of the structure between the charged and discharged states.



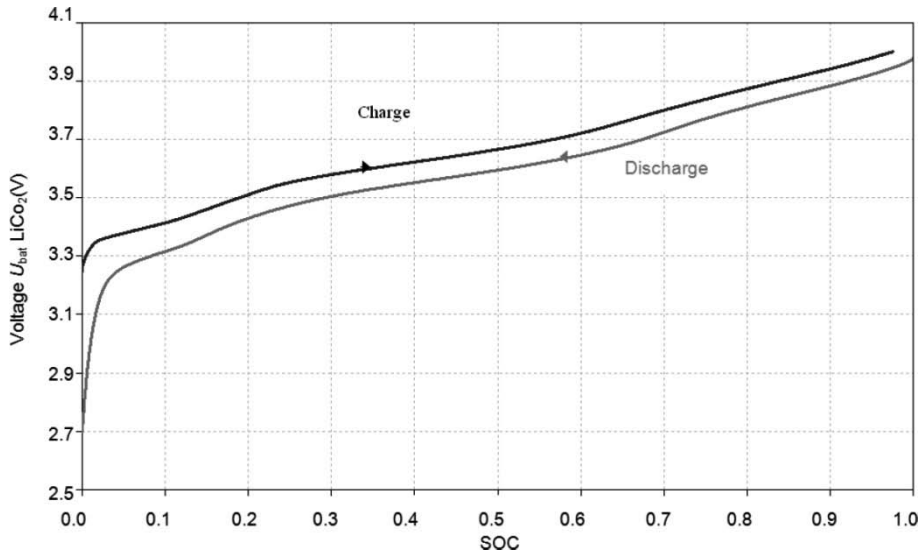


**Figure 6.22.** Voltage hysteresis between charge and discharge at constant current ( $C/10$  during both charge and discharge) of a 10 Ah C-LiCoO<sub>2</sub> element Ah as a function of the SOC

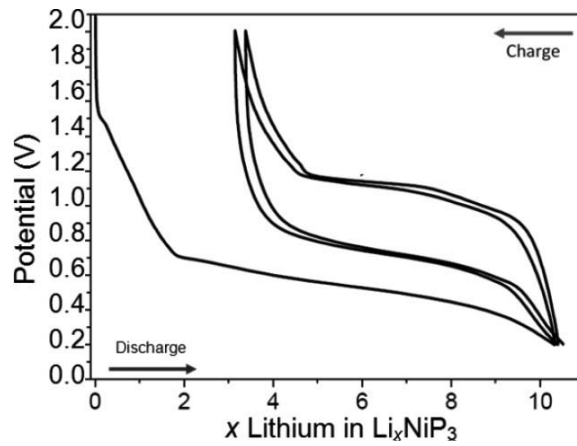


**Figure 6.23.** Profile of potential for the first cycles of a NiP<sub>3</sub> electrode with a current  $C$  versus metal lithium (instead of an SOC, electrochemists indicate the number of lithium ions inserted on the horizontal axis)<sup>32</sup>

32 A. SOARES, Batteries Lithium-ion, spécifiques pour le stockage de l'énergie photovoltaïque, Doctoral thesis, University of Montpellier II, 22 October 2012.

### 6.2.19. Average cycling lifetime

When manufacturers publish the cycling lifetimes of their products (usually determined by measuring the degradation of capacity), they specify the cycling conditions applied at 25°C (unless otherwise stated) and subjected to 1,000 cycles. A few examples are given in Table 6.14.

|         |   |
|---------|---|
| C-LFP   | A123 Systems (C during charge - C during discharge):<br>1000 cycles: 5% capacity lost<br>BYD (C during charge / C during discharge):<br>100% DOD: 23.75% capacity lost<br>PHET (5 C during charge / 10 C during discharge):<br>100% DOD: 12.5% capacity lost<br>VALENCE (8 C during discharge / C/2 during charge):<br>1000 cycles: 26% capacity lost |
| C-LMO   | KOKAM polymer (C during discharge / C during charge):<br>100% DOD: 12.5% capacity lost<br>80% DOD: 2.5% capacity lost<br>20% DOD: 1.7% capacity lost  |
| C-NMC   | SAMSUNG (0.5 C during charge / 1 C during discharge):<br>1000 cycles: 22.2 % capacity lost  |
| LTO-LMO | ALTAIRNANO (2 C during discharge / 6 C during charge):<br>100% DOD: 3.33% capacity lost   |

**Table 6.14.** *Degradation of capacity after 1000 cycles*

The temperature also influences the number of cycles delivered. We have recorded impacts on lifetime when the temperature exceeds 40–45°C, but these impacts are more or less marked depending on the technology and the manufacturer (Table 6.15).

### 6.2.20. Calendar lifetime

Batteries will also degrade even if they are not being used. This is known as calendar aging.

Although published data suggest that lithium-ion batteries, in principle, have calendar lifetimes of over 20 years, we are compelled to note that the

batteries used in mobile systems (cellphones and particularly portable computers) have a much shorter lifetime (2–5 years), often even in the absence of usage. This degradation could be due to insufficiently pure materials and/or insufficiently developed manufacturing conditions.

|                                   |      |  |
|-----------------------------------|------|--|
| C–LFP A123 Systems<br>1000 cycles | 25°C | C during charge - C during discharge:<br>5% capacity lost          |
|                                   | 45°C | 1.3 C during charge – 2.1 C during discharge:<br>10% capacity lost |
|                                   | 65°C | 1.3 C during charge – 2.1 C during discharge:<br>25% capacity lost |
| C–LFP Valence<br>500 cycles       | 25°C | C/2 during discharge / C/2 during charge:<br>22.7% capacity lost   |
|                                   | 45°C | C/2 during discharge / C/2 during charge:<br>24.2% capacity lost   |
|                                   | 60°C | C/2 during discharge / C/2 during charge:<br>93.8% capacity lost   |

**Table 6.15.** *Degradation of the cycling capacity on the basis of the testing temperatures*

More generally, we see aging of the interfaces, which is a slow but irreversible phenomenon that takes place during prolonged periods of storage. This aging occurs particularly at the interface between the lithiated negative electrode and the electrolyte. As previously indicated, this interface comprises a “passivation” film of both an organic and inorganic nature (formed during the first charge by electrochemical decomposition of the electrolyte (organic solvents + lithium salt). When fully charged, the lithiated negative electrode will experience a gradual self-discharge by slow extraction of the lithium, which reacts with the electrolyte as it diffuses through the SEI. The chemical composition of the SEI is altered, causing a progressive increase in the internal resistance of the battery, leading to the degradation of its performances. It is for this reason that it is advisable to leave a battery at rest in an intermediary SOC, so as to limit the reactions (slow but unavoidable) between the inserted lithium and the electrolyte. This is also the reason why, unlike lead–acid accumulators, when a new lithium battery is delivered it is not completely charged.

Figure 6.24 gives a quantified example of calendar aging and cycle aging for a C–Li(Co,Ni,Al)O<sub>2</sub> element. For the example of calendar aging, the

measuring conditions are: storage at 40°C in the fully-charged state with measurement of the capacity (by total discharge) every month, followed by restoration to the fully-charged state. For the example of cycle aging, the measuring conditions are: C/5 and then C/20 during charge and C/5 during discharge, with 50 cycles at 20°C followed by 50 cycles at 40°C. We can see that, in these test conditions, the part played by calendar aging (at 100% SOC) is greater than that played by cycle aging.

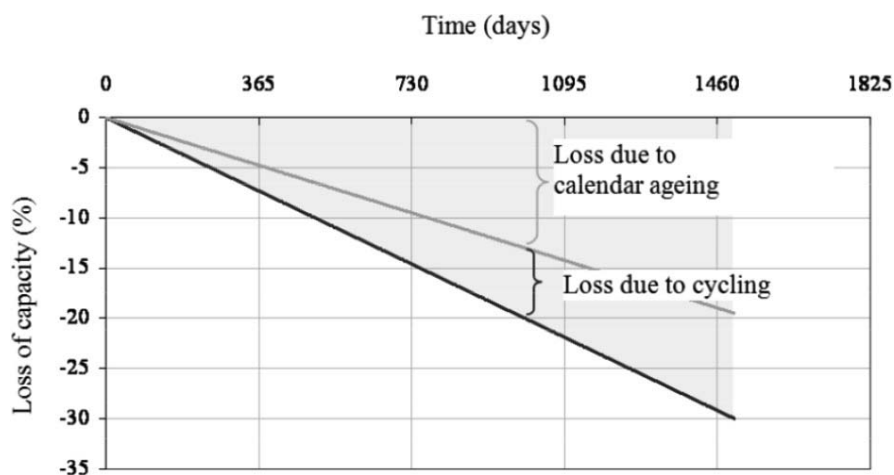


**Figure 6.24.** Degradation of capacity due to calendar ageing and cycle aging for C-Li(Co,Ni,Al)O<sub>2</sub> (C-NCA) elements

In a series of tests where C-LiCoO<sub>2</sub> cells were stored at 55°C and at different levels of charge for 100 days, Chinese researchers at the Shanghai Institute of Microsystem and Information Technology<sup>33</sup> showed that only the cell which was stored in the fully-discharged state was able to almost recover its initial capacity. The fully-discharged state, however, is not advisable for other technologies using manganese-based positive electrodes, because at this SOC, the electrode is in a delithiated state, which lends itself to the phenomenon of dissolution of the manganese, which diffuses through

<sup>33</sup> JIA LI, JIAN ZHANG, XIGUI ZHANG, CHUANZHENG YANG, NAIXIN XU, BAOJIA XI, "Study of the storage performance of a Li-ion cell at elevated temperature", *Electrochimica Acta*, 55, 927–934, 2010.

the separator and then poisons the carbon negative electrode<sup>34</sup>, thereby degrading the overall operation of the element.

When the technology is not explicitly specified (which is usual with “public consumption” batteries, it tends to be preferable to conserve a lithium-ion battery in neither a fully-charged nor fully-discharged state (where reactions that degrade the positive electrode and/or negative electrode may be prevalent), but rather in an intermediary SOC and at low temperature (given that all of the chemical or electrochemical phenomena discussed above are encouraged by high temperatures).

If a lithium battery has to be kept in an extreme SOC, it is preferable to store it in the discharged state, with the exception of batteries with manganese positive electrodes, for which the fully charged state is preferable.

The idea of an intermediary SOC runs counter to the conventional use of a portable computer, whereby the charger means that the battery is always charged to the maximum (so as to maximize the autonomy). In order to increase its lifetime, it would be better to operate it in cycles so it does not spend too long in a fully-charged state, which requires the device to be plugged in. Better still, it should be kept at an intermediary SOC when we know that we will not require autonomy in the near future, and then charge it fully only when we know that we will be for some time without another source of power. Thus, there is a compromise between aging by cycling and calendar aging which is attributable to the battery’s being kept in a charged state more often than not.

Finally, it is also better from a safety point of view to transport elements or batteries in an intermediary SOC. Indeed, this way the battery is less energetic and will therefore be less reactive if exposed to extreme abusive situations (piercing, crushing, severe thermal stresses, etc.) which might occur during these phases.

---

34 M. WOHLFAHRT-MEHRENS, C. VOGLER, J. GARCHE, “Aging mechanisms of lithium cathode materials”, *J. of Power Sources*, 127, 58–64, 2004.

### 6.2.21. Degradation phenomena

The loss of capacity of a lithium-ion battery based particularly on insertion materials at the electrodes is due to the combination of three main phenomena:

- decrease of the quantity of lithium exchanged between the electrodes, consumed by alteration of the composition or (re)formation of the SEI and by the deposition of metal lithium (a phenomenon known as “plating”) involving a decrease in the concentration of lithium salts. The irreversible consumption of lithium is also a phenomenon caused by the self-discharge of a charged element, because of reaction between the electrolyte and the lithium present in the graphite. This reactivity causes a decrease in the composition of the SEI, which becomes more resistive;
- degradation of the active materials in the electrodes: exfoliation (described in section 5.4.1) of the planar structures of the graphite, fracturing of particles by volumetric expansion or by gas emission, disordering of the crystalline arrangements, dissolution of metal cations;
- parasitic reactions: degradation of the polymer binder, local corrosion of the collector, contamination of the active sites.

These phenomena lead to changes in the surface properties of the components (electrodes and collectors), the exchange surfaces and an increase in the internal resistance of the cell. The increase in polarization because of the increase overvoltages and ohmic resistance of the element reduces the available capacity by preventing full discharge or full charge – all the more so with high current regimes.

Figure 6.25 gives a visual representation of these different mechanisms of degradation.<sup>35</sup>

---

<sup>35</sup> J. GROOT, State-of-Health Estimation of Li-ion Batteries: Cycle Life Test Methods, Division of Electric Power Engineering, Department of Energy and Environment, PhD thesis, Chalmers University of Technology, Gothenburg, Sweden, 2012.

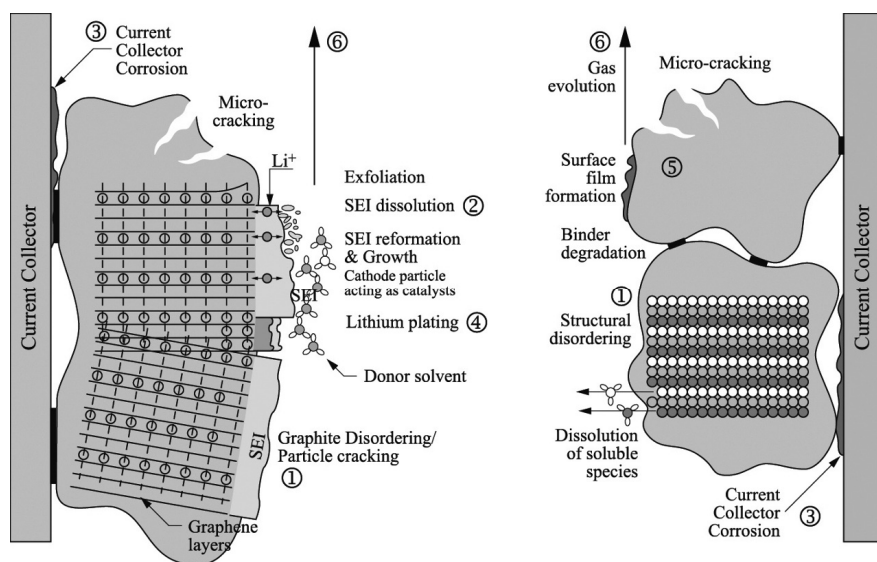


**Figure 6.25.** Diagrammatic representation of the phenomena of degradation in a lithium-ion battery<sup>35</sup>

Let us now go into greater detail about all of these mechanisms, which are mutually correlated – this makes it more complex to understand the mechanisms, their origin and how they work:

1) Damage to the crystalline structure: as described by many authors, including Vetter<sup>36</sup> and Broussely<sup>37</sup>, the intrinsic properties of the active materials do not change drastically over the course of the life of the cell, but aging does occur essentially on the surface of the particles, both with modifications to their structure and their electrochemical properties;

2) Formation and reformation of the SEI: the changes in the volume of the graphite particles (albeit very slight changes) with the insertions and extractions of lithium cause microcracking to occur in the SEI, exposing the lithiated graphite to the electrolyte, which leads to the formation of a “secondary” SEI. This occurs mainly when the depths of discharge (DODs)

36 J. VETTER, P. NOVAK, M.R. WAGNER, C. VEIT, K.-C. MOLLER, J.O. BESENHARD, M. WINTER, M. WOHLFAHRT-MEHRENS, C. VOGLER, A. HAMMOUCHE, “Ageing mechanisms in lithium-ion batteries”, *J. Power Sources*, 147, 269–281, 2005.

37 M. BROUSSELY, Ph. BIENSAN, F. BONHOMME, Ph. BLANCHARD, S. HERREYRE, K. NECHEV, R.J. STANIEWICZ, “Main aging mechanisms in Li ion batteries”, *J. Power Sources*, 146, 90–96, 2005.

are great, because the changes in volume are then maximal. This leads to the consumption of the lithium, and contributes to an imbalance of the electrochemical reactions between the electrodes.<sup>36</sup> Traces of contaminants in the electrolyte introduced during manufacture or resulting from dissolved species from the positive electrode (which is more susceptible to oxidation than the negative electrode at the end of charge of the element), may lead to the dissolution of the SEI by acting as catalysts (the SEI is unstable at the end of discharge of the element). The SEI is re-formed when the element is recharged, to the detriment of the lithium ions available;

3) Corrosion of the collectors, engendered in particular by the presence of water. This contaminant can react with the lithium salt  $\text{LiPF}_6$  to form hydrofluoric acid (HF), which is highly corrosive, and which can damage metallic collectors:



Corrosion of the collectors is also possible when the potential of the cell surpasses the window of potential determined by the choice of the materials.<sup>38</sup>

4) Lithium plating: deposits of metal lithium may occur on the surface of the graphite particles when they are locally taken to low potentials (lower than 0 V versus  $\text{Li/Li}^+$ ). The lithium atoms form metal lithium instead of being intercalated into the graphite matrix. The reaction is not entirely reversible, because lithium can react to form oxides. This phenomenon is more pronounced at low temperature, with a high charge current and if the capacity of the negative electrode decreases as it becomes degraded, ultimately becoming less than that of the positive electrode.<sup>39</sup>

5) Migration of species from one electrode to the other: the secondary reactions at the electrodes upon excessive charging or excessive discharging may lead to the formation of electrolyte-soluble species, which migrate from

---

38 X. ZHANG, B. WINGET, M. DOEFF, J. W. EVANS, T. M. DEVINE, "Corrosion of Aluminium Current Collectors in Lithium-Ion Batteries with Electrolytes Containing  $\text{LiPF}_6$ ", *J. The Electrochemical Society*, 152, B448–B454, 2005.

39 S.S. ZHANG, K. XU, T.R. JOW, "Study of the charging process of a  $\text{LiCoO}_2$ -based Li-ion battery", *J. Power Sources*, 160, 1349–1354, 2006.



one electrode to the other. The dissolved species may undergo reduction and produce additional surface layers.<sup>40</sup>

6) Gas formation: the formation of gases may occur as the product of the secondary reactions mentioned above: dissolution/re-formation of the SEI, corrosion of the collectors, migration of the products of reduction of the electrolyte from the negative electrode to the positive electrode, where they react to form passivation layers and gases are given off as the product of that reaction. The gas formed can increase the mechanical stress to which the electrodes are subject, and in the case of the negative electrode, can accelerate the reactions relating to the re-formation of the SEI. The gas trapped in the pores of the active material can also reduce the specific active surface area of the electrode.

Thus, these phenomena of degradation will be limited or encouraged depending on the usage profiles (thresholds of charge- and discharge voltage, current strengths, DODs, operating temperature) but also on the very design of the cell (purity of the components, ratio of capacity between the electrodes).

#### **6.2.22. Operational safety**

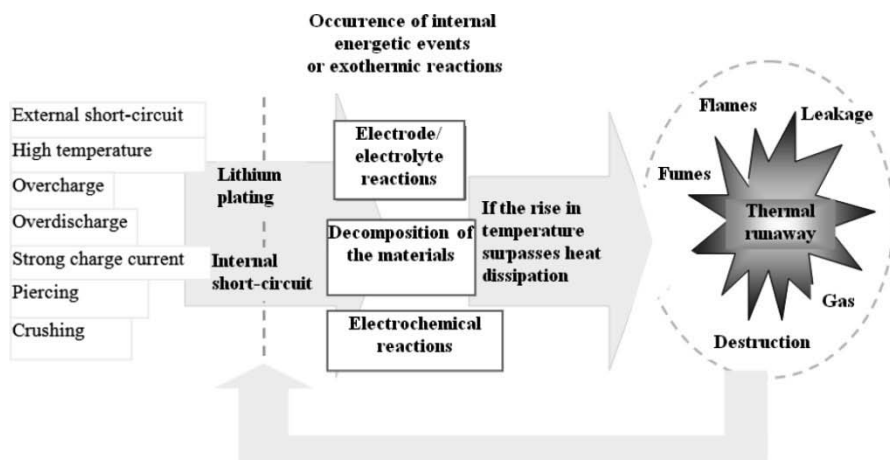
Today, the weak point which is preventing the introduction of this technology in high-energy stationary or on-board applications is its lack of tolerance to abusive operation (such as over-charging or high temperatures), which renders the battery particularly vulnerable to dangers of thermal runaway, which can cause fire and even – in extreme cases – explosions.

Figure 6.26 shows the abusive conditions which can lead to thermal runaway in a lithium-ion battery.<sup>41</sup>

---

40 J.H. ZHENG, Q. SUN, G. LIU, X. SONG, V.S. BATTAGLI, J. “Correlation between dissolution behavior and electrochemical cycling performance for  $\text{LiNi}_{1/3}\text{Co}_{1/3}\text{Mn}_{1/3}\text{O}_2$ -based cells”, *Power Sources*, 207, 134–140, 2012.

41 K. GI-HEON, A. PESARAN “Analysis of Heat Dissipation in Li-Ion Cells & Modules for Modeling of Thermal Runaway”, *The 3rd International Symposium on Large Lithium Ion Battery Technology and Application*, Long Beach, California, 2007.



**Figure 6.26.** Extreme situations which can cause thermal runaway  
(taken from Heon and Pesaran<sup>41</sup>)

Energy management, balancing between the elements making up the battery and heat management therefore have to be perfectly performed. With a significant excess charge, the risk of dangerous phenomena is more marked in the presence of  $\text{LiCoO}_2$  positive materials because with the extensive extraction of lithium from the material, as discussed in section 5.3.1, there is a “subsidence” of the octahedral lamellar structure with the release of oxygen. This newly-formed oxygen violently oxidizes the organic solvents. These solvents (which have a low boiling point, a high saturating vapor voltage and a low flash point) evaporate suddenly, causing an increase of the internal pressure, which can give rise to the explosion of the external casing of the element. On the negative side, lithium can be deposited in metal form on the surface of the graphite. This deposition causes a loss of capacity by loss of the lithium, which is deposited in a very heterogeneous manner and becomes electrochemically unusable.

It should be noted that this danger of deposition of metal lithium on the carbon electrode may also arise in case of charging with very high current, beyond the specifications quoted by the manufacturer. Under such charge currents, the lithium ions are inserted too slowly between the graphene layers, and accumulate on the surface of the grains of carbon, where electrochemical plating of metallic lithium can occur. This phenomenon causes the irreversible reduction of the lithium ions with a corresponding

drop in capacity, with the deposition occurring in a heterogeneous, dendritic manner (see section 4.4.2). In extreme cases, this phenomenon may cause an internal short-circuit.

Lithium ferrophosphate  $\text{Li}_{(1-x)}\text{FePO}_4$  is more stable when faced with abusive situations such as excessive charge (the fully-oxidized form  $\text{FePO}_4$  is perfectly stable) or exposed to high temperatures. Unlike other blended oxides<sup>42</sup>, oxygen cannot react with the organic solvents or cause the sudden oxidation of the aluminum present. It is for this reason that  $\text{LiFePO}_4$  is used for high-capacity batteries, because its intrinsic safety is much better.

On the other hand, excessive discharge (range of voltage less than 2.0 V) does not cause exothermic reactions which are likely to give rise to thermal runaway; however, it does lead to the irreversible degradation of the element. The phenomena cited most frequently occur at the negative electrode with the decomposition of the SEI and corrosion of the copper collector. Recharging restores the potential to the normal range of operation, but the re-formation of the SEI consumes lithium (again irreversibly), and the copper ions present in the electrolyte undergo a reduction reaction on the electrode, thus poisoning it.

These undesirable reactions take place outside of the domain of electrochemical stability of the element, and are described in Figure 6.27.

In case of an increase in operating temperature with a strong current or because of poorly-controlled or uncontrolled environmental conditions, the phenomenon leading to thermal runaway is linked primarily to the decomposition of the SEI of the lithiated carbon electrode, leaving exposed the electrode, which decomposes by reaction between the inserted lithium and the electrolyte. Gas formation occurs, once again leading to an increase in the internal pressure of the element.

### **6.2.23. Transport and storage of lithium batteries**

The very high reactivity of lithium, particularly with humidity from the air and with water, means caution must be exercised when transporting it.

---

<sup>42</sup> As is the case, for instance, in cobalt C- $\text{LiCoO}_2$  elements, an excessive discharge leads to the oversaturation of the LCO, which decomposes to produce lithium oxide  $\text{Li}_2\text{O}$  and cobalt oxide  $\text{CoO}$ .

There are very strict international regulations<sup>43</sup> surrounding land, air or maritime transport of lithium-ion secondary batteries but also metal-lithium secondary batteries or even lithium primary batteries (which contain metal lithium).

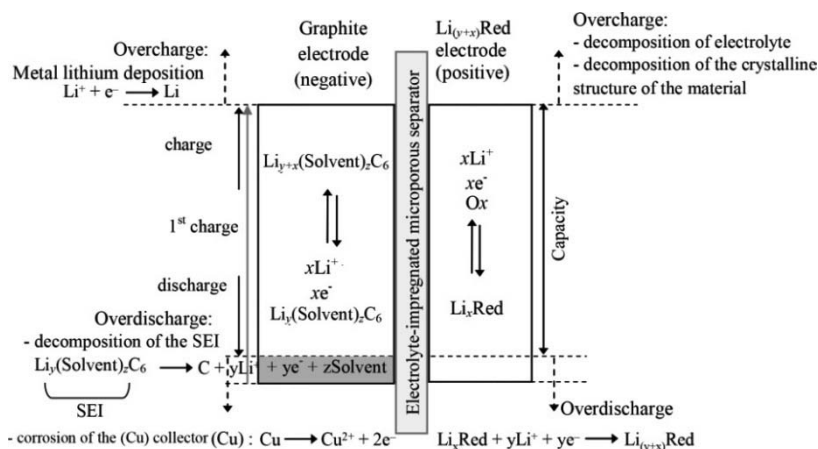


**Figure 6.27.** Domain of electrochemical instability of a lithium-ion battery for a C-LiCoO<sub>2</sub> electrochemical couple

While no particular precaution needs to be taken when taking a battery of less than 96 Wh capacity on a flight in one's laptop, limitations apply when transporting spare batteries or more generally any lithium batteries outside of the devices to which they belong. In these cases it is necessary to package them in such a way that no short-circuit can occur (individual packaging, solid packaging, etc.). If more than a certain quantity of batteries is being transported, specific labels need to be displayed on the packaging.

In the same vein, the storage of lithium-based primary and secondary cells with a view to recycling must be done so that there is absolutely no danger of contact between the terminals of the elements, which could cause intense currents and, consequently, an increase in temperature with the risk of fire and/or explosion.

In case of fire, it is preferable to use CO<sub>2</sub> or argonite extinguishers.

<sup>43</sup> These regulations continue to evolve over time. It is helpful to refer to whatever regulation is in force at the time of transport. The latest update came into force on 1 January 2013. The applicable conditions are displayed, among other places, at the premises of transport contractors (TNT®, UPS®, Chronopost®, etc.) or of battery manufacturers.

### 6.2.24. Packaging

Lithium-ion batteries are available in different formats:

- “coin cell” elements, examples of which are presented in Figure 6.28;
- rolled elements (with rolled electrodes) in a rigid metal casing of aluminum or stainless steel as presented in Figure 6.29 or in a soft sachet;
- “stacked” elements (with the electrodes stacked on top of one another), usually in a soft casing (as opposed to a hard casing) as presented in Figure 6.30. A hard casing can also be used, but is less common.

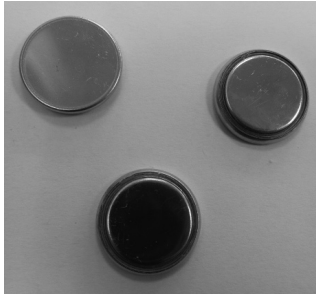


**Figure 6.28.** “Coin cell”-type elements (source: CEA)



**Figure 6.29.** Rolled element (source: CEA)

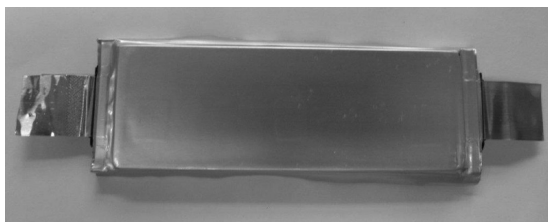


**Figure 6.30.** “Stacked” element (source CEA)

The sachet used to contain the element is schematically composed of two external layers of polymer (polyamide and polypropylene), ensuring both internal and external electrical insulation of the element, and a metal aluminum foil as represented in Figure 6.31. The name usually given to elements in a soft sachet is a “pouch-cell”. As the melting point of the polymer on the internal surface is lower than that of the external polymer, the system can be sealed by the melting of the internal polymer.

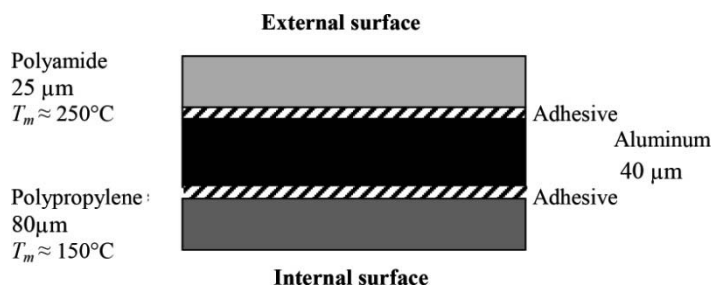


**Figure 6.31.** Schematic makeup of the soft pouch

### 6.2.25. Manufacturing procedures

The manufacture of a lithium-ion battery occurs by a succession of stages as described below. The photos below show pre-industrial or industrial equipment.

#### 6.2.25.1. Powder synthesis phase

Various chemical approaches are used to synthesize powders of active material, even on a nanometric scale. The different materials used are first milled to their optimal particle size distribution (PSD) (e.g. using a pin sand mill such as that shown in Figure 6.32) and then subjected to a heat

treatment. There are also other methods of synthesis, such as CVD<sup>44</sup>, for instance.

Thus, for a cell, we obtain two groups of powders – one group for the negative electrode and the other for the positive electrode.

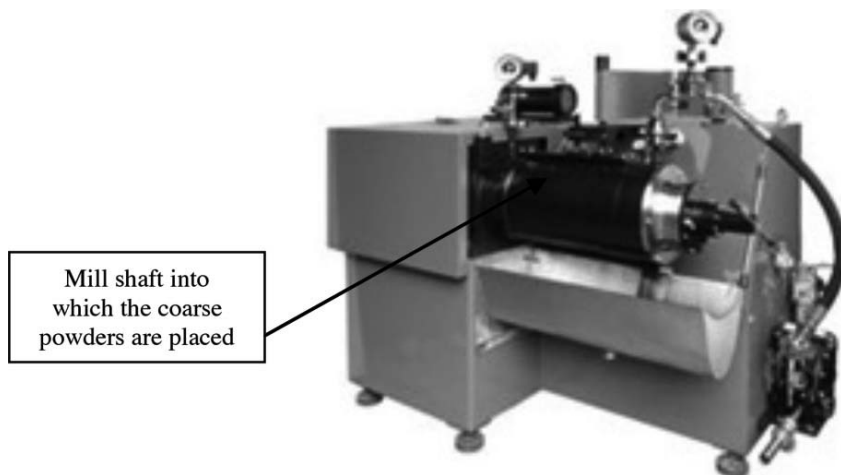


**Figure 6.32.** Pin sand mill for powder manufacture  
(source Sower Group: [www.sowergroup.com](http://www.sowergroup.com))

#### 6.2.25.2. Creation of an ink

The powders, called the “active materials”, are dispersed in a solvent – usually organic (syntheses in an aqueous medium are used today). Then, we add conductive agents (carbon) and a “binder” (usually a polymer) to plasticize the electrode so it can be handled and will absorb the electrolyte (the polymer swells up on contact with the electrolyte) – in the proportion of 4–8% of the mass of the final electrode (with 92–96% being accounted for by the active materials). The solution has the consistency of an ink.

The mixing of the active powders, the electronic conductive carbon and the polymer binder dissolved in a solvent is done by a planetary mixer (Figure 6.33).

---

<sup>44</sup> CVD: Chemical Vapor Deposition, whereby thin films are formed from gases in a vacuum.

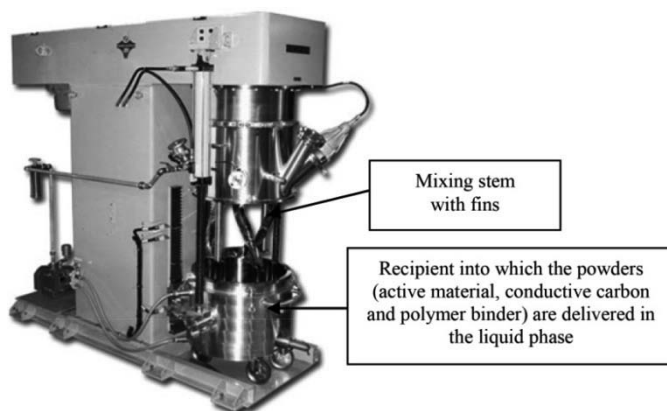


**Figure 6.33.** Planetary mixer (source Texmac: [www.texmac.com](http://www.texmac.com))

#### 6.2.25.3. Deposition of the ink on the current collector

The ink is deposited on the copper or aluminum foils (which serve as a mechanical support and as a current collector) by conventional coating (Figure 6.34) or by other printing techniques (flexography, gravure printing, silkscreen printing, etc.). As happens in the printing industry, the deposition is done by rollers covered with the ink. After passage through a continuous drying tunnel, we obtain a dry electrode roller (the solvent has evaporated).

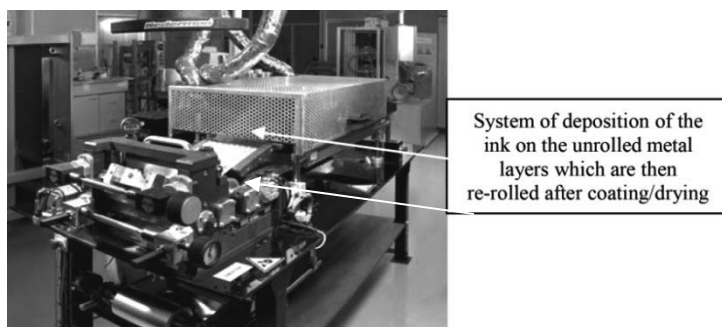


**Figure 6.34.** Coating machine (source Texmac: [www.texmac.com](http://www.texmac.com))

The porosity of the electrode is too significant for the expected electrochemical reactions (it is necessary to find a compromise between sufficient porosity for a large reactional interface surface area and good contact between the particles). The strip of electrode is therefore



compressed, decreasing from 70% to 20–40% porosity, by a process known as “roll pressing” (Figure 6.35).

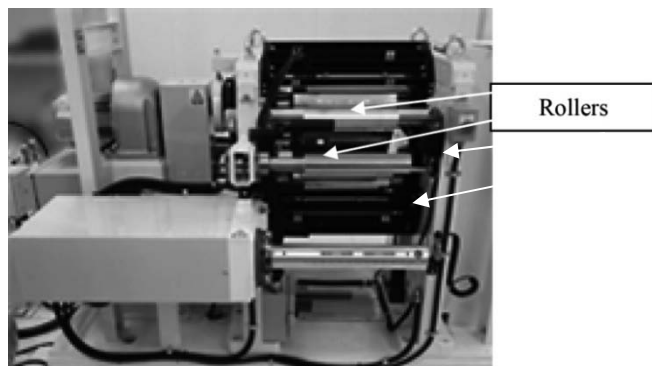


**Figure 6.35.** Roll press machine (source: [www.libtec.or.jp](http://www.libtec.or.jp))

#### 6.2.25.4. *Shaping of the electrode*

When the ink was deposited on the current collectors, the ends of the strip remained bare. Divided lengthwise, they constitute the electrode, with one end performing the role of a collector. The electrode is then wound onto a roll (for cylindrical cells). This task is done by machines called jelly-roll winders (see Figure 6.36). The width of the electrode strip corresponds to the height of the final electrode. It should be noted that cells can also be made in a “stacked” format or, in particular for electric vehicles, in “stacked prismatic cells”. The whole thing is then inserted into a rigid casing soldered shut by a laser or into a heat-sealed soft pouch. All shapes and sizes are envisageable.

#### 6.2.25.5. *Introduction of the electrolyte*

The liquid electrolyte is introduced through an orifice present in the casing or at one of the edges (not yet sealed). This is called the “activation stage”. The electrolyte impregnates the electrodes and the separator: it infiltrates the pores of the material and the separator. In a cell weighing around 100 g, the electrolyte accounts for around 20 g (Table 6.5). In the case of lithium-ion batteries, the lithium-salt-based electrolyte is very sensitive to humidity. Not a single molecule of water must be present, so as to prevent the formation of acid in the element by reaction with the lithium salt (e.g. by the following reaction:  $\text{LiPF}_6 + \text{H}_2\text{O} \rightarrow 2\text{HF} + \text{POF}_3 + \text{LiF}$ ). The

operation is therefore carried out in a so-called “anhydrous or dry room” (i.e. with no humidity), where the quality of the ambient air is controlled, or, in a laboratory, in a glovebox. Specific semi-automatic or automatic *electrolyte filling machines* are used.



**Figure 6.36.** Jelly-roll winder for cylindrical cells (source: CEA)

#### 6.2.25.6. Activation

As with any commercialized battery, a stage of “electrical activation or formation” must take place (Figure 6.37): a charge/discharge cycle is performed in particular conditions which guarantee its optimal operation. The element is then hermetically sealed.

#### 6.2.26. Energy cost throughout lifecycle

An evaluation of embodied energy<sup>45</sup> was published by two Swedish researchers, C. J. Rydh and B. A. Sandén<sup>46</sup>, on SAFT lithium-ion VL50 E

---

<sup>45</sup> Embodied energy is the sum of all the energy needed from the manufacture of a product to its dismantling, including the energy necessary for its operation. This notion of the energy expended throughout the lifecycle therefore includes the energy needs for raw material extraction, transformation, transport, production, manufacture, implementation, etc. – for the product itself, for its constituent materials but also for those materials necessary during its usage and upkeep, and then, at end-of-life, the energy required for its deconstruction and recycling.

<sup>46</sup> C.J. RYDH and B.A. SANDÉN. “Energy analysis of batteries in photovoltaic systems. Part 1: Performance and energy requirement”, *Energy Conversion and Management*, vol.46: 1957–1979, 2005. Cited in Yaël THIAUX, Optimisation des profils de consommation pour minimiser les coûts économique et énergétique sur cycle de vie des systèmes photovoltaïques autonomes et hybrides. Évaluation de la technologie Li-ion, Doctoral thesis, École Normale Supérieure de Cachan, 8 July 2010.

batteries (with C and NCA electrodes) in the context of a photovoltaic application.

The hypotheses taken into account are:

- gravimetric energy density of 120 Wh/kg;
- transport by truck over 3,000 km;
- self-discharge is not considered;
- the overall efficiency of the energy mix of electricity production for manufacture is 35%;
- when they have lost 20% of their capacity, the batteries are declared to be at end-of-life (EOL) and are sent back by truck over the 3,000 km distance, but the materials are not re-used.

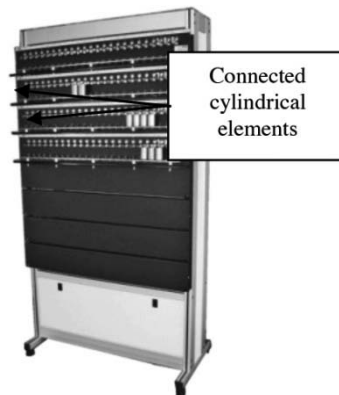


**Figure 6.37.** Training machine (source Pec: [www.peccorp.com](http://www.peccorp.com))

The authors then calculate the primary energy requirement for the construction and transport of the battery; they give it as being 520 kWh of primary energy per kWh of battery capacity.

It is interesting to compare this energy with the amount that said battery would store/deliver over the duration of its lifetime. For instance, for 2,000 cycles with a DOD of 80%, the battery will have exchanged 1,600 kWh electric (4,128 kWh of primary energy if we take the coefficient of primary-to-final energy conversion to be 2.58, which is the value used in France) and consumed 520 kWh of embodied (primary) energy.

### **6.2.27. Purchasing cost**

The cost of manufacture and therefore sale of small lithium-ion batteries is, as yet, high – approximately €2000/kWh. For this reason, in spite of their undeniable qualities, lithium-ion ion batteries are not yet universally employed in portable applications. They are essentially present in technological applications (multimedia, communications tools), where cost is not a crucially important factor. However, such a cost is not suitable for an electric vehicle application, for which it is imperative to drive costs down. It is estimated that the cost of a  $\text{LiFePO}_4$ -based battery needs to drop below €500/kWh, and even tend toward €250/kWh in order to attain such a market. With the pressing demand from vehicle manufacturers and the increased volume, even now we can predict that the costs will go down during the first ten years of commercialization (which is a natural phenomenon for any technological novelty). Today, the purchasing cost is around €2000/kWh for small units for portable devices and €1000–1500/kWh for higher-capacity elements (with the exception of manufacturers in China). We shall quite deliberately distinguish the costs of Chinese-made batteries from those made in other countries in Asia (Taiwan, Japan, South Korea), in the USA or in Europe, because of the significant disparity observed in price. For batteries made outside of China, we see an average cost of €1250/kWh, whereas for Chinese-made batteries the cost is €400/kWh, which represents a cost three times lower for elements with capacities greater than 10 Ah. The tendency toward an increased capacity of the elements manufactured is driven by the requirements of electric vehicle applications and stationary applications.

### **6.2.28. Manufacturers and suppliers/integrators**

The number of manufacturers of lithium-ion elements or batteries in the world is constantly evolving. It is impossible to establish an exhaustive list of these manufacturers unless we exclude new Chinese companies, which have an increasing presence in the market. As it is very difficult to classify these companies by their corporate turnover, we have chosen to classify them by continent (North America, Europe, Asia) and in alphabetical order. Below, we list some of the actors in the manufacturing process (manufacturers and suppliers/integrators) for lithium-ion batteries:

**North America:** A123 Systems (USA, China), ATB (USA), Dow Kokam<sup>47</sup> (USA), Gaia (USA), MAGNA (Canada), Saft (USA, France), Valence (USA), etc.

**Europe:** Evonik (Germany), OMT (Germany), Saft (France, USA), Sunlight Systems S.A (military and submarine batteries, Greece), etc.

**Asia:** AESC (formed by the merger of NEC and NISSAN, Japan), ATL “Amperex Technology Limited” (China), BAK (China), BMI “Battery Manufacturer’s International” (China & Taiwan), BYD<sup>48</sup> (China), E-One Moli Energy Corp. (Taiwan, Canada), ENAX (Japan), Hitachi (Japan), Kokam (South Korea), LG Chem (South Korea), Lischen (China), Maxell (Japan), MBI “Matsushita Battery Industrial” (Japan), NEC (Japan), Panasonic (Japan), PEVE “Primearth EV Energy Co. Ltd” (Japan), PHET “Pihsiang Energy Technology Co. Ltd.”, (Taiwan), Samsung SDI (South Korea), Sanyo (Japan), Sony (Japan), Toshiba (Japan), Yuasa (Japan), etc.

As we can see, the majority of lithium-ion battery production is located in Asia.

### 6.2.29. *Main outlets*

In 2012, the main outlet for lithium-ion batteries, both in terms of number of units sold and turnover, was still cellphones, followed by portable computers. Lithium-ion batteries have also built up a significant presence in digital cameras and camcorders, audio and video players, games consoles, PDAs, etc. In addition, they are increasingly to be found in portable electric tools. Electric vehicles, if they develop as they are currently predicted to, will ultimately come to represent the dominant market. The more distant future should see the development of the market of batteries for grid support. LiPo batteries are primarily used in model-making and in EAPCs, etc.

---

<sup>47</sup> Groupe Industriel Marcel Dassault – France – is one of the three founding partners that set up DOW KOKAM in 2009. Société de Véhicules Électriques (SVE) created by Dassault in 2002 is now the French chapter of Dow Kokam.

<sup>48</sup> BYD is the acronym for “Build Your Dreams”. This company, founded in 1995, has become a world leader in the field of lithium-ion batteries, with a 30% market share.

### 6.2.30. Recycling options

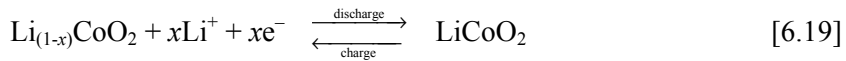
Channels for recycling develop at the same rate as products that need to be recycled. In France, we can cite SNAM (whose site in Viviez near to Rodez in Aveyron produces 300 tons of cobalt derivatives per year, RECUPYL and EURO DIEUZE (with 50% recycling and value creation).

## 6.3. Solution to exercises from Chapter 6

### *Solution to exercise 6.1: Calculation of the theoretical gravimetric capacity and gravimetric energy density of a $\text{Li}_{(1-x)}\text{C}_6\text{-LiCoO}_2$ element*

Let us approach this problem half-reaction by half-reaction:

For the positive electrode, the reaction to take into account is [6.4]:



We know (from section 5.3.1) that for this type of electrode, we must not exceed  $x = 0.5$  for fear of disintegration of the structure. The theoretical gravimetric capacity is therefore:

$$C_{\text{m.th}} = \frac{0.5}{6.9 \times 58.9 + 16 \times 2} \times 26801 = 137 \text{ mAh/g} \quad [6.20]$$

For the negative electrode, the reaction to take into account is [6.5]:



For complete extraction of the inserted lithium, we have  $x = 1$ , with 1 electron exchanged:

$$C_{\text{m.th}} = \frac{1}{6 \times 12} \times 26801 = 372 \text{ mAh/g} \quad [6.22]$$

Considering 100 g of negative material, the capacity of the electrode is 37.2 Ah. This capacity must correspond to the usable capacity of the positive material. The mass of the positive material is therefore equal to  $37.2 \text{ Ah} / 0.137 \text{ Ah/g} = 271.5 \text{ g}$ .

Note that in order to limit the extraction of lithium to  $x=0.5$  in the lithiated cobalt oxide positive electrode, this electrode needs to be oversized in terms of mass.

The theoretical gravimetric energy density for the active material alone is therefore:

$$C_{m.th} = \frac{372 \times 100}{100 + 271.5} = 100 \text{ mAh/g} \quad [6.23]$$

With an average discharge voltage of 3.8 V, the theoretical gravimetric energy density for the active material alone is therefore equal to:

$$W_{m.th} = C_{m.th} \times U_{nom} = 100 \times 3.8 = 380 \text{ mWh/g} = 380 \text{ Wh/kg} \quad [6.24]$$

This value cannot be achieved in practice, because the masses of the electrolyte, the copper collectors on the negative side and the aluminum collectors on the positive side, the external casing (the aluminum metal casing or, to a lesser extent, the soft sachet) reduce this value, which today, on the scale of the element, is 190 Wh/kg.

### ***Solution to exercise 6.2***

The energy stored in a portable computer battery pack notated 11.1 V–3,600 mAh is  $3.6 \text{ Ah} \times 11.1 \text{ V} = 40 \text{ Wh}$ .

A voltage of 11.1 V indicates that there are three cells in series ( $11.1/3 = 3.7$ ). Three assemblies of two cells in parallel are connected in series so that the electronics can measure the voltage of each parallel block of cells (Figure 6.38).

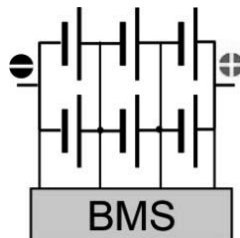


**Figure 6.38.** *Interconnection of the cells to one another and to the BMS*

Given that the current divides into two branches, the capacity of each element is  $3,600 \text{ mAh}/2 = 1,800 \text{ mAh}$ .

The gravimetric energy density of a  $3.7 \text{ V} - 1,800 \text{ mAh}$  cell with a mass of  $40 \text{ g}$  is  $1.8 \text{ Ah} \times 3.7 \text{ V}/0.04 \text{ kg}$  which is  $167 \text{ Wh/kg}$ .

The gravimetric energy density of an  $11.1 \text{ V} - 3,600 \text{ mAh}$  pack with a mass of  $350 \text{ g}$  is  $3.6 \text{ Ah} \times 11.1 \text{ V}/0.35 \text{ kg} = 114 \text{ Wh/kg}$ .

The mass of the nine-cell pack will be  $350 \text{ g}$ , to which we need to add three cells of  $40 \text{ g}$  each and take away three tubes of  $3.5 \text{ g}$  each. This gives us  $459.5 \text{ g}$ . The gravimetric energy density of the nine-cell pack is therefore  $3.6 \text{ Ah} \times (9/6) \times 11.1 \text{ V}/0.46 \text{ kg}$ , which is  $130 \text{ Wh/kg}$ .

### ***Solution to exercise 6.3***

A voltage of  $11.1 \text{ V}$  indicates that there are three cells in series ( $11.1/3 = 3.7$ ). Given the respective masses of a cell and the battery, we conclude that there are six cells ( $350/46 = 7.6$ ). The energy stored in this pack is therefore  $11.1 \text{ V}/3 \times 6 \times 2.5 \text{ Ah}$  or  $55.5 \text{ Wh}$ .

The gravimetric energy density of a  $3.7 \text{ V} - 2,500 \text{ mAh}$  cell with a mass of  $46 \text{ g}$  is  $2.5 \text{ Ah} \times 3.7 \text{ V}/0.046 \text{ kg}$  or  $200 \text{ Wh/kg}$ .

The gravimetric energy density of the pack is  $55.5 \text{ Wh}/0.35 \text{ kg} = 159 \text{ Wh/kg}$ .

### ***Solution to exercise 6.4***

A voltage of  $11.1 \text{ V}$  indicates that there are three cells in series ( $11.1/3 = 3.7$ ). The energy stored in this pack is therefore  $11.1 \text{ V}/3 \times 9 \times 2.7 \text{ Ah}$ , so  $90 \text{ Wh}$ .

The gravimetric energy density of the pack is  $11.1 \text{ V}/3 \times 9 \times 2.7/0.484 \text{ kg} = 186 \text{ Wh/kg}$ .

The density of this pack is  $0.484/0.270 = 1.79 \text{ kg/dm}^3$ .



***Solution to exercise 6.5***

The volume of a cell is  $(\pi \cdot 18^2/4) \times 65 \text{ mm}^3$ , which is  $16.54 \text{ cm}^3$ .

The volumetric energy density stored in each of the cells mentioned is:

|  |      |      |      |      |
|--|------|------|------|------|
| Capacity (mAh)                           | 1800 | 2350 | 2500 | 2700 |
| Energy for 3.7 V (Wh)                    | 6.66 | 8.70 | 9.25 | 9.99 |
| Volumetric energy density for 3 V (Wh/L) | 403  | 526  | 559  | 604  |

The volumetric energy density stored in each of the packs cited is:

|                                  |         |         |         |         |
|----------------------------------|---------|---------|---------|---------|
| Pack                             | 6 cells | 9 cells | 6 cells | 9 cells |
| Capacity (mAh)                   | 3600    | 5400    | 5000    | 8100    |
| Volume ( $\text{cm}^3$ )         | 312     | 312     | 168     | 270     |
| Energy for 11.1 V (Wh)           | 40.0    | 59.9    | 55.5    | 89.9    |
| Volumetric energy density (Wh/L) | 128     | 192     | 330     | 333     |



## Chapter 7

# Present and Future Developments Regarding Lithium-ion Batteries<sup>1</sup>

In this chapter, we shall give some examples of current and future avenues for development of lithium-ion technologies.<sup>2</sup> We have classified these into three categories:

- developments relating to improvement of the operation and safety of present technologies, either commercialized or close to being commercialized for applications on the rise such as electric mobility and grid support;
- developments relating to improvement of the future intrinsic performances of the battery, based on the use of new active materials, new morphologies of active particles or indeed the internal design;
- developments regarding new formats of batteries, aimed at opening the technology up to new applications, such as medical or micro-technological applications.

---

<sup>1</sup> Heartfelt thanks go to Sébastien Patoux, researcher at the CEA and head of the *Laboratoire des Matériaux pour Batteries* for having attentively read through this chapter.

<sup>2</sup> B. SCROSATI, J. GARCHE, “Lithium batteries: Status, prospects and future”, *J. of Power Sources*, 195, 2419–2430, 2010.

## **7.1. Improvement of the operation and safety of current technologies**

### **7.1.1. *Developments of advanced BMSs (Battery Management Systems)***

The development of algorithms to manage the state of charge (SOC, defined in section 2.4.2), state of health (SOH, defined in section 2.4.4) and safety, which are collected under the generic umbrella term of BMS (battery management system) has occupied, and continues to occupy, many academics with the exponential development of portable applications, the advent of electric vehicles, or indeed the provision of storage capabilities to manage the variations in energy production, particularly from renewable sources. Combined with the use of lithium batteries, this monitoring of the SOC, SOH and operational safety has come to play an increasingly important role, because these factors are more vital to control in the case of abusive operation (overcharge, excess temperature range). However, these developments are essential in order to expand the usability of lithium technologies for stationary applications (standalone systems or grid-connected storage systems) and mobile applications (electric vehicles), which imply an increase in the specific energy and power of the battery. Real-time tracking of the SOC of the battery more specifically serves the needs of an EV application, which requires an on-board indicator capable of estimating the level of energy remaining in the battery and inform the driver of the remaining autonomy. In time, it will be possible to program a journey from point A to point B into the on-board computer and have the BMS tell the driver whether the SOC of the battery is sufficient to cover the required distance, taking account of the distance, the level of the terrain (uphill and downhill) and the maximum authorized speed, or suggest an optimal route. However, as soon as the application involves using the batteries in strenuous and intermittent cycles, as with the driving of an EV, this type of stress may damage the storage system and cause an unpredictable loss of capacity, thus necessitating a precise diagnostic of the SOH and a real-time estimation of the actual SOC of the battery. In the context of operational safety, the detection of internal phenomena – be they electrical, thermal or mechanical in nature – which could lead to a thermal runaway in the lithium batteries (which is synonymous with the swelling of the element because of increased internal pressure, breakage of the external casing with release of fumes, sparks or splashes of flaming electrolyte) during abusive use (e.g. excess charging) is of primary importance in order to prevent the total degradation of an element or battery of elements, or even of the whole vehicle.

The indicators developed take account of the influence of environmental and operational factors on the autonomy and lifetime of the battery. The cycle lifetime of a lithium-ion battery is a function of its average operating temperature, which depends on the outside temperature and the heat generated by the application itself, on the DOD attained and the charge conditions applied. High temperatures, deep discharges and poorly-managed charge profiles reduce the lifetime of a battery in terms of the number of cycles. The introduction of the temperature parameter intervenes to improve the estimation of the SOH, but also in the charge/discharge-management algorithms so as to keep the battery within an optimal functional range, even if this means limiting its performances for a given period so as not to degrade its lifetime. For instance, we might limit the recharge currents so as not to degrade the negative electrode (by metal lithium plating on the surface of the graphite) or, at high temperature, limit the discharge currents in order to avoid imposing too great a temperature increase by the passage of a strong current through the element, which could cause thermal runaway.

Thus, we implement robust diagnostic methods, which are as un-intrusive as possible, with a view to management of the battery's operation and predictive maintenance of the components during their operation. These methods are based on electrical or empirical models using measurements of the voltage, current and temperature, and monitoring of the electrical parameters which are representative either of the SOC or the SOH. These electrical parameters are obtained from electrochemical measurements taken by impedance spectroscopy (frequent measurements described in section 2.4.12) or by pulsed current (temporal measurements) such as the internal resistance.<sup>3</sup> Thermal models on the scale of the element or of the pack are also of crucial importance.<sup>4, 5</sup>

These diagnostics tools are globally associated with the battery pack, or indeed more specifically with each individual element, based on the concept

---

3 See section 2.4.10 and V. POP, H.J. BERGVELD, P.H.L. NOTTEN, P.P.L. REGTIEN, Review article: "State-of-the-art of battery state-of-charge determination", *Meas. Sci. Technol.* vol. 16 R93–R110, 2005.

4 C. FORGEZ, D.V. DO, G. FRIEDRICH, M. MORCLETTE, C. DELACOURT, "Thermal modeling of a cylindrical LiFePO<sub>4</sub>/graphite lithium-ion battery", *J. Power Sources*, vol. 195, 2961–2968, 2010.

5 K. GI-HEON, A. PESARAN, "Analysis of heat dissipation in Li-ion cells & modules for modeling of thermal runaway", *The 3rd International Symposium on Large Lithium Ion Battery Technology and Application*, Long Beach, California, 2007.

of a “Smart cell”, whereby the element is equipped with its own local BMS to carry out measurements, manage the cell and communicate with the battery pack. This tool for management and diagnostics on the scale of the element can also take care of its balancing.

### 7.1.2. Development of high-performance management systems

The function of balancing in SOC management systems for lithium-ion batteries takes account of the technology’s intolerance to being over-charged. This necessitates element-by-element management of the charge of the battery so as to reduce the differences in voltage between elements and thus ensure optimum performances in terms of capacity and lifetime of the battery. Prolonged excessive charging of a single element can indeed cause irreversible and potentially dangerous phenomena (depending on the materials and other internal components used). The most modern chargers send current to all of the plugged in elements in a series. Standard equalization mode consists of diverting the current to reduce the current imposed by the charger on those elements whose voltages are highest (Figure 7.1). This derivation can be performed by an electronically-controlled resistor or by a MOS transistor.<sup>6</sup> Thus, no single element will experience too great a voltage at its terminals. The system waits until the elements with lowest voltages have reached the maximum imposed voltage before stopping charge. This involves a dissipation of energy, which reduces the efficiency and increases charge time.

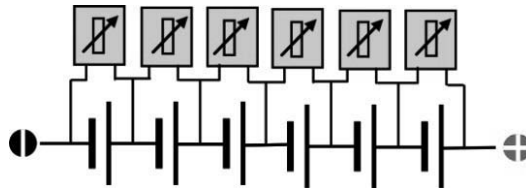


**Figure 7.1.** *Diagram of the principle behind a passive balancer (superfluous current is diverted and dissipated into resistors)*

At present, development efforts are focused on innovative balancing protocols, with as little energy losses as possible and as rapid charge times as possible. With such systems, instead of the energy from the diverted current

---

<sup>6</sup> MOS (Metal Oxide Semiconductor).

simply being dissipated, it is injected back into the ensemble of the battery (Figure 7.2).

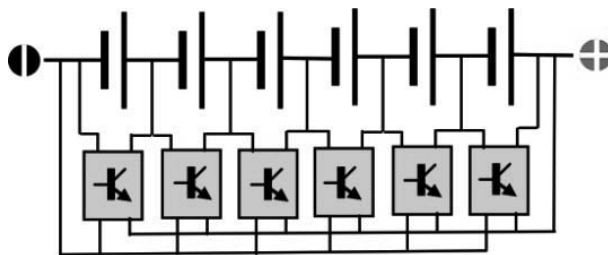


**Figure 7.2.** *Diagram of the principle behind an active balancer (superfluous current is diverted and injected back into the ensemble of the battery)*

### 7.1.3. Synthesis of new solvents

Organic electrolytes present two disadvantages: poor ionic conductivity (10 mS/cm) and high flammability. New electrolytes have been developed, composed solely of cations and anions obtained by the dissociation of inorganic salts.<sup>7-8</sup> They have very low melting points. Thus, they are liquid at ambient temperature and exhibit good ionic conductivity. The electrolytes developed contain cations such as EMI<sup>+</sup> (ethyl-methylimidazolium) or BMI<sup>+</sup> (butyl-methylimidazolium) and anions such as BP<sub>4</sub><sup>-</sup> (tetrafluoroborate) or PF<sub>6</sub><sup>-</sup> (hexafluorophosphate). The main advantages to these compounds are their high thermal stability, which has a range of between -90°C and 400°C, depending on the electrolyte; a large window of electrochemical stability (5 V); an aptitude to be gelled by polymers (polyvinylidene fluoride – PVdF) and a low saturated vapor pressure. The ionic conductivity can attain high values of 25 mS/cm at ambient temperature. However, these electrolytes can only be used in a lithium-ion battery if they contain a lithium salt. Therefore, a lithium salt is needed which is highly soluble in the electrolyte. At present, such salts are expensive, so the only situation in which they could come to be used as electrolytes is if we develop new, less costly techniques to synthesize them in an aqueous medium.

7 J.S. LEE, J.Y. BAE, H. LEE, N.D. QUAN, H.S. Kim, H. Kim, Ionic Liquids as Electrolytes for Li Ion Batteries, *J. Ind. Eng. Chem.*, 10, 1086–1089, 2004.

8 A. LEWANDOWSKI, A. SWIDERSKA-MOCEK, “Ionic liquids as electrolytes for Li-ion batteries – An overview of electrochemical studies”, *J. Power Sources* 194, 60–609, 2009.

#### 7.1.4. Introduction of redox shuttle molecules to prevent over-charging

Given that accidental over-charging is a significant technological risk for the operation of lithium-ion batteries, the addition of “protective” adjuvants into the electrolyte is one of the processes employed, particularly for the development of high-capacity batteries, where such an incident could have serious consequences (fire, explosion, large-scale emission of fumes). This solution is also very advantageous because it has no bearing on the design of the element.

Two types of protection are possible:

- shutdown molecules, whose function is to form a resistant polymer film on the surface of the electrode. However, this protection is irreversible<sup>9</sup>;
- redox shuttle molecules, which facilitate the long-term use of the battery, by way of an internal redox mechanism.

This latter process is able to deal with an imbalance of elements in the battery pack without going through a period of over-charging, where the danger of thermal runaway is significant. With excess charging, the oxidation current at the positive electrode is consumed by the oxidation reaction of the redox shuttle molecule instead of oxidizing the molecules of the electrolyte.

Figure 7.3 is a graphic representation of the operation of a redox shuttle molecule at the electrodes during a period of over-charging.<sup>10</sup>

Over-charge protection is regulated by the redox shuttle molecule, which is oxidized at the positive electrode, given that the oxidation potential of the shuttle molecule is just slightly greater than the end-of-charge potential of the positive electrode, and the molecule will be regenerated (by reduction) at the negative electrode.

---

9 S.L. LI, X.P. AI, J.K. FENG, Y.L. CAO, H.X. YANG, “Diphenylamine: A safety electrolyte additive for reversible overcharge protection of 3.6 V-class lithium ion batteries”, *J. of Power Sources*, 184, 553–556, 2008.

10 Q. WANG, S.M. ZAKEERUDDIN, I. EXNAR, M.L. GRAETZEL, “A new strategy of molecular overcharge protection shuttles for lithium ion batteries”, *Electrochemistry Communications*, 10, 651–654, 2008.



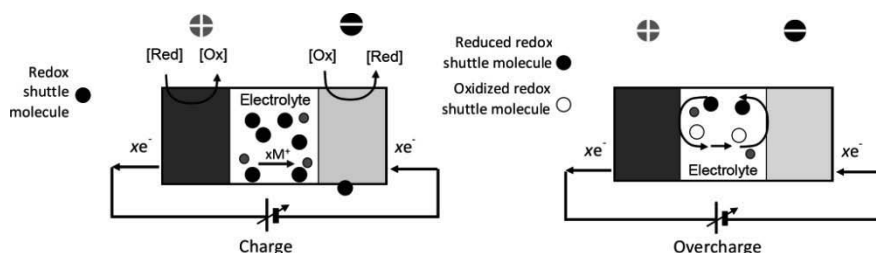


**Figure 7.3.** Diagram of the principle of operation of redox shuttle molecules

For this purpose, redox shuttle molecules need to exhibit the following specific properties:

- good electrochemical reversibility;
- an oxidation potential which is slightly greater than the maximum end-of-charge potential of the cathode;
- high solubility in the electrolyte;
- a good diffusion coefficient.

The earliest research carried out on redox shuttle molecules for Li-ion batteries was performed by Sony in 1991.<sup>11</sup> In the wake of this work, the use of aromatic molecules overtook that of organo-metallic complexes to play the role of a redox mediator during over-charging.

In 2009, K. Amine *et al.*, in a journal article<sup>12</sup>, listed the redox shuttle molecules developed over the past ten years. More recently, in 2011, a new, very exhaustive breakdown of the developments carried out on redox shuttle molecules was published.<sup>13</sup>

The molecule TEMPO – (2,2,6,6-tetramethylpiperidin-1-yl)oxyl – is one of the redox shuttle molecules most frequently envisaged for over-charge protection of 3 V lithium-ion batteries (Figure 7.4).

11 M. ADACHI, K. TANAKA, and K. SEKAI, “Aromatic Compounds as Redox Shuttle Additives for 4 V Class Secondary Lithium Batteries”, *J. Electrochem. Soc.*, 146, 1256–1261, 1999.

12 Z. CHEN, Y. QIN, K. AMINE, “Redox shuttles for safer lithium-ion batteries”, *Electrochimica Acta*, 54, 5605–5613, 2009.

13 L. ZHANG, Z. ZHANG and K. AMINE, Ed. I. Belharouak, “Redox Shuttle Additives for Lithium-Ion Battery”, *Lithium Ion Batteries – New Developments*, Publ. InTech, 173–188, 2012.

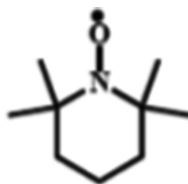


Figure 7.4. TEMPO molecule

However, the work of D. Lemordant *et al.* unearthed problems with the stability of the TEMPO cation after over-charging.<sup>14</sup> Redox shuttle molecules containing a benzyl group then began to be considered more thoroughly. Among the various research teams working on this type of molecules, we can highlight the work of K. Amine *et al.*<sup>15, 16</sup> and that of J.R. Dahn *et al.*<sup>17, 18</sup> on 4-tert-butyl-1,2-dimethoxybenzene (TDB, Figure 7.5) and 2,5-di-tert-butyl-1,4-dimethoxybenzene (DDB, Figure 7.5), covering the use of elements with poor redox potential such as  $\text{LiFePO}_4/\text{Li}_4\text{Ti}_5\text{O}_{12}$ , whose stability over time has been studied. In 2007, it was proposed to alter this molecule by the addition of fluoride groups so as to be able to serve higher usage potentials.<sup>19, 20</sup> Many patents have been filed on these

14 M. TAGGOUGUI, B. CARRE, P. WILLMANN, D. LEMORDANT, “Application of a nitroxide radical as overcharge protection in rechargeable lithium batteries”, *J. of Power Sources*, 174, 643–647, 2007.

15 ZONGHAI CHEN, K. AMINE, “Degradation pathway of 2,5-di-tert-butyl-1,4-dimethoxybenzene at high potential”, *Electrochimica Acta*, 53, 453–458, 2007.

16 Z. ZHANG, L. ZHANG, J.A. SCHLUETER, P.C. REDFERN, L. CURTISS, K. AMINE, “Understanding the redox shuttle stability of 8,3,5-di-tert-butyl-1,2-dimethoxybenzene for overcharge protection of lithium-ion batteries”, *J. of Power Sources*, 195, 4957–4962, 2010.

17 J. CHEN, C. BUHRMESTER and J.R. DAHN, “Chemical overcharge and overdischarge protection for lithium-ion batteries”, *Electrochemical and Solid-State Letters*, 8, 59–A62, 2005.

18 L.M. MOSHUCHAK, M. BULINSKI, W.M. LAMANNA, R.L. WANG, J.R. DAHN, “Direct comparison of 2,5-di-tert-butyl-1,4-dimethoxybenzene and 4-tert-butyl-1,2-dimethoxybenzene as redox shuttles in  $\text{LiFePO}_4$ -based Li-ion cells”, *Electrochemistry Communications*, 9, 1497–1501, 2007.

19 M. TAGGOUGUI, B. CARRE, P. WILLMANN, D. LEMORDANT, “2,5-Difluoro-1,4-dimethoxybenzene for overcharge protection of secondary lithium batteries”, *J. of Power Sources*, 174, 1069–1073, 2007.

20 L.M. MOSHURCHAK, W.M. LAMANN MIKE BULINSKI R.L. WANG, R.R. GARSUCH, J. JIANG, D. MAGNUSON, M. TRIEMERT and J. R. DAHN, “High-Potential Redox Shuttle for Use in Lithium-Ion Batteries”, *J. of Electrochem. Soc.*, 156, A309–A312, 2009.

molecules and others, which may or may not also cover over-discharge.<sup>21, 22, 23, 24, 25, 26</sup>

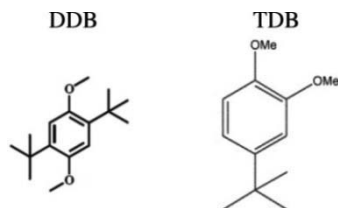


**Figure 7.5.** Example of two redox shuttle molecules

The limitations of these molecules are their solubility in carbonates. They may also decrease the solubility of the lithium salt. Furthermore, the degree of over-charging must be limited, because the redox reaction of the shuttle molecule is exothermic and can cause the temperature of the element to increase. The stability of the performances over time is also a crucially-important criterion: the 3M Company proclaims that the performances of its shuttle molecule are stable over 500 over-charge cycles (DDB, Figure 7.5).

The results on redox shuttle molecules for protection of lithium-ion batteries against small over-charges are therefore extremely promising. The benefits offered by the use of such electrochemical management, on the scale of a module or a pack or the entire system, are very significant, because it is able to:

- eliminate the need for a costly electronic management system:
  - no management on the scale of the element,
  - no balancing circuit;

21 I. EXMAR, Q. WANG, Overcharge and overdischarge protection in lithium-ion batteries, US Patent 8,003,260 B2.

22 J.-H. KIM, H.Y.LEE, S.-H. CHOY, H.-S. KIM, H.-G. NOH, Electrolyte for lithium-ion battery and lithium battery comprising same, US Patent 20110151337 A1.

23 W. WENG, Z. ZHANG, K. AMINE, Redox shuttles for lithium-ion batteries, US Patent 20110294017 A1.

24 L. ZHANG, Z. ZHANG, K. AMINE, Z. CHEN, Redox Shuttles for high voltage cathodes, US Patent 20110294018 A1.

25 Z. ZHANG, L. ZHANG, K. AMINE, Polyether-functionalized redox shuttle additives for lithium ion batteries, WO Patent 2011/149970 A2.

26 J. DAHN, W.M. LAMANN, M.J. BULINSKI, J. JIANG, L. MOSHUR-CHAK, P.T. PHAM, L.R. WANG, Redox Shuttles for high voltage cathodes, WO Patent 2009102604 A1.

- reduce the complexity and the size of the packs:
  - less measuring connecting material, fewer electronic components,
  - gains in terms of potential space and mass in the pack;
- improve the lifetime, performances and safety of the packs:
  - over-discharge protection for each individual element,
  - management of the weakest elements and an overall gain in capacity for the pack.

## **7.2. Improvement of the intrinsic performances (energy, power)**

### **7.2.1. *Synthesis of new materials***

New positive and negative materials are in the process of development, both in terms of the nature of the compounds and in terms of morphology (nanomaterials), with the aim of improving performances regarding energy, power, cost, reliability, lifetime and intrinsic safety. What is done at the level of the material is to develop or implement more energetic structures with the aim of reducing costs. Indeed, over the past few years, the improvements made in the sense of a gain in mass energy density have consisted of developing lighter casings (replacing steel casings with aluminum casings or soft pouches) and optimizing the design of the cells (compromising between the surface area of the electrodes developed and the mass loading<sup>27</sup>). As the limits have been reached in these domains, further progress can only be made by changing the nature or morphology of the active compounds.

#### **7.2.1.1. *New compounds***

Figure 7.6 illustrates the new materials in the course of development, plotting their theoretical mass capacity and their average potential versus lithium. The gain in gravimetric energy density is possible either by increasing the gravimetric capacity of the element or by increasing its nominal voltage.

---

<sup>27</sup> The mass loading of an electrode is the amount of active material coated per unit surface area. The unit usually employed is the mg/cm<sup>2</sup>.

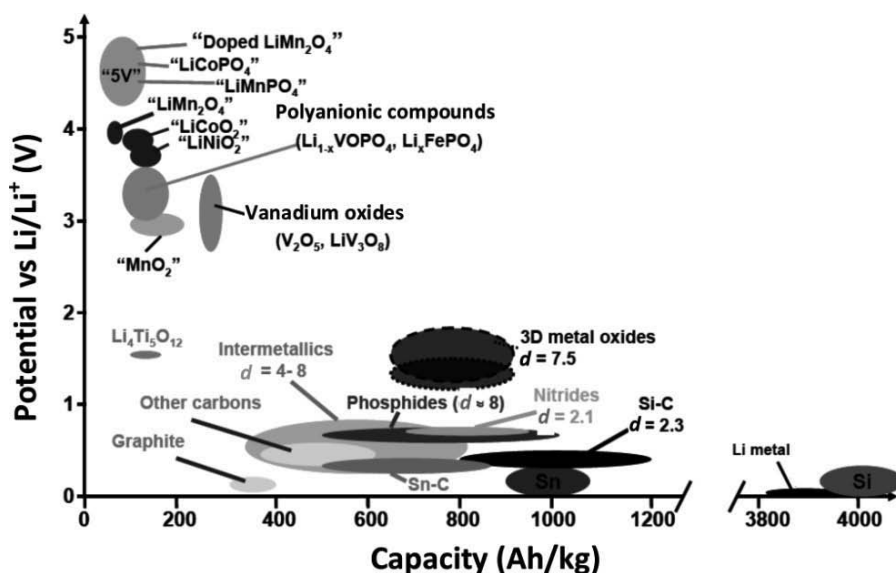


Figure 7.6. New materials for electrodes in the course of development<sup>28</sup>

#### 7.2.1.1.1. Materials for negative electrodes

We can see that a gain in gravimetric capacity is envisageable for the negative electrode with the introduction of new materials which, whilst functioning at low potential with values of less than 1 V versus  $\text{Li}^+/\text{Li}$ , exhibit high theoretical gravimetric capacities, beyond the theoretical gravimetric capacity of graphite which is taken as a reference (372 mAh/g). Such materials include, e.g. compounds of carbon-silica (Si-C), carbon-tin (Sn-C) or intermetallics (see section 4.3). In practice, we then need to take account of the gravimetric capacity which is actually accessible for the electrode (the practical gravimetric capacity) in order to guarantee the electrical performances over time (which depends – amongst other things – on the degree of reversibility of the electrochemical reaction and any mechanical phenomena occurring during the charge/discharge cycles, the morphology of the active particles and the design of the electrode). Considering the whole of the element, increasing the energy by increasing the gravimetric capacity of one of the electrodes – here the negative

<sup>28</sup> J.M. TARASCON & M. ARMAND, “Issues and challenges facing rechargeable lithium batteries”, *Nature*, vol. 414, 359–367, 2001.

electrode – involves oversizing the positive electrode by increasing its mass loading. An adjustment of the balancing of the capacity of the two electrodes is required to deliver the performances expected of the element (energy, cyclability). However, the increase of the mass loading of the electrode has experimental limitations (mechanical adherence, thickness percolation), which therefore reduces the possible gains in terms of energy, whilst maintaining performances in terms of power that are “acceptable” for the intended application (see section 6.2.2).

The first materials to be studied were alloys based on aluminum (Al)<sup>29</sup>, tin (Sn)<sup>30</sup> or silica (Si)<sup>31</sup> because of their very high theoretical gravimetric capacities.

| Negative materials | Theoretical gravimetric capacity<br>(mAh/g) | Nominal voltage<br>(V versus<br>Li <sup>+</sup> /Li) |
|--------------------|---|--|
| Graphite (C)       | 372   | 0.10   |
| Tin (Sn)           | 994 (3 times that of graphite)              | 0.50   |
| Aluminum (Al)      | 2234 (6 times that of graphite)             | 0.36   |
| Silica (Si)        | 3579 (10 times that of graphite)            | 0.40   |

In addition, they exhibit good thermal stability and excellent calendar stability.

Figure 7.7 shows the discharge curves for a number of alloys on the basis of the amount of lithium they contain.

29 Y. HAMON, T. BROUSSE, F. JOUSSE, P. TOPART, P. BUVAT, D.M. SCHLEICH, “Aluminum negative electrode in lithium ion batteries”, *J. of Power Sources*, 97–98, 185–187, 2001.

30 M. WINTER, J.O. BESENHARD, “Electrochemical lithiation of tin and tin-based intermetallics and composites”, *Electrochimica Acta*, 45, 31–50, 1999.

31 WEI-JUN ZHANG, “Lithium insertion/extraction mechanism in alloy anodes for lithium-ion batteries”, *J. Power Sources*, 196, 877–885, 2011.

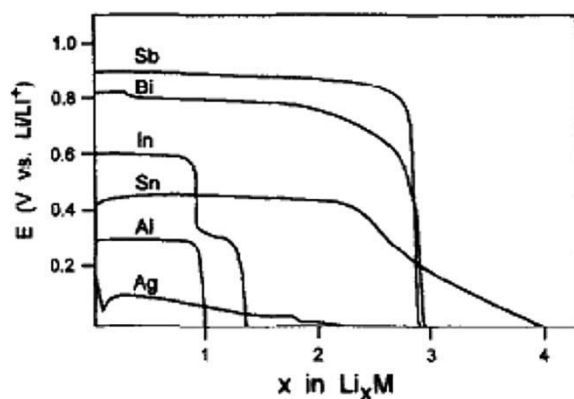


Figure 7.7. Profile of the charge/discharge potential of a number of  $\text{Li}_x\text{M}$  alloys<sup>32</sup>

However, they cannot be used for cycling applications in the “massive” state because of the volumetric expansion of the crystal lattice which occurs during lithiation, and because of the low diffusion coefficients of lithium in the metal, which limit the strengths of current that are applicable.

Figure 7.8 shows the increase in standardized volume (in L/Ah) of a number of compounds before and after total lithiation.

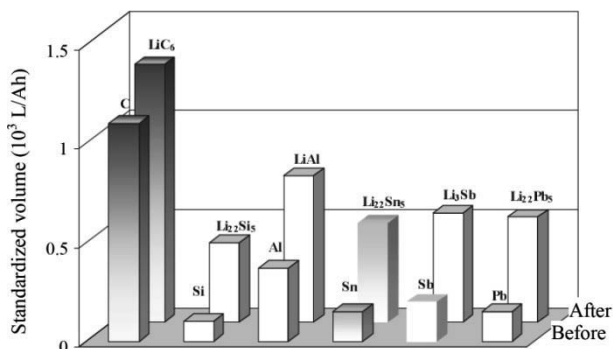


Figure 7.8. Volumetric expansion of a number of alloys compared to graphite<sup>33</sup>

32 J.O. BESENHARD, J. YANG, M. WINTER, “Will advanced lithium-alloy anodes have a chance in lithium-ion batteries?”, *J. of Power Sources*, 68, 87–90, 1997.

33 M. WINTER, J.O. BESENHARD, “Electrochemical lithiation of tin and tin-based intermetallics and composites”, *Electrochimica Acta*, 45, 31–50, 1999.

For instance, the volumetric expansion between Si and  $0.25\text{Li}_{15}\text{Si}_4$  is +280%, but the reaction  $15\text{Li}^+ + 15\text{e}^- + 4\text{Si} \rightarrow \text{Li}_{15}\text{Si}_4$  in question offers the highest known theoretical gravimetric capacity (3,579 mAh/g), a corresponding practical capacity of 2200 mAh/cm<sup>3</sup> and an average lithiation/delithiation potential equal to 0.4 V versus  $\text{Li}^+/\text{Li}$  (therefore not very different from carbon or lithium, which has the effect of preserving a high voltage per element and thus a high gravimetric capacity). In practice, the target gravimetric capacity is 1000 mAh/g. Beyond this value, there is no longer any significant effect on the element's energy, because the positive electrode can no longer ensure balanced capacity.

In addition, the volumetric expansion of the lithiated particle is such that a phenomenon of electrochemical pulverization occurs, whereby large particles crumble into smaller particles. Unpassivized active surfaces are thus created during the course of cycling, leading to the continuous formation of a passivation film, which consumes electrolyte and electrons (irreversible capacity). This is particularly true for metals accepting lithium insertion below 0.8 V versus  $\text{Li}^+/\text{Li}$  such as Sn, Al, Si, etc.

In order to enable this type of material to contain such variations in volume and reduce the mechanical damage (cracking, de-cohesion), research is currently focusing on the nanostructuration of the active material (nanoparticles or nanowires) and testing new formulations for electrodes so as to have good porosity and a binder which absorbs the variations in size (see section 7.2.1.2).

More recently, with a view to finding negative materials with high specific capacities, researchers have turned their attentions to intermetallic materials which obey conversion mechanisms. Until recently, they had not been extensively looked into, because of their poor cyclability – an inherent consequence of the conversion mechanism which requires considerable energy for the charge reversibility, and of the significant volumetric expansion during the charge/discharge cycle. However, recent improvements in cycling have been obtained by adapting the electrode formulation.<sup>34</sup> Hence, their use as an electrode material is no longer precluded.

---

34 V. SIVASANKARAN, C. MARINO, M. CHAMAS, P. SOUDAN, D. GUYOMARD, J.-C. JUMAS, P.-E. LIPPENS, L. MONCONDUIT, B. LESTRIEZ, "Improvement of intermetallics electrochemical behavior by playing with the composite electrode formulation", *J. Mater. Chem.*, 21, 5076–5082, 2011.



Below are two examples of promising conversion materials:  $\text{NiP}_3$  and  $\text{TiSnSb}$ .

### ***NiP<sub>3</sub> compound***

This compound belongs to the family of binary skutterudites<sup>35</sup> ( $\text{MX}_3$ :  $\text{M} = \text{Co}, \text{Rh}, \text{Ir}, \text{Ni}$  and  $\text{X} = \text{P}, \text{As}, \text{Sb}$ ) and crystallizes in a cubic lattice in which the nickel atoms are at the center of octahedrons formed by phosphorus atoms.  $\text{NiP}_3$  reacts with nine lithium ions per formula unit and has a theoretical capacity of 1590 mAh/g, following a reaction process which leads to the formation of nanoparticles of nickel:



The plateau of insertion potential occurs at 0.5 V versus  $\text{Li}^+/\text{Li}$ .

Hitherto, we have not yet been able to obtain relatively good cyclability<sup>36</sup> except by limiting the window of potential and excluding regions with low potential, as illustrated by Figure 7.9, and therefore accepting a decrease in specific capacities. If this cell is subjected to cycling between 0 and 2.5 V, the initial gravimetric capacity is very high (1600 mA/g), but it drops to zero in only ten cycles. If the same type of cell is subjected to cycling between 0.5 and 2 V, the initial gravimetric capacity is much less, but afterward it remains almost constant. If we further reduce the window of potential (first cycle between 0.5 and 2 V, followed by cycles between 0.65 and 2 V), the gravimetric capacity decreases still further without a gain in terms of lifetime. These experiments demonstrate the compromise between capacity and lifetime by choice of the maximum threshold voltage during charge and the minimum threshold voltage during discharge. This compromise is more general than with  $\text{NiP}_3$  batteries alone.

---

<sup>35</sup> Skutterudite is a mineral compound containing cobalt-nickel arsenide with the formula  $(\text{Co}, \text{Ni})\text{As}_3$ . It lends its name to a group of isostructural minerals (i.e. with an identical crystal lattice).

<sup>36</sup> S. BOYANOV, F. GILLOT, L. MONCONDUIT, "The electrochemical reactivity of the  $\text{NiP}_3$  skutterudite-type phase with lithium", *Ionics*, vol. 14, no. 2, pp. 125–130, 2008.

S. BOYANOV, Performances et mécanismes électrochimiques des phosphures de fer et nickel comme anode dans les batteries Li-ion, Doctoral thesis, University of Montpellier II, 29 September 2008.

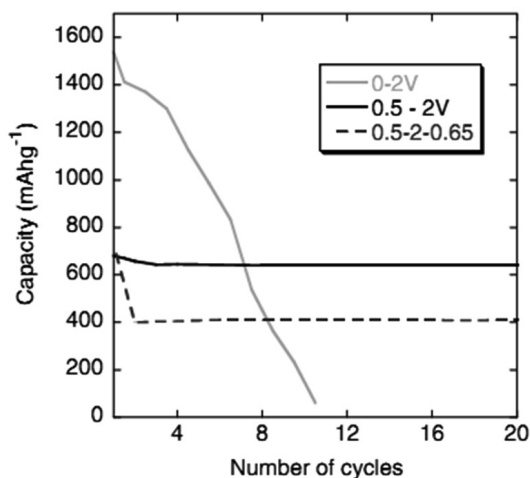
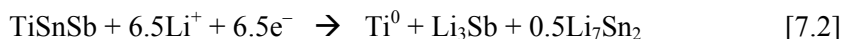


**Figure 7.9.** Behavior of  $\text{NiP}_3$  versus lithium with a  $C_{10}$  cycled current between (2.5 and 0 V), (2 and 0.5 V) and then (0.5 then 2 and 0.65 V)<sup>36</sup>

### ***TiSnSb compound***

The reaction involved is written thus:



$\text{TiSnSb}$  has not yet been used in commercial elements, but it has proved to be highly promising in comparison with other negative materials with an insertion mechanism, thanks to its nominal potential of 0.60 V versus  $\text{Li}^+/\text{Li}$ , which places it between graphite and LTO, and its gravimetric capacity of 600 mAh/g, which is greater than that of graphite.  $\text{TiSnSb}$  is currently in a phase of optimization, and accepts a constant gravimetric capacity of 600 mAh/g over at least 500 cycles in a half-cell with Li.<sup>37</sup> The charge process is not yet fully understood.<sup>38</sup>

37 H. WILHELM, C. MARINO, A. DARWICHE, L. MONCONDUIT, B. LESTRIEZ, "Significant electrochemical performance improvement of  $\text{TiSnSb}$  as anode material for Li-ion batteries with composite electrode formulation and the use of VC and FEC electrolyte additives", *Electrochem. Commun.*, 24, 89–62, 2012.

38 M.T. SOUGRATI, J. FULLENWARTH, A. DEBENEDETTI, B. FRAISSE, J.-C. JUMAS, L. MONCONDUIT, " $\text{TiSnSb}$  a new efficient negative electrode for Li-ion batteries: mechanism investigations by operando-XRD and Mössbauer techniques", *J. Mater. Chem.*, 21, 10069–10076, 2011.

### 7.2.1.1.2. Materials for positive electrodes

For the positive electrode, the gain in energy is achieved by increasing:

– either the operational nominal voltage above 4.0 V with the development of new “high-voltage” compounds: oxides with a spinel structure such as  $\text{LiMn}_{2-y}\text{M}_y\text{O}_4$  where  $M = \text{Cr, Fe, Co, Ni}$ ), called 5 V spinels, or  $\text{LiCoPO}_4$ - or  $\text{LiMnPO}_4$ -type phosphates. The introduction of these high-voltage compounds is conditioned by advances in the definition of new oxidation-resistant electrolytic blends;

– or the theoretical (and subsequently practical) specific capacity, with the synthesis of lamellar-oxide-type compounds, which are over-lithiated and rich in manganese ( $x\text{Li}_2\text{MnO}_3 \cdot (1-x)\text{LiMO}_2$ , where  $M = \text{Mn, Co, Ni}$ ). These compounds are not high-voltage materials: their nominal voltages are approximately 3.4–3.6 V versus  $\text{Li}^+/\text{Li}$ .

A number of examples are given below, compared with  $\text{LiCoO}_2$  which we shall take as a reference:

| Positive materials   | Theoretical gravimetric capacity (mAh/g) | Nominal voltage (V versus $\text{Li}^+/\text{Li}$ ) |
|--|--|---|
| $\text{LiCoO}_2$   | 140                                      | 3.7   |
| $\text{LiNi}_{0.4}\text{Mn}_{1.6}\text{O}_4$ (5V spinel)   | 147                                      | 4.7   |
| Over-lithiated lamellar oxides:<br>$x\text{Li}_2\text{MnO}_3 \cdot (1-x)\text{LiMO}_2$ where $M = \text{Mn, Co, Ni}$ | 300                                      | 3.5   |

### 7.2.1.2. New morphologies: nanomaterials

As explained above, alloy-based active materials offer greater capacity than graphite, but their volumetric expansion is prohibitive for their cycling behavior in the long term (or forces us to considerably restrict the DODs by oversizing the electrode in relation to the positive counterpart material).

One of the solutions (which has proven itself) to deal with the problem is to develop nanostructured electrodes to absorb the variations in volume in the porosity and preserve the mechanical integrity of the particles and the electrode. Research is also being carried out on deposition of thin films devoted to the design of micro-batteries (see section 7.4.3).

The advantage to nanostructuration of the active particles lies in the obtaining of a better lifetime, but also of high power by reducing the distances over which lithium is diffused in the nanoparticles. These developments are gradually being integrated into commercial technologies. For instance, we can cite the results of the work done by M. Alias for her doctorate<sup>39</sup>, or the industrial approach used by American company Amprius ([www.amprius.com](http://www.amprius.com)), reported by the Massachusetts Institute of Technology journal, with a silica-based nanostructured element which would store twice as much energy as the marketed equivalent, and offer a 40% gain in autonomy of portable electronic products. The silica would be in the form of silica nanotubes (hollow nanowires), with the presence of an external layer to reinforce the structure and impose mechanical constraints on it.

Note that this increase in power by way of nanostructuring has also been applied to insertion materials. We can cite the development of a nanostructured lithiated iron phosphate by A123 Systems, (Nanophosphate™ lithium-ion battery), which – by acting on the morphology of the particles – compensates for poor electronic conductivity ([www.a123systems.com](http://www.a123systems.com)), or the development of a nanostructured lithium titanate by Altairnano ([www.altairnano.com](http://www.altairnano.com)). Such developments are tending toward increased power, accelerated charging and longer lifetime.

### 7.3. New formats of batteries

#### 7.3.1. *Development of specific architectures: bipolar*

The so-called bipolar configuration<sup>40, 41</sup> (Figure 7.10) facilitates the connection of elements in series by the sharing of a current collector between the positive and negative electrode, with the current collectors also delimiting distinct electrolytic compartments.

---

39 M. ALIAS, Composés à base de silicium ultra-divisé pour électrodes négatives d'accumulateur lithium-ion, Doctoral thesis, Polytech Nantes, XII.2008.

40 T. BERGER, J. DREHER, M. KRAUSA, J. TÜBKE, "Lithium accumulator for high-power applications", *J. Power Sources*, 136, 383–385, 2004.

41 R.A. MARSH, P.G. RUSSELL, T.B. REDDY, "Bipolar lithium-ion battery development", *J. Power Sources*, 65, 133–141, 1997.

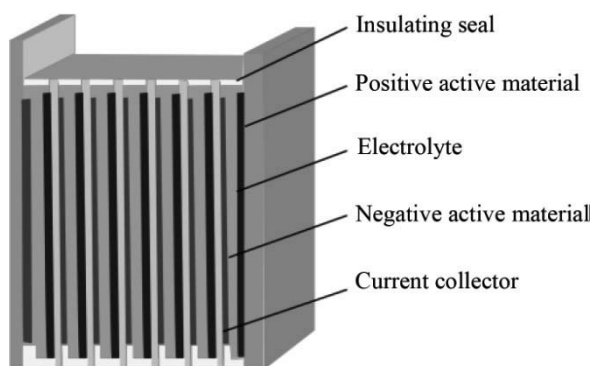


**Figure 7.10.** *Generic architecture for a bipolar battery*

In this configuration, the current is passed from one element to the next via the current collector, and is collected at the battery's terminal plates. This considerably reduces the battery's internal resistance and ensures homogenous distribution of the current (electronic and ionic). These characteristics mean this architecture is a natural choice for the optimization of systems functioning with a strong current.

Applied to lithium-ion technology, this bipolar architecture necessitates the use of a negative electrode that is compatible with an aluminum current collector. Such is the case of  $\text{Li}_4\text{Ti}_5\text{O}_{12}$ . Replacing graphite with this titanium oxide enables us to use the same metal collector as the positive electrode.

### **7.3.2. Development of thin and soft batteries**

Manufacturers are seeking to reduce production costs of batteries by developing less costly electrode-manufacturing processes. Today, electrodes are made by deposition/coating of powders dispersed in an organic or aqueous solvent (for positive materials) onto metal current collectors. Research efforts have turned toward printing techniques from the paper industry, whereby very thin films of active materials can be very precisely deposited to make thin and soft batteries.<sup>42</sup> The intended applications are applications for which it is necessary to have batteries with small

<sup>42</sup> J. HUANG, J. YANG, W. LI, W. CAI, Z. JIANG, "Electrochemical properties of  $\text{LiCoO}_2$  thin film electrode prepared by ink-jet printing technique", *Thin Solid Films*, vol. 516, 3314–3319, 2008.

dimensions – miniatures: medical implants, smart labels, energy-storing clothing, etc.

### 7.3.3. *Development of micro-batteries*

Techniques for the deposition of thin layers (CVD<sup>43</sup>, PVD<sup>44</sup>, photolithography) are under development to create stacks of electrochemical cells of dimensions  $< 3 \times 3$  mm with a thickness of only a few  $\mu\text{m}$ . Depositions are made of silica substrates of 200  $\mu\text{m}$  in thickness. The existing body of literature indicates that the positive electrode can be made of a film of LiTiOS (lithiated titanium oxysulfide (TiOS)); the electrolyte may be a solid polymer, lithium phosphorus oxynitride (LiPON) and the negative electrode made of metal lithium or silica, etc.<sup>45</sup>. We obtain a volumetric capacity of approximately 100  $\mu\text{Ah}/\text{cm}^2$  for a voltage domain between 2 and 2.5 V. The use of silica may enable us to circumvent the stage of integration on chip boards heated to around 200°C instead of lithium, which would melt at such temperatures.

The quoted lifetimes are very high – over 1500 cycles, with no loss of capacity, provided there is not a sealing problem. Self-discharge is very low, and the calendar aging depends on the quality of the casing. The impedance can indeed change over time, because of the evolution of the interfaces by way of lithium loss by corrosion.

The surface capacity of silica in the lithiated state is equivalent to that of lithium, and the volumetric variation of silica with an equal surface capacity exchanged is comparable to that of lithium. The electrochemical mechanism, however, is different, because lithiation of silica occurs by breaking of the Si-Si bond to allow the lithium to penetrate. Management at the end of discharge is crucially important, because to surpass the acceptable threshold of discharge voltage leads to an alteration of the structure of the material, which – having initially been amorphous – becomes crystalline. Then, we notice an alteration of the recharge curve with a very different evolution of the voltage.

---

43 CVD: chemical vapor deposition, whereby thin films are formed from gases in a vacuum.

44 PVD: physical vapor deposition, whereby there is physical deposition in the vaporous phase – e.g. evaporation of a solid material and condensation on the substrate (cathodic sputtering).

45 V.P. PHAN, B. PECQUENARD, F. Le CRAS, “High-performance all-solid-state cells fabricated with silicon electrodes”, *Adv. Funct. Mater.*, vol. 22, pp. 2580–2584, 2012.

This type of micro-batteries benefits from the robustness of CVD processes and from the compatibility of the operating conditions for creating stacks of active layers (positive electrode/electrolyte/negative electrode). Such micro-batteries have already been commercialized by numerous companies (Cymbet, Front Edge Technology, Infinite Power solution, Excellatron, GS Nanotech, etc.). Cymbet and Front Edge Technology, for instance, commercialize micro-batteries to be soldered to imprinted circuit boards. We can also cite ST Microelectronics, who have developed a battery with thin layers and high energy density (EnFilm™ technology). The performances of the micro-battery are 1000 charge/discharge cycles to a 50% DOD. Its dimensions are  $25.4 \times 25.4$  mm with a thickness of only 0.2 mm. This micro-battery with 700  $\mu\text{Ah}$  capacity can generate a strong pulsed peak current (up to 10 mA).

#### **7.4. Conclusion**

In this chapter, we have sketched the broad outlines of the research being conducted to improve the electrical performances of lithium-ion batteries (specific energies and lifetime). In parallel to these developments on lithium-ion technology, lithium-sulfur and lithium-air batteries are in an examination phase and should, in the coming years, become a viable competitor for lithium-ion batteries. They are examined in Chapters 9 and 10.





## Chapter 8

# Lithium-Metal Polymer Batteries<sup>1</sup>

Introduced in 1973, the earliest form of battery technology to use lithium had a metal lithium foil as a negative electrode. Abandoned in a liquid electrolyte medium, this technology is now being developed thanks to the use of a solid polymer electrolyte, based on molten poly(ethylene oxide) (PEO), impregnated with lithium salt. It was Michel B. Armand who, in 1978, proposed the use of such an electrolyte, whose poor ionic conductivity is problematic at ambient temperature but whose viscosity at high temperatures (to ensure sufficient conductivity) mechanically blocks dendrite growth (see section 4.4.2) during charging when the lithium is reduced.

The advantages of lithium are:

- a very low electrochemical potential which offers very high specific energies;
- malleability, which means it can be used in the form of a film and facilitates the making of rollable electrodes with large surface areas;
- good electrical conductivity, which means it can serve both as an active material and a current collector.

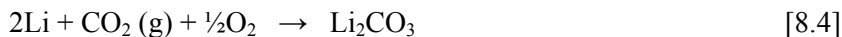
---

<sup>1</sup> This chapter has been enhanced by attentive reviewing by Philippe Azaïs, a researcher at CEA-Grenoble.

Lithium's very low electrochemical potential renders it a very powerful reducing agent. Lithium will react with any other component in its vicinity. On contact with the nitrogen in the air, it forms a layer of nitride by way of the following reaction:



Handled in as dry an environment as possible, the surface of lithium comprises a layer of oxide (and/or hydroxide in the presence of atmospheric water) and carbonate, formed by the reactions:



In the context of the development of this battery technology, the phenomenon of dendrite growth (explained in section 4.4.2) has been studied in great depth, because it occurs even in the presence of a polymer electrolyte, in case of over-charge and aging. As previously indicated (Figure 4.5), a dendrite results from the non-uniform deposition of lithium during its electrochemical reduction.

### 8.1. Principle of operation

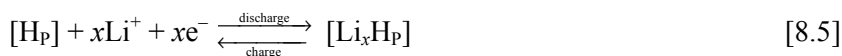
In a lithium-metal polymer battery, the electrochemical chain involved is:



where  $[\text{H}_\text{p}]$  is a positive host structure, which is an insertion material functioning at high potentials, around +3 to +4 V versus  $\text{Li}^+/\text{Li}$ . This voltage is limited, not by the intrinsic operation of the electrodes, but by the PEO, which degrades when subjected to voltages of over 4 V. This maximum voltage imposes limitations on the choice of metal oxides to use for the positive host structure.

The reaction principle behind the operation of a Li-metal battery is given below:

#### Positive electrode



## Negative electrode



## Balance equation



The equations are illustrated in the following figure:

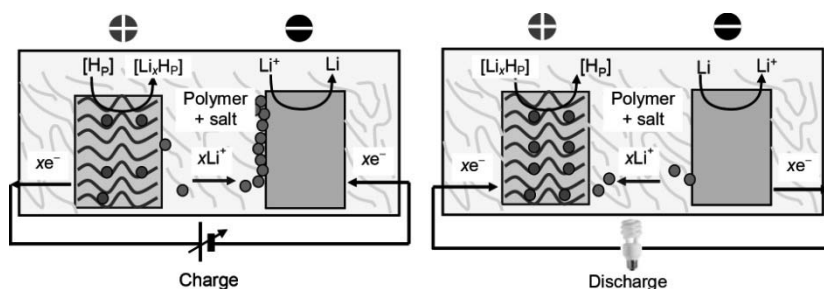


Figure 8.1. Principle of operation of the lithium-metal polymer battery

### 8.1.1. Positive electrode

The active material of the positive electrodes comprises insertion materials intercalating lithium over as broad a range of voltage as possible in view of the PEO (its degradation at the operating temperature occurs at around 4.1–4.2 V versus  $\text{Li}^+/\text{Li}$ ). One might, for instance, use transition metal oxides:  $\text{Li}_{0.2}\text{MoS}_2$ ,  $\text{V}_2\text{O}_5$  and  $\text{LiFePO}_4$  (at Batscap),  $\text{V}_6\text{O}_{13}$ ,  $\text{MoO}_3$ . Carbon can be added to improve electrical conduction, and a polymer for the plasticizing aspect. For reasons of compatibility, we use the same polymer as for the electrolyte – PEO blended with PVDF, in which we dissolve a lithium salt such as  $\text{LiTFSI}$ <sup>2</sup> for its very low hygroscopicity ( $\text{LiPF}_6$  is not usable because it is too hygroscopic). The current collector is aluminum.

<sup>2</sup>  $\text{LiTFSI}$  is the abbreviation for  $\text{LiN}(\text{SO}_2\text{CF}_3)_2$  (lithium bis(trifluoromethanesulfonyl)imide). It corrodes the aluminum of the current collectors with a voltage higher than 4.2 V. However, as PEO requires the voltage to be limited to 4 V, we can use  $\text{LiTFSI}$  with no danger of degradation of the element.

### 8.1.2. *Negative electrode*

The negative electrode comprises a foil of metal lithium, which also serves as a current collector. Between this strip and the outer terminal, it is necessary to use a copper current retriever on the edge of the roll or the stack.

### 8.1.3. *Electrolyte*

The electrolyte is a poly(ethylene oxide) (PEO) film with a dissolved lithium salt LiTFSI. In order to obtain a sufficiently good ionic conductivity, we need to operate the battery at a temperature greater than the glass transition temperature of the polymer. The operating temperature required is 60–80°C, which limits the field of application to large batteries, which notably precludes the mobile market. Under no circumstances must the thermal degradation temperature of the PEO, which is around 120°C, be surpassed.

The aim of current research is to be able to lower this operating temperature by developing new types of polymers (such as LiFSI – Lithium bis(fluorosulfonyl)imide – which is more soluble in PEO), which still offer good resistance to dendrites.

## 8.2. **Manufacturing process**

In 2007, the Bolloré Technologies group bought its main competitor – Avestor in Canada. Now, this company is known as Bathium, and works on the same technology as the sister company of the Bolloré group: Batscap. Since the buyout, Bolloré has held the vast majority of patents over this technology (over a hundred categories of patents dating from 1992). Since 2012, Bolloré Technologies has been commercializing lithium-metal polymer batteries as a pack for applications in cars and buses. The packs are made by the two companies, Bathium and Batscap. This technology was chosen by the *Syndicat Mixte de la Ville de Paris* (Combined Parisian Syndicate) for its electric car-sharing service *Autolib*. It is implemented in the Bluecar<sup>3</sup>. It is based on the company's know-how in the making of thin films to make a “sandwich” structure of different strips (insulator, lithium

---

<sup>3</sup> At the end of 2012, there were already 1,450 Autolib vehicles in service.

foil, electrolyte, positive electrode, aluminum foil to serve as a current collector). This composite film is around  $100\text{ }\mu\text{m}$  in thickness. This technique ensures minimized manufacturing costs. The large surface areas of the electrodes, the thinness of the electrolyte and the operation at high temperature<sup>4</sup> also enhance the battery's performances in terms of power.

### 8.3. Main characteristics

The main characteristics of this technology are those quoted by Batscap (see the photo in Figure 8.2).



**Figure 8.2.** Module developed by Batscap (<https://www.autolib.eu/100-ecologique/>)

#### 8.3.1. Operating voltage

The voltage of the battery, whose elements use a lithium ferrophosphate (LFP)-based positive electrode, varies between 300 and 435 V for a nominal voltage of 430 V. It comprises six modules connected in series. The volume of the battery is 300 liters. Its mass is 300 kg.

#### 8.3.2. Capacity

The capacity at C/4 is given for 75 Ah.

#### 8.3.3. Practical gravimetric energy density

The energy stored in the battery is 30 kWh (75 Ah – 400 V) for a mass of 300 kg. This represents a practical gravimetric energy density of 100 Wh/kg.

---

<sup>4</sup> A rented fleet helps vehicles run more often than personal vehicles. The self-heating of the battery maintains its temperature.

#### **8.3.4. Practical volumetric energy density**

The volume of the module is 300 L. This gives us a practical volumetric energy density of 100 Wh/L.

#### **8.3.5. Power**

The peak power over 30 seconds is given as 45 kW. Hence, the gravimetric power density is 150 W/kg.

#### **8.3.6. Operating temperature**

The internal operating temperature is 60–80°C with an acceptable ambient temperature between –20°C and +60°C.

#### **8.3.7. Self-discharge**

Self-discharge is likely to be low with a  $V_2O_5$  electrode. The same is absolutely not true with an LFP electrode, which exhibits a high degree of self-discharge when the temperature rises. In addition to the intrinsic discharge of the battery, it should not be forgotten that, in order to function, the electrolyte needs to be kept at a temperature far greater than ambient temperature. If the energy needed to maintain the temperature is extracted from the battery, the result is a significant apparent self-discharge. The same is also true if the auxiliary management components consume energy from the battery.

#### **8.3.8. Average cycling lifetime**

Batscap claims an average cycling lifetime of 1000 cycles (lifetime of 200000 km with an autonomy of over 200 km for a complete charge).

#### **8.3.9. Recyclability**

Batscap states that the product is made of non-pollutant and recyclable materials.

## Chapter 9

# Lithium-Sulfur Batteries<sup>1</sup>

### 9.1. Introduction

At present, lithium/sulfur (Li-S) batteries are the subject of a great many investigative research projects the world over, in an academic sphere (the US Department of Energy (DoE) has invested nearly 8 million dollars in research; Japan's "New Energy and industrial technology Development Organization" (NEDO) has invested in research programs) and in an industrial sphere, with the R&D activities carried out by Samsung, Bosch and BASF. This technology is by no means new, because the earliest patents<sup>2</sup> filed on it date from the 1960s, with the concept having first been proposed by Herbert and Ulam in 1957. It was developed between 1960 and 1990 and then abandoned, probably because of the need to use a metal lithium negative electrode.

We are going to look at the reasons why interest in this technology has recently experienced a significant resurgence, and why it is now predicted

---

<sup>1</sup> This chapter is largely inspired by the state of the art given in the Doctoral Thesis of Céline Barchasz, project leader at CEA-Grenoble, entitled Développement d'accumulateurs lithium/soufre, Joseph Fourier University, Grenoble, October 2011.

<sup>2</sup> US Patent 3,043,896, Electric Dry Cells and Storage Batteries, D. Herbert, J. *Ulam*, (1962).

to become a promising alternative to conventional lithium-ion technology.<sup>3,4,5,6</sup>

## 9.2. The element sulfur

Sulfur (symbol S) is a tetravalent non-metallic element, relatively abundant (only 0.06% of the Earth's crust but easily extractable) and non-toxic (but flammable). This compound is found in its native state in the form of a yellow solid in volcanic regions, particularly in the vicinity of hot springs. Elementary sulfur exists in the form of a molecular solid, meaning that it comprises molecules which are held together by Van der Waals forces. The molecules themselves comprise sulfur atoms arranged in the form of rings of eight atoms, so is given the symbol S<sub>8</sub>.

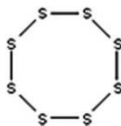


**Figure 9.1.** *Elementary sulfur S<sub>8</sub>*

Elementary sulfur exists, at ambient temperature, in the polymorphous form  $\alpha$  which is the most thermodynamically stable. It crystallizes in an orthorhombic lattice of “centered faces”. Its molar mass is 32.1 g/mol and its density is 2.07 g/cm.

## 9.3. Principle of operation

A Li-S battery comprises a positive electrode of elementary sulfur (S<sub>8</sub>), an organic liquid electrolyte and a negative electrode of metal lithium. More specifically, the positive electrode is usually composite, i.e. prepared using elementary sulfur and non-electroactive adjuvants. A finely powdered electronic conductor (carbon black or acetylene black) is used to improve the

3 X. Ji, L.F. NAZAR, Advances in Li-S batteries, *J. Mater. Chem.*, 20, 9821–9826, 2010.

4 M.-K. SONG, E.J. CAIRNS, Y. ZHANG, “Lithium/sulfur batteries with high specific energy: old challenges and new opportunities”, *Nanoscale*, The Royal Society of Chemistry, 2013.

5 S. S. ZHANG, “Liquid electrolyte lithium/sulfur battery: Fundamental chemistry, problems, and solutions”, *Journal of Power Sources*, 231, 153–162, 2013.

6 S. EVERS, L.F. NAZAR, “New Approaches for High Energy Density Lithium-Sulfur Battery Cathodes”, *Acc. Chem. Res.*, 2012.



electronic conductivity of the electrode, while a polymer binder is added to ensure cohesion between the materials. However, because they are not electrochemically active, the electronic conductor and binder need to be added in a minimal quantity so as not to significantly decrease the gravimetric and volumetric energy densities of the battery.

The electrochemical chain, therefore, is:



The main reactions at the electrodes are given below. When manufactured, the positive electrode is composed of elementary sulfur and the negative electrode of metal lithium, so initially the battery is in the charged state. During discharge, the elementary sulfur is reduced to form sulfur anions  $\text{S}^{2-}$  and the lithium is oxidized into  $\text{Li}^+$  cations. The  $\text{Li}^+$  and  $\text{S}^{2-}$  react to form lithium sulfide ( $\text{Li}_2\text{S}$ ).

### Positive electrode



### Negative electrode

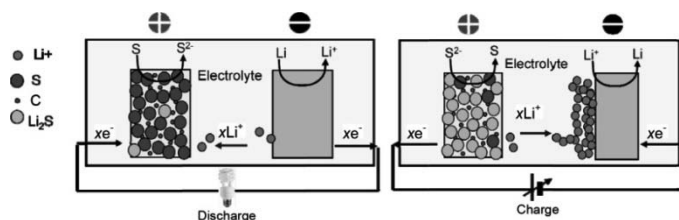


### Balance equation



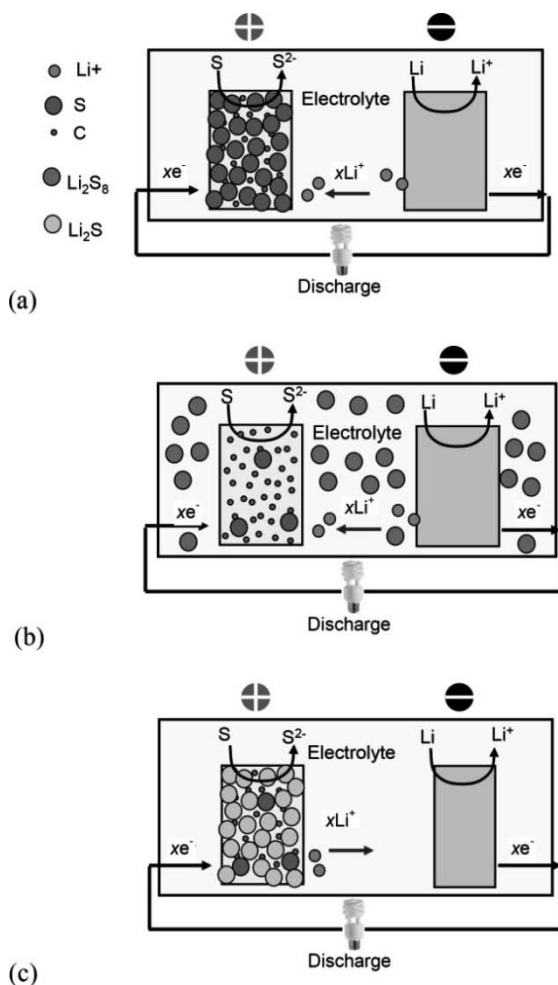
The difference in potential created is around 2.1 V.

Figure 9.2 gives an overview of the functioning of the system.



**Figure 9.2.** Principle of operation of a Li-S battery.  
*During discharge (left), the elementary sulfur is reduced and the metal lithium oxidized.  
 During charge (right), the reverse reactions take place at the electrodes*

The mechanism by which a Li-S battery is discharged is an unusual one, because it does not involve insertion reactions, conversion reactions or alloy formation. Unconventionally, the active material passes successively between the solid state and the dissolved state depending on the SOC of the battery. Most of the reduction mechanism occurs in solution. It is therefore possible to speak of a catholyte (= cathode dissolved in the electrolyte).



**Figure 9.3.** Simplified representation of the state of the system during discharge of an organic-electrolyte Li-S battery (a) charged state; (b) during discharge, (c) discharged state). The dissolution of the active material occurs at the beginning of discharge, whereas the completely reduced product –  $\text{Li}_2\text{S}$  – is insoluble. During the reduction, the metal lithium electrode is, for its part, partially consumed

A simplified representation of the state of the system during discharge is given in Figure 9.3. In the initial state, the active material is present in the solid state in the electrode, in the form of elementary sulfur (a). During the reduction of the sulfur, i.e. during the course of discharge, the cyclic sulfur molecules are reduced and form linear chains of lithium polysulfides, with the general formula  $\text{Li}_2\text{S}_n$ . Because the initial molecule is  $\text{S}_8$ , the first compounds to be formed are long-chain lithium polysulfides such as  $\text{Li}_2\text{S}_8$  or  $\text{Li}_2\text{S}_6$ . These polysulfides of lithium are soluble in the organic electrolytes, so the first stage of discharge consists of the dissolution of the active material in the electrolyte and the production of long-chain lithium polysulfides in solution (b). Then, as the reduction of the sulfur continues, the length of the polysulfide chains is gradually reduced, and compounds such as  $\text{Li}_2\text{S}_5$ ,  $\text{Li}_2\text{S}_4$  or  $\text{Li}_2\text{S}_2$  are formed in solution. Finally, the end product of the reduction is lithium sulfide ( $\text{Li}_2\text{S}$ ), which for its part is insoluble in organic electrolytes. Thus, the final stage in the mechanism of reduction of the sulfur is the precipitation of the sulfurized active material (c).

This is a simplified and approximate representation, because the exact mechanism of sulfur reduction is at present uncertain, and the following contradictory theories have been put forward by various authors:

- a relatively simple mechanism<sup>7</sup> of reduction of the sulfur by the lithium, involving few intermediary reaction products such as  $\text{S}_2^{2-}$  and  $\text{S}_4^{2-}$ ;
- a far more complex mechanism<sup>8, 9, 10</sup> which involves the formation of numerous radical<sup>11</sup> intermediary reaction products such as  $\text{S}_6^{2-}$ ,  $\text{S}_3^{2-}$  and  $\text{S}_3^{\bullet-}$ ;

---

7 K. KUMARESAN, Y.V. MIKHAYLIK, R.E. WHITE, “A mathematical model for a lithium-sulfur cell”, *J. Electrochem. Soc.*, 155, A576-A582, 2008.

8 Y. JUNG, S. KIM, “New approaches to improve cycle life characteristics of lithium-sulfur cells” *Electrochem. Commun.*, 9, 249–254, 2007.

9 B.S. KIM, S.M. PARK, “In situ spectroelectrochemical studies on the reduction of sulfur in dimethyl sulfoxide solutions” *J. Electrochem. Soc.*, 140, 115–122, 1993.

10 C. BARCHASZ, F. MOLTON, C. DUBOC, J.-C. LEPRÊTRE, S. PATOUX, F. ALLOIN, “Lithium/sulfur cell discharge mechanism: an original approach for intermediate species identification”, *Anal. Chem.*, 84, 3973–3980, 2012.

11 A radical species is a species with an un-accommodated electron. These species, such as radical ions, are mainly found in organic chemistry as reaction intermediates. They are unstable and react very quickly to form a different, more stable species. This free electron is symbolized by a superscript point beside the chemical symbol.

– formation<sup>12</sup> solely of the intermediary species  $S_8^{2-}$ ,  $S_4^{\bullet-}$  and  $S_3^{\bullet-}$ .

Thus, as we can see, there is no consensus as to the exact mechanism of reduction of elementary sulfur in an organic electrolyte, with the difficulty lying primarily in the numerous equilibrium points of the reaction, notably dismutation equilibrium and antidismutation<sup>13</sup> equilibrium, which exist in solution for  $S_8$  and make it tricky to study solutions of lithium polysulfides  $Li_2S_n$ .



The theoretical specific capacity of sulfur can be calculated simply using Faraday's law (section 2.3.3.2) where  $n$  = number of electrons exchanged (here  $16/8 = 2$  in accordance with reaction [9.2] for a sulfur atom) and  $M_S$  = molar mass of sulfur (32 g/mol):

$$\frac{1000 \times n \times F}{3600 \times M_S} = \frac{1000 \times 2 \times 96485}{3600 \times 32} = 1675 \text{ mAh/g} \quad [9.6]$$

Thus value needs to be compared with a  $LiCoO_2$  positive electrode with 0.5 lithium exchanged (calculated in section 5.3.1): 137 mAh/g.

Unless otherwise stated, the gravimetric capacities are expressed in milliampere-hours per gram of elementary sulfur contained in the positive electrode. Thus, the corresponding unit is written as mAh/g<sub>S</sub>. In practice, the gravimetric capacity will be low, because the positive electrode also contains inactive materials.

12 P. LEGHIÉ, J.P. LELIEUR, E. LEVILLAIN, "Comments on the mechanism of the electrochemical reduction of sulphur in dimethylformamide", *Electrochem. Comm.*, 4, 406-411, 2002.

13 When it is possible for an element to be both reduced and oxidized simultaneously, with the two reactions being coupled, we speak of a dismutation or antidismutation reaction:

Example of a dismutation mechanism:

$Cl_2^{(0)} + 2OH^- \rightarrow ClO^-^{(+1)} + Cl^-^{(-1)} + H_2O$  where  $Cl_2$  is oxidized into  $ClO^-$  and reduced into  $Cl^-$ .

Example of an antidismutation mechanism:

$ClO^-^{(+1)} + Cl^-^{(-1)} + H_2O \rightarrow Cl_2^{(0)} + 2OH^-$  where  $ClO^-$  is oxidized and  $Cl^-$  is reduced into  $Cl_2$ .

### 9.4. Discharge curve

The classic discharge curve for a Li-S battery is presented in Figure 9.4.

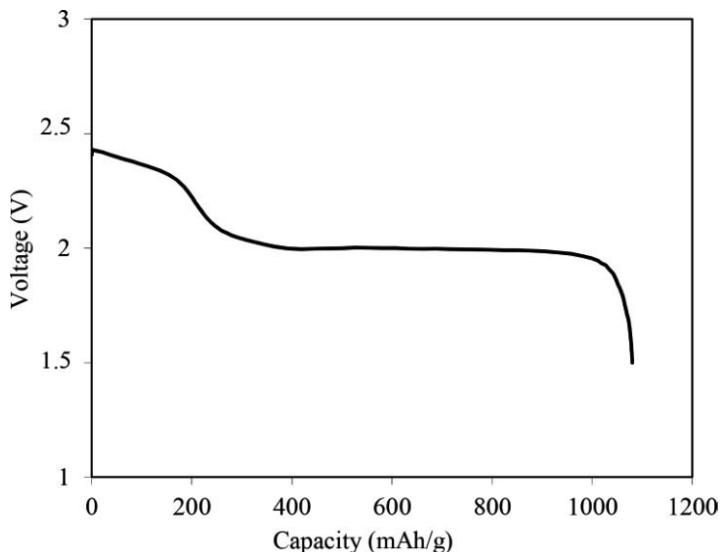


**Figure 9.4.** Classic discharge curve for a Li-S battery (source CEA)

*A priori*, the discharge curve presents two plateaus with different shapes. The plateau that can be seen at high potential, between 2.4 and 2.2 V, is sloped and is relatively short. On the other hand, the plateau that is observable at lower potential, at around 2 V, is relatively flat and much longer. The shape of this discharge curve has yet to be fully accounted for. The profile of discharge of a lithium-ion battery is generally revealing of the mechanism of electrochemical lithiation of the material, and each plateau is linked to a phase transition. However, because in the case of the Li-S battery, we are not dealing with a mechanism of insertion of the lithium ions but rather one of dissolution/precipitation, it is difficult to predict the evolution of the potential during discharge.

Finally, the average discharge potential is around 2.1 V, and from this we can deduce the gravimetric energy density that is theoretically accessible for a kilogram of sulfur by taking the theoretical gravimetric capacity of the positive electrode ( $S_8$ ) in the charged state calculated in equation [9.6]. By finding the product of this theoretical gravimetric capacity of 1675 mAh/g

by the average voltage 2.1 V, we get a theoretically accessible gravimetric energy density of 3517 Wh per kg of sulfur.

### 9.5. Advantages to Li-S

Although in theory, Li-S technology is capable of storing 3517 Wh per kg of sulfur (this value being calculated only for the positive electrode and in the fully-charged state), in practice – given the mass of the whole battery and the intrinsic electrochemical limitations – it is only capable of delivering 500 Wh/kg, or up to 700 Wh/kg as claimed by certain research teams.<sup>14</sup> However, this value is still much higher than that for other technologies. The argument in favor of the use of S-Li technology relates to its high potentiality in terms of its gravimetric and volumetric energy densities in comparison to lithium-ion technologies, as illustrated by Figure 9.5.

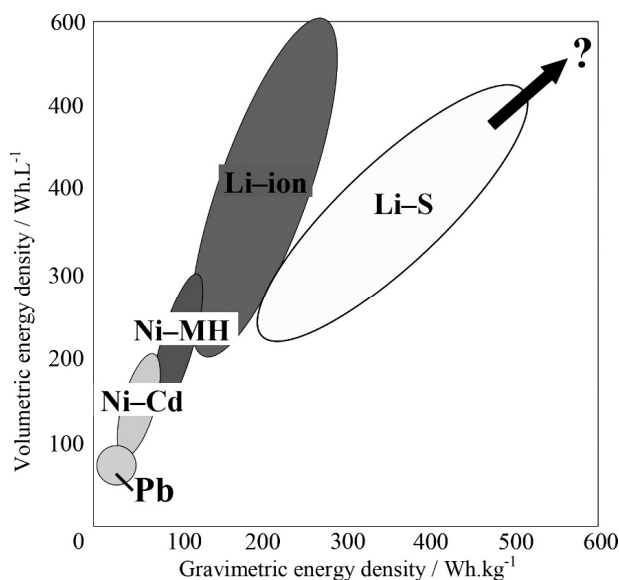


**Figure 9.5.** Comparison of different technologies for rechargeable batteries in relation to the emerging Li-S technology, in terms of gravimetric and volumetric energy densities (source CEA)

<sup>14</sup> This value is considerably higher than that for the couple C-LiCoO<sub>2</sub> used in lithium-ion technology, whose theoretical gravimetric energy density is 416 Wh/kg.

The advantages to this type of battery stems from the high gravimetric storage capacity of the sulfur positive electrode, up to ten times greater than that obtained with conventional positive electrode materials, used in Li-ion technologies (that of LFP is around 160 mAh/g). In addition, sulfur has the not-insignificant advantages of being abundant, affordable and non-toxic<sup>15</sup> – criteria which are also very important when envisaging large-scale commercialization, such as for EVs. Knowing that the cost of the positive electrode currently counts for a third of the total price of the conventional lithium-ion battery, we can quite clearly understand the need to develop alternative storage technologies such as Li-S.

## 9.6. Limitations and disadvantages of a Li-S battery

The limitations of the Li-S battery are many, and need to be resolved in order for commercialization to be possible. These limitations relate to the internal components: the electrode, electrolyte and separator.

### 9.6.1. Positive electrode

Because sulfur is an electronic insulator ( $\sigma = 5 \times 10^{-30}$  S/cm at 25°C), the presence of an electronically-conductive adjuvant (such as carbon black) is required to increase the electronic conductivity of the positive electrode and facilitate the redox reaction. In spite of the efforts which have been made to optimize the carbon black content and formulate the coating solution, the discharge regimes generally obtained with Li-S batteries remain relatively slow.

Elementary sulfur  $S_8$  is partially soluble in organic solvents. Therefore, the dissolved sulfur diffuses through the liquid electrolyte and reaches the negative electrode. It reacts chemically with the metal lithium, causing it to corrode. Hence, self-discharge of Li-S batteries is often significant, both in an open circuit and in operation.

The product  $Li_2S$  is insoluble in organic solvents, and precipitates at the end of discharge onto the positive electrode. As it is also an electronic insulator, it is responsible for the passivation of the positive electrode, and

---

<sup>15</sup> LFP also has the same characteristics, but unlike sulfur, which is to be found in the natural state, LFP has to be synthesized.

can lead to the formation of inactive areas on its surface. Many images taken with a scanning electron microscope (SEM) are presented in the existing literature, illustrating this passivation which appears to evolve, for instance, depending on the cycling regime (Figure 9.6).

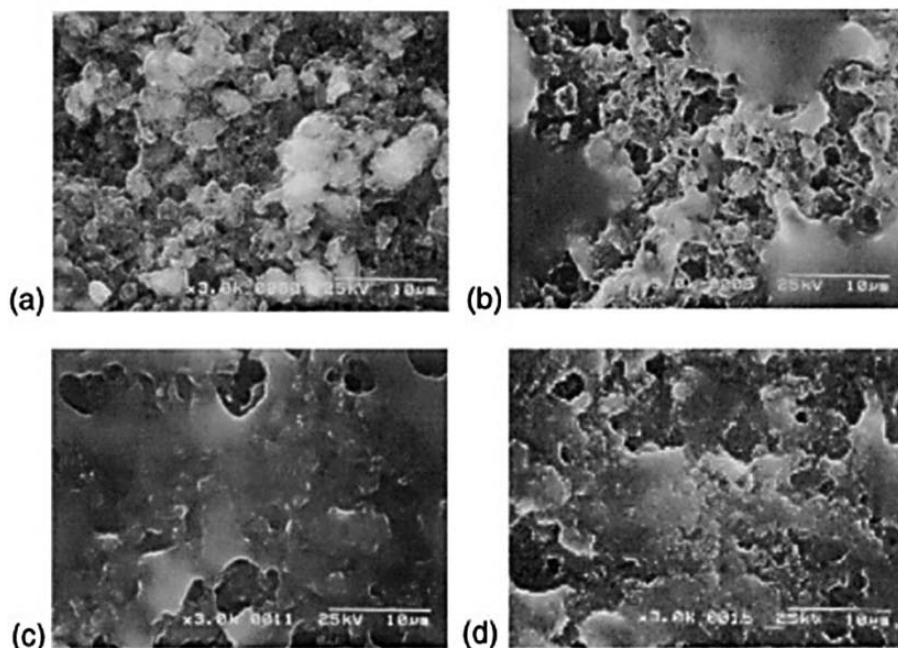


**Figure 9.6.** SEM images presented by Cheon *et al.*<sup>16</sup>, of a sulfur electrode at the end of discharge, covered by a fairly significant deposit of  $\text{Li}_2\text{S}$ . (a) before discharge, (b) after discharge at 1.5 V with a current density of  $0.26 \text{ mA}\cdot\text{cm}^{-2}$ , (c) after discharge at 1.5 V with a current density of  $1.74 \text{ mA}\cdot\text{cm}^{-2}$ , (d) after discharge at 1.5 V with a current density of  $3 \text{ mA}\cdot\text{cm}^{-2}$

In order to remedy this poor electronic conductivity of the active material, a number of different options are under investigation.

<sup>16</sup> S.E. CHEON, J.H. CHO, K.S. KO, C.W. KWON, D.R. CHANG, H.T. KIM, S.W. KIM, "Rechargeable lithium sulfur battery - I. structural change of sulfur cathode during discharge and charge", *J. Electrochem. Soc.*, 149, A1437–A1441, 2002.



#### 9.6.1.1. *Choice of electronically-conductive adjuvant*

The nature of the carbon used as an electronic conductor may vary<sup>17</sup>: carbon black from different sources with particle size distributions (PSDs) of 30–40 nm and specific surface areas of 100–2,000 m<sup>2</sup>/g (BET<sup>18</sup> surface), activated carbons, carbon fibers or indeed carbon nanotubes (CNTs). The type of carbon, its morphology and its mode of dispersion or coating play a part in the resulting electrical properties of the electrode. For instance, carbon fibers or CNTs improve the electronic conductivity of thick electrodes, because their high shape factor enables them to form a good electronic percolation lattice.<sup>19</sup> In the presence of CNTs, a capacity of 900 mAh/g<sub>S</sub> in the first cycle and 75% retention of capacity after 60 cycles (with a charge/discharge current density of 100 mA/g and 68% sulfur in the

---

17 S.E. CHEON, J.H. CHO, K.S. KO, C.W. KWON, D.R. CHANG, H.T. KIM, S.W. KIM, “Structural factors of sulfur cathodes with polyethylene oxide binder for performance of rechargeable lithium sulfur batteries”, *J. Electrochem. Soc.*, 149, A1437–A1441, 2002.

18 The Brunauer, Emmett and Teller (BET) method explains the physical adsorption of gas molecules (N<sub>2</sub> or CO<sub>2</sub>) to a solid surface and is based on the fact that the adsorbed gas molecules tend to form a fine layer which covers the whole of the surface of the solid. Thus, it enables us to measure the specific surface area (m<sup>2</sup>/g) of the sample (generally powders) and the distribution of its pores as a function of their size. The acronym BET comes from the initials of the surnames of S. Brunauer, P. H. Emmett and E. Teller – American scientists who, in 1938, published the first article on the BET method.

19 The term “percolation lattice” in electrochemistry characterizes the movement of the electrons in a composite electrode, i.e. comprising a blend of materials with different electrical properties: an electrochemically-active material which is involved in the main electrochemical reaction (e.g. a manganese oxide), a polymer binder (generally non electro-active) and a material serving to conduct electrons (e.g. carbon black, acetylene black, carbon fibers). This lattice is essential for the electrochemical reaction to take place, conditioned by the circulation of electrons in the electrode, from the current collector to the active site of the material (where the ions participating in the reaction are present). It is the coexistence of the ions and electrons at the same place on the active site which facilitates this “triple contact”, so that the electrochemical reaction can happen. Overall, the quantity of these electronic conductors that is added needs to remain minimal so as to maximize the energy densities of the battery. It is therefore necessary to determine the optimal amount of conductive adjuvant to deliver the best possible electronic conductivity (without sacrificing the electrochemical performances, mechanical strength or total cost). This work is done during the so-called electrode formulation stage. We also find the term “percolation threshold”, which corresponds to the composition for which the behavior of an electrode goes from being insulative to being conductive. Below the percolation threshold, the blend tends to behave as an insulator. Above this threshold, the blend is conductive, and the electrons can easily move around. The percolation threshold can be reached by increasing the amount of conductive material.

electrode).<sup>20</sup> Certain authors also claim 40% initial capacity in the fast regime (with a current density of 1600 mA/g during charge/discharge with 50% of S in the electrode).

#### 9.6.1.2. *Addition of an adjuvant to adsorb lithium polysulfides*

CNTs or certain carbon blacks with large specific surface areas can also be employed, because of their adsorbing effect. Indeed, their use enables us to limit the dissolution of the active material, which largely remains adsorbed to the adjuvant. Certain authors report a capacity during the initial discharge of 1200 mAh/g<sub>S</sub> (at 100 mA/g and with less than 60% S in the electrode), yielding an improved cyclability.

The adsorbing effect on polysulfides can also be obtained with adjuvants, either metal or oxide in nature (oxides of aluminum, vanadium, etc.). For instance, tests would give us a relatively stable specific capacity, greater than 1,000 mAh/g<sub>S</sub>, for more than 50 cycles (with a C/10 current) if we use the compound Mg<sub>0.6</sub>Ni<sub>0.4</sub>O. However, these results need to be carefully interpreted because they are obtained with an electrode whose sulfur content is low (only 20% of its mass).

#### 9.6.1.3. *Method for preparation of the carbon/sulfur composite*

A number of different modes of preparation are used:

- Mixing with the conductive adjuvant and the polymer binder by mechanical agitation in solution before the molding of the electrode. Because of this stage of homogenization, the carbon is evenly distributed around the sulfur particles, and therefore creates a percolation lattice.

- Additional milling to improve the mixture between the components in solution. However, this step may alter the final porosity of the electrode, leading to a loss of capacity. This step of milling can be carried out beforehand in a dry environment. With this pretreatment, the sulfur is coated with carbon and overall the composite presents an improved electronic conductivity in comparison to sulfur alone. Such coating can also be done in the vaporous phase.

---

20 L. YUAN, H. YUAN, X. QIU, L. CHEN, W. ZHU, “Improvement of cycle property of sulfur-coated multi-walled carbon nanotubes composite cathode for lithium/sulfur batteries”, *J. Power Sources*, 189, 1141–1146, 2009.

– Coating of the carbon black with a layer of sulfur (giving rise to a structure with a core and an active skin rather than an active core with a skin as before):

- by precipitation of the sulfur from sulfur dioxide  $\text{SO}_2$  onto nanoparticles of carbon black – e.g. by synthesis in a liquid medium (water or ethanol):  $\text{SO}_2 + 2\text{S}^{2-} + 4\text{H}^+ \rightarrow 3\text{S}_{\downarrow} + 2\text{H}_2\text{O}$ ;

- by physical vapor deposition of sulfur into the pores of the carbon. The drawback to this coating technique is that it causes polarization (see footnote 31 in Chapter 6) which is greater during discharge, probably attributable to the need to expend additional energy to break the C-S bonds formed by close contact between the carbon and sulfur.

Other, innovative approaches to the making of a carbon/sulfur composite structure have been put forward. Of these, we can cite the use of a mesoporous carbon<sup>21</sup> structure (alignment of carbon tubes) which offers a high volume of pores, good electronic conductivity and the possibility of confining the active material in channels left free between the tubes (Figure 9.7).

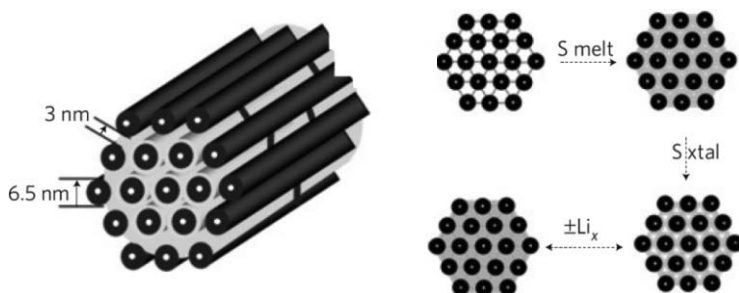


**Figure 9.7.** *Diagram of the principle of preparation of the carbon/sulfur composite*<sup>22</sup>

The use of a carbon exhibiting bimodal porosity with a multitude of pre-existing micropores has also been suggested (Figure 9.8).

<sup>21</sup> A mesoporous carbon combines a large specific surface area with porosity on the nanometric scale. We speak of mesopores when the diameter of the pores is between 2 and 50 nm (reminder: micropores: < 2 nm; macropores: > 50 nm).

<sup>22</sup> X. LI, K.T. LEE, L.F. NAZAR, "A highly ordered nanostructured carbon-sulphur cathode for lithium-sulphur batteries", *Nature Materials*, 8, 500–506, 2009.

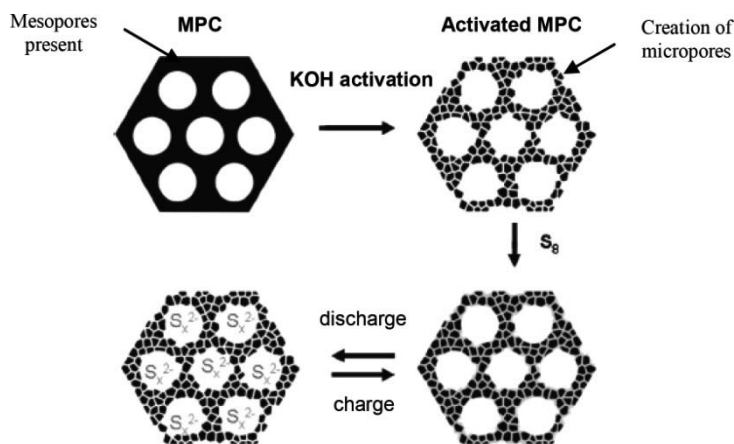


**Figure 9.8.** Diagram of the principle of the carbon/sulfur composite with bimodal porosity and its cycling behavior<sup>23</sup>

In this last example, the idea is also to give the active material favorable environments for its confinement in the electrode regardless of its physical state. Thus, the sulfur, which is initially solid, is contained within the carbon structure. During discharge, the lithium polysulfides are dissolved in the mesoporous channels (greater volume).

However, irrespective of the carbon structure, the confinement of the polysulfides is not perfect, because the electrolyte is still in contact with the sulfurated active material, and we see a progressive increase in the amount of sulfurous compounds in the electrolyte over the course of cycling, which bears witness to this gradual dissolution, followed by a pollution of the negative electrode. Nonetheless, these architectures are capable of accommodating a significant deposit of end-of-discharge products, and offer a buffer structure to deal with the variations in volume of the electrode during cycling (the volume of Li<sub>2</sub>S is twice that of sulfur); hence the improved overall cyclability in the second example.

#### 9.6.1.4. Pretreatment of the active material

The powdered active material can be milled so as to reduce the size of the particles of sulfur and obtain better usage of the active material, and

<sup>23</sup> C. LIANG, N.J. DUDNEY, J.Y. HOWE, "Hierarchically structured sulfur/carbon nano composite material for high-energy lithium battery", *Chem. Mater.*, 21, 4724–4730, 2009.

therefore a greater capacity.<sup>24</sup> Indeed, it has been shown that the PSD of the active material influences the nature of the percolation lattice; thus, the finer the sulfur particles, the greater the surface area of contact between sulfur and carbon, which helps increase the percentage usage of active material (from 35 to 50% usage when the particle size decreases from 20 to 5  $\mu\text{m}$ , for instance). In the same vein, the sulfur can first be sieved to exclude the largest particles.

Other studies attempt to couple elementary sulfur with a conductive polymer such as polythiophene or polypyrrole in order to improve the electronic conductivity of the electrode whilst having an effect of retention of lithium polysulfides. In addition, all authors agree that the presence of this polymer helps to fix the active material to the positive electrode, which prevents it from accumulating during the course of cycling.<sup>25</sup>

#### 9.6.1.5. Formulation of $\text{Li}_2\text{S}$ -based composite electrodes

The safety problems which are inherent to the use of metal lithium for the negative electrode can be resolved by the use of a positive electrode containing a source of lithium, based on lithium sulfide ( $\text{Li}_2\text{S}$  with a theoretical capacity of 1,170  $\text{mAh/g}_{\text{Li}_2\text{S}}$ ). The  $\text{Li}_2\text{S}$  electrode can then be coupled with a negative electrode made of a material such as graphite (C), silica (Si) or tin (Sn).<sup>26</sup> Thus, once again we find ourselves in the category of lithium-ion batteries. Many teams of researchers have come out in favor of lithium-ion-sulfur technology, which has the advantage of eliminating the problem of dendrites (see section 4.4.2). On the other hand, the charge/discharge mechanism of the  $\text{S}_8/\text{S}^{2-}$  electrode in this new type of battery remains unchanged, as do the problems inherent to the electrode: dissolution, poor electronic conductivity of the active material, passivation at the end of the cycle, undesirable shuttle mechanism (see section 7.1.4), etc. The active material  $\text{Li}_2\text{S}$  is, like elementary sulfur, an electronic insulator. Therefore, it has to be coated with carbon (by milling or some other technique).

24 S.E. CHEON, J.H. CHO, K.S. KO, C.W. KWON, D.R. CHANG, H.T. KIM, S.W. KIM, "Structural factors of sulfur cathodes with polyethylene oxide binder for performance of rechargeable lithium sulfur batteries", *J. Electrochem. Soc.*, 149, A1437–A1441, 2002.

25 S. KAKUDA, T. MOMMA, T. OSAKA, G.B. APPETECCHI, B. SCROSATI, "Ambient-temperature, rechargeable, all-solid lithium/polypyrrole polymer battery", *J. Electrochem. Soc.*, 142, L1–L2, 1995.

26 J. HASSOUN, Y.K. SUN, B. SCROSATI, "Rechargeable lithium sulfide electrode for a polymer tin/sulfur lithium-ion battery", *J. Power Sources*, 196, 343–348, 2011.

### 9.6.2. Electrolyte

The dissolution of the sulfurous active material in the electrolyte during cycling causes numerous problems:

- Firstly, the dissolution of these lithium polysulfides can lead to an increase in the viscosity of the electrolyte. These species are highly soluble in the electrolyte, and the concentrations can reach up to 10 mol/L. In such conditions, the electrolyte becomes viscous and the ionic mobility is decreased.

- Similarly, the dissolved lithium polysulfides can diffuse through the electrolyte, corrode the metal lithium negative electrode and cause self-discharge. In the extreme case, if the reaction of these polysulfides reaches the extent that the compound  $\text{Li}_2\text{S}$  is formed, this precipitate can be deposited on the metal lithium negative electrode, partially blocking the electrode. This causes an irreversible loss of active material on the negative electrode, which accounts for the poor cycling resistance of this type of battery.<sup>13, 27</sup>

- Finally, a characteristic which is rare for a lithium battery, the presence of these polysulfides dissolved in the electrolyte leads to the appearance of an undesirable redox shuttle mechanism.<sup>28</sup> Based on the model of the mechanism for protection of lithium-ion batteries against over-charge phenomena (adjuvants to the electrolyte, redox shuttles), this shuttle mechanism occurs naturally during charge in Li-S batteries. The short-chain polysulfides are then oxidized into long-chain molecules at the positive electrode. These long-chain polysulfides are soluble, and are apt to diffuse through the electrolyte and reach the metal lithium electrode, where they are reduced to form short-chain polysulfides. The species again diffuse toward the positive electrode, where they can then be re-oxidized into long chains, and so on. The occurrence of this mechanism fixes the potential of the battery, because the reactions at the electrodes are dictated by the redox shuttle. The battery is then said to be over-charged, as is illustrated in Figure 9.9.

---

27 X. LIANG, Z. WEN, Y. LIU, H. ZHANG, L. HUANG, J. JIN, *J. Power Sources*, 196, 3655–3658, 2011.

28 Y.V. MIKHAYLIK, J.R. AKRIDGE, “Polysulfide shuttle study in the Li-S battery system”, *J. Electrochem. Soc.*, 151, A1969–A1976, 2004.

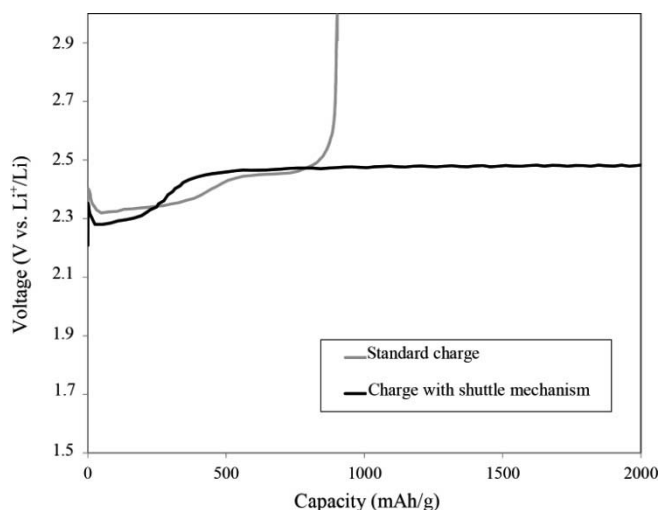


**Figure 9.9.** Curves of galvanostatic charge for two Li-S batteries: one presenting a conventional charge curve, and the other illustrating the phenomenon of overcharge (source CEA)

The shuttle mechanism occurs at constant potential (here around 2.45 V). However, it does not occur in all cases, because it depends on the capacity of the species to diffuse through the electrolyte. Thus, its occurrence is a function of the cycling regime, which determines the time the species have in which to diffuse through the electrolyte (a mechanism which can be seen in a low regime). Similarly, the cycling temperature and the viscosity of the electrolyte solvents play an important role in this shuttle mechanism, because these parameters condition the mobility of the species in the electrolyte (the shuttle mechanism is encouraged at high temperature or low viscosity).

Normally, the redox shuttle is exploited (see section 7.1.4) to protect batteries against over-charge (indeed, certain lithium-ion batteries have very poor tolerance to prolonged charges).<sup>29</sup> Thus, this intrinsic mechanism can logically be seen as a way of protecting S-Li batteries against over-charge phenomena. However, as it occurs at around 2.4 V, the battery has not yet finished charging. If this shuttle mechanism is partial, i.e. if the oxidation at the positive electrode is faster than the reduction at the negative electrode,

<sup>29</sup> K. XU, "Nonaqueous liquid electrolytes for lithium-based rechargeable batteries", *Chemical Reviews*, 104, 4303–4417, 2004.

the battery will continue to charge progressively and the uppermost limit of cycling will be attained only after a prolonged period of over-charge. It is possible to fully charge the battery, but it takes a very long time, which causes a significant loss of faradaic efficiency, because some of the charge current is consumed at the positive electrode to oxidize the short-chain sulfides into long-chain sulfides, rather than to oxidize  $S^{2-}$  into  $S_8$  (two competing electrochemical mechanisms are present). On the other hand, this shuttle mechanism can also continue to occur indefinitely, as long as the charge process is applied if species mobility is encouraged (oxidation of short-chain sulfides into long-chain sulfides during charging at the positive electrode, which again become short-chain molecules when they migrate through the inter-electrode space and are reduced at the negative electrode). This being the case, the battery will never attain a 100% SOC. This shuttle mechanism renders end-of-charge detection very difficult, because it blocks the voltage rise, which is a classic indicator (Figure 9.9).

In order to overcome these difficulties, work is being done on the electrolyte, experimenting with the use of ether molecules such as 1,3-dioxolane (DIOX) or tetrahydrofuran (THF). Solvents such as glyme, whose general formula is given in Figure 9.10 (such as 1,2-dimethoxyethane (DME)), are also commonly used in Li-S batteries. However, these solvents flounder because of their property of solubilization of lithium polysulfides.

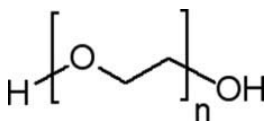


**Figure 9.10.** General chemical formula of glyme-type solvents ( $n = 1, 2, 3, \dots$ )

Just like carbonates, ether-type solvents are not stable in comparison to metal lithium, and are reduced at the negative electrode. However, they cause the formation of a stable passivation layer at the SEI, which ultimately helps to protect the negative electrode. In general, ether-type solvents can be employed in all types of lithium batteries. However, the electrochemical stability of ethers against oxidation is not as good as that of carbonates ( $<4$  V versus  $Li^+/Li$  as opposed to  $\approx 4.5$  V versus  $Li^+/Li$  for carbonates), which is why they are very infrequently used. However, this window of stability is perfectly compatible with the Li-S battery (cycled between 1.5 and 3 V).



Other studies mention the use of solvents from the sulfonate family, including toluene, added into the electrolyte (2–10% volume), which decreases the dissolution and diffusion of polysulfides through the electrolyte. Furthermore, this adjuvant helps improve the saturability of the electrolyte with the positive electrode. Finally, as it has low viscosity, toluene also improves the ionic conductivity of the electrolyte. A number of authors also make a case for the use of ionic liquids, stating that it is possible to decrease/limit the dissolution of the active material in the electrolyte by using this very particular family of solvents.

#### 9.6.2.1. *Dry and gelled polymer electrolytes*

Liquid electrolytes cause significant dissolution of the active material, and encourage its diffusion toward the negative electrode. Thus, an alternative is to use polymer electrolytes.<sup>30, 31</sup>

In this case, we have an electrolyte identical to that which is present in lithium-polymer batteries, made of poly(ethylene oxide) (or PEO) in the presence of a lithium salt, solid at ambient temperature, and which needs to be heated above ambient temperature in order for the battery to work ( $T > 65^{\circ}\text{C}$  for PEO). Thus, the electrolyte, in its molten state, exhibits sufficient ionic conductivity for the lithium ions to pass. This type of electrolyte can be used on its own (without a membrane) because it ensures physical separation of the positive and negative electrodes. This type of polymer electrolyte needs to be differentiated from gelled or plasticized electrolytes, wherein a polymer is mixed with a lithium salt but also with a solvent or a blend of organic solvents, and which function at ambient temperature. In the case of a Li-S battery, dry polymer membranes are often preferred because they present a genuine “all solid” state at ambient temperature, which helps limit the dissolution of the active material and therefore self-discharge. Similarly, in the molten state (viscous polymer), the diffusion of the species is slowed, and there is the hope of being able to contain the lithium polysulfides near to the positive electrode. In addition, this technology limits the formation of dendrites on the metal lithium

---

30 J. HASSOUN, B. SCROSATI, “Moving to a solid-state configuration: a valid approach to making lithium-sulfur batteries viable for practical applications”, *Advanced Materials* vol. 22, issue 45, pp. 5198–5201, December 1, 2010.

31 D. MARMORSTEIN, T.H. YU, K.A. STRIEBEL, F.R. McLARNON, J. HOU, E.J. CAIRNS, J. *Power Sources*, 89, 219–226, 2000.

negative electrode, and can therefore be seen as a means of protection of the metal lithium.

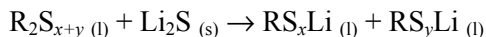
#### 9.6.2.2. *Lithium salts and adjuvants to liquid, polymer or gelled electrolytes*

The salt most commonly used in Li-S batteries is LiTFSI, which exhibits good chemical, thermal and electrochemical stability (no corrosion of the aluminum in the window of potential of the sulfur electrode, no formation of hydrofluoric acid – HF). Similarly, because of its high degree of dissociation in ethers, it enables us to obtain good ionic conductivity values, of around  $5 \times 10^{-3} \text{ S/cm}$  at  $20^\circ\text{C}$ . Hence, it constitutes an alternative to  $\text{LiPF}_6$  salt which is used in conventional lithium-ion batteries but is not very soluble in ether solvents.

Other salts or adjuvants can also be added to the formulation of liquid or polymer electrolytes, in order to lend them specific properties:

– Nitrogenous adjuvants (such as lithium nitrate, whose formula is  $\text{LiNO}_3$ , or indeed nitromethane –  $\text{CH}_3\text{NO}_2$ ), on whose use the American company Sion Power ([www.sionpower.com](http://www.sionpower.com)) holds a patent. These compounds decompose *in situ* on the metal lithium negative electrode and protect it. Thus passivized, the lithium electrode is far less reactive with lithium polysulfides dissolved in the electrolyte, and the shuttle mechanism is eliminated. Similarly, self-discharge appears to be significantly reduced, because the open-circuit potential remains around 2.4 V, whereas a rapid drop in potential to 2.15 V is observed with the classic electrolyte (with no adjuvant). A study has been carried out on the effect of the  $\text{LiNO}_3$  adjuvant on the passivation of the metal lithium electrode, demonstrating the formation of  $\text{Li}_x\text{NO}_y$  and  $\text{Li}_x\text{SO}_y$  compounds on the surface of the electrode which prevent the metal lithium from continuously reacting with the sulfurous active material in solution.

– Organic polysulfide compounds, with the general formula  $\text{R}_2\text{S}_{x+y}$ , which limit the irreversible deposition of  $\text{Li}_2\text{S}$  on the metal lithium electrode.<sup>32</sup> The compound  $\text{Li}_2\text{S}$  reacts with  $\text{R}_2\text{S}_{x+y}$  according to the reaction:




---

<sup>32</sup> B.A. TROFIMOV, M.V. MARKOVA, L.V. MOROZOVA, G.F. PROZOROVA, S.A. KORZHOVA, M.D. CHO, V.V. ANNENKOV, A.I. MIKHALEVA, “Protected bis(hydroxyorganyl) polysulfides as modifiers of Li-S battery electrolyte”, *Electrochim. Acta*, 56, 2458–2463, 2011.

and forms a soluble and electrochemically active product:  $RS_xLi$  (or  $RS_yLi$ ), which limits the loss of capacity over the course of cycling.

- Halogenated electrolyte adjuvant (such as LiBr or LiCl), which reacts with the lithium sulfide precipitated on the negative electrode, dissolving it.

- Addition of lithium polysulfides into the electrolyte, which decrease the solubility of the active material in solution. By the saturation effect, the organic liquid electrolyte soon attains the maximum capacity of dissolved sulfurous species, and therefore the lithium polysulfides from the positive electrode can no longer be dissolved.<sup>33</sup>

#### 9.6.2.3. *Porous separators for liquid electrolytes*

The separator is generally a porous membrane of polyolefins (polyethylene, polypropylene) (as an example, we can cite Celgard®-brand separators) used in combination with a liquid electrolyte to ensure physical separation between the two electrodes.

It is also optimized in Li-S batteries, because it has an impact on the mobility of the species in the electrolyte. With the aim of confining the active material to the positive electrode, a two-layer separator has been developed which is based on polypropylene covered with a copolymer of PVdF-HFP<sup>34</sup> and nanoparticles of clay (montmorillonite). The clay particles prevent the passage of the polysulfide anions through the separator, confining them within the compartment of the positive electrode, and help improve the cycling durability of the technology.

#### 9.6.3. *Negative electrode*

As highlighted previously, the use of a metal lithium electrode is well known for being tricky – particularly because of its tendency to favor the formation of dendrites. Especially when using liquid electrolytes, dendrite formation almost invariably leads to the occurrence of short-circuits during cycling or when the current densities are too high.

---

33 H. YAMIN, A. GORENSHTEIN, J. PENCINER, Y. STERNBERG, E. PELED, “Lithium sulfur battery oxidation/reduction mechanisms of polysulfides in THF solutions”, *J. of Electrochem. Soc.*, 135, 1045–1048, 1988.

34 PVdF-HFP: Poly(vinylidene fluoride-co-hexafluoropropene).

Metal lithium is known to be extremely reactive with organic electrolytes and their impurities. The electrolyte becomes passivized immediately when the battery is activated. The SEI is then composed of the products of degradation of the organic solvents, the lithium salt and the impurities that are present. If this passivation layer formed *in situ* is not a good ionic conductor, the electrode will be blocked and the battery will be faulty. Similarly, if this layer is continuously formed, the lithium electrode will gradually be consumed, and will therefore no longer be available to participate in the electrochemical processes.

The work being done regarding the negative electrode aims to decrease its reactivity with lithium polysulfides, and limit dendrite formation. A number of strategies are possible.

#### 9.6.3.1. *Use of means to protect the metal lithium*

– Deposition of a layer of  $\text{Li}_3\text{N}-\text{CuN}_x$  on the metal lithium, by CVD, followed by the deposition of a ceramic which is conductive of lithium ions (such as LiSICON – “*Lithium Super Ion CONductor*”, e.g.  $\text{Li}_x\text{Al}_y\text{Ge}_z(\text{PO}_4)_3$ ).<sup>35</sup> This “all-solid” layer of electrolyte prevents dendrite formation, by ensuring the rigidity of the lithium/electrolyte interface. The disadvantage to this system, however, lies in the fragility of the ceramic layer. Indeed, this layer is made as thin as possible, because of the poor ionic conductivity of the material (around  $10^{-4}$  S/cm at ambient temperature). With a thickness of only a few micrometers, the layer is liable to crack during cycling (cycles of dissolution/precipitation of the metal lithium, and a negative electrode which swells during charge and contracts during discharge). If it does crack, this can exacerbate the problem of dendrite formation. Note that a fairly similar design has been presented by the company Sion Power, mentioned previously.

– Direct deposition of a layer of ion-conductive ceramic – LiPON, which has the formula  $\text{Li}_x\text{PO}_y\text{N}_z$ , often used as a solid electrolyte in lithium micro-batteries – and a (softer) polymer, on the surface of the lithium. In this latter case, a solution of macromonomers of poly(ethylene glycol) dimethacrylate, mixed with a radical initiator and a liquid electrolyte (which also guarantees ionic conductivity in the polymer layer), is deposited on the surface of the negative electrode. After UV activation, a layer of some ten micrometers in thickness is formed, covering the strip of metal lithium, which helps to

---

35 Patents held by the company PolyPlus ([www.polyplus.com/lisulfur.html](http://www.polyplus.com/lisulfur.html)).

eliminate the phenomenon of the shuttle mechanism, or at least slow it down.

#### 9.6.3.2. *Use of a lithiated negative electrode instead of pure lithium*

– Alloys such as LiAl, LiGe or LiSi, which prevent the formation of dendrites during charge. The operational potential of these negative electrodes is slightly greater than 0 V – ranging between 0.1 and 0.7 V versus  $\text{Li}^+/\text{Li}$  – but the loss of energy is largely compensated for by the gain in the safety of the batteries.

– Lithiated graphite. The graphite electrode is generally prepared in a conventional way, and the step of chemical lithiation is done by bringing the carbon material into contact with a metal lithium foil, or by CVD of the metal lithium. Lithiation can also be performed electrochemically (cycling of the graphite electrode with metal lithium, and then recovery of it). The drawback to this lithiation technique, however, is its industrial feasibility, as it is difficult to implement for large-scale production and with large surface areas.

## 9.7. Conclusion

Through the references cited here, we have shown that the literature on the development of Li-S batteries is abundant, and that there are many and diverse approaches to improving the durability of the technology, which still falls down on the as-yet-insufficient number of cycles that it can deliver. In summary:

- optimization of the positive electrode, with the aim of containing the active material in the electrode as much as possible (use of absorbent adjuvants, structured materials);
- optimization of the composition of the electrolyte in an attempt to reduce the dissolution of the active material and its diffusion toward the negative electrode (development of polymer- or gelled electrolytes);
- improvement of the structure and chemical composition of the separator (adjuvants to the electrolyte help improve the passivation of the metal lithium);

– protection of the metal lithium negative electrode and the sulfurous active material against dendrite formation (use of a  $\text{Li}_2\text{S}$  positive electrode, which provides a source of lithium and opens the way for all materials for the negative electrode other than metal lithium).

Research efforts should resolve these difficulties and render the technology attractive.

## Chapter 10

# Lithium-Air Batteries<sup>1</sup>

### 10.1. Introduction

As the name indicates, metal–air technologies have an air positive electrode using oxygen (of which there are unlimited reserves) and a metal negative electrode. With regard to the air electrode, their operation is similar to that of the well-known fuel-cell technology.<sup>2</sup> Given that one of the electrodes is fed by oxygen from the air, one often finds a very high value of gravimetric energy density, because unlike with other couples, one of the components (oxygen) is not stored in the battery in the charged state.<sup>3</sup> However, the specific powers are necessarily low, because the input of oxygen is limited. Thus, such systems are capable of providing weak currents over long periods of time, and are therefore often used in conjunction with supercapacitors in order to serve power needs.

---

<sup>1</sup> We are grateful for the amiable participation, in the writing of this chapter, of Céline Barchasz, a researcher at CEA-Grenoble, and Charles Gayot, currently a doctoral candidate at CEA-Grenoble whose thesis is precisely on the development of Li–Air technology. We have also been supported by Frédéric Le Cras, dispatched from CEA-Grenoble to the University of Nantes, and by Sébastien Patoux, Head of the *Laboratoire des Matériaux pour Batteries* at CEA-Grenoble.

<sup>2</sup> M.C. PÉRA, D. HISSEL, H. GUALOUS, C. TURPIN, *Electrochemical Components*, ISTE, London, John Wiley & Sons, New York, 2013.

<sup>3</sup> Of course, during discharge, the oxygen combines with the positive electrode, which decreases the gravimetric energy density.

Because of its very low molar mass (6.9 g/mol), lithium, as a metal, is obviously a very attractive choice to make the negative electrode, which led to the introduction of the lithium-dioxygen system (or lithium-air; the molar mass of oxygen is 16 g/mol) as a rechargeable element, first advanced in 1976.<sup>4</sup> Also, in the electrochemical reactions in which they are involved, the lithium at the negative electrode ( $E^0(\text{Li}^+/\text{Li}) = -3.05 \text{ V/NHE}$ ) and the oxygen at the positive electrode ( $E^0(\text{O}_2/\text{OH}^-) = 0.40 \text{ V/NHE}$  in an aqueous medium, and  $E^0(\text{O}_2/\text{O}^{2-}) = 1.12 \text{ V/NHE}$  in an anhydrous medium) offer a significant difference of redox potential of 3.45 V or 4.17 V.

In relation to other couples using lithium, the lithium-air battery is original in the sense that it is not necessary to store the positive active material in the battery itself. For this reason, lithium-air batteries may have a higher gravimetric energy density than conventional lithium-ion technologies such as lithiated metal oxides/carbon. The couple  $\text{Li-O}_2$  has a potentially very high gravimetric energy density: around 12,000 Wh/kg excluding the oxygen, or around 3,600 Wh/kg including the oxygen<sup>5</sup> (see the calculations in the appendix to this chapter – section 10.7). However, these values are theoretical, and do not take account of the mass of the components associated with the supply of oxygen to act as the positive electrode, current collectors, electrolyte, separators, casing, etc. Thus, in the existing body of literature, we find many different values depending on whether the reactants and the reaction products are taken into account, or on other issues such as the internal components and the operating conditions applied. However, it can be estimated that an objective of 1,000 Wh/kg will be judicious.<sup>6, 7, 8</sup> This gravimetric energy density remains the highest out of all the electrochemical couples known today. For comparative purposes, lithium-ion batteries commercialized today offer a practical gravimetric energy density which peaks at around 200 Wh/kg.

---

4 D. N. BENNION, E. L. LITTAUER, “Mathematical model of a lithium water electrochemical power cell.” *J. of Electrochem. Soc.*, 123, 1462–1469, 1976.

5 The mass of the battery increases over the course of discharge, because oxygen is absorbed by the positive electrode.

6 P. BRUCE, S. FREUNBERGER, L. HARDWICK, J.-M. TARASCON, “ $\text{Li-O}_2$  and Li-S batteries with high energy storage”, *Nature Mat.*, 11, 19–29, 2012.

7 J. CHRISTENSEN, P. ALBERTUS, R. S. SANCHEZ-CARRERA, T. LOHMANN, B. KOZINSKY, R. LIEDTKE, J. AHMED, A. KOJIC, “A critical review of Li/air batteries”, *J. of Electrochem. Soc.*, 159, R1-R30, 2012.

8 H.-G. JUNG, J. HASSOUN, J.-B. PARK, Y.-K. SUN, B. SCROSATI, “An improved high-performance lithium-air battery”, *Nature Chemistry*, 4, 579–585, 2012.



However, as mentioned at the start of the chapter on lithium-ion batteries (see footnote 4 in Chapter 4), the low density of the materials (oxygen and lithium) is a negative factor for the volumetric energy density.

Finally, much like air fuel cells<sup>9</sup>, as the input of oxygen is limited, its specific powers are low: 200 W/kg and 500 W/L.

Although there are still numerous technological difficulties to be resolved (rechargeability, carbonation of the lithium, sealing, corrosion, lifetime, limited power, operating temperature, etc.), lithium-air batteries are still promising candidates for energy storage. It is for this reason that we shall devote this chapter to them.

## 10.2. Operational principle

The lithium-air battery consists of a positive electrode of porous carbon, designed to ensure the diffusion and reduction of the oxygen, and a negative electrode of metal lithium. The two electrodes are separated by an electrolyte which is conductive of lithium ions. At present, development efforts are focused mainly on two Li-O<sub>2</sub> technologies, with an aqueous electrolyte or with an organic electrolyte<sup>10</sup>, involving different reactions and stresses. An old study suggested the use of a salts-based electrolyte; there is an argument to be made for this technique, but its use was discontinued.<sup>11</sup>

Generally, the electrochemical chain is written thus:



During discharge, the metal lithium is oxidized into lithium ions with the release of electrons at the negative electrode, as expressed by the half-reaction  $\text{Li} \rightarrow \text{Li}^+ + \text{e}^-$ .

---

<sup>9</sup> Zinc-air batteries are used in auditive prostheses (hearing aids).

<sup>10</sup> K.M. ABRAHAM, Z. JIANG., "A polymer electrolyte-based rechargeable lithium/oxygen battery", *J. of Electrochem. Soc.*, 143, 1-5, 1996.

<sup>11</sup> K. W. SEMKOW, A. F. SAMMEILS, "A lithium oxygen secondary battery", *J. Electrochem. Soc.*, Accelerated Brief Communications, 143, 2084-2085, 1987.

The electrons released are transported via the external circuit to the positive electrode, while the dissociated lithium ions diffuse through the electrolyte to the positive electrode. Still at the positive electrode, oxygen is catalytically reduced at the surface, and – depending on the type of electrolyte used – forms either a hydroxide ion  $\text{OH}^-$  (in an aqueous medium) or a peroxide ion  $\text{O}^{2-}$  (in an organic medium), which combines with the  $\text{Li}^+$  ions present in the electrolyte.

### 10.2.1. Aqueous $\text{Li-O}_2$

Due to the high reactivity of lithium with water, it is not possible for a lithium-oxygen battery to directly use an aqueous solution as an electrolyte, unless the negative electrode (of metal lithium) can be protected against parasitic degradation. One solution to this problem is to form a completely solid electrolyte (polymer or ceramic) or to incorporate a blended electrolyte.<sup>12</sup> This constraint makes it very tricky to design aqueous  $\text{Li-O}_2$  batteries. This accounts for the fact that, although a great deal of research has been devoted to the study of  $\text{Li-O}_2$  with a solid or blended electrolyte, a very large proportion of the articles published relates to  $\text{Li-O}_2$  with an organic electrolyte (technology examined in section 10.2.2).

The principle behind the aqueous  $\text{Li-O}_2$  battery (in a basic medium) is illustrated in Figure 10.1.

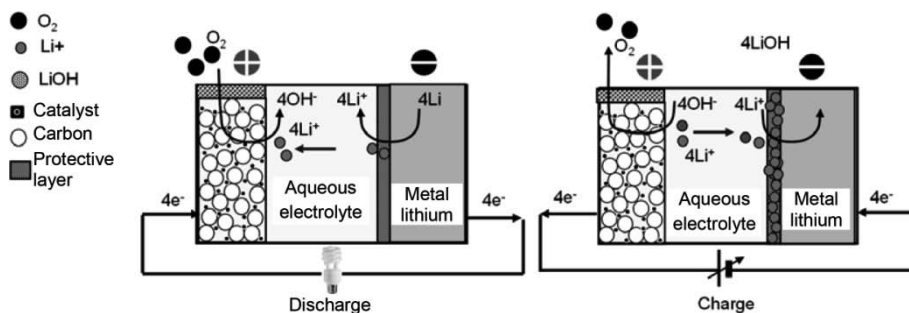


**Figure 10.1.** Diagram of the principle behind an aqueous  $\text{Li-O}_2$  cell (basic medium)

12 T. ZHANG, N. IMANISHI, Y. TAKEDA, O. YAMAMOTO, "Aqueous lithium/air rechargeable batteries", *Chem. Lett.* 40, 668–673, 2011.

In a basic or neutral medium, the reactions at the electrodes are:

– **Positive electrode**



– **Negative electrode**



– **Balance equation**



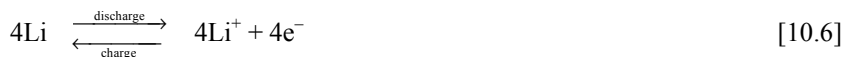
Metal lithium, water and oxygen are consumed during the discharge reaction. The theoretical potential of the reaction is 3.45 V, but the potential measured during discharge tends more to be around 2.85 V (see section 10.4.1.1).

In an acidic medium<sup>13</sup>, the reactions involve protons  $\text{H}^+$ . In the presence of the counter-ion<sup>14</sup> of the acid present, the  $\text{Li}^+$  ions combine to form the corresponding lithium salt. For instance, considering the counter-ion  $\text{CH}_3\text{COO}^-$  of acetic acid  $\text{CH}_3\text{COOH}$  or  $(\text{CH}_3\text{COO}^-, \text{H}^+)$ , lithium acetate  $\text{CH}_3\text{COOLi}$  or  $(\text{CH}_3\text{COO}^-, \text{Li}^+)$  is formed, as is water ( $\text{H}_2\text{O}$ ).

– **Positive electrode**



– **Negative electrode**

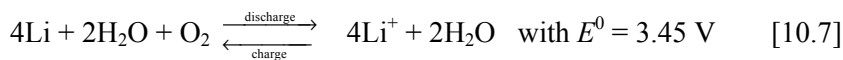



---

13 T. ZHANG, N. IMANISHI, Y. SHIMONISHI, A. HIRANO, J. XIE, Y. TAKEDA, O. YAMAMOTO, N. SAMMES, “Stability of a water-stable lithium metal anode for a lithium-air battery with acetic acid–water solutions”, *J. Electrochemical Society*, 157, A214–A218, 2010.

14 When speaking of an acid, the part without the  $\text{H}^+$  is called the counter-ion. For instance, with acetic acid, whose formula is  $\text{CH}_3\text{COOH}$ , the counter-ion is  $\text{CH}_3\text{COO}^-$ .

### – Balance equation

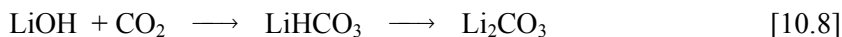


Physical protection of the metal lithium against the water is the essential criterion for operation of the cell to be possible and viable in the long term. This physical protection, which is conductive of  $\text{Li}^+$  ions, ensures the integrity of the lithium without direct contact with the aqueous electrolyte.

Two other issues also need to be considered:

– in a basic or neutral medium, the concentration of the product formed,  $\text{LiOH}$ , increases progressively with the advancement of the reaction, and the number of moles of  $\text{LiOH}$  may surpass the solubility limit of 5.25 M (at  $20^\circ\text{C}$ ). Beyond this point,  $\text{LiOH}$  precipitates in the form of monohydrated lithium hydroxide ( $\text{LiOH} \cdot \text{H}_2\text{O}$ ). This precipitation complicates the operation of the cell, which needs to allow for such a precipitation to occur by allowing reversible storage of  $\text{LiOH} \cdot \text{H}_2\text{O}$  (development of an *ad hoc* membrane for protection of the lithium), or preventing it. This phenomenon conditions the specific energies and the energy densities that are accessible;

– the cell also needs to be able to function whilst preventing the precipitation of  $\text{Li}_2\text{CO}_3$  (because of the presence of  $\text{CO}_2$  in the air) via the reaction:



#### 10.2.2. Organic $\text{Li-O}_2$

The principle behind the organic (or anhydrous)  $\text{Li-O}_2$  battery is illustrated in Figure 10.2.

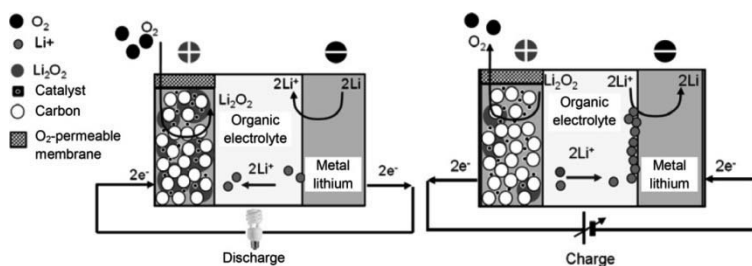


Figure 10.2. Diagram of the principle behind an anhydrous  $\text{Li-O}_2$  cell

The reactions at the electrodes are given below. The oxygen is reduced by an electrochemical reaction involving either two electrons (equation [10.9]) or four electrons (equations [10.9] and [10.12]).

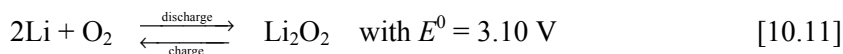
– **Positive electrode**



– **Negative electrode**

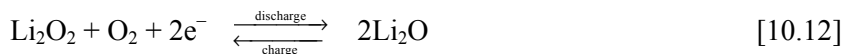


– **Balance equation**

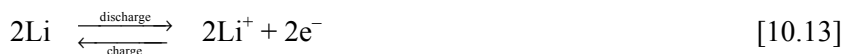


Depending on the discharge current and the composition of the electrolyte, a portion of  $\text{Li}_2\text{O}_2$  may be discharged earlier to form  $\text{Li}_2\text{O}$ .

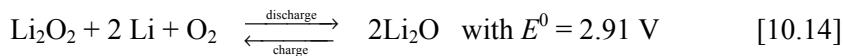
– **Positive electrode**



– **Negative electrode**



– **Balance equation**



By combining equations [10.11] and [10.14], we get:



Certain authors also indicate the possibility of a competing reaction, involving a superoxide ion:<sup>15</sup>

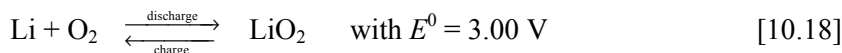
– **Positive electrode**



– **Negative electrode**



– **Balance equation**



If the superoxide ion has a sufficient lifetime, it reacts with another electron to form  $\text{O}_2^{2-}$ :



and again we have equation [10.9].

A chemical reaction also takes place which is similar to that described above, leading to the formation of  $\text{Li}_2\text{O}_2$  from  $\text{LiO}_2$ .



Because the measured potentials of these two reactions of reduction of  $\text{O}_2$  are very similar (3.10 V with two electrons involved and 2.91 V with four electrons involved), lithium peroxide ( $\text{Li}_2\text{O}_2$ ) or indeed lithium oxide ( $\text{Li}_2\text{O}$ ) may be the most abundant product at the end of discharge. The use of specific catalysts may encourage one of the two reactions over the other.

---

15 V. S. BRYANTSEV, V. GIORDANI, W. WALKER, M. BLANCO, S. ZECEVIC, "Predicting solvent stability in aprotic electrolyte Li-air batteries: nucleophilic substitution by the superoxide anion radical ( $\text{O}_2(\bullet-)$ )", *The Journal of Physical Chemistry A*, 115, 2399–12409, 2011.

The alternative mechanism suggested at the positive electrode with the transitory presence of the superoxide ion  $\text{O}_2^{\cdot-}$  is not desirable, because carbonate-based electrolytes are already known not to be compatible with the superoxide ion, similarly to other families of organic solvents.

Regardless of which reactions occur, during the course of a discharge, the reduction products ( $\text{LiO}_2$ ,  $\text{Li}_2\text{O}$  and  $\text{Li}_2\text{O}_2$ ) will progressively fill up the pores which are accessible to oxygen.

For organic Li- $\text{O}_2$  technology, the key criterion is that the cell be able to function with reversible storage of  $\text{Li}_2\text{O}_2$ .

### 10.3. Electrolytes

Four types of electrolyte have been developed for two technologies of Li- $\text{O}_2$  batteries (Figure 10.3):

- aqueous electrolyte<sup>16</sup> (basic  $\text{LiOH}$ );
- non-aqueous, organic electrolyte;<sup>17, 18, 19</sup>
- dual electrolyte – aqueous on the side of the positive electrode, and organic on the side of the negative electrode, with the two compartments being separated by a solid electrolytic wall;<sup>20</sup>
- solid, polymer or ceramic electrolyte.<sup>21</sup>

---

16 H. HE, W. NIU, N. M. ASL, J. SALIM, R. CHEN, Y. KIMA, “Effects of aqueous electrolytes on the voltage behaviors of rechargeable Li-air batteries”, *Electrochimica Acta*, 67, 87– 94, 2012.

17 J. READ, “Characterization of the lithium/oxygen organic electrolyte battery”, *J. of Electrochem. Soc.*, 149, A1190–A1195, 2002.

18 J. READ, “Ether-based electrolytes for the lithium/oxygen organic electrolyte battery”, *J. of Electrochem. Soc.*, 153, A96–A100, 2006.

19 S. S. ZHANG, D. FOSTER, J. READ, “Discharge characteristic of a non-aqueous electrolyte  $\text{Li}/\text{O}_2$  battery”, *J. Power Sources*, 195, 1235–1240, 2010.

20 P. ANDREI, J. P. ZHENG, M. HENDRICKSON, E. J. PLICHTA, “Modeling of Li-air batteries with dual electrolyte”, *J. of Electrochem. Soc.*, 159, A770–A780, 2012.

21 T. ZHANG, N. IMANISHI, S. HASEGAWA, A. HIRANO, J. XIE, Y. TAKEDA, O. YAMAMOTO, N. SAMMES, “Li/polymer electrolyte/water stable lithium-conducting glass ceramics composite for lithium–air secondary batteries with an aqueous electrolyte”, *J. of Electrochem. Soc.*, 155, A965–A969, 2008.

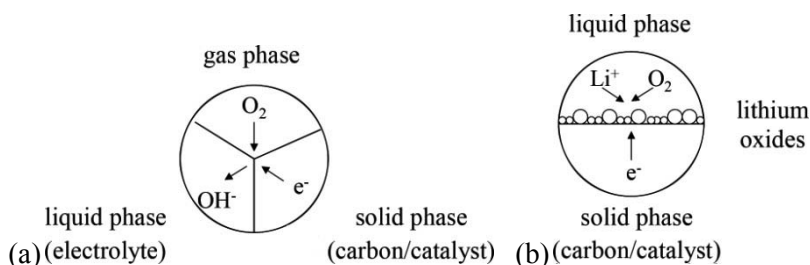


Figure 10.3. Representation of the interactions involved for (a) an aqueous electrolyte; (b) a non-aqueous electrolyte<sup>22</sup>

Figure 10.3(a) describes the interactions between gas, liquid and solid which occur at the positive electrode when an aqueous electrolyte is used. Oxygen, in the gaseous phase, combines with electrons from the carbon electrode/catalyst according to the reaction at the positive electrode in an aqueous electrolyte:



The compound  $\text{OH}^-$  formed is dissolved in the aqueous solution.

Figure 10.3(b) shows the interactions between the liquid and solid which occur when a non-aqueous electrolyte is used. Oxygen is in the electrolyte solution and combines with electrons from the carbon/catalyst system and lithium ions from the electrolyte.

We can see that the major difference between an aqueous and a non-aqueous electrolyte is that the reduction products  $\text{Li}_2\text{O}$  and  $\text{Li}_2\text{O}_2$  for the latter, non-aqueous system are not soluble in the electrolyte, and form a thin deposit on the surface of the carbon positive electrode (Figure 10.3(b)).

It is for this reason that we frequently find a value for the specific capacity of organic lithium-oxygen batteries which is standardized in relation to the carbon electrode: the mass of carbon is used in calculating the specific capacity because the products of reduction during discharge block the available pores. The reduction products can be dissociated reversibly to re-form the initial reactants (oxygen and lithium ions).

<sup>22</sup> R. PADBURY, X. ZHANG, "Lithium-oxygen batteries – Limiting factors that affect performance", *J. Power Sources*, 196, 4436–4444, 2011.



It has been shown that when the solubility of oxygen in organic electrolytes increases, the specific capacity of the battery also increases because of the greater concentration of oxygen available for the reduction reaction. The other parameters such as conductivity and viscosity have their own effect on the specific capacity of the battery: for instance, a low viscosity and a high conductivity of the electrolyte ensure that the lithium ions can access the positive electrode. This demonstrates the importance of choosing the best electrolyte for non-aqueous lithium-oxygen batteries.

The electrochemical stability of liquid electrolytes containing carbonates has been studied in relation to a lithium electrode. It has been shown that the reduction reactions on lithium involve an  $O_2$  radical to form a lithium alkyl carbonate ( $RO-(C=O)-OLi$ ) and lithium carbonate ( $Li_2CO_3$ ). This shows that carbonate-type solvents greatly influence the reaction products, which runs counter to the redox mechanisms discussed above.

#### 10.4. Main limitations

Research is actively being pursued to deal with the limiting factors, to produce commercially-viable lithium-air batteries (sufficient lifetime in terms of charge/discharge cycles, operation with oxygen from the air).<sup>23</sup>

We can cite the development of:

- negative electrodes which are stable and protected against humidity;
- structures of positive electrodes which are improved and optimized in terms of micro-porosity to facilitate the diffusion of oxygen, whilst preserving high electrical conductivity;
- electrolytes offering solubility and a high oxygen diffusion coefficient and a good conductivity of lithium ions;
- catalysts which facilitate the reaction of oxygen formation and reduce the overvoltages of oxygen release at the electrode.

---

23 I. KOWALCZK, J. READ, M. SALOMON, “Li-air batteries: a classic example of limitations owing to solubilities”, *Pure Appl. Chem.*, 79, 851–860, 2007.

### 10.4.1. General limitations<sup>22</sup>

#### 10.4.1.1. Overvoltages

The standard potential of the lithium-oxygen battery given by Nernst's equation considers only the thermodynamic properties of the active materials contained in each of the two electrodes. The standard potential can be affected by kinetic factors. The potentials of charge and discharge may therefore deviate from the standard potential, because of the presence of these terms of overvoltages linked to the kinetics of the reactions. The overvoltages represent the extra energy required to drive reactions whose current density is high, in addition to the energy defined by the thermodynamics. Figure 10.4 shows a typical charge/discharge curve with the overvoltages – positive during charge and negative during discharge.

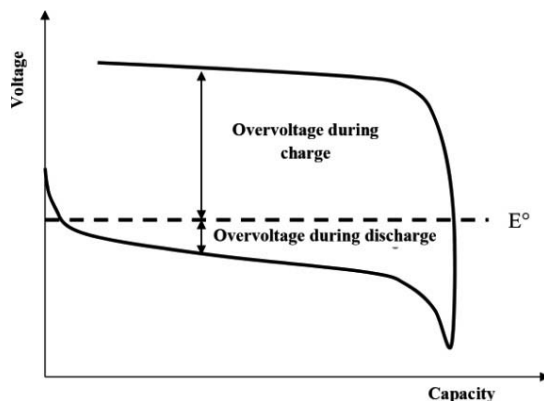


**Figure 10.4.** Charge/discharge curve with the overvoltage during charge and discharge<sup>22</sup>

These phenomena are present in Li-O<sub>2</sub> batteries when a non-aqueous electrolyte is used; thus the overvoltages are linked to the insoluble reduction products formed, such as Li<sub>2</sub>O<sub>2</sub>. During discharge, lithium peroxide increases the internal resistance of the cell and reduces the reaction kinetics, which is shown by the negative overvoltage. Finally, when the reduction products block the porous lattice of the positive electrode, the reduction reaction is interrupted and the current strength at which the reaction takes place determines the value of the capacity attained. The hysteresis between the profile of voltage during charge and discharge is due to the significant difference in potential which is necessary to dissociate the lithium peroxide during charge. The use of a catalyst in the electrochemical reactions helps

reduce the overvoltages, and thereby to reduce the hysteresis between the charge and discharge curves.

#### 10.4.1.2. Catalysts

A decrease of the hysteresis between the voltage curves during charge and discharge, with a view to improving the energy efficiency of the lithium battery, can be achieved by incorporating a bi-functional platinum-gold/carbon (Pt-Au/C) catalyst into the carbon positive electrode, for example. The use of a catalyst can facilitate the charge reaction by reducing the voltage required to dissociate the reduction products into metal lithium and oxygen. Figure 10.5 compares typical charge/discharge curves for lithium-oxygen batteries with and without a manganese dioxide catalyst.<sup>22</sup>

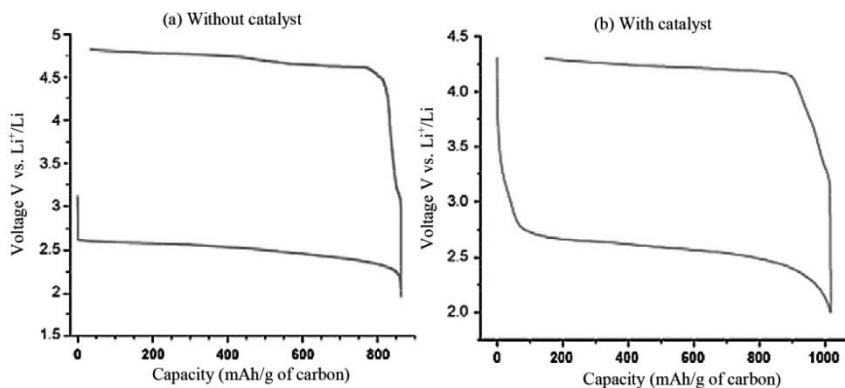


**Figure 10.5.** Charge/discharge curves (a) with and (b) without the manganese dioxide catalyst (electrodes made of the same type of carbon, discharged with the same current density)<sup>22</sup>

In this particular case, the introduction of the catalyst improves the capacity from 850 to around 1000 mAh/g, and decreases the charge potential by around 0.5 V. We can conclude from these results that the catalyst has improved the charge reaction by reducing the charge potential, and increased the kinetics of the discharge reaction, which leads to an increase in the specific capacity of the battery.

In addition, it should be noted that the voltages required to charge the lithium-oxygen battery are very high ( $>4.5$  V), which may damage the

electrolyte. The degradation of the electrolytic solution decreases the performances and also the lifetime of the lithium-oxygen battery.

#### 10.4.1.3. *Diffusion and solubility*

Diffusion is an important mechanism in the operation of a Li-O<sub>2</sub> battery. Firstly, at the positive electrode, the oxygen penetrates into the porous electrode at the electrode/oxygen interface and diffuses through the network of pores to combine with the lithium ions from the electrolyte and the electrons from the external circuit. The diffusion of the oxygen is linked to the porosity of the carbon positive electrode, because it offers an easy path for the oxygen through the electrode. The oxygen solubility also affects the kinetic of the battery, because it has to dissolve in the electrolyte at the electrode/oxygen interface before it can diffuse through the porous lattice of the positive electrode to combine with the lithium ion and electrons. The oxygen dissolved in the electrolyte is less mobile than oxygen in the gaseous phase, which further decreases the reaction kinetics and affects the overall performances of the battery. However, it has been shown that increasing the partial pressure of oxygen improves its diffusion and the concentration of oxygen in the positive electrode, which corresponds to an increase of the specific capacities. Furthermore, it is important that the lithium ions be able to diffuse easily through the electrolyte from the negative to the positive electrode.

#### 10.4.1.4. *Filling of the positive electrode with electrolyte*

The filling of the positive electrode with electrolyte is also a criterion that needs to be considered, which can affect the overall efficiency and capacity of the lithium-air battery.

The reference cited in footnote 22 demonstrates this. Based on the mode of electrolyte filling, it classifies positive electrodes into three categories: flooded, dry or wetted, as illustrated by Figure 10.6.

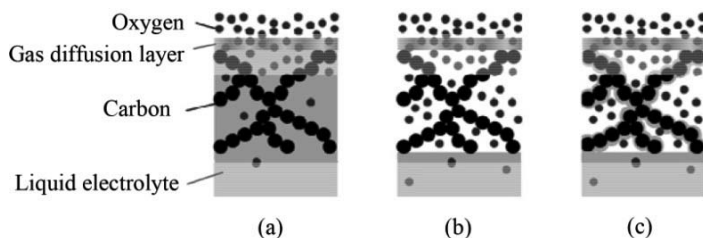


**Figure 10.6.** *Electrolyte filling in the positive electrode: (a) flooded; (b) dry; (c) wetted*<sup>22</sup>

Case 1: In a flooded positive electrode, oxygen needs to dissolve in the electrolyte at the electrode/oxygen interface and, as previously indicated, oxygen dissolved in the electrolyte is less mobile than oxygen in the gaseous phase. Consequently, the kinetics of this system is slow, because of the stage of dissolution of the oxygen in the electrolyte.

Case 2: In a positive electrode which is insufficiently filled with electrolyte (dry), the oxygen can penetrate more easily and more deeply into the positive electrode. However, the lithium ions present in solution are not present at the interface between the positive electrode and the electrolyte.

Case 3: In a positive electrode in an intermediary state of filling (wetted), the conditions are optimal, creating a more uniform concentration of oxygen- and lithium ions in the positive electrode. This means that an optimal surface area of the positive electrode is used during the discharge reaction.

Figure 10.7 gives an account of the discharged capacities of three Li-O<sub>2</sub> batteries with different levels of electrolyte filling.

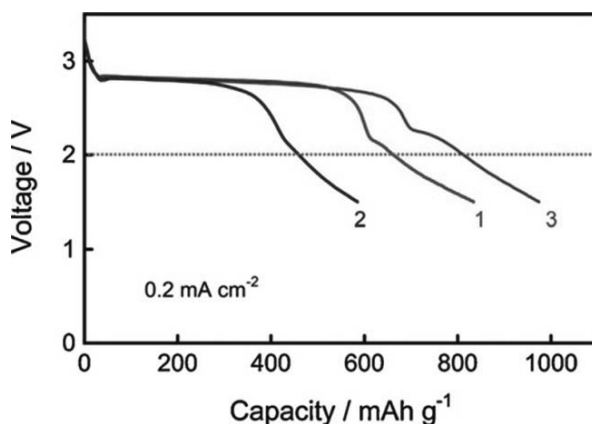


**Figure 10.7.** Discharge curves for three Li-O<sub>2</sub> batteries with different levels of electrolyte filling with a 0.2 mA/cm<sup>2</sup> current, (1) with insufficient electrolyte (dry), (2) with excess electrolyte (flooded), (3) with the right amount of electrolyte (wetted)<sup>19</sup>

#### 10.4.1.5. Porosity and amount of carbon

The amount of reduction products formed during discharge correlates directly to the porosity of the electrode. As previously indicated, the reduction products are insoluble in a non-aqueous electrolyte (Li<sub>2</sub>O, Li<sub>2</sub>O<sub>2</sub>).

Thus, deposits form on the surface of the positive electrode, preventing the discharge reaction, which leads to a reduction in specific capacity. Also, lithium peroxide ( $\text{Li}_2\text{O}_2$ ) is a poor electrical conductor, so as the discharge reaction progresses, the internal resistance increases as lithium peroxide is deposited, thereby limiting electron transfer. It has been shown that when the porosity increases, the specific capacity of the battery increases.<sup>19</sup> An optimization of the size of the pores is necessary in order to improve the kinetics and the capacity of the battery. A different study<sup>24</sup> indicates that pores of diameter less than 10 nm are insufficient to maintain oxygen diffusion and accommodate the reduction products during discharge. Another important factor to consider is the combination between the porosity and the carbon content of the positive electrode. If the carbon content increases, the porosity of the positive electrode decreases, reducing the kinetics of the reaction and leading to a lower specific capacity. However, it is important to optimize the amount of carbon contained in the positive electrode so as to preserve good electronic conductivity.

#### 10.4.1.6. *Surface area of carbon and porosity*

The surface of the carbon electrode is also important for the battery's performances. As a general rule, a larger surface area enables a greater quantity of catalyst to be dispersed, and offers more reaction sites for the electrochemical reactions. However, it has been proven that carbons with large specific surface areas do not always correspond to a greater specific capacity.<sup>24</sup> This further highlights the importance of the porosity, and especially the diameter of the pores.

In the context of these developments, we can cite the development of a carbon electrode with a honeycomb-like structure.<sup>25</sup>

#### 10.4.1.7. *Operating conditions*

It is important to control the operating conditions of lithium-oxygen batteries during discharge. The performances are sensitive to:

- The depth of discharge applied, which has a significant effect on the specific capacity and even the reversibility of the reactions (Figure 10.8).

<sup>24</sup> X.H. YANG, P. HE, Y.Y. XIA, "Preparation of mesocellular carbon foam and its application for lithium/oxygen battery", *Electrochem. Commun.* 11, 1127–1130, 2009.

<sup>25</sup> X. LIN, L. ZHOU, T. HUANG, A. YU, "Hierarchically porous honeycomb-like carbon as a lithium-oxygen electrode", *J. Mater. Chem. A*, 1, 1239–1245, 2013.

The first scenario (see curve (a) in Figure 10.8) corresponds to cycling with a significant DOD. A very significant loss of capacity is observed as early as the third cycle. The second scenario (curve (b) in Figure 10.8) limits the discharge capacity to 1000 mAh/g for a current density of 0.1 mA/cm<sup>2</sup>. The curve of capacity discharged remains stable until the tenth cycle. The last scenario (curve (c) in Figure 10.8) is intermediary between the first two, and represents discharge to a limited DOD with a gradual decrease of the capacity discharged as the cycles continue. As previously indicated, during discharge, the reduction products are deposited on the surface of the carbon electrode, which increases its internal resistance. After a deep discharge, the positive electrode is not completely recharged, i.e. the charge voltage is not sufficient to decompose the lithium peroxide, leading to a significant drop in the specific capacity for subsequent cycles. However, by controlling the DOD, it is possible to maintain sufficient porosity so that, during charge, the reactions can take place, ensuring the maintenance of the specific capacity as cycles progress. This shows that the DOD is an important factor which affects the specific capacity of the lithium-oxygen batteries, and is a parameter which needs to be controlled if we are to achieve acceptable performances.

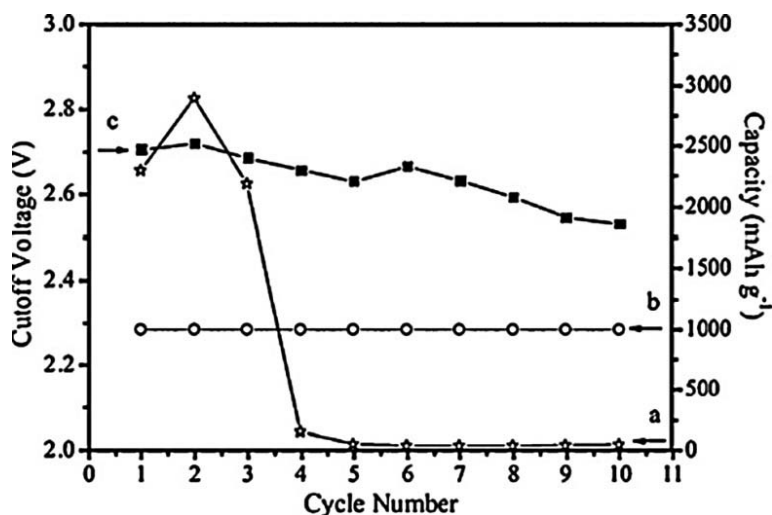


**Figure 10.8.** Cycling performance of the lithium-oxygen battery, (a) with a deep discharge, (b) limiting the capacity to 1,000 mAh/g with a current density of 0.1 mA/cm<sup>2</sup> (c) with limited DOD

– The current density (Figure 10.9). Experience tells us that maintaining a low current density (typically between 0.05 and 0.1 mA/cm<sup>2</sup>) improves the overall specific capacity of the battery.<sup>19</sup> However, in practice, a battery with a high operational current density is desirable in order to obtain high power.

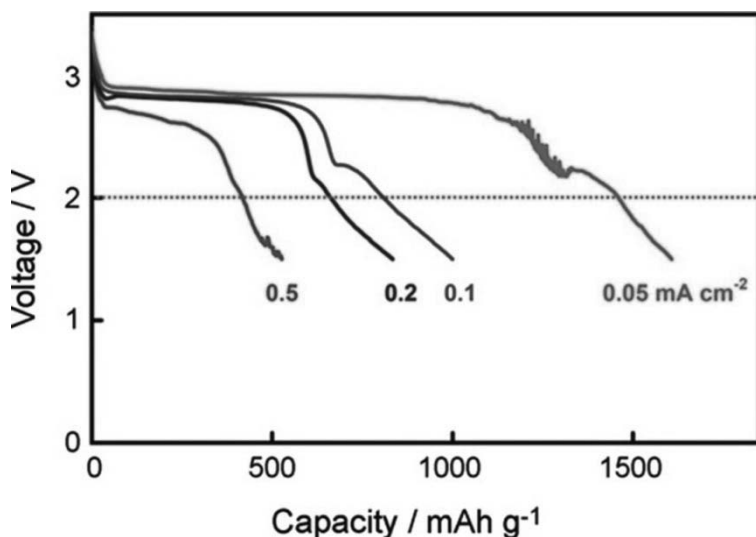


**Figure 10.9.** *Specific capacity as a function of the discharge current*<sup>18</sup>

Thus, a key objective in the development of high-performance lithium-oxygen batteries is also to maximize the kinetics of the reaction at the electrode so that high current densities can be applied to the element, whilst preserving a high and stable specific capacity.

### 10.5. Main actors

The main actors in the development of this technology are:

In the USA:

– Yardney Technical Products, Inc. / Lithion (Pawcatuck, Connecticut), who designed a prototype of large dimensions (256 cm<sup>2</sup>) with a liquid organic electrolyte (molar LiPF<sub>6</sub> in an equal-parts mixture of



EC/DEC/DMC<sup>26</sup>). An adjuvant appropriate for oxygen transport is added into the electrolyte to increase the oxygen diffusion coefficients. The performances attained with low current densities (0.05 mA/cm<sup>2</sup>) are 2500 mAh/g and, at high current densities (2 mA/cm<sup>2</sup>), drop to 200 mAh/g (www.yardney.com);

- PolyPlus Battery Company (Berkeley, California), who have published interesting results in an aqueous electrolyte with the integration of a protective layer of ceramic LISICON on the surface of the lithium (www.polyplus.com);

- LiOX Power, a startup company in Pasadena, California (www.liox.com);

- Excellatron Solid State LLC, who develop lithium-air batteries for applications such as cellphones, airplanes and the space industry (www.excellatron.com);

- IBM<sup>27</sup> (Almaden Lab in San Jose, California) (www.research.ibm.com/labs/ almaden).

In Asia:

- the Japanese company Toyota<sup>28</sup> for the EV application, claiming performances of 800 mAh/g of carbon (sufficient to deliver 2,100 Wh/kg, approximately) at 0.02 mA/cm<sup>2</sup> and 25°C and a capacity of 60% in relation to the initial capacity after 100 cycles for an element using a Li/PC<sup>26</sup>, LiTFSA<sup>29</sup> (1 M)/carbonated positive electrode impregnated with MnO<sub>2</sub> (catalyst)/O<sub>2</sub>;

- Japan's AIST (Advanced Industrial Science and Technology), who have developed a cell with blended electrolyte with two compartments: in the compartment on the negative side, an organic electrolyte and in the compartment on the positive side, an aqueous electrolyte. The two compartments are separated by a solid electrolytic wall. The intended

---

<sup>26</sup> These are alkyl carbonates: EC: Ethylene carbonate; DEC: Diethyl carbonate; DMC: Dimethyl carbonate; EMC: ethyl methyl carbonate; PC: propylene carbonate.

<sup>27</sup> P. ALBERTUS, G. GIRISHKUMAR, B. McCLOSKEY, R. S. SÁNCHEZ-CARRERA, B. KOZINSKY, J. CHRISTENSEN, A. C. LUNTZ, "Identifying capacity limitations in the Li/oxygen battery using experiments and modeling", *J. of Electrochem. Soc.*, 158, A343–A351, 2011.

<sup>28</sup> F. MIZUNO, S. NAKANISHI, Y. KOTANI, S. YOKOISHI, H. IBA, "Rechargeable Li-air batteries with carbonate-based liquid electrolytes", *Electrochemistry*, Vol. 78, No. 5, p. 403, 2010.

<sup>29</sup> LiTFSA: Lithium bis(trifluoromethanesulfonyl) amide.

applications are the consumer product and military markets ([www.aist.go.jp](http://www.aist.go.jp)).

With regard to France, in addition to institutional laboratories, EDF has coordinated a National Research Agency project – “*LIO: Faisabilité d'une batterie Lithium-air*” (Feasibility of a Lithium–air battery) (project director: Ph. Stevens) devoted to the development of a complete aqueous-electrolyte lithium-air cell with all its components. The metal lithium is protected by a first surface layer of LIPON (lithium phosphorus oxynitride) and then by a ceramic membrane of LISICON (Li Super Ionic Conductor:  $\text{LiM}_2(\text{PO}_4)_3$  with  $M=\text{Ti, Zr, Ge, Hf}$ ). The declared performances are 100 mAh/cm<sup>2</sup> (sufficient to deliver 500 Wh/kg) for current strength of 2 mA/cm<sup>2</sup> at 30°C, and up to 6 mA/cm<sup>2</sup> at 60°C. The lifetime is 38 cycles with a current strength of 10 mAh/cm<sup>2</sup>.

## 10.6. Conclusion

Lithium–air technology is not yet sufficiently mature to envisage commercialization in the near future – particularly because the lifetime of the cells is too short. With the most optimistic of hypotheses, it might become a possibility in ten years' time. The packaging is a crucial element for the improvement of the performances, with oxygen permeability of the polymer membrane of the air positive electrode. The perspectives show that the gravimetric energy density could reach up to 1000 Wh/kg, which is around ten times that of present-day lithium-ion technology. The design of cells with bipolar electrodes (see section 7.3.1) could increase the gravimetric power densities.

With an oxygen reserve of 20 liters stored in a canister and a compressor to recharge the system, the embedded energy density would be 370 Wh/kg (including the canister and compressor) for a 15 kWh battery. This is still interesting in comparison to present lithium-ion technology. This arrangement helps deal with the problem of lithium's sensitivity to ambient humidity, because the system – including the oxygen – is entirely enclosed.

The lithium-air battery could be of interest for all applications requiring high gravimetric energy densities. For small portable systems, the degree of oxygen storage is prohibitive, but this problem could be circumvented by using oxygen for the air, except for space applications.

### 10.7. Appendix: calculation of theoretical gravimetric energy densities

The gravimetric energy densities of lithium-air technology given in the literature are very variable from author to author, because the working hypotheses chosen are very different.

For an aqueous electrolyte, the reaction to be considered is [10.4]. It involves four electrons, and is again given below:



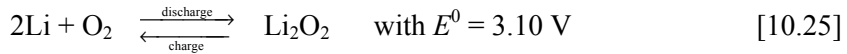
Considering that oxygen is provided by the ambient air as and when needed:

$$\begin{aligned} E_{\text{th}} &= E_{\text{nom}} \times Q_{\text{th}} = 3.45 \times \frac{4}{4 \times 6.9 + 2 \times (2 \times 1 + 16)} \times 26801 \\ &= 5815 \text{ mWh/g} = 5815 \text{ Wh/kg} \end{aligned} \quad [10.23]$$

Considering that oxygen is stored in the battery (e.g. stored in a canister):

$$\begin{aligned} E_{\text{th}} &= E_{\text{nom}} \times Q_{\text{th}} = 3.45 \times \frac{4}{4 \times 6.9 + 2 \times (2 \times 1 + 16) + 2 \times 16} \times 26801 \\ &= 3869 \text{ mWh/g} = 3869 \text{ Wh/kg} \end{aligned} \quad [10.24]$$

For an organic electrolyte, we begin with reaction [10.11], which is rewritten below:



Considering oxygen to be provided by the ambient air as and when needed:

$$\begin{aligned} W_{\text{m.th}} &= E_{\text{nom}} \times C_{\text{m.th}} = 3.1 \times \frac{2}{2 \times 6.9} \times 26801 \\ W_{\text{m.th}} &= 12041 \text{ mWh/g} = 12041 \text{ Wh/kg} \end{aligned} \quad [10.26]$$

Considering oxygen to be stored in the battery (e.g. stored in a canister):

$$W_{\text{m.th}} = E_{\text{nom}} \times C_{\text{m.th}} = 3.1 \times \frac{2}{2 \times 6.9 + 2 \times 16} \times 26801$$

$$W_{\text{m.th}} = 3628 \text{ mWh/g} = 3628 \text{ Wh/kg} \quad [10.27]$$

Here, we only take account of the molecular masses of the species charged at the electrodes. In practice, we have to take account of all the associated components: separators, electrolyte, current collectors, container and oxygen canister if present.

## Chapter 11

# Lithium Resources<sup>1</sup>

Nowadays, billions of batteries are sold every year for energy storage in cellphones and portable computers, digital cameras, portable electrical devices, etc. For these applications alone, the requirement of lithium is quoted in tens of thousands of tons. Yet with the future emergence of electric vehicles and stationary storage systems intended to better integrate electrical production from intermittent renewable energies with the grid, the associated lithium requirement quoted is far greater than that for mobile devices. In terms of quantity, the number of batteries to be produced, even for electric vehicles alone, will doubtless be similar, but their unitary requirement in terms of energy will be several orders of magnitude greater. Hence, it is not

---

<sup>1</sup> This chapter is inspired by work carried out between 2010 and 2011 by Camille Grosjean for his thesis, prepared between 2009 and 2012 to obtain his doctorate from the University of Corsica Pascal Paoli, based in Corte. Entitled “Usages de batteries lithium-ion comme fonction de stockage d’électricité à la convergence des besoins de l’habitat solaire et du transport électrique”, the work for this thesis was carried out at the Institut National de l’Énergie Solaire (INES), based at Bourget du Lac, and at the Laboratoire du Stockage de l’Électricité (LSE). It was financed by the Laboratoire d’Innovation pour les Technologies des Énergies nouvelles et les Nanomatériaux (LITEN), one of the Grenoble branches of the Commissariat à l’Énergie Atomique et aux Énergies Alternatives (CEA). Supervised by Philippe Poggi, Professor at Corsica University, and Marion Perrin, and engineering researcher at CEA/LITEN and head of the Laboratory for Electricity storage (LSE), this thesis was upheld at the Centre de Recherches Georges Peri in Ajaccio on 17 December 2012.

unreasonable to wonder: “Will there be enough primary material to supply the industrial needs of electrical energy storage by lithium batteries?”.

This chapter gives a detailed examination of the availability of worldwide lithium resources and the techniques used to extract it. We then turn our attention to their possible impact on the market and on the lithium battery industry, particularly in view of the significant foreseeable demand represented by the electric vehicle market.<sup>2</sup>

### 11.1. State of the art in terms of availability of lithium resources

The concept of the electric vehicle re-surfaced in the late 1990s, with the advent of lithium batteries for the mobile electronics market. In 1998, Nicholson and Evans<sup>3</sup> evaluated the past, current and future directions for the lithium market. Because of his involvement as a geologist in mining prospecting campaigns on the Bikita field, Evans was one of the first to witness the emergence of the lithium market in the early 1970s. From then on, he made it his mission to re-assess the inventory of world lithium resources.<sup>4</sup> With Kunasz<sup>5</sup>, another forward-looking geologist, the way was opened for more complete inventories and market analyses, whose successive publications marked the evolution of the uses of lithium in all the

---

2 The lithium-ion battery is, *a priori*, the most likely energy storage solution in the short term to cope with the constraints in terms of volumetric and gravimetric energy densities for the function of on-board storage for an electric vehicle. As this function represents the prospect of a significant market for lithium batteries, mention will be made of it throughout this chapter.

3 P. NICHOLSON, R. K. EVANS, “Evaluating new directions for lithium market”, *Journal of Minerals*, 50 (5), pp. 27–29, May 1998.

4 R. K. EVANS, “Lithium reserves and resources”, *Energy*, 3 (3), pp. 379–385, June 1978.

R. K. EVANS, “Western world lithium reserves and resources”, The Institute of Metals, Aluminium- Lithium Alloys III, Proceedings of the 1985 Conference, 1986.

R. K. EVANS, The current status of the lithium business, Internal Communication, Amax Mineral Resources Company, Golden, Colorado, 1988.

R. K. EVANS, An abundance of lithium, March 2008.

R. K. EVANS, An abundance of lithium: part two, July 2008.

5 I. A. KUNASZ, “Lithium, how much?”, *Footnote Prints*, 48, 1, pp. 23–27, 1980.

I. A. KUNASZ, “Reservas mundiales de litio”, *El litio*, un Nuevo recurso para Chile, 1986.

I. A. KUNASZ, “Lithium resources”, *Industrial minerals and rocks*, pp. 631–642, 1994.

associated sectors of application.<sup>6</sup> Very early on in the history of lithium, although it was already the subject of research in the energy domain, the uncertainty about the true amount of resources available raised the question of world lithium availability for industrial purposes.<sup>7</sup> In fact, even before nuclear physicists began to take an interest in lithium to help make the tritium which is involved in fusion,<sup>8</sup> lithium was already in demand for applications in electric vehicles. In 1996, Will<sup>9</sup> was the first to publish an article about the availability of lithium for industrial applications. However, his study was a little too anchored in economics, and was not sufficiently detailed on points relating to geology and geostrategy. In addition, the structure of the industry has changed since then. Tahil<sup>10</sup> exploited more recent data in coming to the concluding that the use of lithium in electric vehicle batteries was not a long-term option, in view of the insufficiency of production resources in relation to the requirement of the entire industry. However, by applying to lithium the “cumulative availability curve” method which they had previously applied to copper, Yaksic and Tilton<sup>11</sup> came to the opposite conclusion, deeming that lithium was not under threat of depletion, thanks to an inexpensive and promising process of extraction from

---

6 T. F. ANSTETT *et al.*, International strategic minerals inventory report – Lithium, United States Geological Survey (USGS) circular 930-I, 1990.

H. J. ANDREWS, The industry of lithium, FMC Corp., Lithium Division, La Paz, 1991.

J. A. OBER, Lithium, USGS minerals yearbook, 1994–2006.

D. KINGSNORTH, *Overview of lithium market*, Sons of Gwalia Ltd., 2001.

M. MORA, Análisis de la estructura mundial de la industria del litio y criterios de priorización de proyectos de investigación científica y tecnológica, Universidad de Chile, 2003.

D. JIMENEZ (oral presentation), Industrial Minerals Conference, Montreal, 2003.

A. EBENSPERGER *et al.*, “The lithium industry: its recent evolution and future prospects”, *Resources Policy*, 30, pp. 218–231, 2005.

The economics of lithium, 11th Edition, Roskill, 2009.

7 A.L. HAMMOND, “Research news: lithium: will short supply constrain energy technologies?”, *Science*, 191, pp. 1037–1038, 1976.

8 D. FASEL, M. Q. TRAN, “Availability of lithium in the context of future D-T fusion reactors”, *Fusion Engineering and Design*, 75–79, pp. 1163–1168, 2005.

9 F. G. WILL, “Impact of lithium abundance and cost on electric vehicle battery applications”, *Journal of Power Sources*, 63 (1), pp. 23–26, November 1996.

10 W. TAHIL, The trouble with lithium, Implication of future PHEV production for lithium demand, Meridian International Research (MIR), Jan. 2007.

W. TAHIL, “The trouble with lithium 2”, *Under the Microscope*, MIR, May 2008.

11 A. YAKSIC, J.E. TILTON, “Using the cumulative availability curve to assess the threat of mineral depletion: the case of lithium”, *Resources Policy*, 2009.

salt lake brines. Following in their footsteps, Gruber and Medina<sup>12</sup> went further in their thinking, contrasting the different founts of information and precisely evaluating the lithium content of all known sources. At the same time, Clarke and Harben<sup>13</sup> created a wall-map on the basis of this type of data, transforming what had previously been only natural sciences and geology into geoeconomy.

This chapter evaluates the worldwide availability of lithium resources, comparing updated data which reflect the reality of the market, particularly in terms of the evolution of market share and price of lithium, which are likely to impact the manufacturing costs of electric vehicles. Particular attention is paid to the origin and nature of all types of resources and to the current structure of the lithium industry. Finally, the question of the bottleneck relating to geostrategic aspects will be debated and prospective avenues for improvement will be given with a view to solving the problems raised here.

## 11.2. Comparison of resources with the needs of the electrical industry

On the market, there is a multitude of lithium-based products (Figure 11.1). Lithium carbonate ( $\text{Li}_2\text{CO}_3$ ), mineral concentrates and lithium hydroxide ( $\text{LiOH}$ ) are the most commonly commercialized forms, together representing 80% of the market share.<sup>14</sup> Mineral concentrates are raw materials, used to produce glasses and ceramics, whilst lithium carbonate and hydroxide are chemical products used as ingredients involved in the making of batteries, greases, aluminum alloys, etc.

In 2007, the majority application amongst all uses for lithium derivatives was the manufacture of glass and ceramics, representing 37%, as opposed to only 20% for batteries (Figure 11.2). Considering only lithium-ion batteries, which are the most widely sold in the current market, lithium is mainly present in the positive electrode (90%) and in the electrolyte (9%) (Figure 11.3). However, its hitherto marginal use in negative electrodes could rise, in view of the interest shown by researchers and industrialists in

---

12 P. GRUBER, P. MEDINA, Global lithium availability: a constraint for electric vehicles?, University of Michigan, April 2010.

13 G.M. CLARKE, P.W. HARBEN, Lithium Availability WallMap (LAWM<sup>®</sup>), 2008.

14 "The economics of lithium", 11<sup>th</sup> Edition, Roskill, 2009.



materials based on Lithium Titanate Oxide  $\text{Li}_4\text{Ti}_5\text{O}_{12}$  (LTO), used in place of graphite to encourage fast recharging.<sup>15</sup>

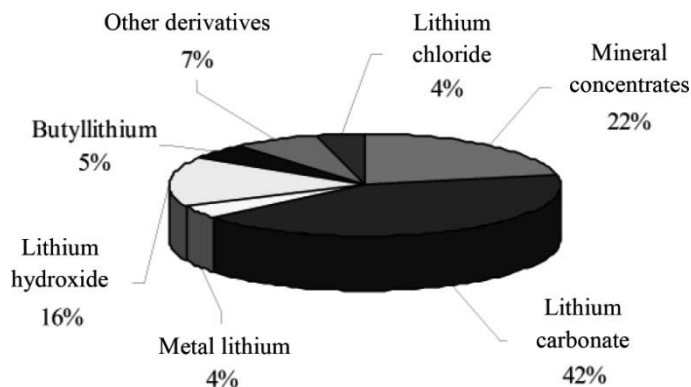


**Figure 11.1.** Market share distribution of lithium-based commercial products (taken from “The economics of lithium”, 11<sup>th</sup> Edition, Roskill, 2009, available at [www.giiresearch.com/report/ros79366-economic-lithium.html](http://www.giiresearch.com/report/ros79366-economic-lithium.html))

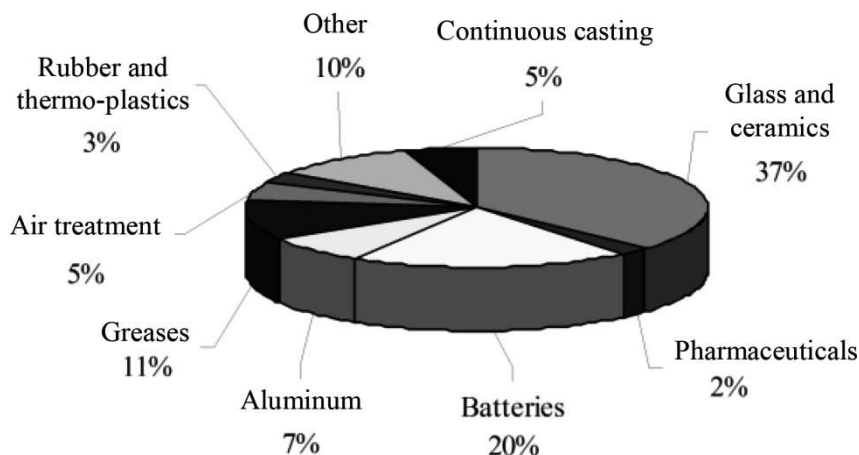


**Figure 11.2.** Distribution by application of world lithium consumption in 2007 (taken from G. M. Clarke, P. W. Harben, “Lithium Availability WallMap” (LAWM<sup>®</sup>), 2008)

15 A. S. PRAKASH *et al.*, “Solution-combustion synthesized nanocrystalline  $\text{Li}_4\text{Ti}_5\text{O}_{12}$  as high-rate performance Li-ion battery anode”, *Chemistry of Materials*, 22 (9), pp. 2857–2863, 2010.

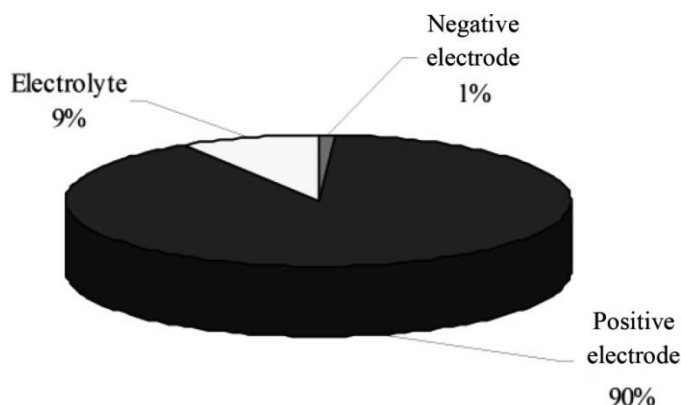


**Figure 11.3.** *Distribution of lithium by function in lithium-ion batteries*  
 (taken from “The economics of lithium”, 11<sup>th</sup> Edition, Roskill, 2009, available at  
<http://www.giiresearch.com/report/ros79366-economic-lithium.html>)

Thus, apart from mineral concentrates which can be used in the raw form with no treatment, all other lithium-based commercial products can be derived from lithium carbonate. Therefore, in the rest of this chapter, the study of lithium will be reduced to the examination of supply and demand of lithium carbonate.

In 2009, barely 80 tons (t) of strategic stores of lithium carbonate were declared worldwide, in one country alone – South Korea.<sup>16</sup> In fact, we can assimilate global lithium production to its consumption; supply and demand are in clear and constant increase, with 12500 t produced in 1998<sup>17</sup>; 13,000 t in 2000<sup>18</sup>; 20,340 t in 2005<sup>19</sup>; and, depending on the information source, 21,300 or 22,800 t in 2008.<sup>20, 21</sup> The average annual rate of growth between 2000 and 2008 was around 6%, though this was followed in 2009 by a sudden drop due to the global economic crisis.<sup>21</sup> We can also the degree of dependency of each consumer sector on lithium resources. In particular, the demand expressed for the industrial areas of batteries and aluminum

16 C. HOCQUART, Rare Earths (REE), IFRI Energy Breakfast Roundtable, 2010, Brussels.

17 P. NICHOLSON, R. K. EVANS, “Evaluating new directions for lithium market”, *Journal of Minerals*, 50 (5), pp. 27–29, May 1998.

18 “The economics of lithium”, 11<sup>th</sup> Edition, Roskill, 2009.

19 J.A. OBER, Lithium, USGS minerals yearbook, 1994–2006.

20 G.M. CLARKE, P.W. HARBEN, Lithium Availability WallMap (LAWM<sup>®</sup>), 2008.

21 “The economics of lithium”, 11<sup>th</sup> Edition, Roskill, 2009.

increased despite the crisis, which shows as an artificial increase in their market share.

In all likelihood, as certain studies predict<sup>22</sup>, there is a high chance that lithium will be replaced or abandoned in most of its current outlets, except for batteries, where the extremely captive uses will undoubtedly elevate the lithium-ion battery industry to a leading position amongst lithium-consuming sectors. This is all the more likely when one considers that in this analysis we have only taken account of the amount of lithium used in batteries for portable electronic devices. The situation becomes critical when we imagine that millions upon millions of electric vehicles will soon be circulating, supplied by as many battery packs, which will swell an already-captive demand for lithium. The amount of lithium needed to manufacture a battery pack for an average-size electric car is estimated at 3 kg (which equates to 16 kg of lithium carbonate). With worldwide annual production of 21000 t, this means that a maximum of 7 million battery packs could be made each year, assuming that electric vehicle batteries entirely monopolize the lithium market. At present, according to the *Comité des Constructeurs Français d'Automobiles* (CCFA), 1.2 billion vehicles are in circulation the world over, and a total of 65 million new vehicles are registered every year. Hence, if we consider a market share of batteries for electric vehicles using a quarter of annual lithium production, the number of packs that can be made falls to less than 2 million, which is around 3% of the number of new cars being registered. In total, therefore, we can say that world lithium production is, at present, clearly insufficient to quickly satisfy the needs for lithium-ion batteries of a future market of electric vehicles. The question lies entirely in whether the lithium industry is capable of increasing its level of production, and at what cost. Examination of the structure of the lithium industry and the processes and resources upon which it is founded gives us vital information to answer this question.

### **11.3. State of the art of extraction techniques and known production reserves**

Lithium carbonate is primarily produced from two resources: salt lake brine and spodumene ore. Their respective modes of exploitation are detailed below.

---

22 A. EBENSPERGER *et al.*, "The lithium industry: Its recent evolution and future prospects", *Resources Policy*, 30, pp. 218–231, 2005.

Spodumene is an ore rich in lithium, contained in a particular type of rock called pegmatite. Historically, it was the first resource to have facilitated lithium exploitation on an industrial scale, but only in few-and-far-between sites (particularly the Greenbushes mine in Australia), and often as a by-product of the extraction of rare earth elements such as tantalum (Ta) or niobium (Nb), or indeed other elements such as rubidium (Rb) and cesium (Cs). In hard rock ores such as pegmatites, the lithium content (1–4%) and the degree of recuperation (60–70%) are high, which means that the mining sites are profitable. However, their exploitation is complicated, because of the hardness of the rocks and the difficulty in accessing pegmatite veins, which form open-air surface mines, with the appearance of vast belts across the landscape.

The various phases of exploration, exploratory drilling, chemical analysis of samples and testing of treatment processes are as many stages in the preparation of the complex but commonplace process that is peculiar to mining exploitation, comprising the digging of an open-air quarry, the excavation and transport of tons of rocks and the processing of them in a nearby factory. Based on synthesis by acid leaching or caustic leaching, the treatment of ore from hard rocks such as spodumene is quick (5 days) and can be carried out throughout the year. However, quite apart from the pollutant fuels and chemical products that it involves, this mode of lithium extraction has the disadvantage of using blast furnaces and milling and crushing machines which are very energy-hungry. In financial terms, mining operation and installations require enormous investments. Conversely, the cost of their expansion is much more bearable, because it involves merely increasing the pace of the convoys of trucks and diggers that extract the raw material to be processed. In that sense, lithium extraction by mining appears highly advantageous because it can adapt to a possible increase in lithium demand. On the other hand, it is damaging in terms of environmental impact because of the machines present on site, the ore-transport trucks and the pollution linked to the actual process which is used to turn the raw material extracted into commercializable lithium carbonate.

Salt lake brines are water resources presenting a high concentration of mineral salts. They can be accessed in the open air or at a shallow depth under the surface of the extensive salt flats situated in particularly dry regions, where the climatic conditions favor the appearance and endurance of the mineral salts. These salt lakes or salt flats are also referred to as “salars” – a word drawn from Spanish. Amongst other elements, salt lake

brines contain lithium, with contents which are low (0.017- 0.15%) and very variable from one salar to another, but also from one site to another within the same salar (e.g. by a ratio of ten).<sup>23</sup> The largest source in the world is the Uyuni salt flats in Bolivia. This site contains one third of the world's reserves. The Atacama salt flat in Chile is the second-largest source in terms of resources. It represents around 40% of global production, because Bolivia only sanctioned lithium extraction from Uyuni relatively recently (2008). Other salars can be found in China, Argentina, the US and Canada (see section 11.5).

The significant differences thus observed result in a tricky initial phase of estimation of the resource which is based on a long, drawn-out process of exploration made up of multiple samples taken by drilling, chemical analysis of the cores taken, precipitation testing of the salts in solution and treatment in a manned installation, i.e. in a small-scale factory.

This lengthy process means that production cannot truly begin until two or three years after initial prospecting. Once production has begun, lithium extraction is very simple and relatively eco-friendly<sup>24</sup>, because it involves simply pumping the brines to the surface and natural evaporation of them by the combined effect of the sun and the wind. From one decanting basin to another, there is another string of steps which take time to isolate lithium salts from the rest of the mineral salts in solution. Gradually, the color of the basins tends toward blue as the lithium content increases, as the other salts precipitate and are removed. Typically, it takes 1–2 years before the lithium carbonate thus processed is ready to be commercialized. It may take longer still in areas which are at latitudes subject to the effects of winter, as the evaporation phase can only be done on a seasonal basis. Such is the case with sites currently being developed in Tibet and China. Such a long extraction process is not ideal if we wish to be able to adapt to the possible sudden change in the amount of lithium demanded by the market.

In addition to the two major resources cited above, it should be pointed out that large amounts of lithium are to be found in the seas and oceans.

---

23 F. RISACHER, B. FRITZ, "Quaternary geochemical evolution of the salars of Uyuni and Coipasa, Central Altiplano, Bolivia", *Chemical Geology*, Elsevier Science Publishers, 1991.

24 Like any industrial process, this method of lithium extraction inevitably has consequences for the environment. The pumping of brine requires energy. Evaporation basins require large surface areas.

However, they are present in such a low concentration (170 ppb – parts per billion) that it would be a highly complex and costly task to industrially isolate lithium chloride from all the other mineral salts in solution. There is only one laboratory in Japan working on this<sup>25</sup> but, even after several years of research and improvement, ultimately yielding a very pure product, their extraction process is far more costly (\$80/kg) than that based on salt lake brines (\$2–3/kg) or spodumene ores (\$6–8/kg).

In spite of processes which are simple, inexpensive and more ecologically friendly than mining extraction, producing lithium carbonate from salt lake brines poses the problem of the great dispersion of the concentration of lithium, lack of assurance linked to their degree of recuperation and very long periods necessary both for the construction of the production installations and their extension in the context of increased activity. This type of exploitation is also dependent on the presence of workers and the mobilization of means of transport in isolated desert areas, far from living quarters and consumption centers. Lithium extraction by mining exploitation of hard-rock minerals is far safer, with high lithium contents extracted, high degrees of recuperation and short treatment processes which facilitate adaptation of the supply to changing demand. However, the excavation, transport and thermochemical processes used are damaging in terms of environmental impact and cost – all the more so, given that energy prices are predicted to rise. Thus, regardless of the difference between their production cost, there is a place in the market for both the classic modes of lithium production – from salt lake brines and spodumene ore. Both techniques will doubtless come to play a very important role in the lithium industry.

#### **11.4. Nature and geological origin of all potential lithium resources**

Besides spodumene, lithium carbonate can also be produced from other ores which are also included in pegmatite rocks. Containing 1.5–6% weight of lithium, such ores have very varied names – among them amblygonite, eucryptite, lepidolite, petalite or zinnwaldite. Due to its high iron content, petalite is used particularly in glassmaking. Lepidolite was one of the first ores to be exploited for the production of lithium salts and the making of specialized glass, but it has gradually come to be less and less used because

---

25 Y. MIYAI *et al.*, “Recovery of lithium from seawater using a new type of ion-sieve adsorbent based on  $\text{MgMn}_2\text{O}_4$ ”, *Separation Science and Technology*, 23(1–3), pp. 179–191, 1988.

of its high fluorine content. Although these ores share with spodumene the stage of mining exploitation, they differ from it by their varied parameters of composition, hardness and lithium content. This imposes an additional limitation on any possible industrial exploitation because the treatment process will have to be adopted – differently for each type of ore and with an infinite number of extraction by-products which are as varied as the compositions.

Apart from the hard rock ores present in pegmatites bordering granite terrains<sup>26</sup>, lithium can be extracted from two other types of rocks belonging to the silicate family: hectorite (which is a soft, oily clay) and jadarite (which is a chalky powder aggregate). Both are white in color, and are labeled as “evaporites”, because they are supposed to be gain from sedimentation and evaporation of salt flats. In fact, salt lake brines and evaporites result from the same complex geological mechanism: endorheism. This results in the hydrological enclosure of expanses of fresh- or salt-water. These retention and drainage basins are enriched with minerals by leaching and dissolution of the surrounding rocky slopes. Two distinct phenomena lend these endorheic basins the appearance typical of them: sedimentation, resulting from the deposition of alluvia carried by the rains, and evaporation, resulting from the combined effects of the sun and the wind. Hectorite is a particular case of evaporite, because it occurs as the result of the alteration of tuff and volcanic ash in calderas, alkaline lakes where they are confined and subjected to heat from geysers and hot water springs.

Finally, lithium can be produced from two other types of brine extracted from the ground or from deep underground. Drawn from geothermal springs or oil fields, these brines are contained in subterranean pockets of water and saline aquifers where they become enriched with lithium on contact with the surrounding granite plains. Lithium extraction from such resources is highly promising, because it relies on effluents which are the by-product of already-profitable installations whose primary initial goal is to produce heat and electricity, and respectively gas and crude oil. Firstly, new processes have

---

26 450 million years ago, when the magma of the Earth was cooling, the molten magma at a temperature of 400 to 700°C found its way through the Earth’s crust up to the surface, infiltrating the faults and cracks in blocks of granite that had already cooled and hardened. This portion of molten magma became enriched in minerals on contact with the granite (rare earth elements; alkali metals: lithium, rubidium and cesium), forming pockets, veins, lodes and threads of pegmatite which were distributed radially around the granite blocks and carried away, before finally becoming hardened definitively in their turn.

been developed to eliminate the silica contained in geothermal fluids – a material which tends to obstruct and corrode the pumps and heat exchangers in geothermal power plants. Secondly, besides the nature of effluent (available for free and at a reduced energy cost), lithium extraction for petroleum brines facilitates the future reorientation of the oil industry in a direction which is favorable for the durable integration of electric vehicles.

### **11.5. Global geographic distribution of raw lithium resources**

Having painted a picture of the lithium industry and listed the types of resources which are envisageable for its production, we shall now analyze the questions of global availability and local distribution of these resources.

World lithium resources have already been evaluated and quantified by researchers, NGOs and private enterprises, although there is no consensus regarding the figures or the way in which they should be calculated: in 2005, the United States Geological Survey (USGS) established that there were 15 million tons (Mt) of lithium reserve base and 6.8 Mt of reserves, while Clarke and Harben<sup>13</sup> mentioned 39.4 Mt of resources and 27.7 Mt of reserve base in 2008.

As with oil, with the tested, proven or presumed reserves, we can see that the global summary of resources depends on the qualifiers used: “resource”, “reserve base” and “reserves”. The resource is the raw quantity of lithium in the Earth’s crust in a form which renders it potentially exploitable. The “reserve base” is the proportion of lithium resources which satisfy certain physio-chemical criteria relating to production and mining, such as lithium content, quality, breadth of depth of the deposit. As such, it serves as the basis for defining which resources are profitably exploitable (“reserves”), those which are as yet marginal (“marginal reserves”) and those which are nearly at the point of being profitable (“sub economic resources”). In fact, the reserves are by definition that portion of the reserve base which it is economically viable to extract and produce at the time when the resources are evaluated, although the installations may not necessarily be in place and operational. Thus, we can understand that the inventory of the quantities of resources and reserve bases can change over time, with the evolution of the economic context, technological progress, reduction of cost of extraction or – conversely – increase cost of primary materials, particularly those of metals, crude oil and, of course, lithium.



By summarizing the data already available and adding information about new sources, primarily in China and Russia, we have evaluated resources as being between 37.1 Mt and 43.6 Mt. Of these resources, 62% come from brines and 38% from ores. However, the new discoveries relate mainly to mining-type sources with pegmatites. When we compare these figures to the specific needs of the electric vehicle industry, the 37.1–43.6 Mt equivalent lithium (i.e. 197.4–231.9 Mt of lithium carbonate  $\text{Li}_2\text{CO}_3$ ) guarantee enough lithium resources for 12.3–14.5 billion electric vehicles, i.e. ten times the current number of vehicles on the road according to the data from the CCFA. Even if we are speaking of resources rather than reserve bases or reserves, this is a result which indicates that, overall, there is a sufficient quantity of lithium available on Earth to supply lithium-ion batteries for the future market of electric vehicles. However, whilst it is pertinent to consider a global inventory in order to give an idea of the extent of the potential lithium market, it should be noted that the precise geographic location of the resources has an important part to play, as regional influences can result in an imbalance between supply and demand. In fact, it is very useful and educational to examine the geographic distribution of lithium resources (Figure 11.4).

The largest amount of lithium is situated in the ABC triangle, formed by Argentina, Bolivia and Chile. With 43.6% of resources present in that region of the world, it is understandable that at present, most lithium comes from salt lake brines from South America. North America and Australasia represent almost all of the rest of the resources, each with around 25%. Thus, although it is set to become one of the largest consumers of lithium in the world, with numerous auto manufacturers openly involved and investing in electric vehicles in Germany, France and the UK, Europe seems to be the poor parent of the future classification of world lithium producers, holding less than 3% of world resources.

With regard to brines, those of North America come mainly from geothermal springs and oil fields, whereas those of China are from salt lakes. Globally, brine resources are highly concentrated in areas which are far from typical consumption centers, with the exception of certain sites in the US and Canada. Mineral resources from rocks are distributed much more evenly across the planet, with sources available on all the continents. However, in view of the difference in cost of production of this resource in comparison to salt lake brine, very few mining sites in Canada, Australia and China are currently producing.

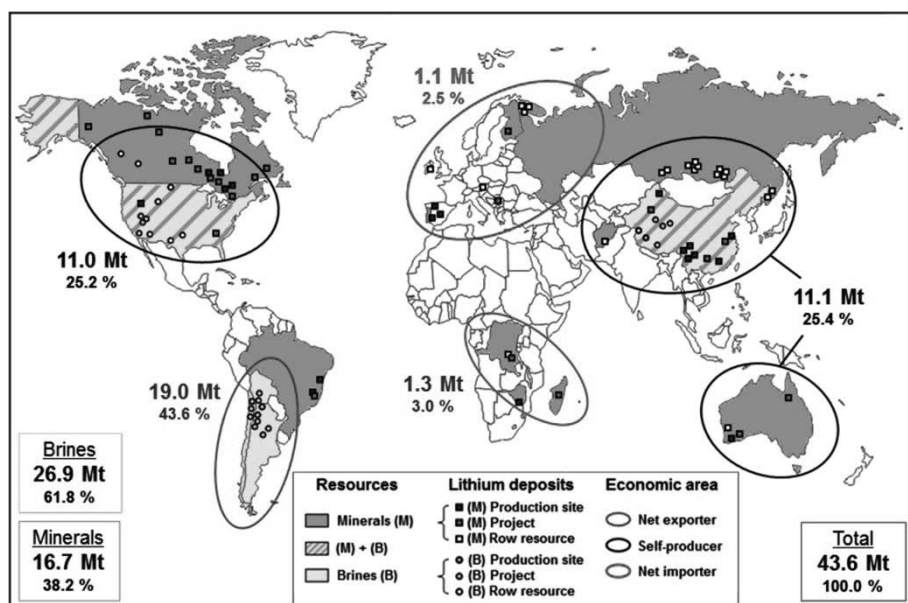


**Figure 11.4.** Cartographic overview of global distribution of sources of brines and lithiated minerals (source Camille Grosjean, see footnote 1)

Ultimately, therefore, lithium resources appear to be greatly polarized geographically, which implies that we must prepare for a significant imbalance in the market in the near future. This will be especially true because some producing countries are politically contentious places which are likely to nationalize lithium exploitation, such as Bolivia, and/or come together to set prices, e.g. by way of an organization of lithium-producing countries. Europe will assuredly be the greatest victim of this geostrategic bottleneck, because it does not have the resources although it will, *a priori*, be a very heavy consumer of lithium. South America will obviously profit massively from lithium trading, because its non-existent domestic consumption will make it a net exporter of low-cost lithium carbonate from salt lake brines. Australia, Asia and North America will probably achieve a balance between their production and consumption. Finally, as attested by the agreements recently signed between the two countries,<sup>27</sup> the proximity of mining sources in the source of Russia will constitute an undeniable

<sup>27</sup> RusNano (Russian Corporation of Nanotechnologies) and the Chinese group Thunder Sky signed a joint venture agreement to build the first Li-ion battery factory in Russia.

advantage for China, which already has a remarkable headstart in terms of electric vehicles, both with models already commercially available and numerous factories for battery production, which place it in a perfect position to negotiate the movement of electrical mobility.

### 11.6. Evolution of the cost of lithium

Figure 11.5 shows the price of lithium carbonate<sup>28</sup> between 1970 and 2010, from data from by the USGS and, between 1990 and 2010, from data from the Chilean customs service.<sup>29</sup>

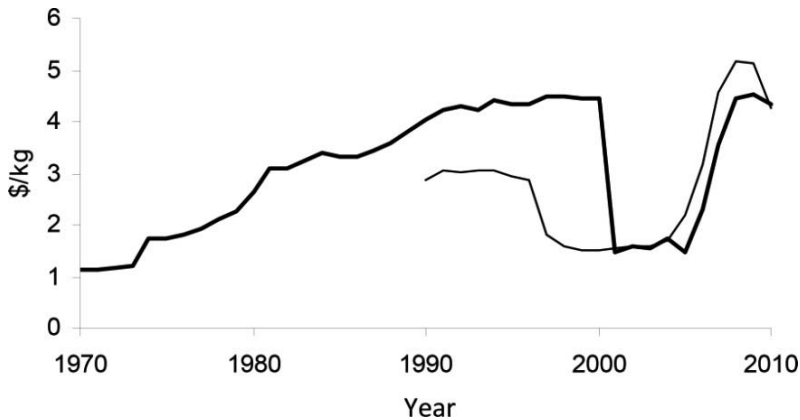


**Figure 11.5.** Evolution of the price of lithium carbonate: heavy line: 1970–2010 according to USGS, available at <http://minerals.usgs.gov/ds/2005/140/ds140-lithi.pdf>; thin line: 1990–2010 according to the Chilean Customs Service, available at <http://www.lithiumsite.com/market.html>

Looking at the past trend in the prices of lithium (Figure 11.5), one might be taken aback by the erratic shape of the curve, with the price remaining stable between 1970 and 1990 before fluctuating with fairly significant upward and downward peaks in 1997 and 2008 respectively. These variations relate to the structure of the lithium industry and to factors which touch on consumer sectors, reflecting an imbalance between lithium supply

<sup>28</sup> 5.3 kg of lithium carbonate contain 1 kg of lithium.

<sup>29</sup> According to [www.lithiumsite.com/market.html](http://www.lithiumsite.com/market.html), Chile accounts for nearly half of all world lithium production (in all forms). Hence, it is a good indicator of the price of lithium.

and demand. Between 1970 and 1990, a number of industrialists exploited hard rock ores as a source of lithium in the form of mineral concentrated, extracted primarily in Australia and the USA but also Portugal and Spain, and used by the glass and ceramics industry. As these applications were not entirely dependent on lithium usage, the prices remained stable so as to avoid any substitution, and the slow pace of exploitation mirrored that of demand. Afterward, however, the German company Chemetall bought up the small companies which had, until then, exploited the mining sources of lithium throughout the world. Thereby the company found itself at the head of a monopoly, which concentrated world lithium production activities, causing the slight increase in the price of lithium observed between 1990 and 1996. From 1997 onwards, the means of lithium extraction changed radically, with the exploitation of salt lake brines leading to the sale of lithium carbonate, and no longer only of mineral concentrates. From 1997 to 2000, the Chilean company SQM (*Sociedad Química y Minera de Chile* – Chemical and Mining Company of Chile) became a market leader by significantly lowering its production costs thanks to this extraction technique, thus forcing other operators to close many of their conventional mining sites which had become unprofitable. The outlets for lithium also changed during this period, with the development of cells and rechargeable batteries usable for mobile applications, and with the desire of the auto and aeronautics industries to make their products lighter by using aluminum alloys containing lithium. From 2005 to 2006, we therefore see a short-lived increase in price because of the passing bottleneck experienced by the market because of production problems in Chile, at the Atacama salt flat, at a time when the dedicated demand for batteries was increasing particularly significantly. From 2007 to 2008, the average cost of lithium exportation saw an unprecedented rise, attaining a record value of \$6.4/kg, undoubtedly because of the marked increase in fuel prices. Finally, more recently, the effects of the economic crisis have been felt in the industrial activity of lithium-consuming industries and sectors, which reduced their demand, forcing a mechanical lowering of the costs of lithium, as production then became far greater than demand.

At this stage, one may wonder about the part played by the cost of lithium in the final cost of a battery for a portable device or an electric vehicle.

An 18650 cell, which is used almost universally in portable computers, contains 0.8 g of lithium for a capacity of 2.7 Ah. At \$6/kg, the cost

attributable to lithium is less than \$0.005. For a 9-cell battery, the cost of the lithium (7.2 g) is \$0.043: a tiny proportion of the final cost.

For an average-sized electric vehicle, the mass of lithium needed to create a battery pack is around 3 kg. At \$6/kg, the cost of the lithium works out at less than \$20: once again, a very small part of the final cost of the battery pack. Amongst other things, this is attributable to the quality of manufacture, which has to ensure a lifetime which is compatible with the usage of the vehicle, but also to the brace of processes needed to assemble cells into a battery pack (connections, mechanics, offsetting of R&D costs, etc).

In case of geopolitical tension and/or a demand that is greater than the factories' capacity to provide lithium, an increase in the cost of this metal would not have a prohibitive impact on the cost of a battery pack.

### **11.7. Summary**

With the rise of lithium-ion batteries, the technological advance of electric vehicles raises the question of the evolution of the availability and price of lithium for the automobile industry. Although lithium has many uses in other fields of application, the inventory of resources shows that there is enough lithium on Earth to serve the needs of this application. In addition, even if the price of lithium were to quintuple, the impact on the price of batteries would be minimal. However, lithium shortages could threaten supply to the electric vehicle market (and the grid support market), because the available resources are highly concentrated geographically. Also, current production capabilities would not, as they stand, be able to deal with the highly-likely sharp increase in demand for lithium. In order for the vehicle industry to survive and thrive, for grid support applications to emerge and for new applications for lithium to appear, we need to build up strategic lithium stores and sign long-term supply contracts. Furthermore, we can try to exploit – in as ecologically sustainable a manner as possible – the many sources of brines and ores which have yet to be explored.



## PART 3

# Other Types of Batteries





## Chapter 12

# Other Types of Batteries<sup>1</sup>

### 12.1. Introduction

Other types of batteries have been introduced to serve specific needs (electric vehicles, electricity storage for grid support, etc.). For this discussion, we have chosen to focus on sodium-sulfur (Na-S) batteries and nickel-chloride-based batteries, which are both so-called “high temperature” battery systems, and lastly redox flow systems.

These technologies have one point in common. Unlike the technologies presented hitherto, in these batteries, the electrodes are liquid and are separated by a solid membrane. In the operation of many batteries, the active material will not occupy the same volume in different states of charge. The successive charges and discharges impose mechanical stresses on the electrodes, which are one of the causes of degradation on the scale of the components and, consequently, aging of the element. With liquid electrodes, these phenomena of volumetric expansion/contraction disappear.

The following sections will discuss these three technologies in turn.

---

<sup>1</sup> The writing of this chapter owes much to the knowledge of Marion Perrin (affiliation given in footnote 1 of Chapter 11).

## 12.2. Sodium–sulfur technology

Following a number of application attempts in electric vehicles in the 1960s, today the sodium–sulfur battery) is used mainly in stationary applications for grid support:

- peak shaving (PS) at times of heavy consumption on the electricity grid, with significant requirements in terms of energy (long discharge durations);
- power quality (PQ), requiring high power capability but for short durations.

This technology has mainly been developed from 1980 onwards by the Japanese firm NGK Insulators, which specializes in ceramics. It began being commercialized in 2002. The largest operational Na–S battery (34 MW) was installed in Japan in 2008 on a 54 MW wind farm. Today, nearly 200 installations have been completed, with an installed power of 300 MW and a stored energy greater than 1500 MWh.

### 12.2.1. Operational principle<sup>2,3</sup>

The Na–S battery comprises a sulfur positive electrode, a sodium negative electrode and a  $\beta$  alumina ceramic ( $\beta$ -Al<sub>2</sub>O<sub>3</sub>), which is conductive of sodium ions, which separates the two electrode compartments. The element is hermetically sealed and functions at temperatures at which both the electrodes are liquid. To liquidize the electrodes and keep them in the liquid state, the element is kept within a temperature range of 300–400°C. As specified in the introduction to this chapter, the electrolyte is a solid ceramic. The structure of the element is given in Figure 12.1: sodium is generally present in the central compartment<sup>4</sup> made of  $\beta$  alumina.

---

<sup>2</sup> K.B. HUESO, M. ARMAND, T. ROJO, “High temperature sodium batteries: status, challenges and future trends”, *Energy Environ. Sci.*, 6, 734–749, 2013.

<sup>3</sup> T. OSHIMA, M. KAJITA, “Development of sodium-sulfur batteries”, *J. Appl. Ceram. Technol.*, 1, 269–276, 2004.

<sup>4</sup> In nickel chloride batteries (section 12.3), sodium is in the external compartment.

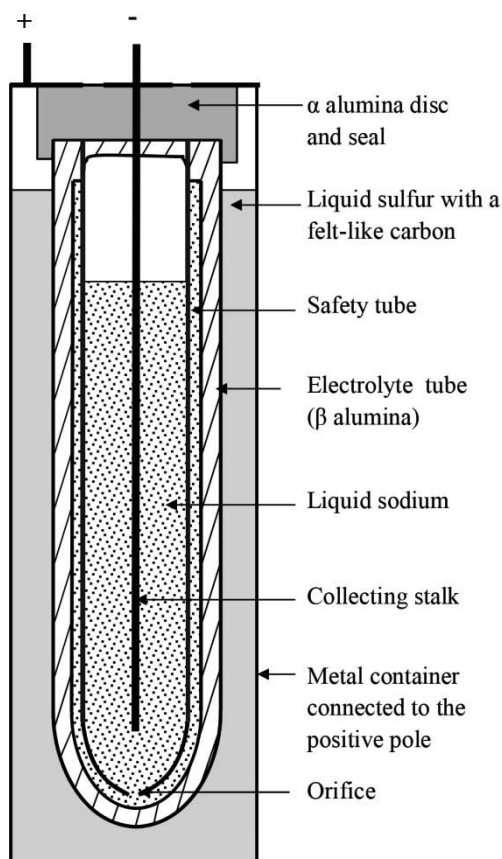
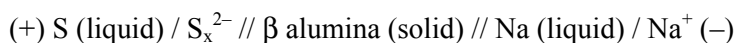


**Figure 12.1.** *Diagram of a sodium-sulfur element*

Inside the ceramic electrolyte (in tubular form) is placed a safety tube with a small hole. By capillary action, the sodium passes through and covers the whole of the surface of the solid electrolyte. If the ceramic is broken, this hole limits the amount of sodium that can reach the ceramic, thus limiting the chemical reactions in case of an accident. The drawback is that it also limits the charge and discharge currents that we can apply: hence, it takes at least six hours to charge or discharge the element.

The electrochemical chain involved is:



where (+) denotes the positive terminal, S sulfur, Na sodium, (–) the negative terminal.

During discharge, the sodium atoms are oxidized and migrate through the  $\beta$  alumina wall to combine with the sulfur. At the beginning of discharge, the compound at the positive electrode is sodium pentasulfide ( $\text{Na}_2\text{S}_5$ ) – a liquid which is immiscible with the liquid sulfur (S). The voltage of the element is therefore 2.08 V at 350°C. Once the sulfur has been completely consumed, the discharge can be prolonged by progressive transformation of the sodium pentasulfide into successive polysulfides, less rich in sulfur, with the general formula  $\text{Na}_2\text{S}_x$ . These polysulfides constitute a single phase as long as the average value of  $x$  is between 5 and 2.7. If discharge is prolonged beyond the formation of a 2.7-sulfide group, we witness the formation of crystals of  $\text{Na}_2\text{S}_2$  and then solid  $\text{Na}_2\text{S}$  at the temperatures in question. However, this reaction must not be allowed to occur because it is irreversible. When the composition of the positive material changes from  $\text{Na}_2\text{S}_5$  to  $\text{Na}_2\text{S}_3$ , the voltage of the element drops from 2.08 to 1.78 V. Hence, the voltage per element must not be allowed to drop below 2.08 V.

The charge/discharge reactions are written as:

*Positive compartment*



where  $x = 1$  to 5.

*Negative compartment*



*Balance equation*



These equations are illustrated in Figure 12.2:

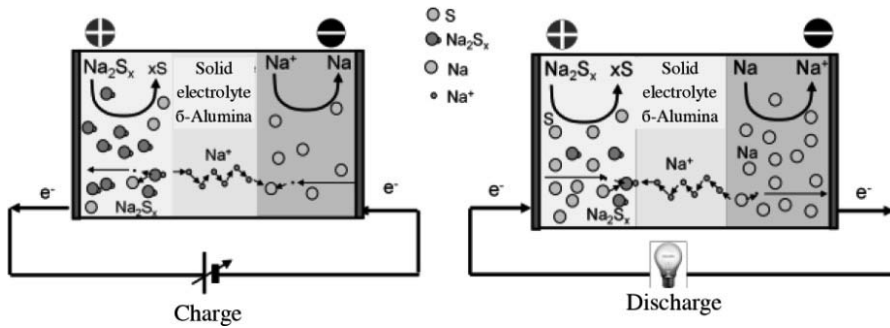


Figure 12.2. Principle of operation of the sodium-sulfur battery

At 60% DOD (or 40% SOC), all the sulfur has been consumed and only Na<sub>2</sub>S<sub>5</sub> remains at the positive electrode<sup>3</sup>, the molar mass of the active materials considered in equation [12.3] with  $x=5$  is, for 2 moles of sodium and 5 moles of sulfur:  $2 \times 23 + 5 \times 32.1 = 206.5$  g. With two moles of electrons exchanged, Faraday's law (see section 2.3.2.2) can be used to calculate the theoretical gravimetric capacity:

$$C_{m,th} = \frac{2}{206.5} \times 26801 = 260 \text{ mAh/g} \quad [12.4]$$

If we multiply by the voltage, 2.08 V, the theoretical gravimetric energy density of the battery is 539 Wh/kg.

### 12.2.2. Main characteristics

The main characteristics of sodium-sulfur technology are shown below:

- nominal voltage per cell: 2.08 V;
- gravimetric energy density: over 200 Wh/kg for an element to a little over 100 Wh/kg for a battery of 240 elements;
- volumetric energy density: over 350 Wh/L for an element to 170 Wh/kg for a battery;

- maximum power penalized by the reduced conductivity of the ceramic electrolyte: we cannot obtain complete charge/discharges with durations of less than 5–6 hours;

- energy efficiency: 70–80% due to the electrical resistivity of the ceramic, which gives rise to the Joule effect every time the battery is charged and discharged. These efficiency values do not take account of possible losses because of the heating of the battery;<sup>5</sup>

- invulnerability to ambient temperature;

- long published calendar lifetime: 15 years;

- long cycling lifetime: 2,500 cycles of 100% DOD, or 4,500 of 90% DOD, or 6,500 of 65% DOD;

- aging is essentially due to the wearing of the ceramic and of the metal/ceramic interface. Therefore, this technology can tolerate very little thermal cycling. The system specifications warn that the battery must not be subjected to more than 2–10 hot-to-cold cycles or the warranty is invalidated. Another cause of aging of the metal/ceramic interface are the vibrations which are inevitable in a vehicle<sup>6</sup> when the system is on board;

- rapid response: the switch can instantly be made between 100% charge power and 100% discharge power;<sup>7</sup>

- no gas emissions, silent operation;

- sodium is extremely abundant on Earth, particularly in the form of NaCl (common salt);

- sulfur is also very abundant on Earth. It is found in the form of sulfides (pyrite, cinnabar, galena, sphalerite, stibine) and sulfates (gypsum, baryte). It is to be found in free form in volcanic gases and derivatives (hot springs, fumaroles). Sulfur is also removed from fossil fuels, to prevent their combustion from releasing sulfurous anhydride, which causes acid rain;

---

5 Because of the high internal resistance of ceramics, a single charge/discharge cycle per day is sufficient to maintain the temperature of the cells. In the absence of use, it takes around ten days for the liquids to solidify.

6 For this reason, this technology – initially developed for electric vehicles – is now used mainly for stationary applications.

7 The same is true – with the exception of the inductances of the cables – for all “immobile” electrolyte batteries. It would not be true for redox flow systems, for which we would have to reverse the direction of the circulation of the reactants.

- relatively low cost for a modern technology, because the constituent materials are abundant on Earth and cost little to extract: €330/kWh for high-energy units, and €370/kWh for a complete AC/AC system of 1 MW and 6 MWh (with a charger and inverter);
- low maintenance requirement;
- only one manufacturer in the world: NGK (Japan);
- battery<sup>8</sup> only available as high-power unit: minimum of around 1 MW (Figure 12.3);
- safety: the presence of sodium, which is highly reactive with air, necessitates the exercise of numerous precautions with its use and manufacture to avoid fire hazards. If the ceramic breaks, this creates very unstable polysulfites which can cause a fire.<sup>9</sup> A sodium fire does not spread, but is difficult to put out;
- unlike nickel chloride batteries, the sodium–sulfur battery is assembled in the fully charged state by filling it with sodium and sulfur.

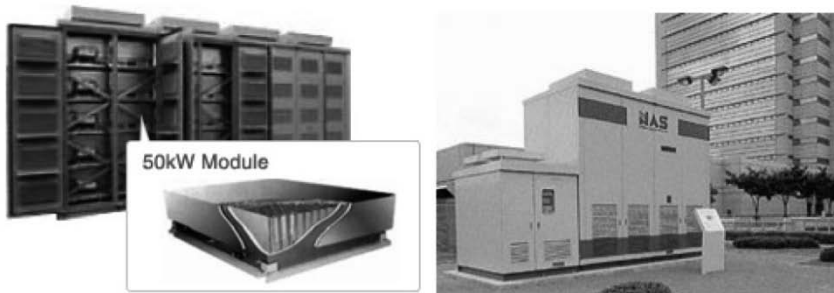


**Figure 12.3.** Sodium–sulfur batteries (source: NGK Website)

### 12.3. Nickel chloride batteries

ZEBRA technology (invented in 1985 by the group *ZEolite applied to Battery Research Africa* headed by Johan Coetzer in Pretoria, South

---

<sup>8</sup> A Na-S battery comprises several elements connected in series and/or in parallel. These elements are placed in a thermal enclosure equipped with electrical resistors to keep the reaction temperature at around 300°C.

<sup>9</sup> A fire occurred with a Na–S battery made by Tepco (Tokyo Electric Power Company) on 21 September 2011, leading NGK to request the provisional shutdown of all Na–S batteries.

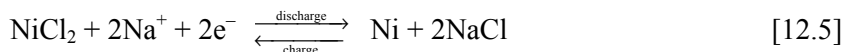
Africa)<sup>10</sup> is a variant of sodium–sulfur technology where sulfur is replaced with a metal chloride such as  $\text{NiCl}_2$  (nickel chloride) or  $\text{FeCl}_2$ . It was specifically developed for applications in electric vehicles, freight transport and public transport: the ZEBRA battery is more particularly intended to serve buses and utility vehicles. As with the Na–S battery, the vibrations felt in a vehicle may cause premature aging of the ceramic/metal interface. Today, such batteries are also being considered for stationary applications.

### 12.3.1. Operational principle<sup>11, 12, 13</sup>

The ZEBRA battery comprises a  $\text{NiCl}_2$  positive electrode in a central compartment with NaCl salt, impregnated with  $\text{NaAlCl}_3$ , which is a liquid mixture of NaCl and  $\text{AlCl}_3$  (considered to be a secondary electrolyte). The negative electrode is liquid sodium confined in a second, outer compartment. The wall separating the two compartments is made of a  $\beta$  alumina ceramic (or  $\beta\text{-Al}_2\text{O}_3$ ), conductive of sodium ions, considered to be the primary electrolyte. The element is sealed hermetically and functions at temperatures equal to or higher than  $300^\circ\text{C}$  so that the active components remain in the liquid state.

The charge/discharge reactions are written thus:

*Positive compartment*



*Negative compartment*



<sup>10</sup> Also known as *Zero Emission Batteries Research Activity*.

<sup>11</sup> J.L. SUDWORTH, “The sodium/nickel chloride (ZEBRA) battery”, *J. Power Sources*, 100, 149–163, 2001.

<sup>12</sup> C.-H. DUSTMANN, “Advances in ZEBRA batteries”, *J. Power Sources*, 127, 5–92, 2004.

<sup>13</sup> X. LU, G. XIA, J. P. LEMMON, V. SPRENKLE, Z. YANG, “Sodium-beta alumina batteries: status and challenges”, *JOM, Energy Storage Technologies*, 62, 31–36, 2010.



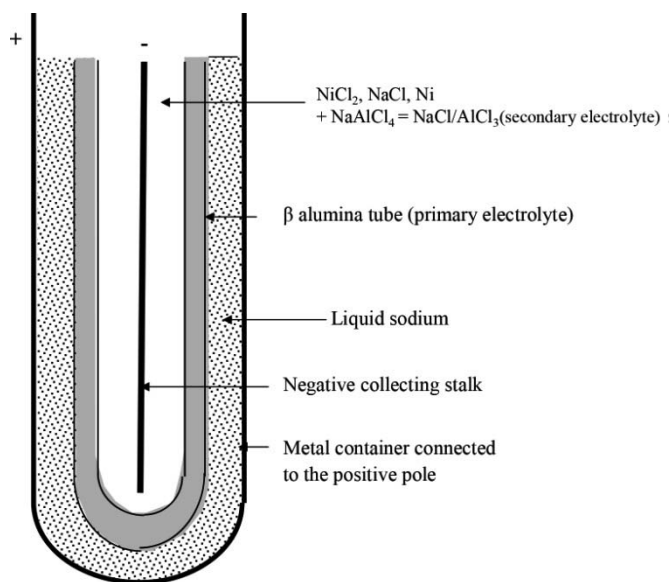


Figure 12.4. Diagram of a sodium–nickel chloride element

Balance equation



The nominal voltage per cell is 2.58 V.

These equations are illustrated in Figure 12.5 below.

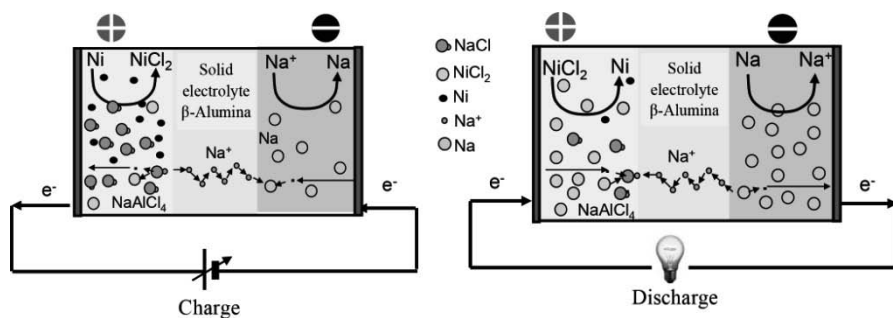


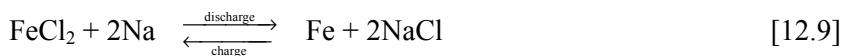
Figure 12.5. Principle of operation of the Na–NiCl<sub>2</sub> battery

Considering the case of the Na-NiCl<sub>2</sub> battery (equation [12.7]), the molar mass of active materials is, for 1 mole of NiCl<sub>2</sub> and 2 moles of Na: 58.7 + 2 × 35.5 + 2 × 23 = 175.7 g. With two moles of electrons exchanged, Faraday's law gives us the theoretical gravimetric capacity:

$$C_{m,th} = \frac{2}{175.7} \times 26801 = 305 \text{ mAh/g} \quad [12.8]$$

If we multiply by the voltage of 2.58 V, the theoretical gravimetric energy density is 787 Wh/kg.

Note that in the case of FeCl<sub>2</sub> being used as the positive active material, the balance equation is:



The nominal voltage per cell is, in this case, 2.35 V, the theoretical gravimetric capacity is 310 mAh/g and the theoretical gravimetric energy density is 729 Wh/kg.

### 12.3.2. Main characteristics

The main characteristics of nickel chloride batteries are given below, quoted for the models which are commercially available at present:

- nominal voltage of an element: 2.58 V at 300°C;
- gravimetric energy density: 140 Wh/kg for a cell, but this drops to between 70 and 90 Wh/kg for a complete 4–10 kWh pack with auxiliary components, BMS, etc. (Figure 12.6);
- volumetric energy density: 280 Wh/L for a cell and 60–110 Wh/L for a pack;
- theoretical faradaic efficiency of 1, as there are no secondary reactions;
- maximum gravimetric power density penalized by the reduced conductivity of the ceramic electrolyte<sup>14</sup>: 150–200 W/kg. The battery

---

<sup>14</sup> A thinner ceramic than in Na-S elements leads to a lower internal resistance, which enables us to increase the possible currents. In addition, we can see an excess of nickel powder on the positive electrode to enhance the conductivity of that electrode.

cannot be charged or discharged in less than two hours (or at a stretch, one hour);

- operating temperature: between 250 and 430°C, with an optimum between 270°C and 300°C;

- lifetime: 2000–3000 charge/discharge cycles to 80% DOD;

- it takes time to re-warm a discharged and cold battery because of the poor heat conductivity of the electrode: it takes several hours or even several days to restore the temperature of the battery. Thus, it is advisable not to let it cool down. That said, thermal cycling is a possibility;

- operational ambient temperature: –20° to +60°C;

- the self-discharge of a pack may be significant: 10–12% per day because of the need to consume energy to maintain the temperature of the battery. However, a daily charge/discharge cycle helps maintain the optimal operating temperature;

- no maintenance required;

- the battery is made with NaCl. Sodium will only form when the battery has been assembled and heated at the operating temperature before being charged. If the ceramic breaks during transportation, we obtain NaCl. Hence, this technology is intrinsically safer from this point of view than Na–S technology.

### **12.3.3. Availability**

Firstly, it is noteworthy that the resources and annual production of the basic constituents (NaCl, Al, Ni, Fe, etc.) are significant.

Having been developed in South Africa, this battery technology became a German and then Swiss preserve, with the company MES-DEA S.A. Today, it is developed by the Italian company FIAMM under the name FIAMM SoNick ([www.fiammsonick.com](http://www.fiammsonick.com)) which, for instance, commercializes 48 V batteries for telecoms applications and, more generally, for emergency supply with modules of 80, 120, 160 and 200 Ah in capacity (Figure 12.6).



**Figure 12.6.** FIAMM SoNick 48 TL-200 battery (source: [www.fiammsonick.com](http://www.fiammsonick.com))

In 2011, General Electric in the USA began producing nickel chloride batteries under the name Durathon. They are intended for grid-connected renewable energy storage, telecoms applications and, more generally, backup power supply and industrial transport needs.

The cost of nickel chloride batteries is approximately €350–€380/kWh for a pack.

#### 12.4. Conclusions about high-temperature batteries

These sodium-based high-temperature battery technologies are at a level of maturity and reliability which places them in a good position for large-scale grid-connected storage applications. They have a higher specific energy than lead batteries and their cost is significantly less than that of lithium batteries. Unlike many other technologies (such as lead or lithium), their peak power is limited, which places them at a disadvantage for applications in electric vehicles. However, if power peaks are required, they can be used in conjunction with supercapacitors. Finally, because of their internal operation at high temperature, these batteries are particularly suitable in environments where the ambient temperature is high (above 40 or 45°C), where the lifetime of other battery technologies falls rapidly.

#### 12.5. Redox flow systems

Redox flow batteries (or systems) are present in ranges from ten to several hundred kW, and even beyond a MW for grid support or transport,

for storage of renewable energies, for uninterruptible power supply, etc. owing to their numerous intrinsic advantages, such as the decorrelation of power and capacity (for vanadium-based technology), the absence of self-discharge when completely deactivated<sup>15</sup> and a competitive cost. The architecture of such a storage system is illustrated in Figure 12.7.

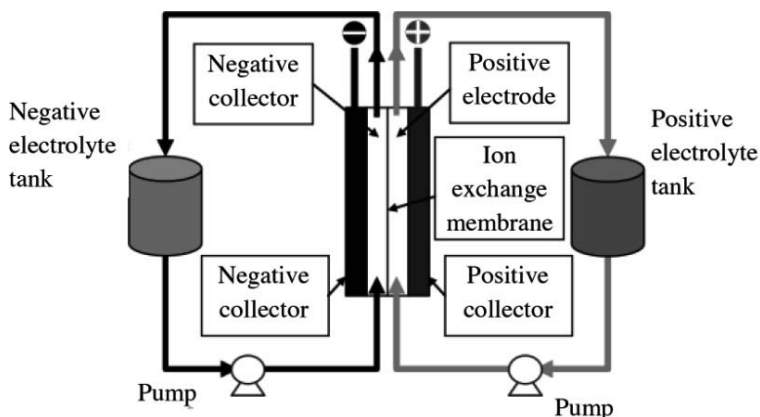


**Figure 12.7.** *Elementary redox flow cell*

In redox flow batteries, the chemical compounds responsible for energy storage are liquid and remain in solution in the electrolyte. This mode of operation enables us to circumvent the limitation of conventional electrochemical batteries wherein electrochemical reactions create solid compounds which are stored directly in the electrodes where they are formed. The mass that it is possible to accumulate locally is therefore necessarily limited by the volume and mass of the electrodes, which sets a maximum capacity.

The electroactive compounds are two soluble redox couples which are oxidized and reduced (section 2.2.4) in a “reactor” which forms the electrochemical cell. These two compounds have the ability to store electrical energy (during charge) and to restore this energy during the discharge phase. The core of the cell comprises two compartments separated by a proton exchange membrane (PEM), such as a Nafion<sup>®</sup> membrane as

<sup>15</sup> That is, in disconnected mode, with all valves closed and pumps turned off. For rapid response capability, it needs to be left functioning. The internal losses and those due to the pumps cause an apparent self-discharge of around 10% per day.

used in fuel cells.<sup>16</sup> The reactants are contained in two storage tanks and circulate in a closed circuit through the core of the cell where the electrochemical reactions take place. This type of design offers a high degree of flexibility in its assembly because the characteristics of energy and power can be dissociated: the power of the system is determined by the surface area of the membrane and by the number of elementary cells used; the energy by the concentration and volume of the electrolyte (and thus of the tanks). Hence, the energy and power can very easily be adapted to serve the needs of charge or discharge in the space of a few hours, as in the case of peak shaving or temporal adaptation of production and consumption, or to needs of several days or even weeks, as required by standalone applications with PV or wind-power systems.

This separation between the reactor and the tanks is one of the advantages of redox flow batteries in terms of transport, as the assembly of the batteries and electrolyte filling are done on site. Thus, during transport, the battery is not electrochemically active.

This modularity also means that, in the medium term, we can expect a moderate cost per kWh delivered. Indeed, it is estimated that the manufacturing costs could be the lowest in comparison to all other storage systems.

Recharging is naturally done by injecting a current into each cell, but can also be done by replacing the electrolytes (for instance, if rapid recharging is needed for an electric vehicle<sup>17</sup>).

It should be noted, however, that it is necessary to put numerous mechanical components (pipes, pumps, etc.), electrical components (power supply), electronics (BMS) and regulators (e.g. to regulate the flowrate of fluids depending on the power requirement) in place around the core of the battery.

---

16 For further explanations about fuel cells, see: M.C. PERA, D. HISSEL, H. GUALOUS, C. TURPIN, *Electrochemical Components Ltd*, ISTE, London, John Wiley & Sons, New York, 2013.

17 Very strict usage precautions must be taken, because it involves handling highly acidic electrolytes. The electrolytes can later be “recharged” in a stationary battery.

In addition, the response time of the system is proportional to the time it takes to get the fluids circulating. Finally, these batteries cannot function below a minimum level of power.

On the other hand, the declared lifetime is very long: 100000 hours and over 10000 charge/discharge cycles, although possibly at the cost of replacing certain components (as with fuel cells, the PEM is the weak point of the device). With this in mind, certain manufacturers claim an infinite lifetime. Nevertheless, the maintenance requirement is minimal.

Different technologies for redox flow batteries have been introduced.<sup>18</sup> The choice of electrodes is dictated by a small overvoltage during the charge and discharge processes to obtain good energy efficiency and significant overvoltage in relation to water to prevent its electrolysis. The most common technology is that based on vanadium oxides, dissolved in sulfuric acid. The four oxides of vanadium present the (very rare) peculiarity of all being soluble in sulfuric acid, so the substance remains dissolved irrespective of the SOC of the element.

#### **12.5.1. Vanadium redox battery**

The use of vanadium in batteries was suggested by the Frenchman P.A. Pissort<sup>19</sup> in 1933. This battery was then investigated in a number of different countries. The present technology stems mainly from work carried out at the University of New South Wales ([www.vrb.unsw.edu.au](http://www.vrb.unsw.edu.au)) in Australia in the 1980s.

#### **12.5.2. Operational principle**

The operational principle of a vanadium–vanadium redox flow cell (vanadium redox battery or VRB) is illustrated in Figure 12.8.

---

<sup>18</sup> A.Z. WEBER, M.M. MENCH, J.P. MEYERS, P.N. ROSS, J.T. GOSTICK, Q. LIU, “Redox flow batteries: a review”, *J. Appl. Electrochem.*, 41, 1137–1164, 2011.

<sup>19</sup> P.A. PISSOORT in a patent filed in France: number FR 754065.

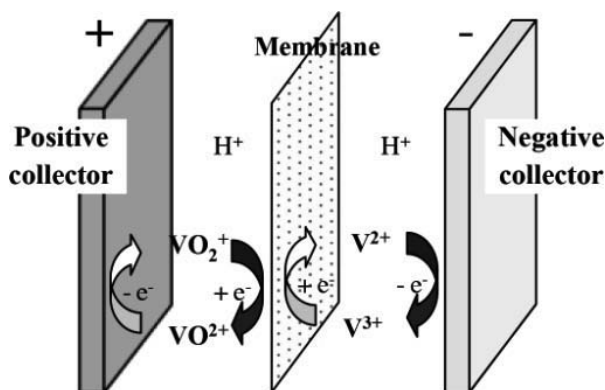
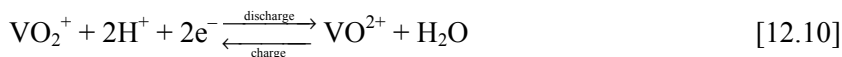


Figure 12.8. Principle of operation of a VRB

The electrolyte in the positive compartment contains  $\text{VO}_2^+$  and  $\text{VO}^{2+}$  ions (dissolved in sulfuric acid). In the negative compartment, the electrolyte contains  $\text{V}^{3+}$  and  $\text{V}^{2+}$  ions. During charge, the  $\text{VO}_2^+$  ions from the positive electrode are turned into  $\text{VO}^{2+}$  ions, and an electron is extracted by the positive terminal. At the negative electrode, the  $\text{V}^{3+}$  ions are turned into  $\text{V}^{2+}$  ions by the addition of an electron. During discharge, of course, these processes are reversed. The exchange of protons ( $\text{H}^+$ ) takes place via the PEM.

The electrochemical reactions which take place at the electrodes are shown below:

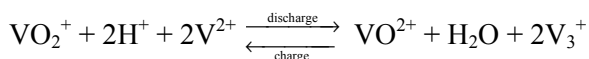
*Positive compartment*



*Negative compartment*

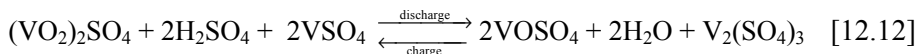


*Balance equation*





or, if we consider sulfuric acid as a solvent on both positive and negative sides:



The nominal voltage per cell is 1.70 V.

### 12.5.3. Main characteristics

Firstly, from the viewpoint of a system, it is not possible to electrically connect too many cells (or reactors) in series to the same tanks because, if all the positive (or respectively negative) compartments are connected to the same tank, this causes a sort of short-circuit between the cells. These leakage currents are minimized by using long pipes with small diameter. The total voltage for a whole system is limited to around 50 V. To obtain higher voltages, all of the components (core, tanks, pumps, controlling electronics, etc.), as connected in series.

In addition, because of the mode of participation of the electrodes, modular arrangements can be made to cope with energy- or power-oriented requirements.

On the scale of a cell, the molar mass of the active materials considered in equation [12.12] is, for 1 mole of  $(\text{VO}_2)_2\text{SO}_4$ , 2 moles of  $\text{H}_2\text{SO}_4$  and 2 moles of  $\text{VSO}_4$ :  $(2 \times (50.9 + 16 \times 2) + 17 + 4 \times 16) + (2 \times 1 + 17 + 4 \times 16) + (50.9 + 17 + 4 \times 16) = 461.7$  g.

With two moles of electrons exchanged, Faraday's law (see section 2.3.2.2) gives us the theoretical gravimetric capacity:

$$C_{\text{m.th}} = \frac{2}{461.7} \times 26801 = 116 \text{ mAh/g} \quad [12.13]$$

With a nominal voltage of 1.70 V, the theoretical gravimetric energy density is established as 197 Wh/kg.

On the scale of a cell, the practical gravimetric energy density ranges from 25 to 35 Wh/kg<sup>20</sup> considering only the liquid electrolytes.

For a whole system of several tens of kWh, the gravimetric energy density falls to less than 10 kWh/kg and between 7 and 14 Wh/L. These values are lower than those for a lead–acid battery and *a fortiori* are far lower than those for nickel- or lithium batteries. However, the VRB is one of the very few systems which can be adapted for interseasonal storage (no self-discharge if the pumps are shut down, and the tanks are sufficiently large to store the amount of energy desired with a cell core appropriate for the power required).

The efficiency of a charge/discharge cycle is expected to be 90% in favorable conditions (low current densities) but nearer to 75% in less favorable conditions. Complete discharges are acceptable, but overcharges are prohibited so as to avoid reaching the level of voltage where electrolysis of water would occur. Hence, as with lead–acid batteries, the end of charge can be done with low current so as not to attain too high a voltage and electrolyze the water, or with a controlled voltage, where the current strength decreases with the SOC. The durations for a complete charge may be over 10 hours.

Discharges are possible with any current strength, but the capacity drops noticeably for discharges in the space of an hour.

The level of maintenance required is more than for conventional battery technologies because of the mechanical elements (pumps, piping, etc.), and the lifetime of the PEM. However, it is not prohibitive (Prudent Energy recommends a 2-hour intervention every 9000 hours of operation, and 8 hours of service every 27000 hours).

The lifetime is set as at least 20 years, on the condition that the system is properly managed. We need to:

- avoid precipitation of the electroactive species in the porous carbon collectors;
- use a PEM that is stable over time;
- use good-quality mechanical components.

---

<sup>20</sup> Here, the specific capacity is limited by the solubility of vanadium oxides in sulfuric acid.

The solubility of the reactants in the electrolyte is an important point for the operation of the system, given that the maximum concentration of the species is conditioned by the solubility of the least soluble species. The concentration of dissolved species thus governs:

- the energy density;
- the power density;
- the charge/discharge efficiencies.

It should be noted that low concentrations mean reduced charge transfers and therefore low current densities, in addition to which we see more prevalent polarization and, for a given power level during charge or discharge, oversizing of the pumping power. In addition, as the solubility is temperature-dependent, the range of operating temperature for modern systems using vanadium sulfates and containing a chloride in the electrolyte is relatively restricted: between  $-5$  and  $50^{\circ}\text{C}$ .

Finally, from an environmental standpoint, vanadium is a toxic product but it remains confined. It is essential to use a double container to prevent dispersion in case of leakage. On the other hand, the patent advantage is that the electrolyte can still be reused even after 20 years of use.

#### **12.5.4. Availability**

We can cite some examples of installations of VRBs commercially available with manufacturer references:

Gildemeister<sup>21</sup> ([en.cellcube.com/en/index.htm](http://en.cellcube.com/en/index.htm)) offers a first CellCube model of 10 kW power with 100 kWh energy storage. Its reaction time is less than 60 ms. Its energy efficiency may reach up to 80%. The power consumed by the auxiliaries in standby mode is 150 W. There is no self-discharge when the device is completely shut down (electrolytes in their tanks). Its volume is  $23\text{ m}^3$ . When charged, its mass is 10,300 kg. From this we can deduce maximum specific energies and powers: 9.7 Wh/kg, 4.35 Wh/L, 1 W/kg and 0.43 W/L.

---

<sup>21</sup> Formerly Cellstrom.

Gildemeister also offers a 200 kW model with 400 kWh storage<sup>22</sup> (Figure 12.9). Its reaction time is less than 60 ms. Its energy efficiency may reach up to 70%. The power consumed by the auxiliaries in standby mode is less than 100 W. There is no self-discharge when the device is completely shut down (electrolytes in their tanks). Its volume is 85 m<sup>3</sup>. When charged, its mass is 60,000 kg. We can deduce its maximum specific energies and powers: 6.7 Wh/kg, 4.7 Wh/L, 3.33 W/kg and 2.35 W/L.

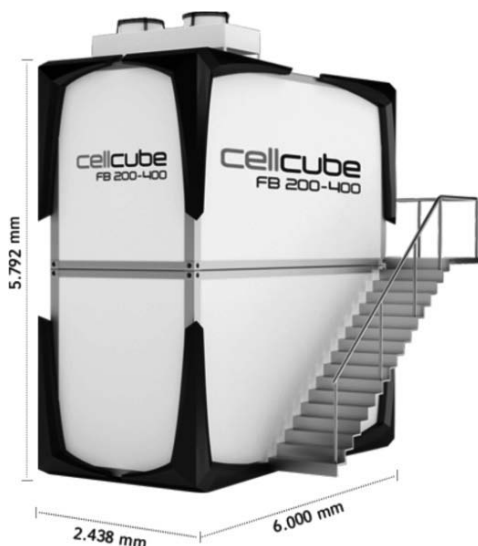


**Figure 12.9.** 200 kW and 400 kWh VRB  
(source Gildemeister, [www.dmg.com](http://www.dmg.com))

Prudent Energy ([www.vrbpower.com](http://www.vrbpower.com)): 5–7 kW; 42–56 V; 100000 hours; 5300 kg and 2.84 m<sup>3</sup> with 40 kWh of storage, so a gravimetric energy density of 7.55 Wh/kg, a volumetric energy density of 14 Wh/L, a maximum gravimetric power density of 1.3 W/kg and a maximum volumetric power density of 2.5 W/L.

We can also cite GEFC (China, [www.gefc.com/en/Products.aspx?id=79](http://www.gefc.com/en/Products.aspx?id=79)), who offer 2.5–50 kW batteries, or visit the Website of Cellennium (Thailand, [www.vanadiumbattery.com](http://www.vanadiumbattery.com)).

<sup>22</sup> The deliverable energy depends on the strength of the discharge current. On output from the battery (and therefore before passage through the inverter), we can recover 220 kWh during discharge over 1 hour, 280 kWh over 2 hours and 400 kWh over 5 hours.

The cost per unit stored energy may be low for low-power cores because the tanks are inexpensive in comparison to the PEMFC and the auxiliary devices. The cost per kWh is thus more attractive with high storage capacities. It currently sits at around €2000/kWh for small systems with a complete environment (inverters, protections, etc.) and is around €600/kWh or even €300/kWh for large systems. The cost objectives are set at around €150/kWh for discharge durations of 8 hours or more.

In terms of land usage, the dimensions, for a given level of energy, are greater than with lead–acid technology, for instance.

#### 12.5.5. Other redox flow battery technologies

Two other technologies have been developed and demonstrated: polysulfide–Bromide (PSB) and zinc–bromide (ZnBr). The principle of their operation is shown in Figure 12.10.

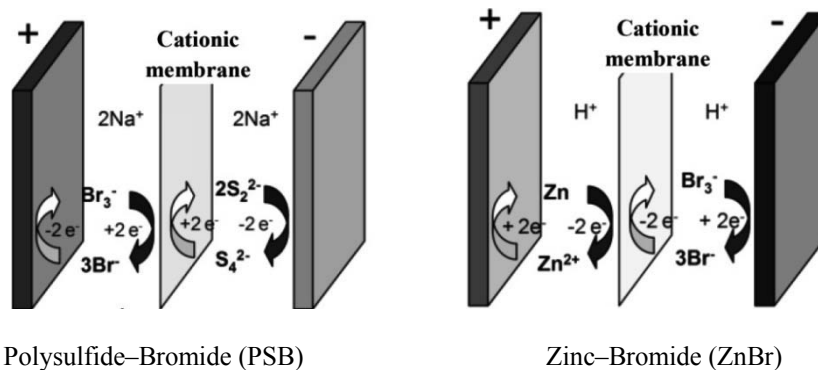


**Figure 12.10.** Principles of operation of PSB and ZnBr redox flow technologies

The zinc–bromide system is commercialized by ZBB Energy (Australia, [www.zbbenergy.com/](http://www.zbbenergy.com/)), Premium Power (USA, [www.premiumpower.com](http://www.premiumpower.com)) and RedFlow ([redflow.com/](http://redflow.com/)).

As for the polysulfide–bromide system, the studies and commercialization that began seem to have been discontinued: Prudent Energy ([www.vrbpower.com](http://www.vrbpower.com)) has adopted the technology initially developed by the company Regenesys, but does not appear to have relaunched it.

**12.5.6. Conclusion about redox flow batteries**

Redox flow battery systems are promising devices, because the tendency is toward the development of “low-cost” systems, and future developments seem to be leaning toward choosing less toxic redox couples, more abundant materials, more stable membranes and effective recycling processes. Electrolytes can always be reused provided there is no precipitation of oxides – a phenomenon which occurs at low temperature.

## Conclusion

Over the course of the different chapters of this book, we have described the operational principles and performances but also the limitations of lithium-ion and lithium-metal batteries, high-temperature batteries and redox flow systems. Whether the technology has reached maturity or is still in the process of development, it must be noted that no single technology is, at present, capable of simultaneously serving the very diverse requirements of portable, stationary or on-board applications, either for reasons of cost, intrinsic performances, availability or recyclability. Numerous and lengthy research projects both at an academic and an industrial level still need to be conducted to further improve these electrical energy storage devices.

Whilst it is true that lithium batteries have come to supplant nickel-based batteries in a large number of small-scale applications (such as in portable devices) or medium-scale ones (e.g. electric vehicles), they are now in competition with other technologies for energy storage on a large scale. Only with full-scale and long-term experiments will we be able to validate the most appropriate technology.

Innovative solutions are under investigation for a more distant future.<sup>1</sup> We have quite deliberately not discussed these in the context of this book,

---

<sup>1</sup> Lectures by J.-M. TARASCON (University of Picardie): Le futur du stockage électrochimique de l'énergie – *Colloque ANR-NTE* at Cité des Sciences et de l'Industrie de Paris, 20 November 2009; – Comment vivre sans les énergies fossiles? Le rôle du stockage électrochimique – Institut de Botanique de l'Université Montpellier II, 29 February 2012.

because they involve concepts which are extremely *avant-gardist*. As in many other domains, researchers are drawing inspiration from models of living things (biomimicry). Thus, we could design batteries using materials that are created and recycled by nature. In another domain, we would like to be able to synthesize battery elements at ambient temperature using sunlight.

Researchers are becoming aware that the development of new batteries needs to be carried out within a framework of sustainable development (green chemistry). This involves considering – from the very start – the use of available resources, and their geographical location (which means discounting materials, for instance, whose sources are concentrated in too limited or poorly distributed geographical areas); the whole lifecycle of the system (i.e. from manufacture through operation to recycling), even if this consideration is made to the detriment of the gravimetric and volumetric performances (on this point, stationary applications are less demanding than on-board applications). From this point of view, sodium<sup>2</sup>, which is immediately below lithium in the Periodic Table (Figure 4.8), is very abundant all over the world, mainly in the form of NaCl. The same abundance is seen for iron and zinc, which are also prospective candidates for the making of low-cost batteries. However, in order for the overall balance to be positive, the lifetime also needs to be appropriate for the requirement, and generally extended. Finally, safety aspects must remain a major concern for researchers.

To introduce very low-cost, long-life batteries would facilitate the democratization of electricity storage – and such democratization could constitute a powerful vector to accelerate the penetration of those renewable energies which are most abundantly available but are highly variable, such as the sun and the wind (photovoltaic and wind power conversion). Developing countries could also benefit more widely from access to energy.

To conclude, the aim of this book has been to help students and potential users of high-tech electrochemical batteries (using lithium or other technologies) by providing useful and practical information, and raising certain questions and ideas. Has this objective been fulfilled? We hope so.

---

<sup>2</sup> J.-M. TARASCON, Histoire et évolution des technologies d'accumulateurs. Collège de France (UPL51353). 2 February 2011.



# Index

1,2-dimethoxyethane (DME), 280  
1,3-dioxolane (DIOX), 280

## A, B

aging, 36–39  
alkyl carbonates,  
158, 305  
Avogadro's number, 31, 32  
base transceiver station (BTS),  
11, 94  
battery, 40–66, 74–78, 101–107,  
113, 121–130, 219, 220, 236–238,  
252–255, 271–285, 335–340, 343,  
349, 350  
management system (BMS),  
236–238  
biphasic, 144, 154, 178  
insertion, 153, 178  
butyl-methylimidazolium  
(BMI), 239

## C

calendar aging, 39, 212  
cell, 22, 23, 52, 53, 60–62, 70, 71,  
187, 188  
chemical vapor deposition (CVD),  
223, 254  
constant phase element (CPE),  
58, 59

## D

dendrites, 131, 132  
diethyl carbonate (DEC), 158, 305  
dimethyl carbonate (DMC), 158, 305

## E

electrically assisted pedal cycles  
(EAPC), 6, 160, 171  
electric vehicle (EV), 9, 10, 104, 107  
electrode, 23, 69, 7, 130, 138–165,  
167–177, 225, 245–251, 259, 260,  
271, 272, 277, 283–285, 300, 301  
element, 22, 23, 58–62, 168–179,  
230, 264  
ethyl-methylimidazolium (EMI), 239  
end of life (EOL), 36–39  
energy density, 63, 64, 198–206, 230,  
261, 262, 307, 308  
ethylene carbonate (EC), 158, 305

## F, G

Faraday law, 31–33  
galvanostatic method, 49, 50  
global sytem for mobile  
communications (GSM), 94

## H, I

half cell, 23  
element, 23

hexafluorophosphate ion ( $\text{PF}_6^-$ ), 239  
 hybrid electric vehicle (HEV), 7–9,  
 44, 180  
 initial charging process, 33, 149  
 insertion/extraction or removal, 122,  
 123, 315–318  
 intercalation/de-intercalation, 122,  
 123, 129, 130, 145  
 irreversible capacity, 124, 127, 248

## L

leaf, 105, 107  
 lifetime, 36–39, 210–213, 262  
 lithium  
   cobalt dioxide (LCO), 168–171  
   iron phosphate (LFP), 62  
   bis(fluorosulfonyl)imide  
     (LiFSI), 260  
   hexafluorophosphate ( $\text{LiPF}_6$ ),  
     159  
   phosphorus oxynitride (LiPON),  
     254, 306  
   superionic conductor (LISICON),  
     284, 306  
   bis(trifluoromethanesulfonyl)imide  
     (LiTFSI), 159, 305  
   ion, 105–107, 136–138  
   manganese oxide (LMO), 105,  
     142, 175, 176  
   titanium oxide (LTO), 152, 175,  
     176, 180, 195  
   nickel cobalt aluminum oxide  
     (NCA), 142  
   nickel manganese cobalt oxide  
     (NMC), 142

## M, N, O

mass loading, 181, 244  
 material, 25, 122, 123,  
 128–130, 146–152, 244–252,  
 276, 277  
 modules, 26, 27, 172, 199  
 mole, 31, 32  
 monophasic insertion, 153

normal hydrogen electrode (NHE),  
 70, 131  
 olivine, 143, 144

## P

pack, 26, 27, 200, 201, 203  
 poly  
   acrylonitrile (PAN), 160  
   ethylene (PE), 159, 160, 283  
   ethylene oxide (PEO), 121, 160,  
     257, 273, 281  
   methyl methacrylate (PMMA), 160  
   propylene (PP), 158, 159,  
     222, 283  
   vinylidene difluoride (PVDF), 160,  
     239  
   vinylidene fluoride-co-  
     hexafluoropropene  
     (PVdF-HFP), 283  
 peugeot 106, 105,  
 polarization, 27, 185, 207  
 potentiostatic method, 49, 50  
 prismatic element, 171, 225  
 physical vapor deposition (PVD),  
 254, 275

## S, T

self-discharge, 67, 262  
 solid electrolyte interphase (SEI), 25,  
 118, 149  
 spinel, 138, 142, 155  
 Stand-alone Emergency Lighting  
   Unit (SELU), 16  
 tetra  
   fluoroborate ion ( $\text{BF}_4^-$ ), 239  
   hydrofuran (THF), 280  
 Toyota prius, 8, 106, 173  
 transition metals, 132, 133, 138–142  
 twizy, 106, 108

## V, W

vinylene carbonate (VC), 33  
 warburg, 53–56, 79–82  
   line, 53, 54